

COORDINATED OPERATIONS OF DISTRIBUTED WIND GENERATION IN A  
DISTRIBUTION SYSTEM USING PMUS

by

MANOAJ SRIKUMAR VIJAYARENGAN

B.E., ANNA UNIVERSITY, CHENNAI, INDIA, 2010

A THESIS

submitted in partial fulfillment of the requirements for the degree

MASTER OF SCIENCE

Department of Electrical and Computer Engineering  
College of Engineering

KANSAS STATE UNIVERSITY  
Manhattan, Kansas

2012

Approved by:

Major Professor  
Dr. Noel N. Schulz

# **Copyright**

MANOAJ SRIKUMAR VIJAYARENGAN

2012

## **Abstract**

Wind energy is becoming one of the most widely implemented forms of renewable energy worldwide. Traditionally, wind has been considered a non-dispatchable source of energy due to the uncertainty of wind speed and hence the variable availability of wind power. Advances in technology allow the consideration of the impact of distributed wind turbines and farms on distribution systems. It is possible to combine the clean energy attributes of wind with the quickly dispatchable nature of a storage facility in order to provide the maximum amount of locally available power economically to the loads present on the distribution feeder. However, a monitoring and control system needs to be provided that is capable of detecting the changes associated with the distribution feeder load and also the variable generation output from the wind farms. This task can be accomplished using a Phasor Measurement Unit (PMU) which has very high sampling rates and hence can measure very rapid and dynamic changes in power levels associated with distribution feeder load and wind generation. The data which is obtained from these PMUs can be used to calculate the amount of distributed generation and storage that can be dispatched locally at the distribution feeder, thus resulting in a reduction in the peak load levels associated with the distribution feeder as seen by the substation monitoring system. Simulations will work to balance load requirements, wind generation output, and distributed storage providing a stable system utilizing maximum renewable resources. The standard IEEE 37-node distribution test feeder is used in the study. Probabilistic models are implemented for distribution feeder load, and the models are analyzed through simulations. Four different combinations of charging and discharging methods have been investigated. Two analytically different algorithms have been used for wind and battery dispatch, one based on forecasted load information and the other based on historical measurements obtained from PMUs. The strategies being investigated can also be used to implement other important applications such as distribution system state estimation, protection and instability prediction.

## Table of Contents

List of Figures .....	vi
List of Tables .....	xiv
Acknowledgements .....	xv
Dedication .....	xvi
Chapter 1 - Introduction.....	1
1.1 Introduction and Motivation .....	1
1.2 Summary of Results.....	3
1.3 Outline .....	4
Chapter 2 - Background and Literature Review .....	5
2.1 Background.....	5
2.1.1 Distribution System Structure.....	5
2.1.2 Distribution System Load Profile .....	5
2.1.3 Wind Energy Generation .....	7
2.1.4 Distributed Storage .....	7
2.1.5 Phasor Measurement Units .....	8
2.2 Literature Review .....	8
Chapter 3 - Research Objectives and Proposed Solution.....	12
3.1 Research Objectives.....	12
3.2 Proposed Solutions .....	12
Chapter 4 - Test Cases, Data and Tools.....	18
4.1 Test Cases and Data .....	18
4.1.1 Average Normalized Load Profile for a group of houses .....	18
4.1.2 IEEE 37 node test feeder.....	20
4.1.3 Distributed Wind Generation .....	22
4.1.4 Standard NAS (Sodium Sulfide) battery specifications.....	23
4.2 Tools .....	25
4.2.1 Backward Forward Sweep Power Flow Algorithm .....	25
4.2.1.1 Node Renumbering .....	26

4.2.1.2 Method .....	27
4.2.1.3 Distributed Generation .....	30
Chapter 5 - Algorithm and Analysis .....	32
5.1 Storage Dispatch Operation Algorithms .....	32
5.1.1 Test Setup of Feeder Components and Measurements .....	32
5.1.2 Testing for conventional base cases .....	34
5.1.3 Dispatch operations for forecasted load information .....	35
5.1.4 Dispatch operations for historical load information from PMUs .....	41
Chapter 6 - Results and Discussion .....	43
6.1 Results obtained for base cases of load flow .....	43
6.1.1 Results obtained for base cases of load flow without wind generation .....	43
6.1.2 Results obtained for base cases of load flow with wind generation .....	49
6.2 Results obtained for wind generation and battery storage integration for forecasted load information.....	60
6.3 Real time operation of storage dispatch with wind generation based on historical PMU measurements.....	91
Chapter 7 - Conclusions and Future Work .....	112
7.1 Conclusions.....	112
7.2 Future Work.....	113
References .....	114
Appendix A – Test Feeder Information .....	118
A.1 Test feeder Line, Load and Transformer details .....	118
A.2 Phase Impedance Matrices for various configurations .....	120
Appendix B – Input Files and Software Code .....	121
B.1 Code for Input file used in Fifteen-minute Analysis.....	121
B.2 Code for Input file used in One-second Analysis .....	131
B.3 Code for Analysis used for fifteen-minute forecasted load data.....	136
B.4 Code for Analysis used for one-second forecasted load data .....	142
B.5 Code for Analysis used for one-second load data based on historical PMU measurements .....	149

## List of Figures

Figure 2.1 Aggregated Residential load curve [26] .....	6
Figure 2.2 Aggregated Commercial load curve [26] .....	6
Figure 2.3 Aggregated Industrial load curve [26] .....	6
Figure 2.4 Functional block diagram of PMU [6] .....	8
Figure 3.1 Wind charging only .....	13
Figure 3.2 Sustained average load charging .....	13
Figure 3.3 Free running discharge .....	14
Figure 3.4 Conservative Discharging .....	15
Figure 3.5 Conversion of 15-minute load profile into One-second load profile .....	16
Figure 4.1 Aggregated 15-minute demand histogram for ten houses for a day [26] .....	18
Figure 4.2 Coincidence factor as a function of number of houses [26] .....	19
Figure 4.3 15-minute average normalized demand histogram for a day .....	19
Figure 4.4 One-second normalized demand curve for a day .....	20
Figure 4.5 IEEE 37 node test feeder .....	22
Figure 4.6 NAS Battery Cell module and Cell structure [15] .....	24
Figure 4.7 Node Renumbering [2] .....	26
Figure 4.8 Renumbered IEEE 37 node Test Feeder .....	27
Figure 4.9 Flowchart of the backward forward sweep power flow algorithm .....	30
Figure 5.1 Dispatch Operations Simulation Test Setup* .....	33
Figure 5.2 Flowchart for base case testing with or without wind generation .....	34
Figure 5.3 Flowchart for battery dispatch operation for wind charging with free running discharge .....	36
Figure 5.4 Flowchart for battery dispatch operation for wind charging with conservative discharge .....	37
Figure 5.5 Flowchart for battery dispatch operation for sustained average load charging with free running discharge .....	39
Figure 5.6 Flowchart for battery dispatch operation for sustained average load charging with conservative discharge .....	40
Figure 5.7 Flowchart for real time battery operation with wind generation using PMUs .....	42

Figure 6.1 Individual demand of phases a, b and c of the feeder for 15 minute data .....	44
Figure 6.2 Individual voltages of phases a, b and c for node 32 for 15 minute data .....	44
Figure 6.3 Power losses for the entire feeder for 15 minute data .....	45
Figure 6.4 Average normalized 15-minute load profile of the feeder without wind generation ..	45
Figure 6.5 Individual demand of phases a, b and c of the feeder for one second data .....	46
Figure 6.6 Individual voltages of phases a, b and c for node 32 for one second data .....	47
Figure 6.7 Power losses of the entire feeder for one second data.....	47
Figure 6.8 Total three phase demand of the feeder for one second data .....	48
Figure 6.9 Average normalized 15-minute demand histogram for the feeder obtained from one second demand.....	48
Figure 6.10 Individual phase demands with direct wind generation connection and high wind for fifteen minute data .....	50
Figure 6.11 Individual phase voltages for node 32 with direct wind connection and high wind for fifteen minute data .....	50
Figure 6.12 Power losses for the feeder with direct wind connection and high wind for fifteen minute data.....	51
Figure 6.13 Normalized fifteen minutes load histogram as seen by the substation with direct wind connection and high wind .....	51
Figure 6.14 Individual phase demands with direct wind generation connection and medium wind for fifteen minute data.....	52
Figure 6.15 Individual phase voltages for node 32 with direct wind connection and medium wind for fifteen minute data.....	53
Figure 6.16 Power losses for the feeder with direct wind connection and medium wind for fifteen minute data.....	53
Figure 6.17 Normalized fifteen minutes load histogram with direct wind connection and medium wind.....	54
Figure 6.18 Individual phase demands with direct wind generation connection and low wind for fifteen minute data .....	55
Figure 6.19 Individual phase voltages for node 32 with direct wind connection and low wind for fifteen minute data .....	55

Figure 6.20 Power losses for the feeder with direct wind connection and low wind for fifteen minute data .....	56
Figure 6.21 Normalized fifteen minutes load histogram with direct wind connection and low wind.....	56
Figure 6.22 Individual phase load demand for one second basis data with direct wind generation connection .....	57
Figure 6.23 Individual phase load voltages for one second basis data with direct wind generation connection .....	58
Figure 6.24 Feeder power losses for one second basis data with direct wind generation connection .....	58
Figure 6.25 Overall demand of the feeder for one second basis data with direct wind generation connection .....	59
Figure 6.26 Fifteen minute average normalized demand of the feeder for one second basis data with direct wind generation connection .....	59
Figure 6.27 Battery charging and discharging for fifteen minute data with high wind generation in free-running discharge and wind charging .....	60
Figure 6.28 Battery state of charge for fifteen minute data with high wind generation in free-running discharge and wind charging .....	61
Figure 6.29 Normalized overall feeder load demand for fifteen minute data with high wind generation in free-running discharge and wind charging.....	61
Figure 6.30 Battery charging and discharging for fifteen minute data with high wind generation in free-running discharge and sustained average load charging .....	62
Figure 6.31 Battery state of charge for fifteen minute data with high wind generation in free-running discharge and sustained average load charging .....	63
Figure 6.32 Normalized overall fifteen minute demand histogram with high wind generation in free-running discharge and sustained average load charging .....	63
Figure 6.33 Battery charging and discharging for fifteen minute data with high wind generation in conservative discharge and wind charging .....	64
Figure 6.34 Battery state of charge for fifteen minute data with high wind generation in conservative discharge and wind charging .....	65



Figure 6.35 Normalized demand histogram for fifteen minute data with high wind generation in conservative discharge and wind charging .....	65
Figure 6.36 Battery charging and discharging with high wind generation in conservative discharge and sustained average load charging .....	66
Figure 6.37 Battery state of charge with high wind generation in conservative discharge and sustained average load charging .....	67
Figure 6.38 Normalized demand histogram with high wind generation in conservative discharge and sustained average load charging.....	67
Figure 6.39 Battery charging and discharging for fifteen minute data with medium wind generation in free-running discharge and wind charging.....	68
Figure 6.40 Battery State of charge for fifteen minute data with medium wind generation in free-running discharge and wind charging .....	68
Figure 6.41 Normalized overall feeder load demand for fifteen minute data with medium wind generation in free-running discharge and wind charging.....	69
Figure 6.42 Battery charging and discharging for fifteen minute data with medium wind generation in free-running discharge and sustained average load charging .....	69
Figure 6.43 Battery state of charge for fifteen minute data with medium wind generation in free-running discharge and sustained average load charging .....	70
Figure 6.44 Normalized overall fifteen minute demand histogram with medium wind generation in free-running discharge and sustained average load charging .....	70
Figure 6.45 Battery charging and discharging for fifteen minute data with medium wind generation in conservative discharge and wind charging .....	71
Figure 6.46 Battery state of charge for fifteen minute data with medium wind generation in conservative discharge and wind charging .....	72
Figure 6.47 Normalized overall fifteen minute demand histogram with medium wind generation in conservative discharge and wind charging .....	72
Figure 6.48 Battery charging and discharging for fifteen minute data with medium wind generation in conservative discharge and sustained average load charging .....	73
Figure 6.49 Battery state of charge for fifteen minute data with medium wind generation in conservative discharge and sustained average load charging .....	73

Figure 6.50 Normalized overall fifteen minute demand histogram with medium wind generation in conservative discharge and sustained average load charging .....	74
Figure 6.51 Battery charging and discharging for fifteen minute data with low wind generation in free-running discharge and wind charging.....	74
Figure 6.52 Battery state of charge for fifteen minute data with low wind generation in free-running discharge and wind charging .....	75
Figure 6.53 Normalized overall feeder load demand for fifteen minute data with low wind generation in free-running discharge and wind charging.....	75
Figure 6.54 Battery charging and discharging for fifteen minute data with low wind generation in free-running discharge and sustained average load charging .....	76
Figure 6.55 Battery state of charge for fifteen minute data with low wind generation in free-running discharge and sustained average load charging .....	76
Figure 6.56 Normalized overall fifteen minute demand histogram with low wind generation in free-running discharge and sustained average load charging .....	77
Figure 6.57 Battery charging and discharging for fifteen minute data with low wind generation in conservative discharge and wind charging .....	78
Figure 6.58 Battery state of charge for fifteen minute data with low wind generation in conservative discharge and wind charging .....	78
Figure 6.59 Normalized overall fifteen minute demand histogram with low wind generation in conservative discharge and wind charging .....	79
Figure 6.60 Battery charging and discharging for fifteen minute data with medium wind generation in conservative discharge and sustained average load charging .....	79
Figure 6.61 Battery state of charge for fifteen minute data with medium wind generation in conservative discharge and sustained average load charging .....	80
Figure 6.62 Normalized overall fifteen minute demand histogram with medium wind generation in conservative discharge and sustained average load charging .....	80
Figure 6.63 Battery charging and discharging for one second forecasted load data in free-running discharging and wind charging modes.....	82
Figure 6.64 Battery state of charge for one second forecasted load data in free-running discharging and wind charging modes.....	82

Figure 6.65 Overall one second actual load demand after peak reduction for one second forecasted load data in free-running discharging and wind charging modes.....	83
Figure 6.66 Fifteen minute average normalized load demand after peak reduction for one second forecasted load data in free-running discharging and wind charging modes.....	83
Figure 6.67 Battery charging and discharging for one second forecasted load data in free-running discharging and sustained average load charging modes.....	84
Figure 6.68 Battery state of charge for one second forecasted load data in free-running discharging and sustained average load charging modes.....	84
Figure 6.69 Overall one second actual load demand after peak reduction for one second forecasted load data in free-running discharging and sustained average load charging modes .....	85
Figure 6.70 Fifteen minute average normalized load demand after peak reduction for one second forecasted load data in free-running discharging and sustained average load charging modes .....	85
Figure 6.71 Battery charging and discharging for one second forecasted load data in conservative discharging and wind charging modes.....	86
Figure 6.72 Battery state of charge for one second forecasted load data in conservative discharging and wind charging modes.....	86
Figure 6.73 Overall one second actual load demand after peak reduction for one second forecasted load data in conservative discharging and wind charging modes .....	87
Figure 6.74 Fifteen minute average normalized load demand after peak reduction for one second forecasted load data in conservative discharging and wind charging modes .....	87
Figure 6.75 Battery charging and discharging for one second forecasted load data in conservative discharging and sustained average load charging modes.....	88
Figure 6.76 Battery state of charge for one second forecasted load data in conservative discharging and sustained average load charging modes.....	88
Figure 6.77 Overall one second actual load demand after peak reduction for one second forecasted load data in conservative discharging and sustained average load charging modes .....	89

Figure 6.78 Fifteen minute average normalized load demand after peak reduction for one second forecasted load data in conservative discharging and sustained average load charging modes .....	89
Figure 6.79 Battery power charging and discharging under real time operation at full capacity in free-running mode only.....	93
Figure 6.80 Battery state of charge under real time operation at full capacity in free-running mode only.....	94
Figure 6.81 Overall actual one second demand under real time operation at full battery capacity in free-running mode only .....	94
Figure 6.82 Fifteen minute average normalized demand under real time operation at full battery capacity in free-running mode only .....	95
Figure 6.83 Battery power charging and discharging under real time operation at full capacity in free-running mode and conservative discharging .....	96
Figure 6.84 Battery state of charge under real time operation at full capacity in free-running mode and conservative discharge .....	96
Figure 6.85 Overall actual one second demand under real time operation at full battery capacity in free-running mode and conservative discharge .....	97
Figure 6.86 Fifteen minute average normalized demand under real time operation at full battery capacity in free-running mode and conservative discharge .....	97
Figure 6.87 Battery power charging and discharging under real time operation at half capacity in free-running mode and conservative discharging .....	99
Figure 6.88 Battery state of charge under real time operation at half capacity in free-running mode and conservative discharge .....	99
Figure 6.89 Overall actual one second demand under real time operation at half battery capacity in free-running mode and conservative discharge .....	100
Figure 6.90 Fifteen minute average normalized demand under real time operation at half battery capacity in free-running mode and conservative discharge .....	100
Figure 6.91 Battery power charging and discharging under real time operation at half capacity and double pulse operation in free-running mode and conservative discharging.....	102
Figure 6.92 Battery state of charge under real time operation at half capacity and double pulse operation in free-running mode and conservative discharge .....	102

Figure 6.93 Overall actual one second demand under real time operation at half battery capacity and double pulse operation in free-running mode and conservative discharge .....	103
Figure 6.94 Fifteen minute average normalized demand under real time operation at half battery capacity and double pulse operation in free-running mode and conservative discharge.....	103
Figure 6.95 Battery power charging and discharging under real time operation at half capacity and higher initial energy in free-running mode and conservative discharging.....	105
Figure 6.96 Battery state of charge under real time operation at half capacity and higher initial energy in free-running mode and conservative discharge .....	105
Figure 6.97 Overall actual one second demand under real time operation at half battery capacity and higher initial energy in free-running mode and conservative discharge .....	106
Figure 6.98 Fifteen minute average normalized demand under real time operation at half battery capacity and higher initial energy in free-running mode and conservative discharge.....	106
Figure 6.99 Battery power charging and discharging under real time operation at quarter capacity in free-running mode and conservative discharging .....	107
Figure 6.100 Battery state of charge under real time operation at quarter capacity in free-running mode and conservative discharge .....	108
Figure 6.101 Overall actual one second demand under real time operation at quarter battery capacity in free-running mode and conservative discharge .....	108
Figure 6.102 Fifteen minute average normalized demand under real time operation at quarter battery capacity in free-running mode and conservative discharge.....	109

## List of Tables

Table 4.1 50 kW NAS Battery module specifications [14] .....	24
Table 4.2 Computer Specifications .....	25
Table 4.3 Load Model Equations [2] .....	28
Table 6.1 Comparison of feeder losses for different wind generation levels .....	54
Table 6.2 Summary of results obtained for one second load forecasted operation of wind generation with battery storage .....	90
Table 6.3 Battery Specifications for real time test system in free-running mode only at full capacity .....	93
Table 6.4 Battery Specifications for real time test system in free-running mode and conservative discharge at full installed capacity .....	95
Table 6.5 Battery Specifications for real time test system in free-running mode and conservative discharge at half capacity .....	98
Table 6.6 Battery Specifications for real time test system in free-running mode and conservative discharge at half capacity for double pulse operation .....	101
Table 6.7 Battery Specifications for real time test system in free-running mode and conservative discharge at half capacity for higher initial energy .....	104
Table 6.8 Battery Specifications for real time test system in free-running mode and conservative discharge at quarter capacity .....	107
Table 6.9 Summary of results obtained for real time operation of wind generation with storage dispatch using historical PMU information .....	110
Table A.1 Underground Cable Configuration .....	118
Table A.2 Spot Loads .....	118
Table A.3 Transformer data .....	119
Table A.4 Line Segment data .....	119

## **Acknowledgements**

I would like to thank the members of my master's thesis committee Dr. Noel Schulz, Dr. Anil Pahwa and Dr. Shelli Starrett for their valuable contributions, advice, guidance, encouragement, and corrections during the entire study and research of this work.

I would like to thank Dr. Ruth Miller and my friend and colleague Dulan Weerasinghe for their valuable inputs, contributions, and guidance during the study and research of this work. I would like to thank the department of Electrical and Computer Engineering for funding this research work.

## **Dedication**

I would like to dedicate this research work to my parents who have always been there to support and encourage me.



# **Chapter 1 - Introduction**

## **1.1 Introduction and Motivation**

The electric power distribution network is often the most overlooked but also the most complex part of the entire power system. While the measurements currently available from the power system are sufficient to ensure the proper working of the generation and transmission system infrastructure, under contingency issues, the distribution system often bears the brunt of all emergency measures taken to bring the system back to its original stable state. This includes measures such as load shedding leading to branch outages, and more recently, islanding of certain parts of the distribution grid to local distributed generation. For quite a few years now, there has been an increasing interest in the installation of renewable energy generation at the transmission as well as the distribution levels, but these still constitute a very small percentage of all the power generated in North America [28]. Under current NERC regulations [29], all forms of renewable generation are currently required to disconnect from the system under abnormal or emergency conditions. The main reason for this regulation is that most renewable energy resources, such as wind and solar, are non-dispatchable due to uncertainty associated with the respective natural resources of wind and sunlight. This leads to a variable availability in power generated from these sources. The focus of this thesis research is on issues faced when working with interconnected wind energy. When wind energy is considered, the issues encountered relate to dynamic changes associated with system voltages and other parameters that would make the system stability a challenge. The challenges arise also due to lack of sufficiently dynamic measurement information required to assess the state of the system. Under present day conditions, the only measurements available from the distribution system may include aggregated load demand of the distribution feeder as seen by the substation monitoring system.

Utilities have started to realize that observability of the distribution system is important in order to have a clear understanding of load dynamics and to assess the state of the system. So, many utilities across North America have begun installing smart meters in the form of Advanced Metering Infrastructure (AMI) in their distribution grids [30]. But this only gives a detailed picture in terms of load demand but not in terms of the actual state of the system. Also, these measurements are not time stamped in any way. In this research, the utilization of Phasor Measurement Units (PMU) in order to ensure the proper working of distributed wind generation with storage has been investigated. The smart grid initiative was taken to improve the efficiency

and reliability of the overall power system. This research aims to improve efficiency by working at the lowest level of the power system hierarchy. In a smart grid environment, some of the available aspects are renewable energy and advanced measurement infrastructure giving enormous amounts of data. This research aims to make use both of these aspects of the smart grid at the distribution level. The emphasis is on the use of dynamic measurements in order to control the amount and instance of consumption of wind energy or storage. Distributed storage aids this process by working to use stored power from wind energy when it is most required. Even a slight reduction in an individual feeder's load at a given instance of time due to wind and storage can result in aggregated savings of many megawatts of power for the upper generation and transmission system levels, resulting in benefits such as reducing overloads of transmission lines, reduction of required spinning reserve and installed capacity, and improvements in the life expectancy of various equipment including the delaying of buying new equipment.

The penetration of wind energy in the U.S. in the distribution system has been increasing steadily over the last few years partly because of the smart grid initiative. Established practices in the distribution system consist of directly connecting the wind turbines to the distribution grid so that they are always online. But this approach may not yield satisfactory results when the wind generation profile and the load profile in a given distribution feeder are negatively correlated. This research aims to solve this problem with the addition of distributed storage. The batteries directly store the wind energy by taking the turbines offline when the load is below a certain predetermined level. When the load is above this level, the wind turbine energy is directly supplied in order to satisfy load requirements, but the battery is also discharged in order to minimize the part of the load that needs to be satisfied by the bulk power from the source node at the substation. This effectively results in the system trying to keep the substation monitored load as close to a predetermined value as possible. The peak load of the feeder reduces, resulting in various benefits as described earlier when this solution is implemented for multiple feeders.

The other aim of this research is to demonstrate that the usage of dynamic measurements recorded by PMUs will help to reduce the capacity of the storage system required for a certain penetration of wind energy. This is an important problem to investigate as storage is one of the most expensive technologies to implement in a distribution system. The fact remains that presently, PMUs are also expensive to implement, but the benefits that PMUs provide to any part of the power system can outweigh economic costs as the use of the technology becomes more widespread.

## 1.2 Summary of Results

The change in the profile of the substation monitored feeder load due to direct connection of the wind farm to the distribution feeder is presented initially. We consider the initial wind generation penetration as 30% of the peak feeder load. This number can be increased in future studies. The initial capacity of distributed storage is considered as equal to the installed wind generation capacity. The improvements in the load profile of the distribution feeder are presented for co-ordination between wind generation and distributed storage. The analysis is done for 15-minute forecasted load and wind generation data for a 24 hour period initially and then later for a one second basis load and wind generation profile. Four different combinations of charging and discharging methods of the batteries are investigated in this research. They are given below and will be explained in more detail in the thesis

- i. Wind charging and Free-run discharging
- ii. Wind charging and Conservative discharging
- iii. Sustained average load charging and Free-run discharging
- iv. Sustained average load charging and Conservative discharging

All the four combinations described above are investigated and the results presented for both 15-minute basis data as well one-second basis data. The use of wind energy and storage in a distribution system with three-phase unbalanced backward and forward sweep power flow algorithm has been undocumented so far in literature and has been newly implemented in this research. Additionally, conservative discharging of the battery based on instantaneous stored energy level or state of charge, wind generation availability and load requirement is an approach that has been newly investigated in this research. Two methods have been implemented to do this process, one without the direct use PMU measurements and one with the use of direct historic PMU measurements. In all cases, the results presented pertain to the following.

- Load profile of the distribution feeder as seen by the substation monitoring system
- Voltage profile of the node where the wind farm and the storage have been installed
- Charging and discharging of the battery for each time instant
- Energy level curve of the battery based on charging and discharging
- Line losses of the distribution feeder due to installation of the wind farm and battery storage.

All of these results give a detailed picture of the dynamics of load, wind generation and storage, and also provide the results required in order to reduce required battery capacity as dynamic measurements become more available.

### **1.3 Outline**

The first chapter provides an introduction into the problem that the research will try to address and also an explanation of the results that are obtained. Chapter 2 will explain some background about various concepts and methods used in this research and also present literature review about various methods and solutions that have been implemented before in order to solve the problem addressed here. There will also be an explanation of new contributions including techniques and methods developed. Chapter 3 will explain in greater detail the objectives of this research, and the approach and steps in the process of achieving this objective. Chapter 4 will present the creation of test cases and the data that was used in the analysis part of the research. Chapter 5 will explain the tools, such as algorithms for backward forward sweep power flow and battery charging and discharging. Chapter 6 will discuss in detail the results that were obtained in the analysis and research and give the explanation of these results. Chapter 7 will provide conclusions and suggest possibilities for future work.

## **Chapter 2 - Background and Literature Review**

### **2.1 Background**

This section will explain some background about various concepts and methods used in this research. Some fundamentals about various components of this research such as distribution systems, wind generation and storage techniques and parameters, and PMUs, have been explained.

#### **2.1.1 Distribution System Structure**

In North America, distribution systems are usually constructed in a radial structure as they are very easy to implement and also are the least expensive and easy to operate and maintain [26]. The other important attribute of the North American distribution systems is that the three phase loads are predominantly unbalanced. So, a single phase equivalent analysis using methods such as the Newton Raphson power flow algorithm would yield inaccurate or unsatisfactory results. So, in distribution system analysis of unbalanced radial feeders, backward forward sweep power flow algorithm is often used [31]. This method follows a three phase equivalent programming structure for voltage, current and impedance and is based on the iterative solution of the basic ladder network from circuit theory. It also considers factors such as mutual impedance between phase conductors. A detailed explanation of this algorithm will be given in chapter 4.

#### **2.1.2 Distribution System Load Profile**

In a typical distribution system, the loads vary according to the time of day, day of the week, weather, and season. The load profiles are different for different nature of loads. The profile or shape of the load curve varies based on the type of load and they are classified into the following types:

i. Residential load

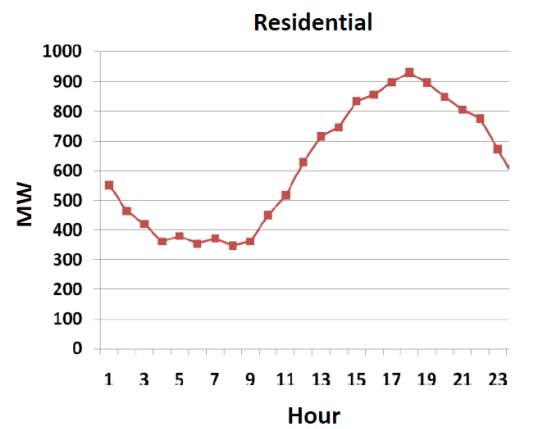


**Figure 2.1 Aggregated Residential load curve [26]**

ii. Commercial load

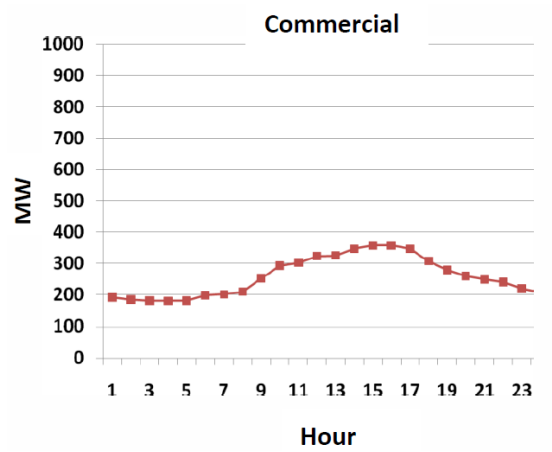


**Figure 2.2 Aggregated Commercial load curve [26]**

iii. Industrial load

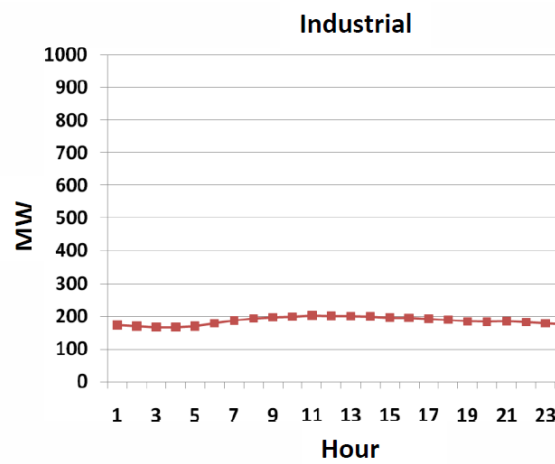


**Figure 2.3 Aggregated Industrial load curve [26]**

As it can be seen from the figures given above, the residential load is the maximum contributing factor to the dynamics of the distribution feeder load curve. So, the 15-minute average normalized load profile of a group of houses has been used in order to create the test cases for this research. A detailed explanation will be provided in chapter 4.

### **2.1.3 Wind Energy Generation**

Wind energy generation is usually modeled using a Rayleigh or Weibull probability distribution [9]. But in order to clearly observe the effects of different levels of wind generation on the storage system of the distribution feeder, actual data from a wind turbine has been used in this research. Data was recorded for a low wind day, medium wind day, and high wind day on a 15-minute basis for a 24 hour period. There is also a one-second basis wind data file for a 24 hour period [27]. For a wind turbine, the reactive power generated is not a function of rotor dynamics and is produced by the converter that helps connect the wind turbine to the power system. This converter's reactive power output can be controlled between set minimum and maximum values independent of wind power generation. So, for the study of behavior of distributed storage, reactive power generation at constant power factor is considered, i.e., it is always a given fraction of the real power generation. Also, due to this assumption, in the power flow study, wind generation node is considered as negative load node instead of voltage controlled node. If the wind node were to be considered as a voltage controlled node, the reactive power generation of the turbine would have to be a variable for every time instant, as the objective of reactive power generated would be to maintain the positive sequence voltage of the node as close to the nominal value as possible [2].

### **2.1.4 Distributed Storage**

In order to operate a battery as distributed storage, the specifications required are rated power, energy capacity, charging and discharging efficiency, and time delay. The rated power limits the charging and discharging rate of the battery. The energy capacity is a measure of the state of charge and determines the efficient operation of battery for the given load requirement. The efficiency of the battery determines the fraction of wind power that actually charges the battery and the losses through the power converter when the battery is online or connected to wind farm. The time delay is of importance in this study as PMU measurements are involved. PMUs can sample data at 30 samples per second, but the delay of the battery is a few

milliseconds to one second [21]. So, the apparent average of 30 measurements from one PMU has been simulated in this study and used in the analysis as one second measurements.

### 2.1.5 Phasor Measurement Units

Phasor measurement units measure the voltage and phase angle of a node using a time-synchronized GPS (Global Positioning System) signal.

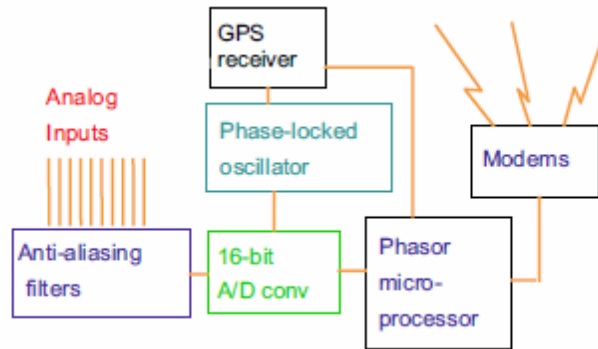


**Figure 2.4 Functional block diagram of PMU [6]**

The device uses digital signal processors and measures voltage signals at 30 samples per second [12]. This is a huge improvement over earlier systems such as SCADA (Supervisory Control and Data Acquisition) which used to provide a measurement every four seconds. So, a very clear and informative picture about the state of the system can be obtained because direct information about the system state is available. In earlier methods, phase angle would have to be estimated using iterative methods. The values of voltage and phase angle can now be directly plugged into power flow programs as they are readily available. Thus, power flow solutions are greatly accelerated. Instantaneous dynamic information about load and wind generation can be extracted by processing these measurements, which also aids in the progress of this research.

## 2.2 Literature Review

Some of the major elements of power systems handled in this research work are distribution systems and their unbalanced power flow, wind generation, battery storage technologies, and Phasor Measurement Units (PMU). The work done relies heavily on the usage of the unbalanced backward forward sweep power flow method which was first introduced in [1]. The abilities of the algorithm to handle different types of distributed resources was investigated in [2] and [17] using actual system information from a Shipboard Power System



(SPS). Although the abilities of backward forward sweep power flow to handle distributed generation as both PQ as well as PV have been demonstrated, the negative PQ load version has been used in this research taking into account the wind generation dynamics that have been used here. The IEEE 37 node test feeder has been selected as the case for study in this research work. The information regarding IEEE test feeders is available on the website of the IEEE Power and Energy Society [32]. A clear understanding of the data required for analysis of these feeders can be obtained in [3]. Wind generation and its interconnection with the distribution systems provide some exciting challenges. The impact of different kinds of wind generators and increasing penetration into a distribution system has been discussed in [8]. A detailed probabilistic analysis of changes in voltage profile of a distribution system with increasing wind generation penetration has been done in [7]. The optimal allocation of wind generation at multiple locations in a distribution system based on probabilistic approaches applied to the loss minimization function has been discussed in [9]. However, for the scope of this research which deals with a case study of a small distribution feeder, we consider the centralized location of all the wind generation and storage at a single weakest node in the system. This node has the lowest voltage profile among all the nodes in the system when a base case of power flow is run on it. In distribution systems, the load modeling used to handle various types of loads plays a major role as they affect the system voltage dynamics. This has been investigated in [11] and the various load models have already been incorporated into the backward forward sweep power flow. The relationship between wind generation penetration levels and the effect that they have on distribution system have been discussed in [13]. With the right amount of penetration of wind generation, it has been shown that incorporating wind generation into the distribution system can have beneficial effects.

The Phasor Measurement Units have many benefits for the distribution system as a clear view of system dynamics can be obtained using this technology. Phadke and Thorp first pioneered this technology and the benefits of usage of PMU have been discussed in [6]. The placement of PMUs for maximum observability in a distribution system has been discussed in [4], but the utility standard is to place PMUs at the point of interconnection of wind farms to the system in order to clearly observe wind farm dynamics. Since the test system used in this research work is a small distribution system, we consider a centralized wind farm location and so we have PMUs installed there. We also have a PMU installed at a node closest to the source node in order to have a clear picture about dynamic bulk amounts of power delivered to the

distribution system even in the presence of support from energy storage. A stochastic analysis of PMU placement for maximum observability has also been done in [5] along with consideration to state estimation functions. The overall benefits that can be obtained by the usage of PMUs in power distribution networks have been discussed in detail in [12]. A major interest in present day power systems, namely the usage of PMUs in a distribution system for interconnection of islanded systems has been discussed in detail in [10]. This is one of the reasons that PMU could become beneficial in future installations when high penetration of renewable energy is expected.

The utility standard NAS battery has been considered as the energy storage system in this research. The NAS (Sodium Sulfur) battery has been used widely across the world in utility operations. The basic specifications and properties of NAS battery have been explained in [14]. The effective utilization of a NAS battery at a large installation in a university in Japan has been demonstrated in [15], proving the operational efficiency and advantages of the NAS battery. The methods used in the basic charging and discharging operations of NAS battery, on which the methods used in this research are loosely based, have been discussed in [22]. A comparison of different storage technologies suitable for storage of wind power has been discussed in [20], and the NAS battery has more benefits among other battery technologies. The benefits of using storage technologies in order to support wind generation operations has been discussed in [16] and [23]. The potential for battery technologies for combined usage with wind generation, including the special benefits of using the NAS battery have been discussed in [19]. The actual simulation of NAS battery with wind generation based on forecasted load operation has been discussed for a balanced system in [18], and the unbalanced mode of operation of NAS battery with wind generation in order to achieve the same functions discussed in this research work have been based on this work. The operation of a wind farm with the specific case of an NAS battery has been investigated in [21]. The applications of combining wind power generation with energy storage in a smart grid environment have been discussed in [24]. The actual simulation of a wind farm with battery storage has been done in detail in [25].

As it can be seen, all of the individual components of the processes being analyzed in this research work have been discussed in literature, but investigations of the combination of these technologies for effective control of the problem addressed here have been undocumented. The usage of PMUs in order to integrate wind energy and storage into the distribution system has been undocumented. Also, there is no published literature on the combined operation of wind

generation and storage instantaneously in order to achieve load reduction and dispatch of distributed renewable resources. All of these issues have been investigated in this research.

## **Chapter 3 - Research Objectives and Proposed Solution**

This section will explain the problem that this research tries to address and the steps that are proposed to solve this problem.

### **3.1 Research Objectives**

Typically, in a distribution system, the wind turbines are directly connected to the distribution feeder and always stay interconnected except in case of contingencies, during which they are required to disconnect from the main system. There is no correlation between distribution feeder load and wind generation profiles. With increasing penetration of wind energy into the distribution grid, there are worst cases of load to wind profile relationship where there is negative correlation. If the load profile is close to base load and there is high wind generation, the part of the load to be supported by the conventional generation from source node may become alarmingly low, and if there is heavy loading while there is very little wind generation, there is maximum possible need for the generation from the centralized energy source node to satisfy. This problem has been addressed in this research. The approach of using storage to help balance this situation requires results to reduce the size of the battery in order to support wind energy storage and peak power reduction effectively. The criteria that are used to charge and discharge the battery play a major role in the capacity utilization of the storage system. This research also provides insight into strategies used to utilize the energy storage system effectively. The availability of dynamic load information also decides the capacity utilization of the battery. This has also been tested using instantaneous measurement information from PMUs.

### **3.2 Proposed Solutions**

The solution to the problem explained above is studied by using the forecasted load data for a given distribution feeder. The assumption is 30% wind generation penetration in the system. This amount of wind generation penetration has been assumed so as to be significant enough to suit modern day smart grid standards, but also to not dominate the energy consumed from the centralized energy source node. The initial assumption is to start with a battery capacity equal to the installed wind generation. The strategy uses the average load of the feeder as the deciding criterion for charging or discharging the battery. Two different charging schemes have been studied.

- i. In one approach, when the value of feeder load at any given instant is below the average load, the wind energy generation for that instant of time is used completely to charge up the battery. The load is satisfied completely using the conventional generation only.

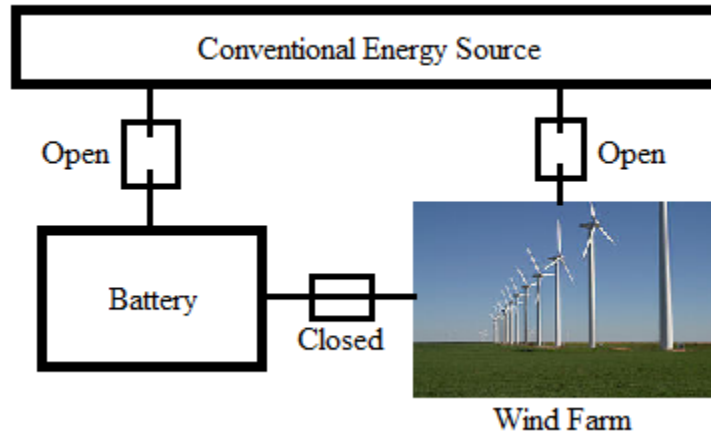


**Figure 3.1 Wind charging only**

- ii. In the other approach, as long as the load is below the average value, the wind energy is fully used to charge up the battery, but the difference between the average load and the instantaneous load value is also extracted from conventional generation to charge the battery such that the feeder load is always at the average value. This method could be suitable for low wind generation days in particular, but assumes a more advanced charge controller that can determine the instances when battery charging using conventional generation is necessary.

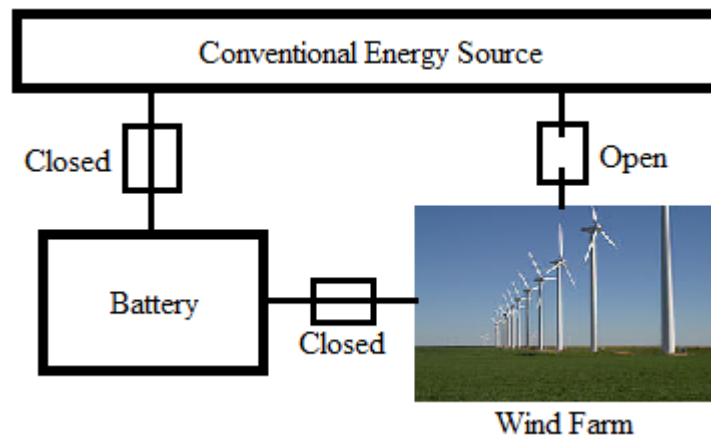


**Figure 3.2 Sustained average load charging**

In both of these charging methods, the battery can only be charged up to its maximum energy capacity, and if battery has been completely charged up, the wind energy is directly supplied to the system to satisfy the load irrespective of whether load at that instant is above or below the average value.

Similarly, the discharging of the battery can be done in two ways, the Free-running discharge method, or the Conservative discharging method.

- i. In the Free-running method, during the discharging of the battery under instantaneous load being higher than average, the wind energy is directly provided to the feeder to satisfy load requirements, and the battery is discharged such that the substation monitored feeder load is as close to the average value as possible. This ensures peak reduction when battery capacity is available for discharge, but under low wind conditions, the risk of the battery being in idle state for longer periods of time than preferred is possible. This may result in unsatisfactory peak reduction when there is low wind generation and the battery capacity has hit minimum.

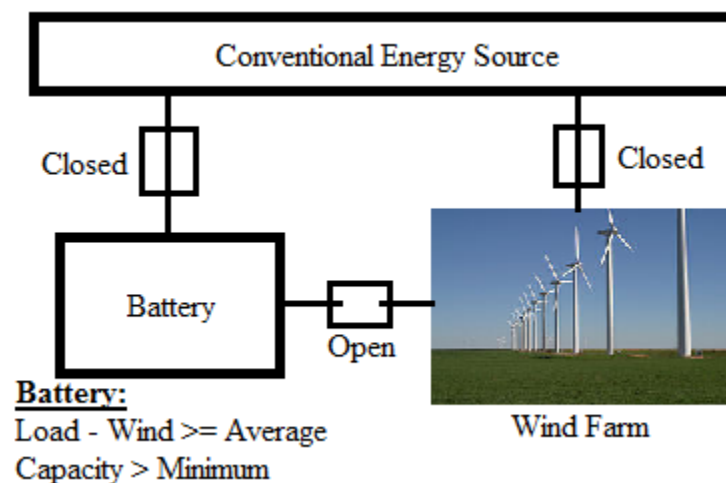


**Figure 3.3 Free running discharge**

- ii. The problem that arises from the above method can be solved using the Conservative discharging method. The amount of discharge for a given feeder load instance beyond the wind generation is determined considering the average load requirement starting from that time instant up to the final time instant, the energy capacity left in the battery for that instant of time, and the maximum possible power rating of the battery. This ensures that

there is at least a minimum possible reduction in the peak load of the feeder, and also ensures that the battery capacity is fully utilized, irrespective of size of the battery.

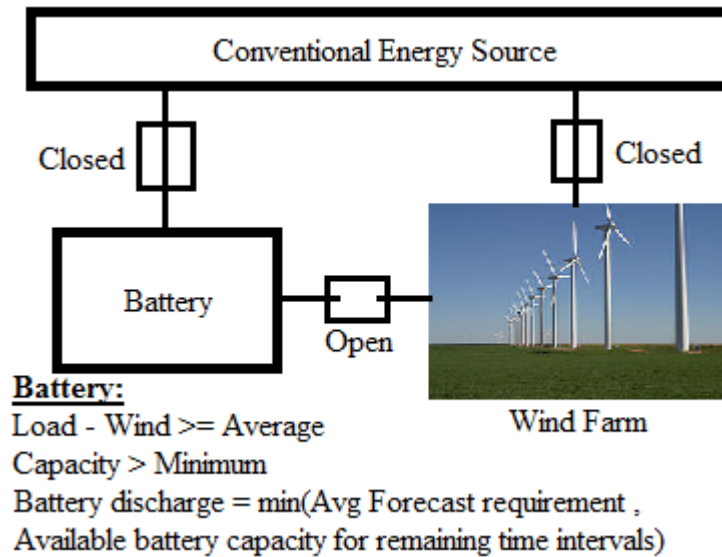


**Figure 3.4 Conservative Discharging**

In both of these discharging methods, the battery can only be discharged up to the minimum level fixed, and if the battery has hit the minimum level, the wind generation is connected directly to the feeder if the load is above the average value.

The charging and discharging techniques discussed above are implemented for the 15-minute average forecasted 24 hour load profile of the IEEE 37-node test feeder initially while considering low wind, medium wind and high wind generation data taken from a real Northwind 100 kW wind turbine [27]. The data is multiplied by a factor of 8 in order to account for 30% wind generation penetration given that the capacity of the feeder under test is 2500 kVA. So, the installed wind generation capacity is 800 kW. The reactive power is generated by the converter under constant power factor, i.e., the reactive power is always a constant fraction of the real power of the wind turbine. Here, 45 kVAR of reactive power for 100 kW of real power is considered as per the specifications of the wind turbine. This gives a power factor of 0.912 uniformly used throughout this research. The peak reduction performance of the feeder, voltage profile, battery power charging and discharging values, and energy capacity utilization of the battery are investigated for all the cases.

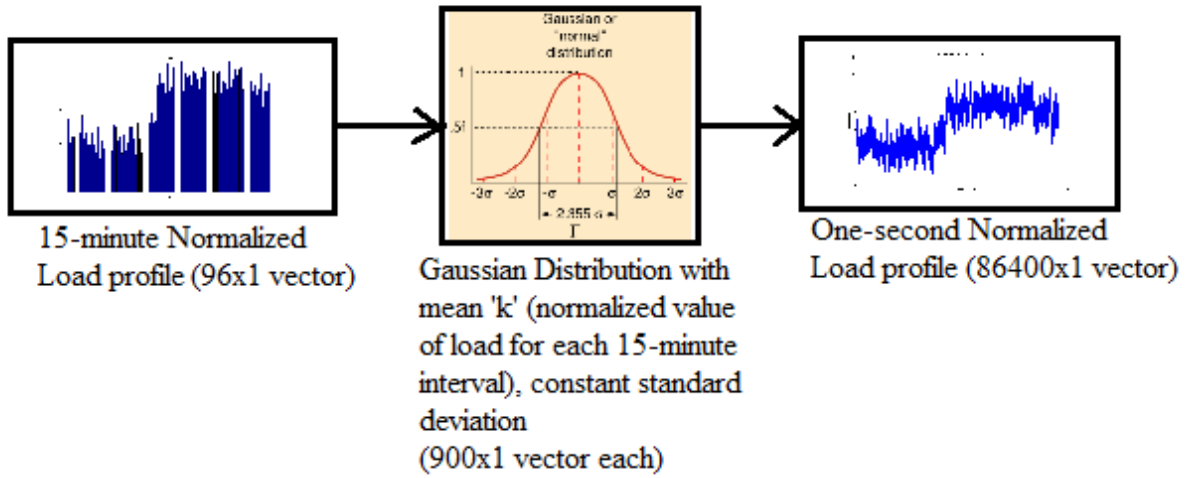


**Figure 3.5 Conversion of 15-minute load profile into One-second load profile**

The one-second data is created for the feeder by using the 15-minute data and using a Gaussian distribution to create one second load fractions for every 15-minute period. The mean of the Gaussian distribution for a given 15-minute period is the value of the 15-minute average load fraction for that period. The value of standard deviation is chosen such that the values of load fraction are always positive. For this, the minimum value of the 15-minute load fractions is selected and this is divided by a factor of 3. The resulting value is the maximum value of standard deviation that can be used. The decided value is usually a little lesser than this maximum value in order to have all of the probabilistic values positive. The calculation described is based on the fact that most of the values fall within the six-sigma interval of the Gaussian distribution. Using the one second data, it is possible to demonstrate that as instantaneous values are available due to use of PMUs, the battery capacity initially assumed is never used completely as many instances of intermittent charging and discharging of the battery are observed as we have more measurements within a given time period.

The final part of the research is an attempt to predict the required dispatch from the battery using previous time instances' recorded load information from PMUs for real time operation as opposed to earlier attempts which use forecasted load information. It is possible to set different values for the window of time for which historical load information obtained by processing PMU measurements can be calculated. For the sake of uniformity, the time window used in the study described in this research has been set at five minutes. The maximum value of load above the average value for a period of five minutes prior to a current time instant is



calculated using PMU measurements. From this value, the wind generation of the current time instant is subtracted in order to yield the battery discharge value for the current time instant. So, the need for forecasted load information is completely eliminated.

## Chapter 4 - Test Cases, Data and Tools

### 4.1 Test Cases and Data

This section will explain about the test cases that were used to analyze the problem including the creation of the normalized distribution system load profile, IEEE distribution system test feeders and their specifications, standard NAS (Sodium Sulfide) battery specifications and so on.

#### 4.1.1 Average Normalized Load Profile for a group of houses

The 15-minute averaged load data for a day for each house in a group of houses present in a real distribution feeder is available in a test case file [26]. A Matlab program is used to extract this information for each house in the feeder. The load information is extracted for each house from a group of ten selected houses that have legitimate realistic load information and then aggregated. The final aggregated 15-minute averaged demand histogram for a group of ten houses is given below.

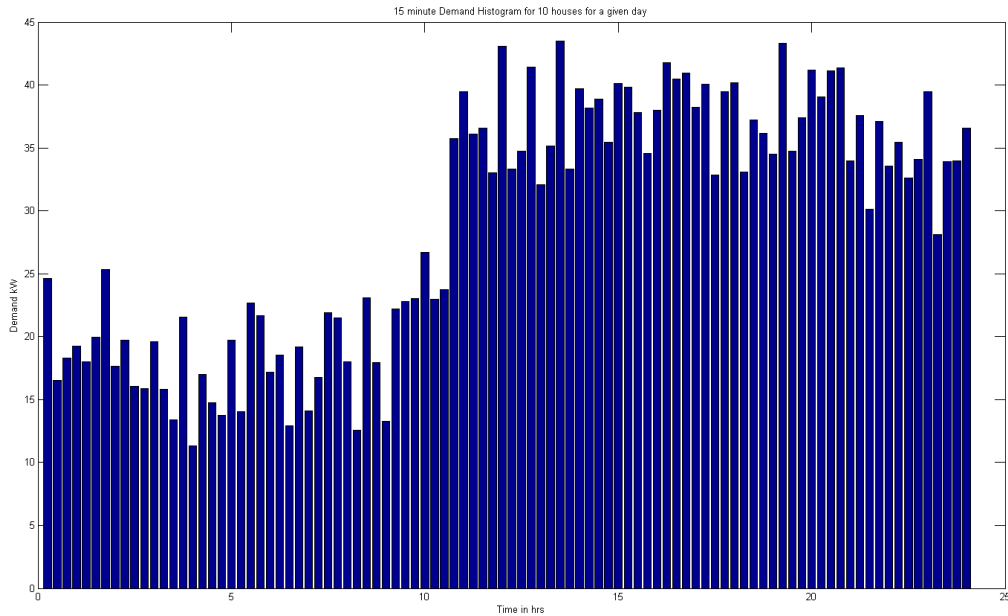


**Figure 4.1 Aggregated 15-minute demand histogram for ten houses for a day [26]**

But for a distribution feeder, beyond a certain value of load, the coincidence factor becomes a constant value as shown in the figure below.

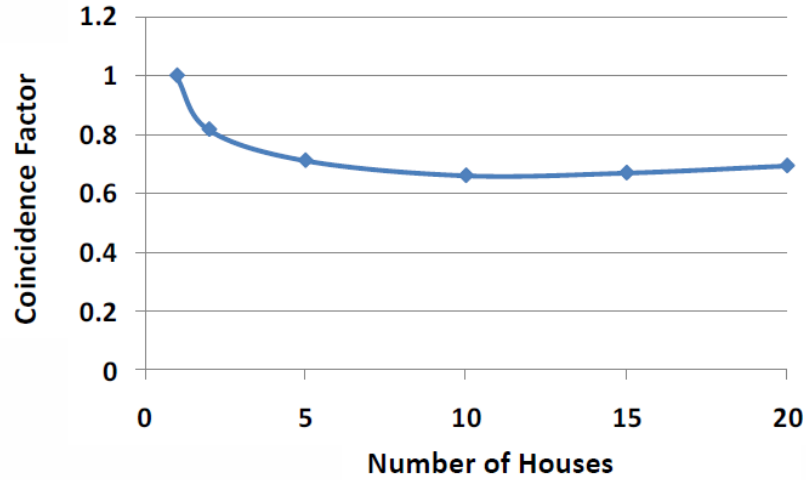


**Figure 4.2 Coincidence factor as a function of number of houses [26]**

So, it is possible to normalize the load profile of the group of houses shown before to a factor of one or 100% and use it for any distribution feeder as a whole as the demand follows a similar profile on a given day for all feeders. After normalization, the 15-minute averaged and normalized demand histogram for a distribution feeder may be obtained as given below.

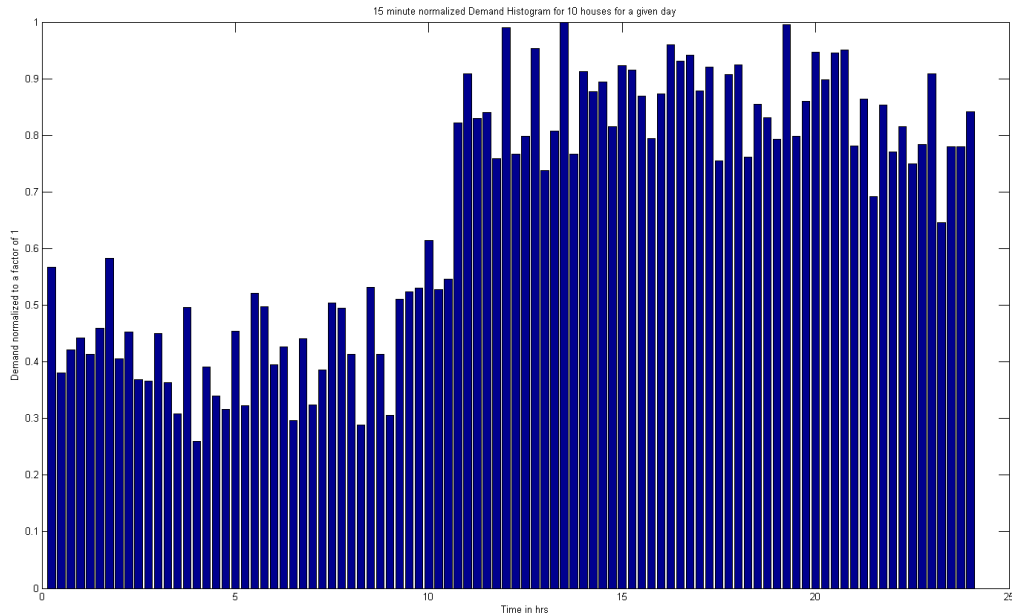


**Figure 4.3 15-minute average normalized demand histogram for a day**

When the one second calculation of dispatch operations of storage is considered, the 15-minute normalized load profile is converted into an equivalent one second load curve by using the normalized demand factor for each fifteen minute interval as the mean of the Gaussian

distribution and using a value of constant standard deviation in such a way that the demand factor does not become a negative value. For the above fifteen minute normalized demand histogram, the lowest value of recorded load factor was 0.2598. In a Gaussian distribution, 97% of the values tend to fall between the six-sigma interval  $[-3\sigma \ 3\sigma]$ . So, an ideal value for the standard deviation can be calculated as follows

$$\text{Standard Deviation } \sigma < 0.2598/3 = 0.866$$

On repeatedly plugging in values of  $\sigma$  less than this value and then reducing to get the load factor to always be greater than 1, the value of  $\sigma$  is fixed to be 0.065 for this test case. The one second normalized load curve that was obtained is given below.

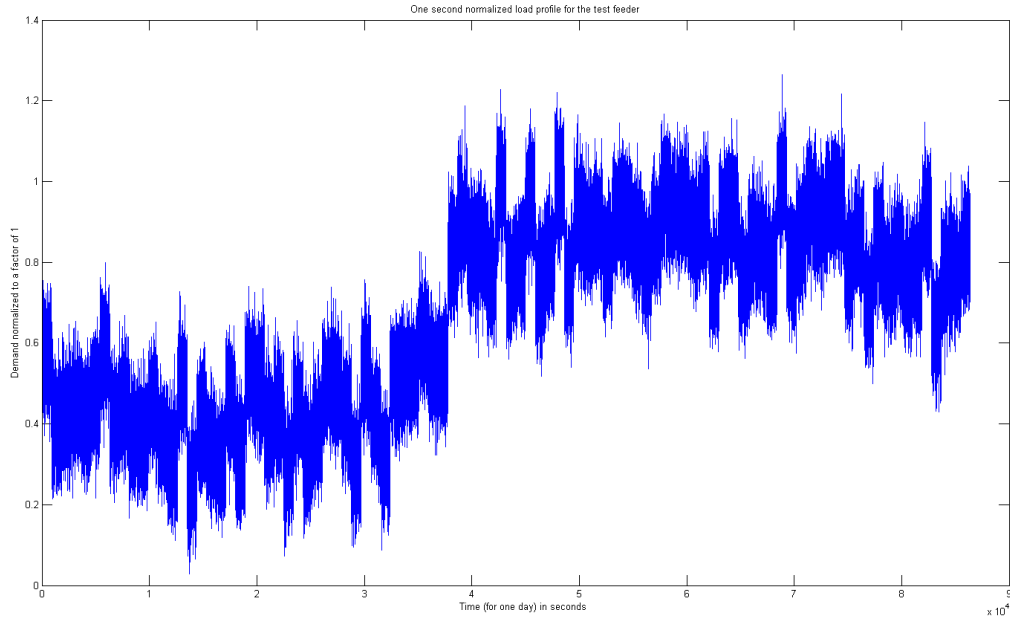


**Figure 4.4 One-second normalized demand curve for a day**

It is observed that load factor exceeds one in some intervals for this curve, but this is realistic as this load dynamic is not captured in a typical distribution feeder when fifteen minute average load is calculated.

#### **4.1.2 IEEE 37 node test feeder**

The IEEE 37 node test feeder is selected as a standard case in order to study the dispatch operation of battery storage with distributed wind generation. It is an actual test feeder in use in

Australia. It is completely underground and has been selected for this research as it is the simplest to analyze because of the following reasons:

- i. The limited number of nodes makes it easy to renumber the nodes for backward forward sweep power flow analysis
- ii. It is completely composed only of Delta configuration lines and transformers, making the study easier.
- iii. It has no additional circuit components such as capacitors, switches and uniformly distributed loads, and it also has only four types of line configurations, making the analysis very simple and straightforward.

The information for the feeder is given in appendix A. The figure 4.5 shows the feeder. It may be noted that regulator information for the feeder is also available, but has not been used in this analysis as there is a need to clearly observe the effects of distributed wind generation and storage on the voltage profile of certain nodes in the feeder. The regulator would tend to improve the voltage profile and prevent the observation of actual effects.

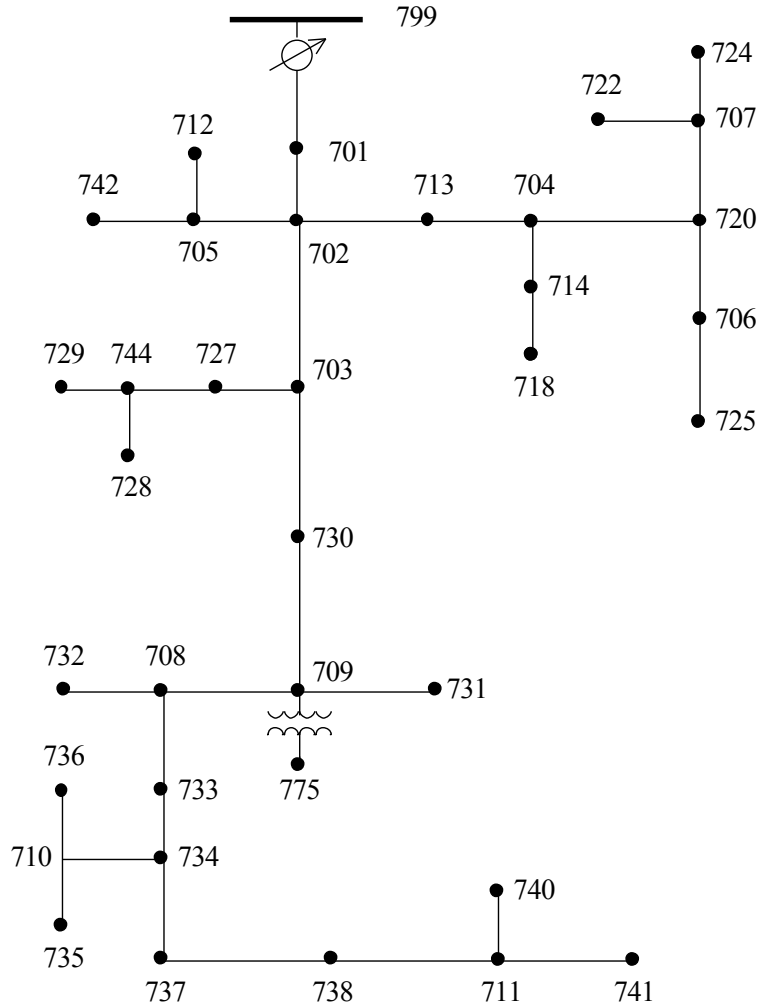


**Figure 4.5 IEEE 37 node test feeder**

The spot load data given with the test feeder specifications is considered as the 15-minute peak load corresponding to a load factor of 1. All the other cases are considered as the load fractions of this peak load. For the purpose of analysis, this puts forward the assumption that all the loads present in the feeder have the same load factor at any given instant.

### 4.1.3 Distributed Wind Generation

The real power generation data of an actual wind turbine manufactured by Northwind has been used in this research. This is a wind turbine present in Riley County, Kansas and the data is available online publicly for research purposes [27]. The real power rating of the turbine is 100 kW although the generation can go up to 120 kW when wind is abundant. The reactive power of

the turbine is independent of wind dynamics and is generated by the converter used to connect the turbine online. The converter can produce any value between  $\pm 45$  kVAR based on user settings. In order to simplify the analysis, generation at constant power factor is considered. A value of +45 kVAR of reactive power generation for 100 kW of wind generation is considered. So, this constant fraction of active power is maintained throughout the operation of the wind turbine. For this analysis, a wind power penetration of 30% of feeder peak load has been considered. Given that the peak load of the feeder is about 2500 kVA, 800 kW of installed wind generation capacity is assumed by multiplying the generation of one wind turbine by a factor of eight. Although the combined wind power generation of eight wind turbines in reality would be a lot smoother function of time, the criticality of this case would prove as a test of the abilities of the control strategies being tested in this research. This wind generation information for one day on a fifteen minute averaged basis is obtained for three different wind scenarios: low wind, medium wind and high wind. This is because, fifteen minute analysis is less time consuming and so, it is possible to observe the effect of wind generation on the operation of battery very easily. The information obtained has been attached in appendix B.

In order to perform the one second analysis for the test system, one single case of wind generation data from the Northwind turbine on a one second basis has been taken. This is because; the wind generation information for a day on a one second basis is memory intensive and requires about 6 to 7 megabytes of space for an Excel file, containing 86400 rows and 6 columns. This information cannot be attached to this thesis as the file could consume a large amount of space exceeding the allowed length of this document.

#### **4.1.4 Standard NAS (Sodium Sulfide) battery specifications**

The battery used to investigate dispatch operations of wind generation in this research is the utility standard NAS battery [14]. This is a tried and tested battery popularly used in utility load support operations and more recently, islanding. It is widely used in Japan and has some very useful advantages making it an attractive option for large scale battery energy storage system operations [15]. The battery has almost no self-discharge characteristics. It operates at a very high temperature of 285-300 °C, and the resistance goes down with the increase in temperature. It has a high efficiency of more than 81% which is greater than most other battery technologies (Table 4.1). It also has a very long life-cycle of about 15 years. The specifications of the NAS battery for one unit have been given below.

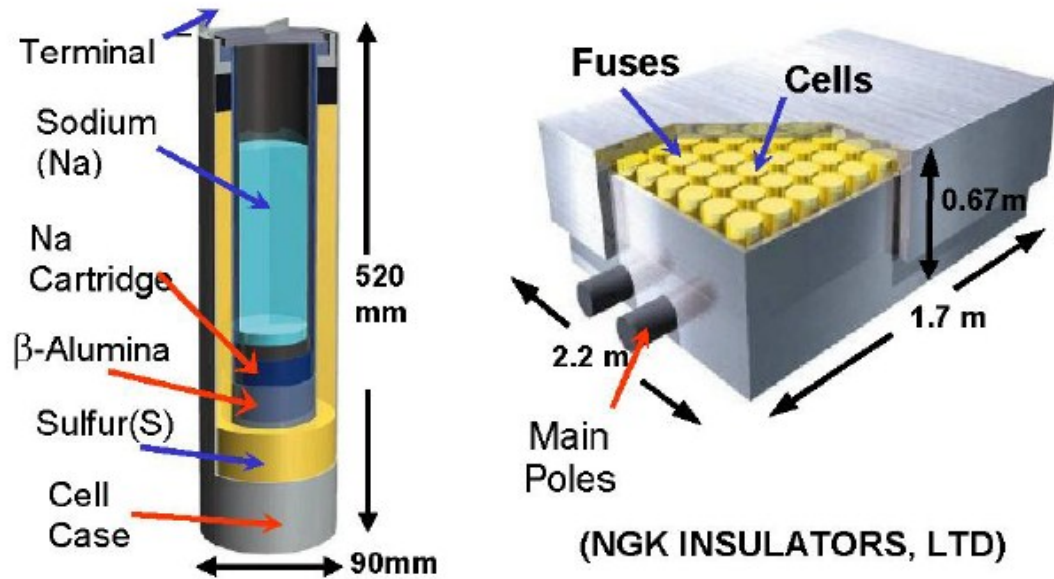


Figure 4.6 NAS Battery Cell module and Cell structure [15]

<b>Output</b>	52.1 kW
<b>Voltage</b>	58V / 116V
<b>Current</b>	726A / 363A
<b>Capacity</b>	375 kWh
<b>Efficiency</b>	~ 83%
<b>Weight</b>	3.5 ton
<b>Energy Density</b>	160 kWh/cu-m
<b>Number of Cells</b>	320

Table 4.1 50 kW NAS Battery module specifications [14]

Although the specified output rating is 52.1 kW, in actual practice, 50 kW is the observed output power. Initially, the installed battery capacity for the test studies is assumed to be equal to the installed wind generation capacity of 800 kW. So, the initial value of total installed battery capacity is also 800 kW. Sixteen units of the specified battery module are assumed, making the energy capacity 6000 kWh which is considered the measure of the state of charge of the battery. Initially a realistic value of battery efficiency of 81% is assumed which is close to the actual value, so that the charging and discharging efficiencies are 90% each, respectively. In order to



ensure effective operation, the limits of the battery are set such that the battery can only be discharged up to a minimum charge of 20% of maximum value. Beyond this state, the battery is switched off. Also, if the battery is charged up to the maximum value, it is switched off in case the load is low and charging operations are still possible.

## 4.2 Tools

All of the simulations required for this research are carried out using a standard Dell Desktop Personal Computer with the following specifications

<b>Processor</b>	Intel® Core™2 Duo @ 3.00 GHz
<b>Installed Memory</b>	4.00 GB (3.50 GB usable)
<b>System Type</b>	32 Bit
<b>Operating System</b>	Microsoft Windows 7 Enterprise Service Pack 1

**Table 4.2 Computer Specifications**

The software tool used to create the code and run the simulations is Matlab R2011b. Matlab is uniquely suited to analyze the problems described in this research as it is effective at handling matrices and some of the major components of this research including Backward forward sweep power flow and battery storage utilization require large amounts of calculation and logic intensive matrix analysis.

### 4.2.1 Backward Forward Sweep Power Flow Algorithm

The backward forward sweep power flow algorithm is the best method to analyze unbalanced radial distribution systems as it is a detailed three phase analysis method that takes into consideration even factors such as mutual impedance between phase conductors. It is based on the iterative solution of the simple ladder network from circuit theory and provides a high level of accuracy in the power flow solution. It is essential in this research as it is a constant part of all the analysis approaches used in the solution to the problems addressed here. It also

provides the PMU measurements that will be used in the final stages of this research. In actual practice, PMU measurements would be measured in the field and then plugged into the power flow solution. But here, as the historical PMU measurements of previous time instants are primarily utilized to dispatch the battery, the voltage measurements of certain nodes solved by using the power flow problem are recorded as PMU measurements.

#### 4.2.1.1 Node Renumbering

In the backward forward sweep power flow analysis, the speed of the solution can be greatly enhanced by using proper node renumbering as the number of laterals branching off from the main feeder determines the number of equations and unknowns in this algorithm. So, a breadth first order is followed in the renumbering of the nodes. Whenever a lateral branches off from a given feeder, the lateral is numbered first before returning to the main feeder. An illustrative example is given below.

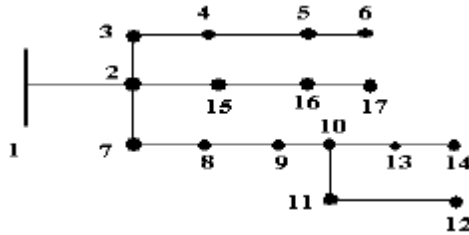


**Figure 4.7 Node Renumbering [2]**

In this way, the IEEE 37 node test feeder is renumbered for analysis in this research and the renumbered feeder has been given below in figure 4.8.

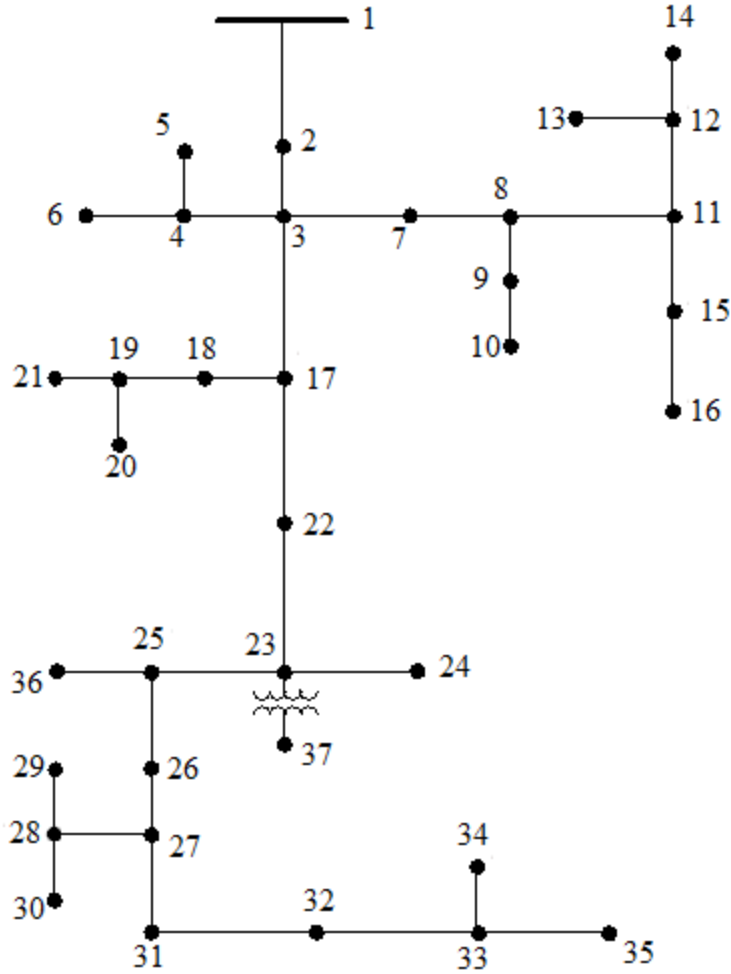


**Figure 4.8 Renumbered IEEE 37 node Test Feeder**

#### 4.2.1.2 Method

The backward forward sweep power flow algorithm has been explained in great detail in [2], but some of its features used in this research have been described in this section. In the backward forward sweep power flow analysis, the first step involves the calculation of voltages and currents of the feeder starting from the terminal nodes and progressing towards the source node. This is called as the forward sweep. In the first iteration, the terminal voltages are assumed to be at the three phase nominal voltage of the given feeder. Then, the currents and voltages of each node and the line currents between nodes are progressively calculated using the following equations.

$$V_i = V_{i+1} + ZI_{i+1} \quad (4.1)$$

$$I_i = I_{i+1} \quad (4.2)$$

Where  $I_{i+1}$  is the line current from the given node  $i$  to the succeeding node  $i+1$ . The line current calculations are performed by the summation of node currents and line currents of succeeding nodes. The node currents are calculated based on the type of load as given below

- i. Constant Power loads: The real and reactive power injections are kept constant. These are similar to the traditional PQ loads in single phase equivalent power flow problems.
- ii. Constant Impedance loads: Using the given real and reactive power values, the node impedance at nominal voltage is calculated and kept constant for all the iterations. The node current is calculated from this impedance value and the node voltage for that iteration.
- iii. Constant Current loads: The magnitude of node current at nominal voltage is calculated from the given real and reactive power values and kept constant. The phase angle value is calculated for each iteration and attached to this current magnitude value.

The node current calculation equations for various load models are given in the table below.

Load Type	Wye	Delta
Constant PQ	$IL_i^{ph} = \left( \frac{S_i^{ph-n}}{V_i^{ph-n}} \right)^*$	$IL_i^{ph} = \left( \frac{S_i^{ph-ph}}{V_i^{ph-ph}} \right)^*$
Constant Z	$Z_i^{ph-n} = \frac{ V_i^{ph-n} ^2}{S_i^{ph-n*}},$ $IL_i^{ph-n} = \frac{V_i^{ph-n}}{Z_i^{ph-n}}$	$Z_i^{ph-ph} = \frac{ V_i^{ph-ph} ^2}{S_i^{ph-ph*}},$ $IL_i^{ph-ph} = \frac{V_i^{ph-ph}}{Z_i^{ph-ph}}$
Constant I	$IL_i^{ph-n} =  IL_i^{ph-n}  *$ $\angle_{\delta_i^{ph-n}} - \theta_i^{ph-n}$	$IL_i^{ph-ph} =  IL_i^{ph-ph}  *$ $\angle_{\delta_i^{ph-ph}} - \theta_i^{ph-ph}$

**Table 4.3 Load Model Equations [2]**

The second step of every iteration is the backward sweep which assumes the sources node 1 to be at nominal voltage and then uses the line currents calculated in the forward sweep process to calculate the voltages of all nodes starting from source and progressing towards the terminal nodes. The equations used are given below.

$$V_i^{new} = V_{nominal} - ZI_i \quad (4.3)$$

The above equation applies only for node 1.

$$V_{i+1} = V_i^{new} - ZI_{i+1} \quad (4.4)$$

There is a possibility of the feeder containing other circuit components such as capacitors, line transformers and switches as well. These are modeled in the following ways.

- i. Line transformers are modeled as in [ ] and the update equations from the various transformer matrices may be given as follows. These equations can be applied irrespective of transformer type.

Forward Sweep

$$V_i = a_t V_{i+1} + b_t I_{i+1} \quad (4.5)$$

$$I_i = d_t I_{i+1} \quad (4.6)$$

Backward Sweep

$$V_{i+1} = A_t V_i^{new} - B_t I_{i+1} \quad (4.7)$$

- ii. Switches are modeled as zero impedance branches.

Forward Sweep

$$V_i = K * V_{i+1} \quad (4.8)$$

$$I_i = K * I_{i+1} \quad (4.9)$$

Backward Sweep

$$V_i^{new} = K * V_{nominal} \quad (4.10)$$

$$V_{i+1} = K * V_i^{new} \quad (4.11)$$

where K could be 0 or 1 depending on the state of the switch.

- iii. Capacitors are modeled as constant impedance matrices similar to constant impedance loads.

For Wye connected capacitor bank

$$Z_i^{ph-n} = \frac{|V_i^{ph-n}|^2}{S_i^{ph-n*}}, \quad IC_i^{ph-n} = \frac{V_i^{ph-n}}{Z_i^{ph-n}} \quad (4.12)$$

For Delta connected capacitor bank

$$Z_i^{ph-ph} = \frac{|V_i^{ph-ph}|^2}{S_i^{ph-ph*}}, \quad IC_i^{ph-ph} = \frac{V_i^{ph-ph}}{Z_i^{ph-ph}} \quad (4.13)$$

The load flow involves the comparison the source node voltage with the nominal voltage at the end of every forward sweep. If the difference is beyond a certain set value of tolerance, the next

iteration is calculated. The flowchart for the backward forward sweep power flow algorithm follows.

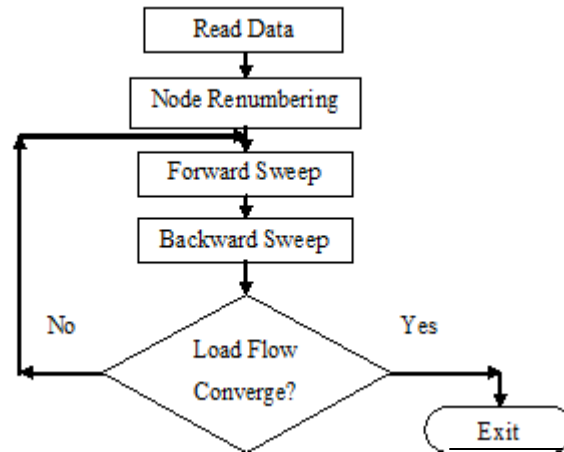


**Figure 4.9 Flowchart of the backward forward sweep power flow algorithm**

#### 4.2.1.3 Distributed Generation

The backward forward sweep power flow algorithm can be used to handle distributed generation in the form of voltage controlled or PV nodes where they are installed by slightly modifying the calculation process. But in this research, wind energy has been handled as a constant power factor input and so, for any given time instant, the value of  $P$  and  $Q$  are constants. So, distributed wind generation has been considered as negative PQ load in the power flow process. Wind turbines can be installed at multiple nodes, but for the sake of simplicity, for the IEEE 37 node test feeder, centralized location of all the generation has been considered at a single node. The wind generation is included into the power flow process by subtracting the given values of real and reactive power generation from wind from the actual load of the node where it is connected in the feeder.

The battery dispatch, which is also a constant three phase value for any given time instant is handled in a similar fashion. The difference lies in the fact that battery charging and discharging is always a real value. In the case of charging of the battery, the real power generation from wind is directly added to the energy level of the battery and not treated as negative PQ load. In the case of discharging, the battery dispatch is subtracted from the feeder node where the wind farm and battery have been connected as negative  $P$  similar to the way

wind generation was handled as explained earlier. The power flow is calculated after these values have been plugged in to the input data.

This chapter has discussed the base cases on which some of the studies were done in order to investigate the addition of wind generation and battery storage along with the measurements of PMUs. There was also a discussion about the IEEE 37-node test feeder on which all the studies were done in this research. The backward forward sweep power flow algorithm that was used throughout this research in order to provide measurements required in the calculation of dispatch for wind generation and battery storage has also been discussed in some detail. The final section also discussed the methods used to include wind generation and batteries in the power flow process as negative PQ load.

## **Chapter 5 - Algorithm and Analysis**

### **5.1 Storage Dispatch Operation Algorithms**

In this section, various approaches that were used in this research in the dispatch operation of battery storage with wind generation are discussed. The first method describes the use of forecast data in order to perform the ideal operation of battery storage with wind generation. This method is tested for both the fifteen minute basis data as well as the one second data in order to observe the effects of battery storage operation with wind generation on the overall load of the feeder, individual phase loads, three phase voltage profile of the node where wind farm and battery have been installed, battery power charging and discharging profile, battery energy level profile, losses of the feeder, and the fifteen minute averaged normalized demand profile.

The second method, which is more realistic and suited to real time utility operations, is based on calculations done using historical PMU measurements and is tested only for one second data. The effects on various system parameters is also observed as discussed above.

#### **5.1.1 Test Setup of Feeder Components and Measurements**

The Backward forward sweep power flow algorithm which was described earlier is used for the IEEE 37 node test feeder at peak load conditions without any wind generation initially. The purpose of this power flow solution is to determine the weakest node, i.e., the node with the lowest voltage profile. This node will become the site of installation of the wind farm as traditionally followed in real world applications. As the battery storage takes power from the wind farm when in charging mode, this node will also be the site of the battery installation. The Phasor Measurement Units (PMU) are installed at two locations for this test feeder while larger feeders with more number of feeders can have more installations. The PMUs are installed for this system at node 738 (renumbered to 32) and node 701 (renumbered to 2) as they are the most critical nodes in the system. Node 701 is the node that is present right after the source node. The voltage difference between the source node and this node is a direct measure of the net load on the feeder at any time instant and so can be very advantageous for monitoring and operations purposes. This property has been taken advantage of in this research when real time operation is considered. The wind farm and battery node is given a PMU because voltages at this node are a direct measure of the wind generation and battery charging or discharging for the system. The



test system setup has been given below. It may be mentioned that the PMUs being used are distribution level PMUs that have reduced functionalities as opposed to transmission level PMUs that have multiple functions.

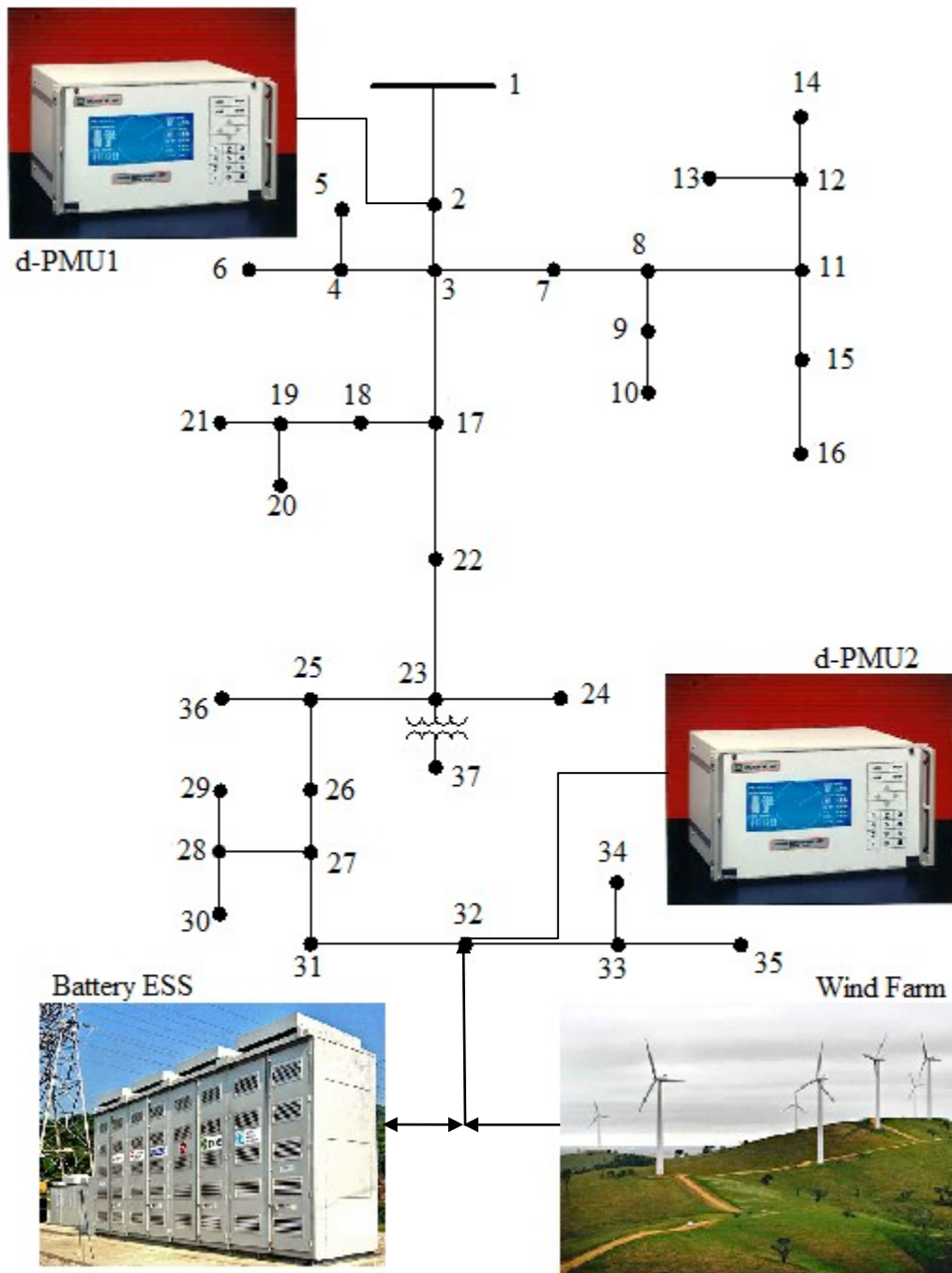


**Figure 5.1 Dispatch Operations Simulation Test Setup\***

\*Pictures courtesy of [www.macrodyneusa.com](http://www.macrodyneusa.com), [www.zmescience.com](http://www.zmescience.com), [www.wastedenergy.net](http://www.wastedenergy.net)

### 5.1.2 Testing for conventional base cases

The initial testing involves running the power flow algorithm without any wind generation and then with wind generation considered in the system. The fifteen minute data is analyzed with low, medium and high wind generation data and the one second data is tested for one single case of wind generation. The results obtained from these test runs will act as comparison data for results that will be obtained later using wind generation and battery combined in the system. The flowcharts for algorithms used for instantaneous power flow in conventional cases have been given below.

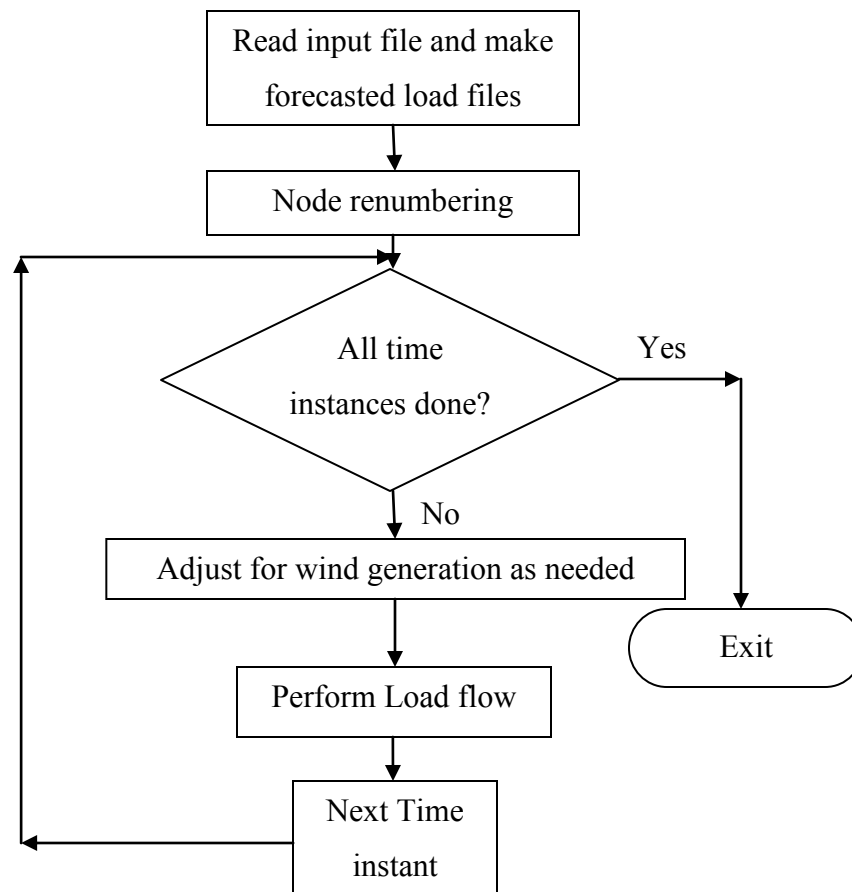


**Figure 5.2 Flowchart for base case testing with or without wind generation**

The only difference in the above method when wind energy is considered is that the given value of wind generation for that time instant is treated as negative PQ load and subtracted from the actual load of the node where wind generation has been installed. In the case of the IEEE 37 node test feeder, node 738 (renumbered to 32) has been considered as the wind generation node.

### 5.1.3 Dispatch operations for forecasted load information

The dispatch operation of the battery with distributed wind generation using forecasted load information can be used to determine the ideal characteristics of battery charging and discharging in order to perform load support operations purely using wind generation, as described earlier. Two different approaches have been tried in order to discharge the battery and additionally, two methods of charging the battery have also been investigated. So, a total of four different combinations are possible. These methods have been tested for both the fifteen minute forecasted load as well as the one second forecasted load information. The four methods have been described below and their respective flowcharts have been presented.

- i. **Wind charging with free running discharging mode:** In this method (Figure 5.3), for all the time instances, if the load for a given time instant is less than the daily average load of the feeder, the wind farm is directly connected to the battery for charging. If the forecasted load is above the average, the wind farm is connected to the feeder and the battery is also discharged in such a way that the overall feeder load seen by the substation is equal to the average forecasted load of the feeder. If the battery has hit any of its limits, i.e., if maximum level has been reached during charging, or if minimum level has been reached during discharging, the battery is switched off and wind generation is directly connected to the feeder. This method is subject to the available capacity in the battery as beyond a certain time instant, apart from the battery capacity, if wind generation becomes reduced as well, peak reduction in feeder load may not be possible if battery is shut off too soon.
- ii. **Wind charging with conservative discharging mode:** In this method (Figure 5.4), for all the time instances, if the load for a given time instant is less than the daily average load of the feeder, the wind farm is directly connected to the battery for charging. If the forecasted load is above the average, the wind farm is connected to the feeder and the battery is also discharged, but the availability of battery capacity for all the remaining time instances of the day is calculated for every time instant such that the full available capacity of the battery is utilized over the entire length of the day. This value is compared with the average load requirement of the remaining time intervals and the minimum of these values is selected. This method may not succeed in maintaining the feeder load

close to the average load all the time, but ensures that there is at least a certain minimum value of load reduction at every time instant. There is also full battery capacity utilization irrespective of battery size.

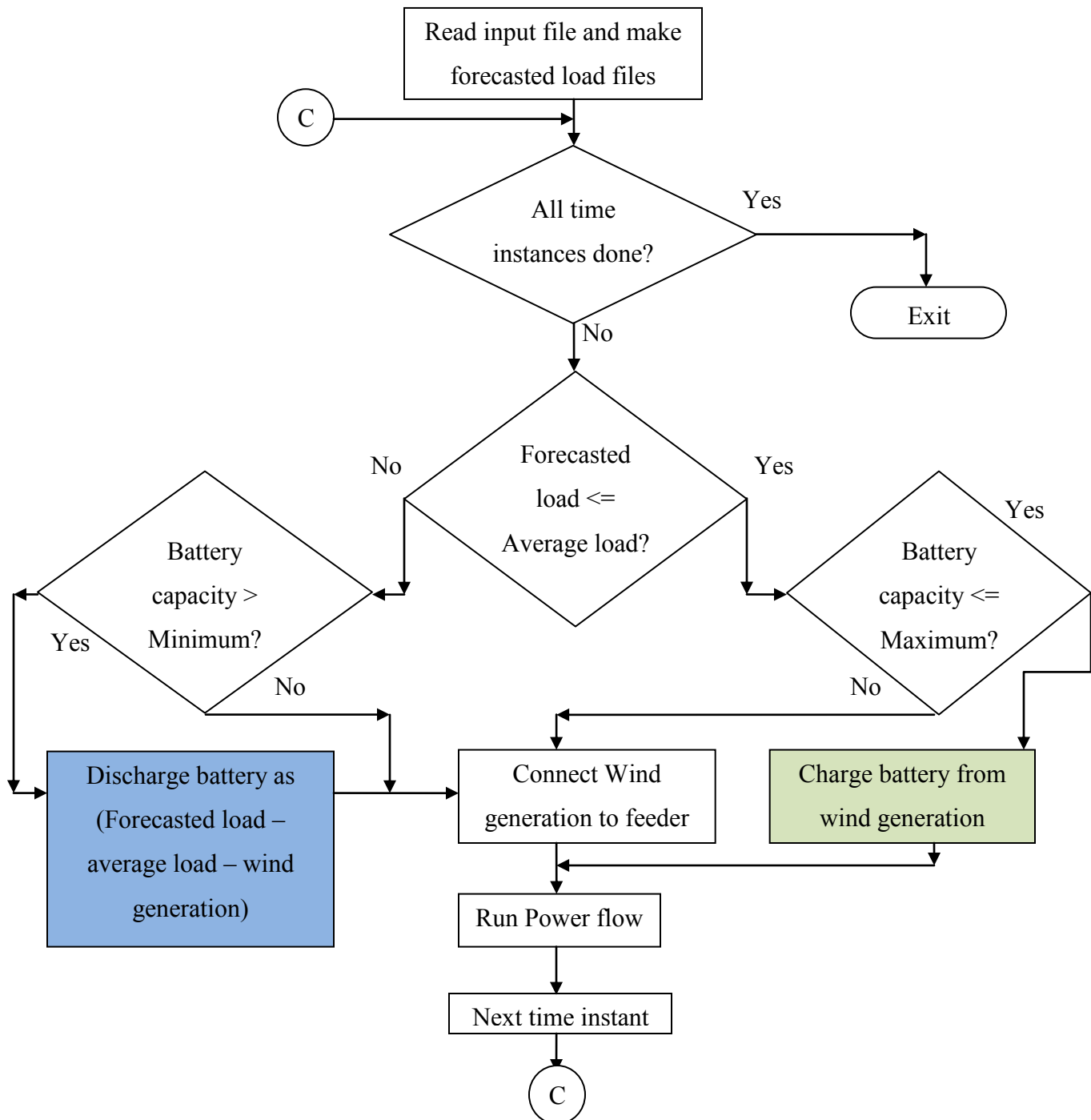


**Figure 5.3 Flowchart for battery dispatch operation for wind charging with free running discharge**

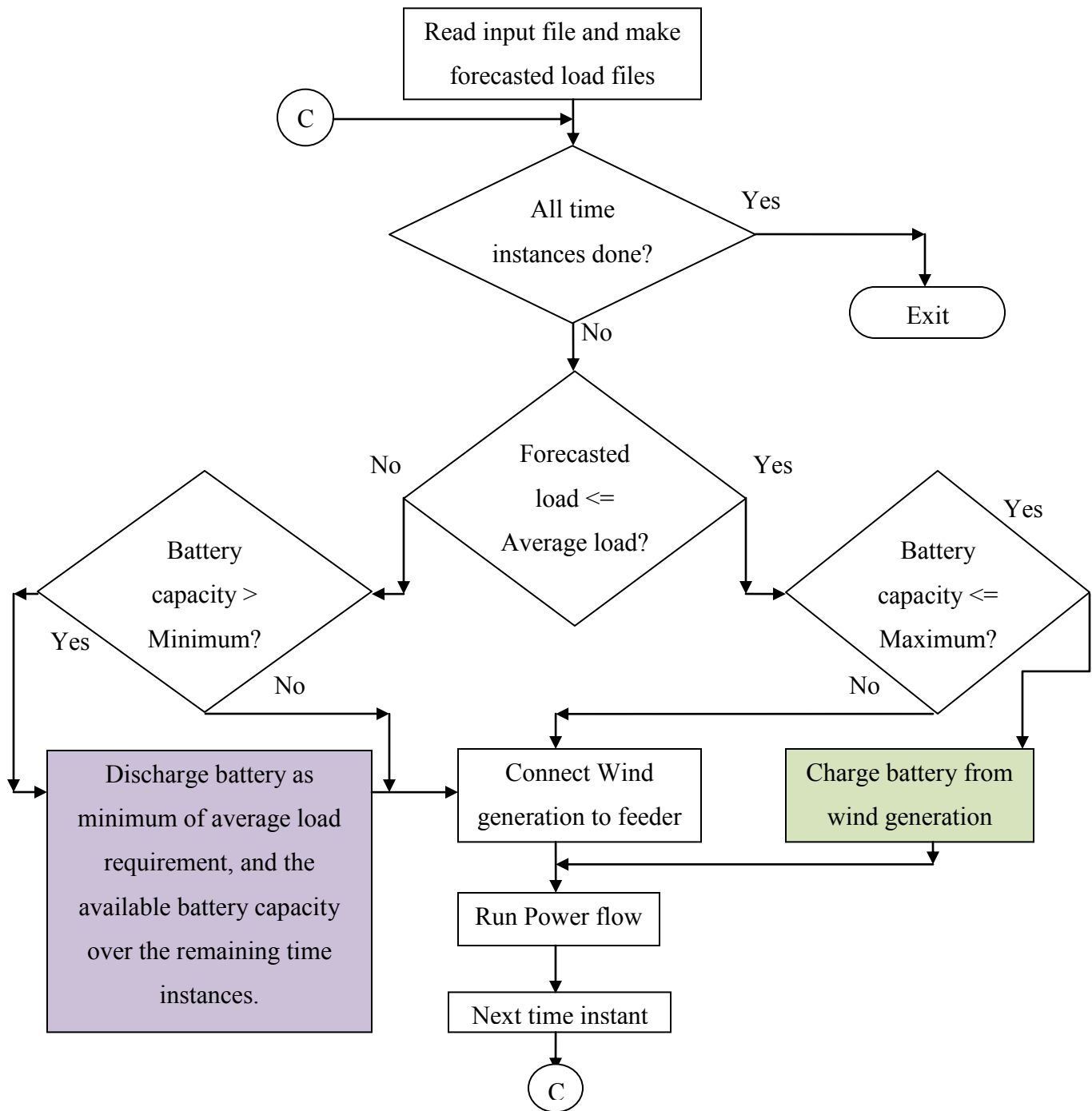


**Figure 5.4 Flowchart for battery dispatch operation for wind charging with conservative discharge**

- iii. **Sustained average load charging with free running discharge:** In this method (Figure 5.5), if the forecasted load is below the average load of the feeder, the battery is charged from the wind generation and also the difference between average and forecasted load is taken from the main supply in order to charge up the battery. The resulting feeder load during times of battery charging is equal to the average load. If forecasted load is above average load, the wind farm is directly connected to the feeder, and also load component above the average load apart from wind generation is supplied by the battery irrespective of available capacity. This method ensures that there is always sufficient battery capacity in order to perform efficient peak reduction during heavy load conditions. The catch lies in the fact that this method requires a highly advanced charge controller for the battery that is currently not available but, this method may become possible in the future. Under current conditions, however, this method cannot be implemented in real time.
- iv. **Sustained average load charging with conservative discharge:** This method (Figure 5.6) uses the same charging strategy as described above, but if the forecasted load becomes greater than the average load, the average load requirement over the remaining time instances is calculated along with the available battery capacity over the remaining time instances. The minimum of these two calculations is taken as the battery discharge. Again, this method also ensures full capacity utilization of the battery irrespective of size.

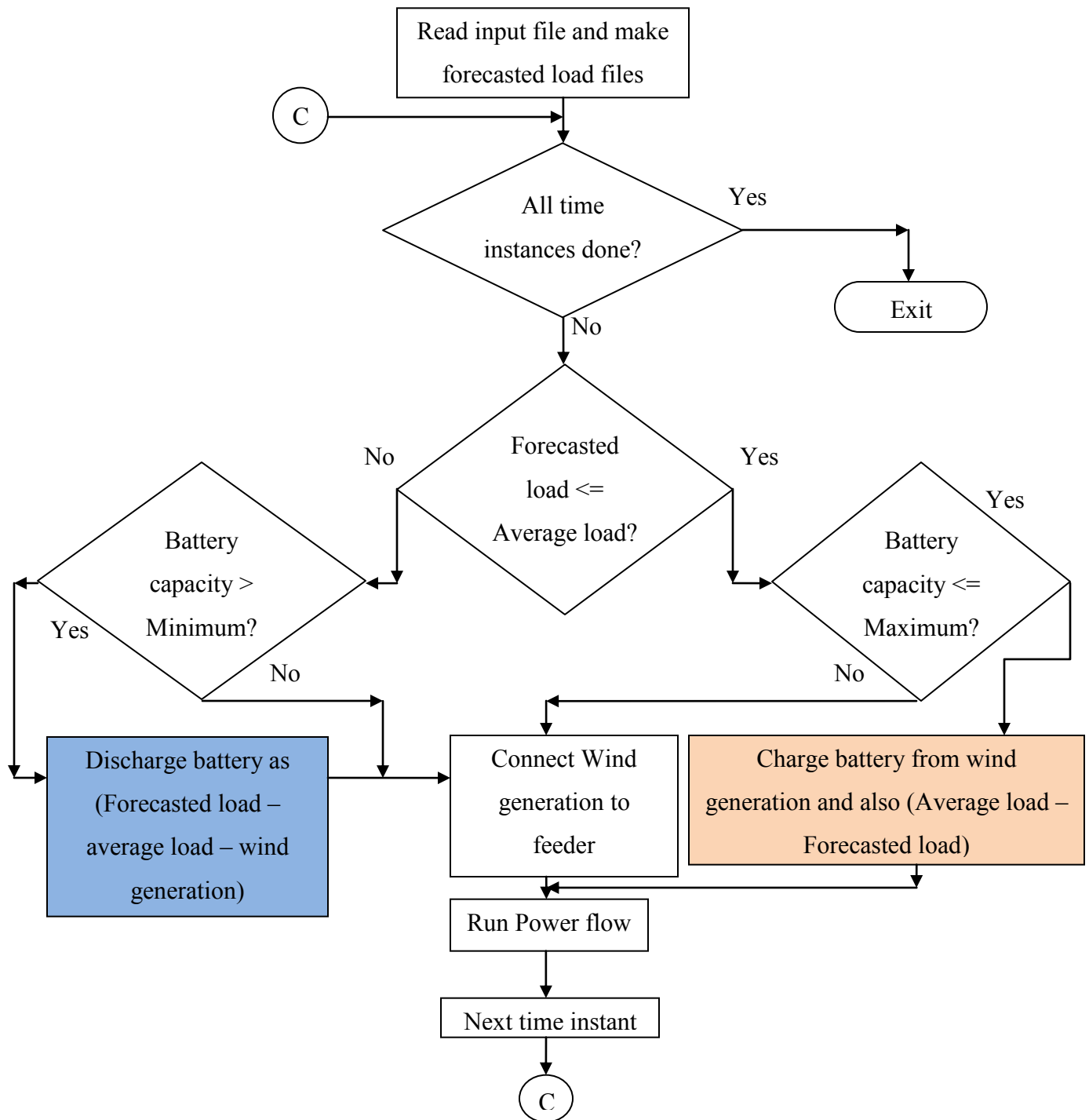


**Figure 5.5 Flowchart for battery dispatch operation for sustained average load charging with free running discharge**

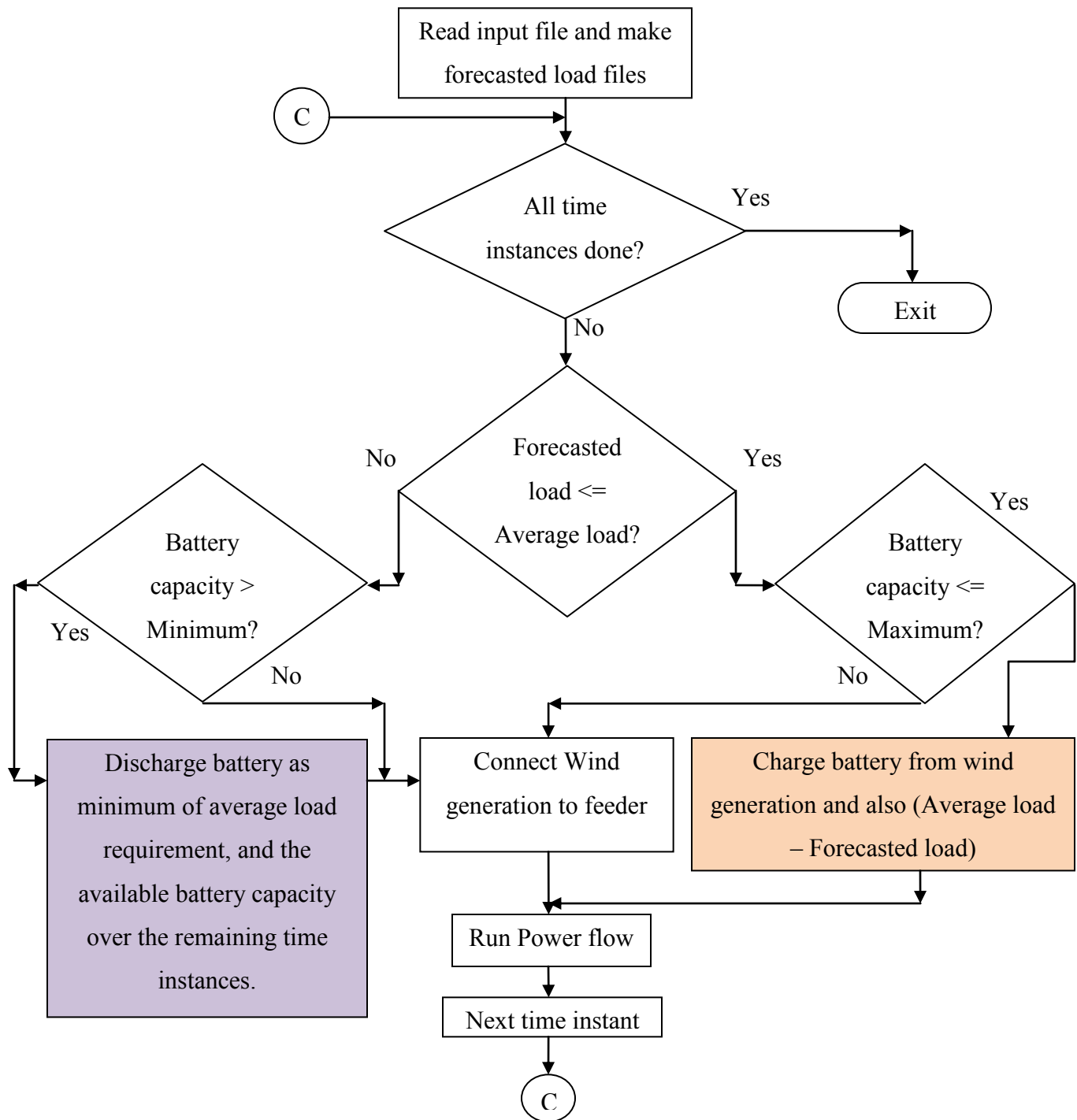


**Figure 5.6 Flowchart for battery dispatch operation for sustained average load charging with conservative discharge**



#### **5.1.4 Dispatch operations for historical load information from PMUs**

The actual real time operation of battery storage with wind energy using historical PMU measurements can be achieved using this method (Figure 5.7). The only information that this method requires during operation is an approximate value of the average load of the distribution feeder. This method is applied only for the one second data as the required results cannot be obtained with fifteen minute data. The decision of charging or discharging the battery is based on the maximum value of the load in a given group of previous load instances. This value of load is calculated by taking into account the PMU measurements of the node that is close to the source node.

For the test system, as described earlier, the PMU is at node 701 (renumbered to 2). This method also ensures that there is always some measure of reduction in the load of the feeder during heavy load conditions. This is ensured by changing the discharging of the battery to the conservative discharging mode described earlier when the battery capacity falls below a certain set value that is still above the minimum level of the battery. The mixed approach is adopted for the discharging of the battery as it is observed in the forecasted load studies that free running mode seems to perform relatively well for one second data except during the last time instances of the day.

The charging of the battery is done using only the wind generation in this case as it is intended for real time purposes and the sustained average load approach is currently not suitable for real time operation. The simulation of this method does not utilize the full capabilities of the PMU however. PMUs can sample data at up to thirty samples a second, while the scope of this study is limited to a much lower rate of one sample per second. This is because actual wind generation information obtained is available for research on a minimum basis of one second, and also, the operational dynamics of distribution system load do not require the resolution offered by the full potential of PMU sampling information. This is evidenced by the fact that conventional utility standards rely on a minimum averaged load sampling of one sample every fifteen minutes, which is much higher than the sample periods being investigated in this research.

The initial condition followed in the implementation of this algorithm is that for the first sample period, the wind generation is used to charge up the battery irrespective of load. This is in order to ensure that PMU measurements are available for any given sampling interval as soon as the initial sampling interval has been crossed. The flowchart for this method has been given below

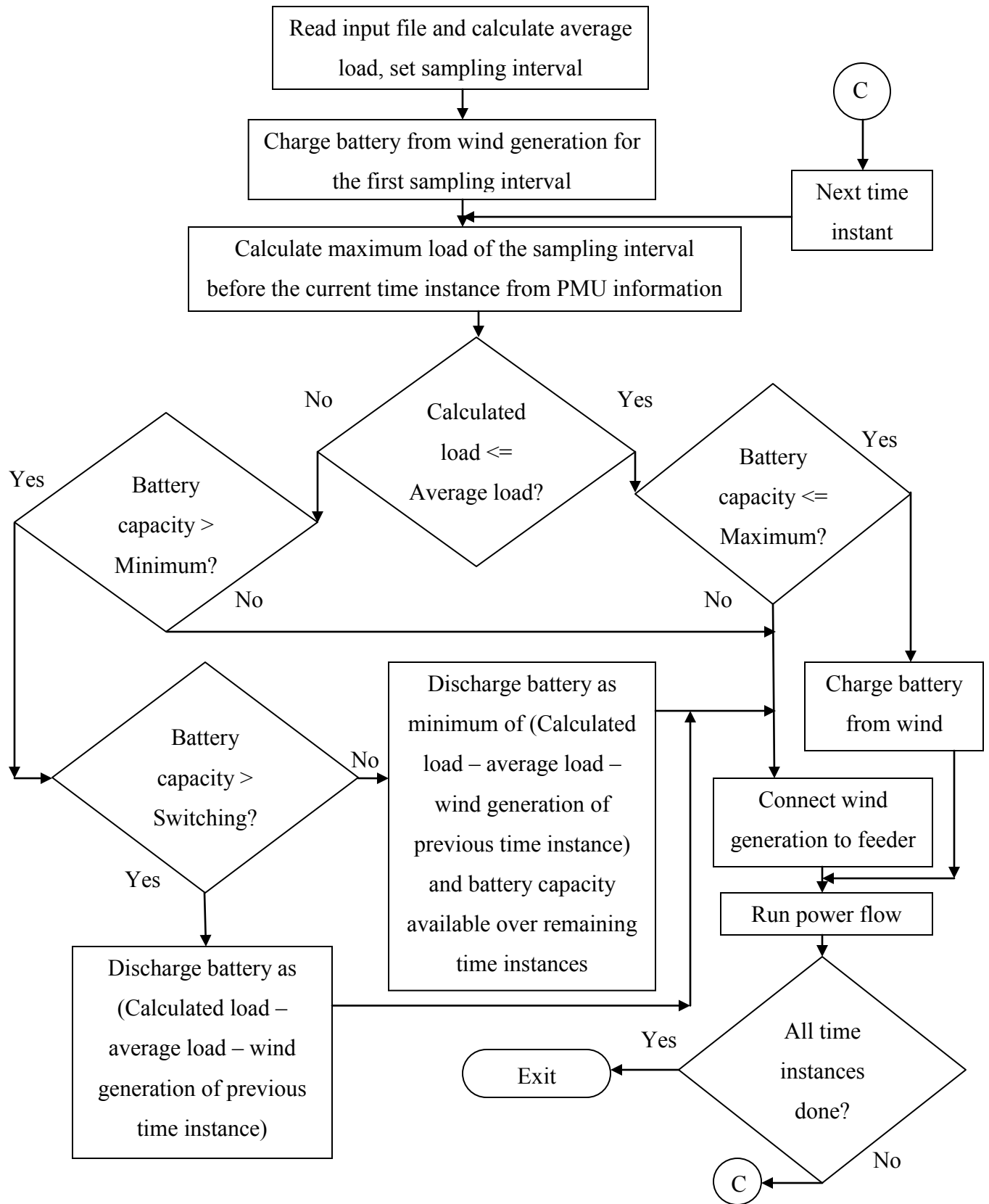


**Figure 5.7 Flowchart for real time battery operation with wind generation using PMUs**

## **Chapter 6 - Results and Discussion**

### **6.1 Results obtained for base cases of load flow**

The base cases of load flow for both the 15 minute as well as one second data serve as a measure of comparison of the benefits of using battery storage with wind generation. The most basic load flow without any wind generation or battery gives the peak load of the feeder and also the heavy power losses that are encountered because of the usage of source power alone. In the next sub-sections, the base cases of load flow with and without wind generation have been shown for the fifteen minute basis demand as well as the one second basis demand data.

#### **6.1.1 Results obtained for base cases of load flow without wind generation**

The following results were obtained for the 15-minute basis forecasted load data for the IEEE 37 node test feeder. The analysis was carried out for all the load instances over a period of 24 hours. The results obtained here will serve as a comparison to the peak reduction achieved using direct wind connection as well as the dispatch operation of the battery storage as it is a case of maximum source power usage from the conventional generation. In order to clearly observe the effects of using PMU information in the battery dispatch process, the results need to be presented in such a way that they can be compared to the simplified fifteen minute normalized demand histogram. The final comparison of all the methods tested in this research work is with the normalized histogram of the base case. The other comparison factor is the power loss in the feeder without any wind generation or battery storage. All the other results are obtained in order to check for normal operation without any unstable or irregular conditions. The voltage profile plot shown for all cases is that of the node where the wind generation and battery storage have been installed. This node is selected as it is subjected to maximum irregularity at every time instant as both the wind generation and the battery storage keep changing. If this voltage is within allowable limits, it can be said with confidence that the other nodes in the feeder are also within normal operating voltages. The plots obtained for base case of feeder load without any form of distributed generation are given below.

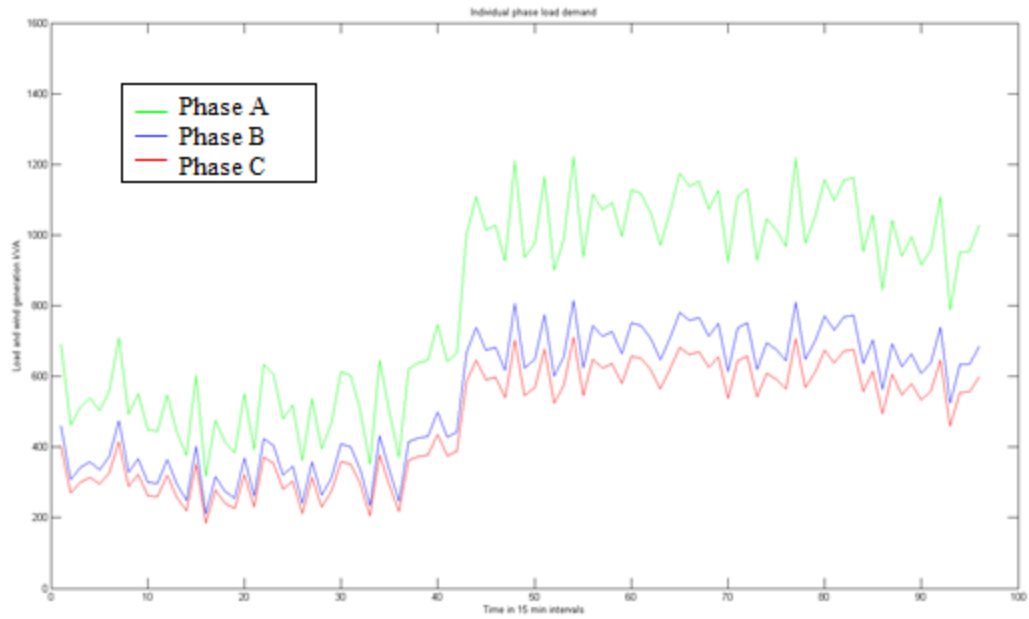


**Figure 6.1 Individual demand of phases a, b and c of the feeder for 15 minute data**

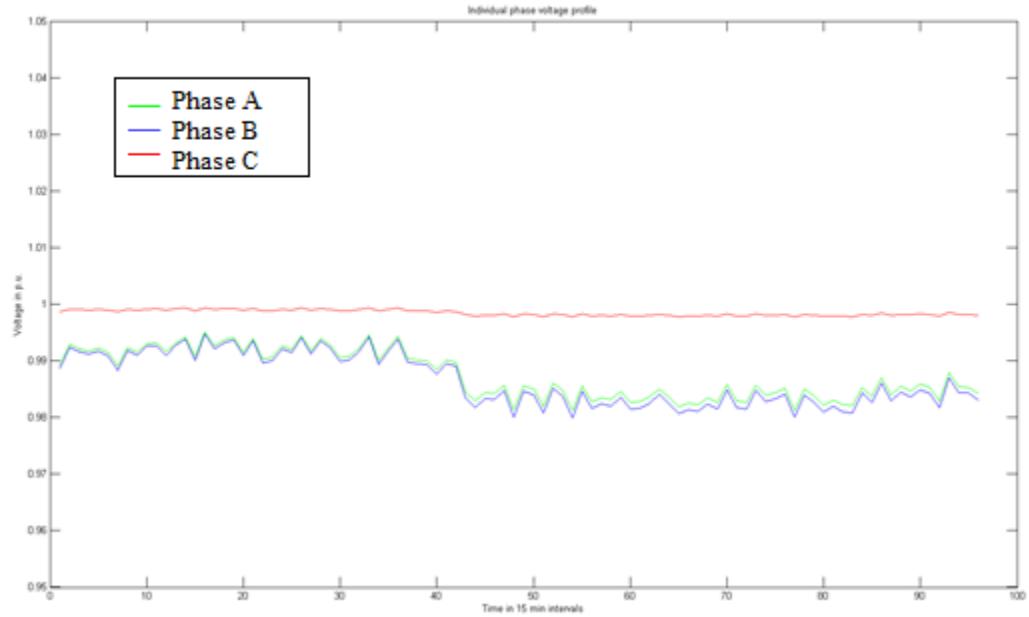


**Figure 6.2 Individual voltages of phases a, b and c for node 32 for 15 minute data**

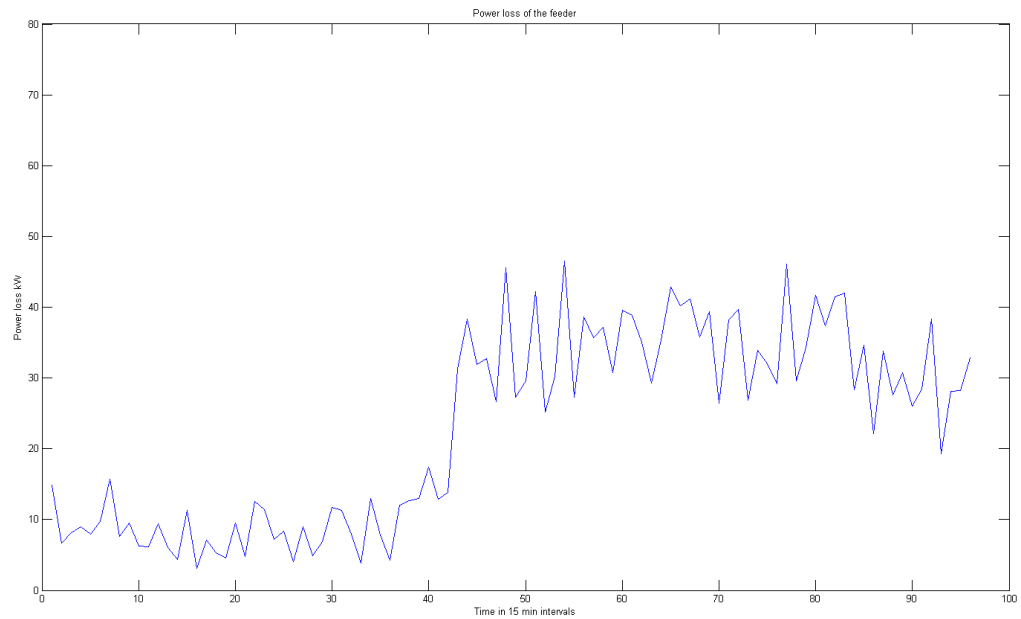


**Figure 6.3 Power losses for the entire feeder for 15 minute data**

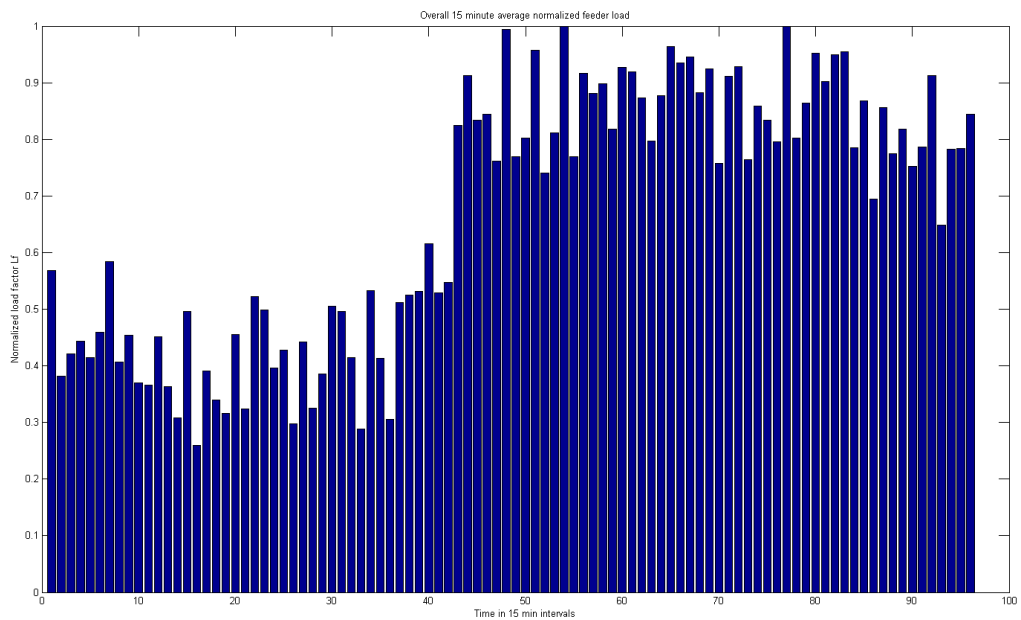


**Figure 6.4 Average normalized 15-minute load profile of the feeder without wind generation**

As it can be seen from the above plots, the load on the feeder follows a standard pattern which results in base load as well as peak load conditions. The above results are for a standard three phase backward forward sweep power flow for all the 96 fifteen minute time intervals of the day. It is also seen that the losses of the feeder are directly related to the amount of power drawn from the conventional generation. The objectives to be achieved are to reduce the peak load conditions that are seen in the 15-minute demand histogram, and also the minimization of losses that arise from more power consumption from conventional generation. It will be observed later that when the first objective is met, the second objective is also met as a result.

The 15-minute load data is multiplied with a Gaussian distribution in order to get one second forecasted data for the purpose of analysis as explained in chapter 4 on test cases. The base case without any distributed wind generation or battery is also run for the one second data. The results obtained are used to show the actual operational dynamics of the load of the feeder and the increase in actual peak load of the feeder when one second data is used. The fifteen minute averaged demand histogram is also created from the one second demand data in order to provide a direct comparison to 15-minute data. The results obtained are given below in figures 6.5 through 6.9.

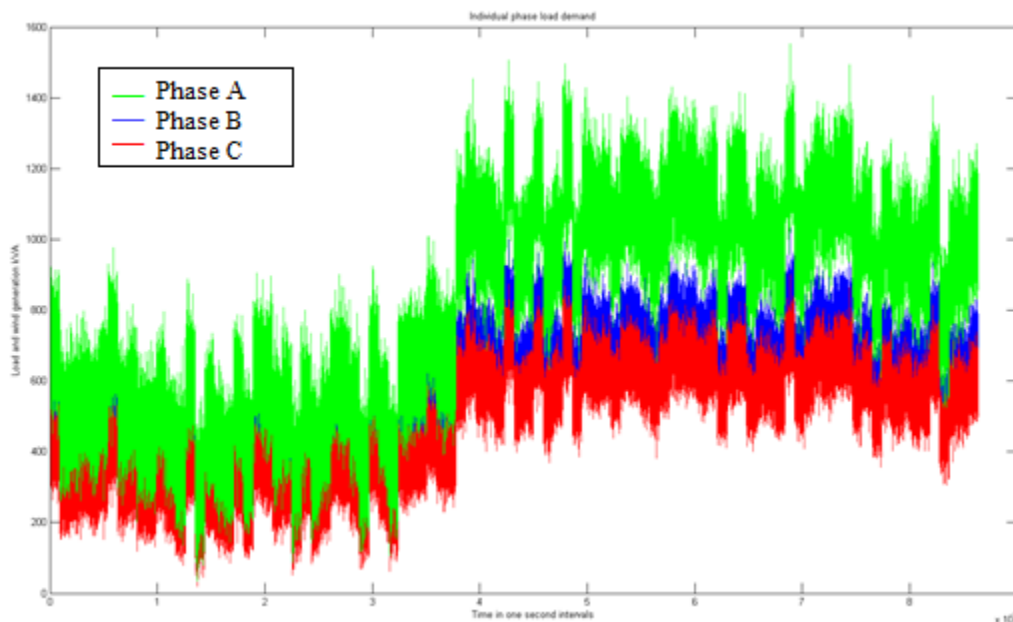


**Figure 6.5 Individual demand of phases a, b and c of the feeder for one second data**

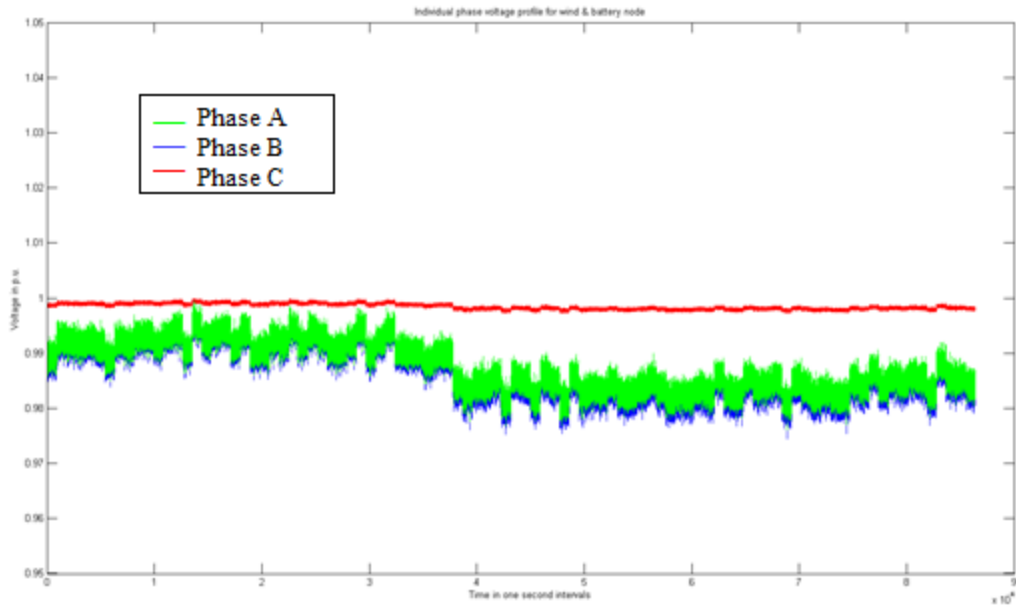


**Figure 6.6 Individual voltages of phases a, b and c for node 32 for one second data**

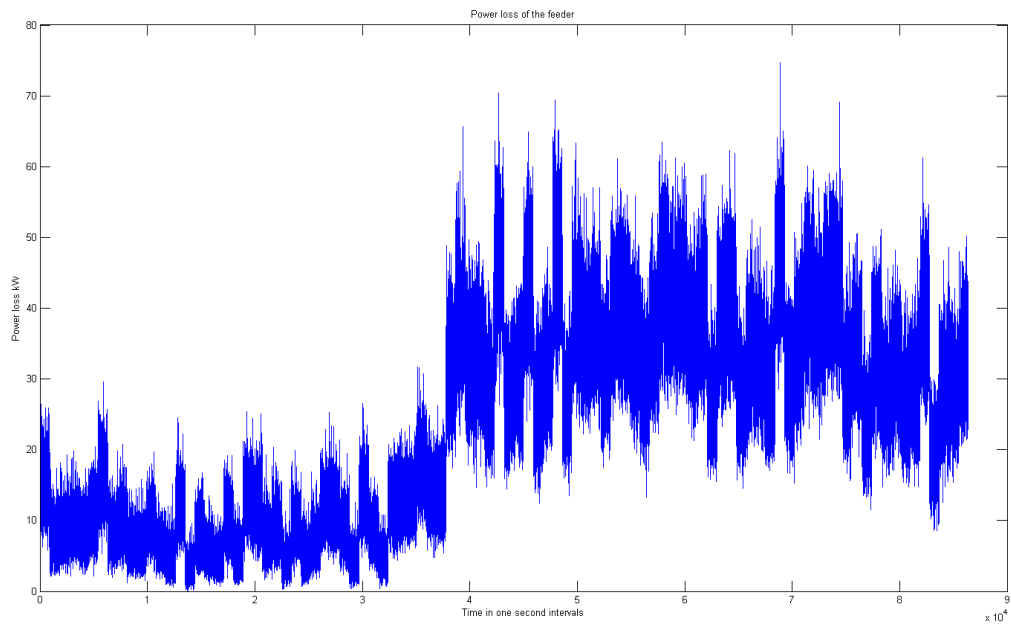


**Figure 6.7 Power losses of the entire feeder for one second data**

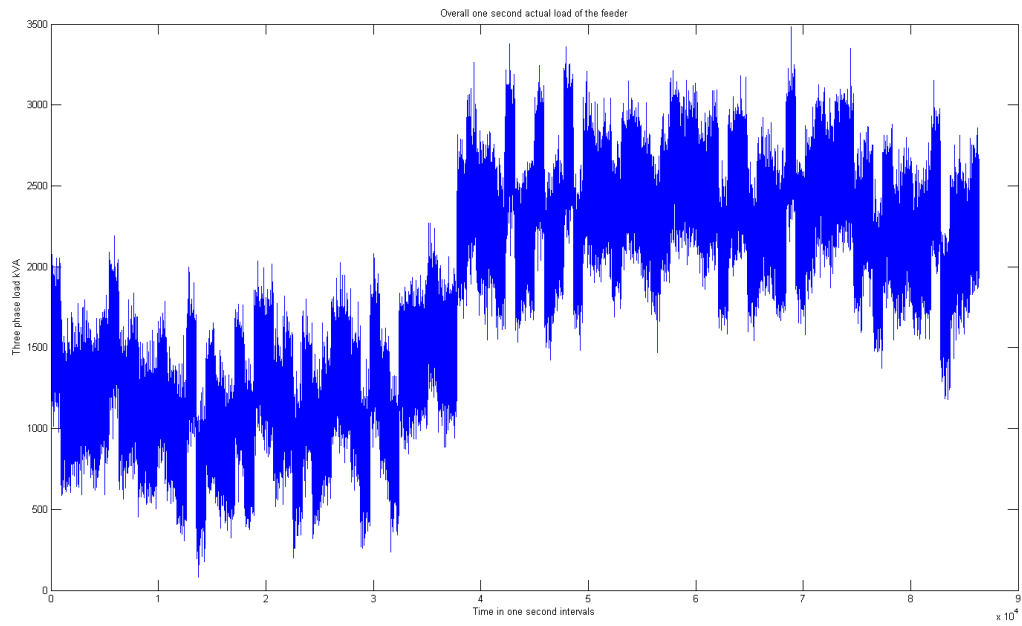


**Figure 6.8 Total three phase demand of the feeder for one second data**

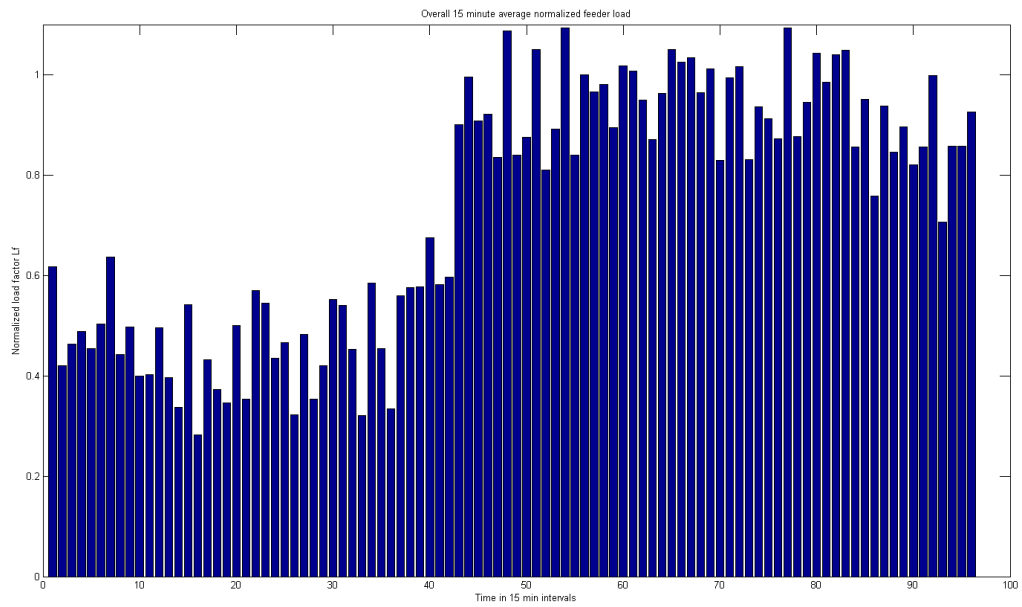


**Figure 6.9 Average normalized 15-minute demand histogram for the feeder obtained from one second demand**



It is observed from the one second approximation of the 15-minute load profile that actual values of load seen by the distribution feeder are much higher than the planned average 15-minute load capacity of the feeder. Although load differences in actual cases may not be as high as the probabilistic case tested here, there is a need to address the problem of increasing load levels with time. This is one of the reasons why peak reduction algorithms are of great importance in modern power system studies. The criticality of the one second basis test case being analyzed in this research will help in the design of robust and foolproof algorithms in the future when actual utility implementation of the algorithms using PMU become possible.

### **6.1.2 Results obtained for base cases of load flow with wind generation**

Current approaches used in utility operation of wind turbines mostly involve the direct online connection of wind farm generation. The load is partially satisfied all the time by the available value of wind power. There is no control strategy involved except in the case of contingencies such as excessive wind during which the turbines are offline. Wind energy in this case can be used up when its requirement is not of great importance and alternatively, there might be no support when there are heavy load conditions. It is also rare to observe an idealized characteristic for wind generation for a given day when load and wind are positively correlated, i.e., the wind generation is highest when the load levels are high. This is the only scenario when maximum peak reduction using wind generation alone is possible. The fifteen minute direct wind connected case power flow data have been presented below for low wind, medium wind and high wind conditions. It does not make sense to calculate peak reduction metrics for direct wind connection as the peak reduction in this case is a function of magnitude, and also the time of wind availability which can be different on different days.

The power flow results obtained for a given day with high wind generation are given below. The results obtained are for the individual phase demands after wind connection (Figure 6.10), voltage profile of the feeder where wind farm and battery have been connected (Figure 6.11), the losses of the feeder after wind generation (Figure 6.12), and the normalized fifteen minute demand after wind connection (Figure 6.13).

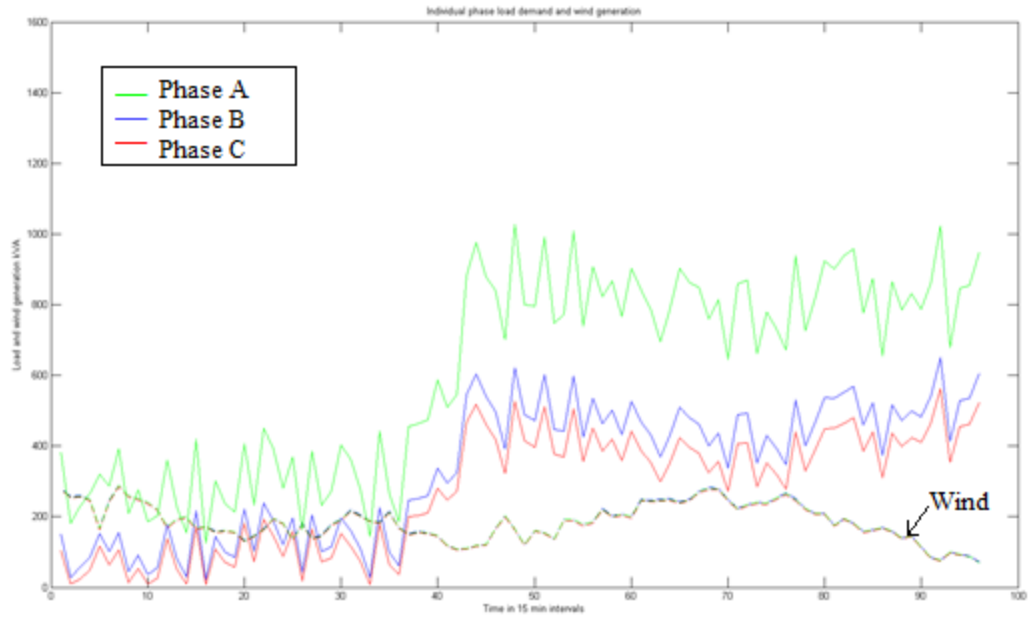


**Figure 6.10 Individual phase demands with direct wind generation connection and high wind for fifteen minute data**

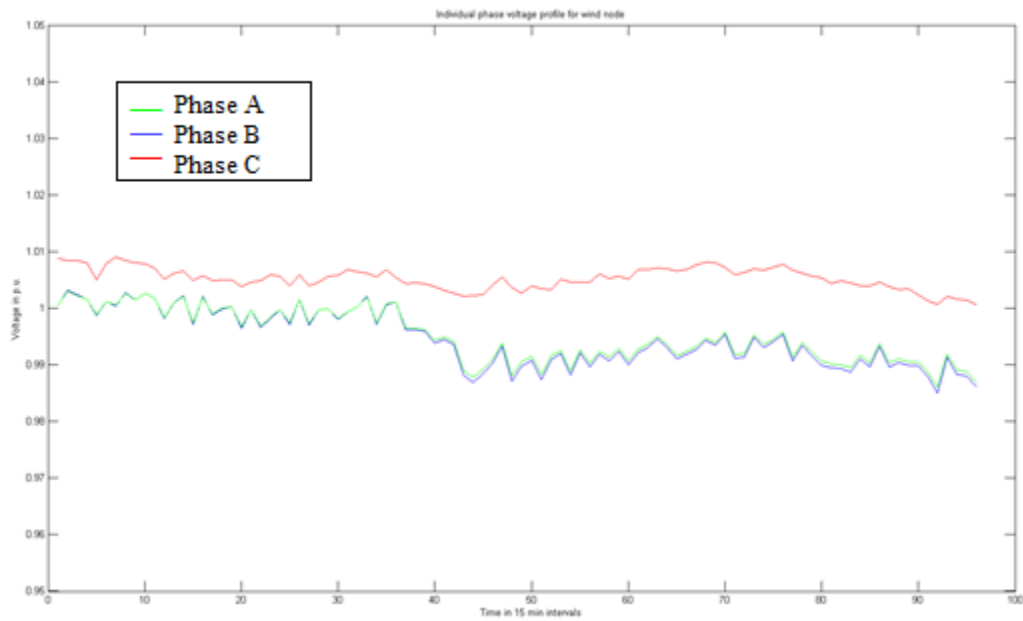


**Figure 6.11 Individual phase voltages for node 32 with direct wind connection and high wind for fifteen minute data**

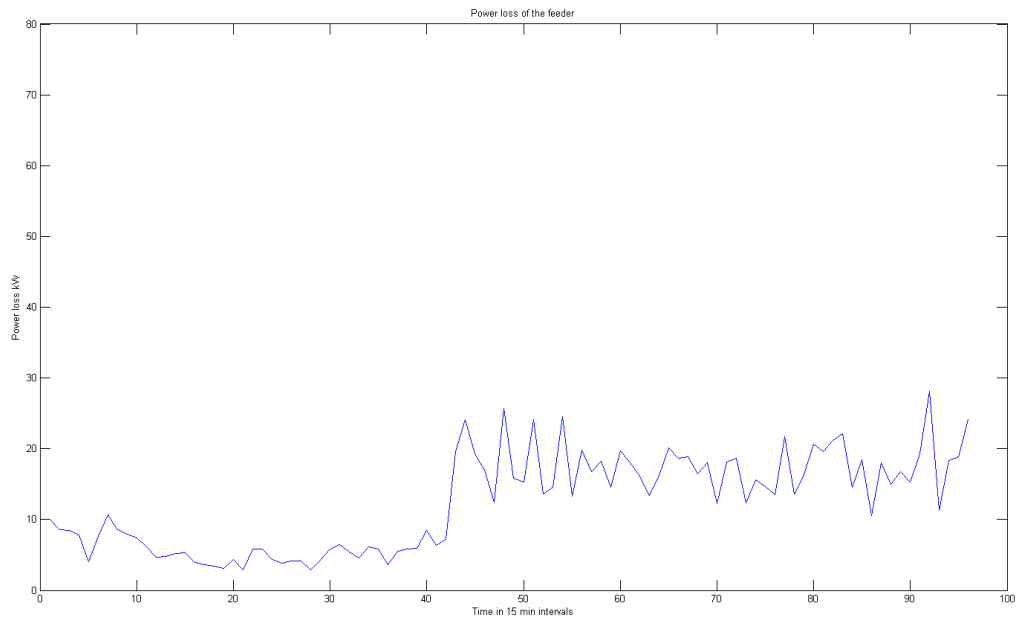


**Figure 6.12 Power losses for the feeder with direct wind connection and high wind for fifteen minute data**

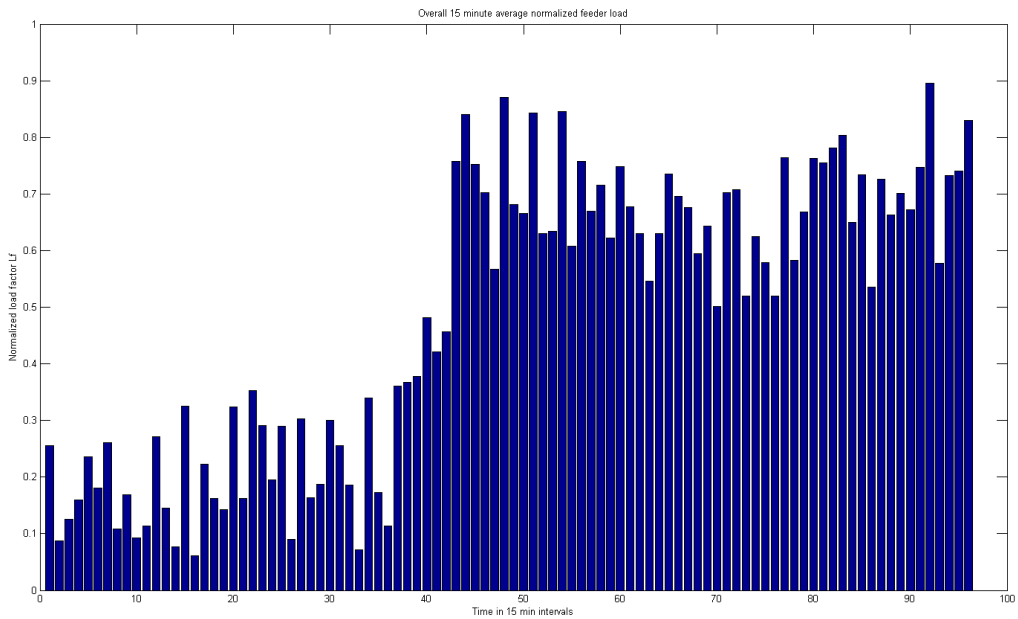


**Figure 6.13 Normalized fifteen minutes load histogram as seen by the substation with direct wind connection and high wind**

As it can be seen from the results above, direct wind connection yields good results when high wind generation is available, but there is a direct relation between the amount of wind generation and peak reduction achieved in a given instance. During instances when the feeder is lightly loaded, the load can drop to dangerously low levels so as to cause unstable conditions such as the Ferranti effect, although this is a rarity as it has to happen simultaneously in multiple feeders.

The power flow results for medium wind generation for a given day for fifteen minute data have been given below from figure 6.14 through 6.17.

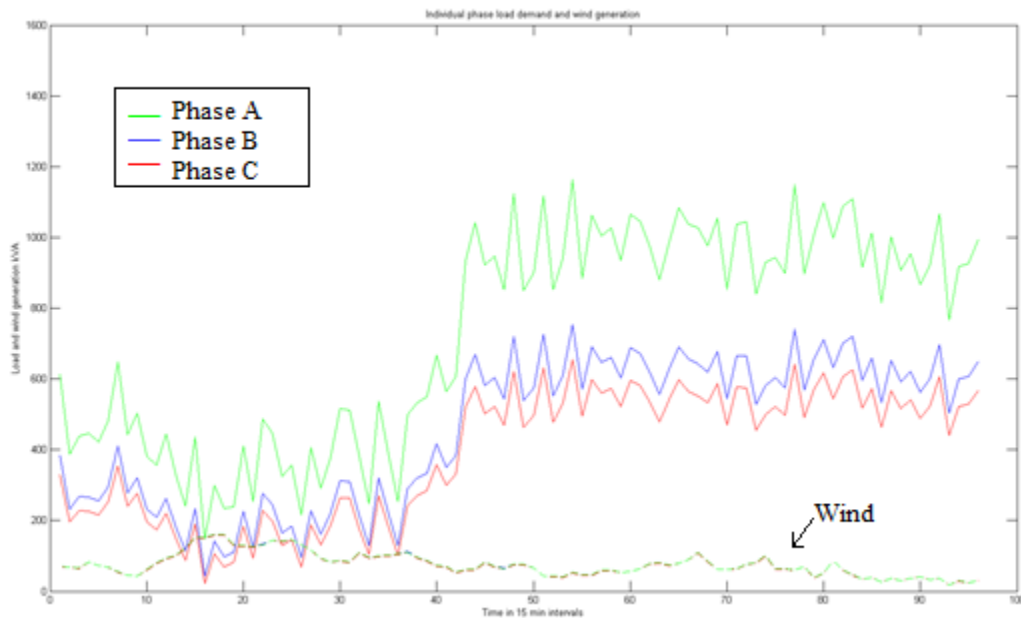


**Figure 6.14 Individual phase demands with direct wind generation connection and medium wind for fifteen minute data**

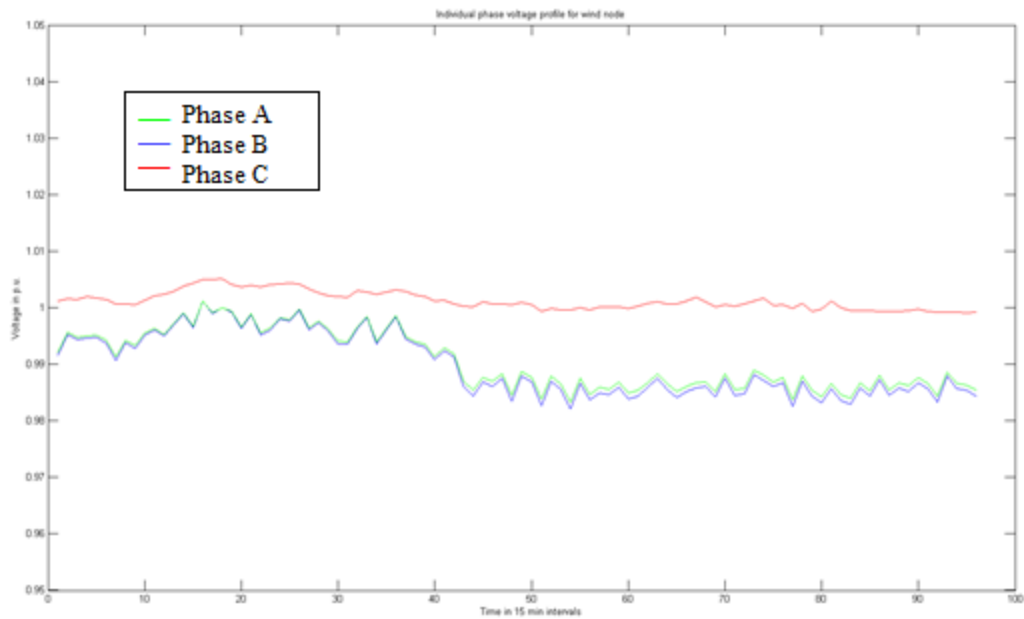


**Figure 6.15 Individual phase voltages for node 32 with direct wind connection and medium wind for fifteen minute data**

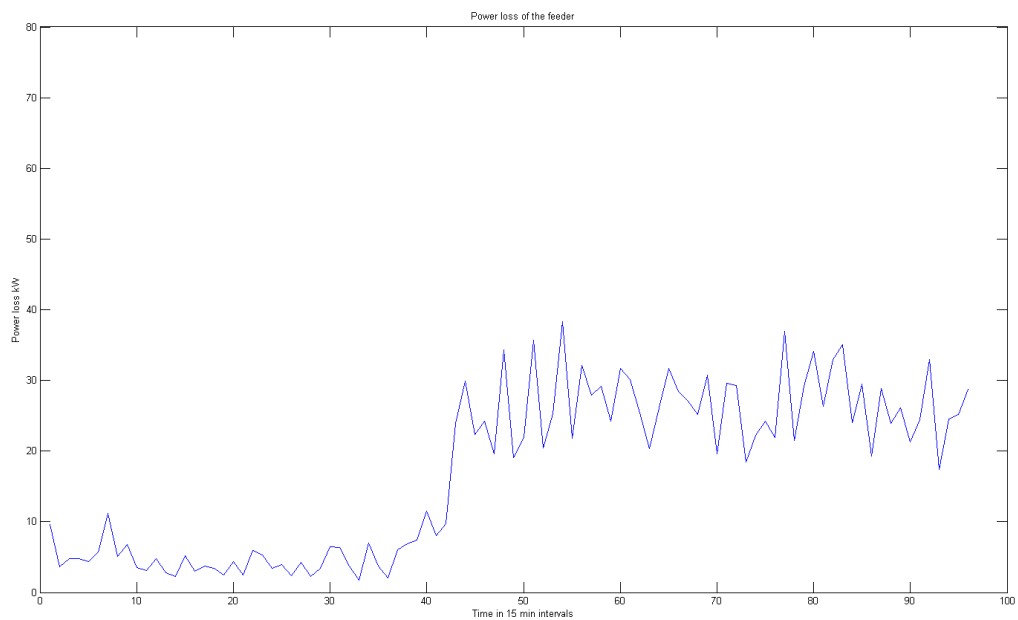


**Figure 6.16 Power losses for the feeder with direct wind connection and medium wind for fifteen minute data**

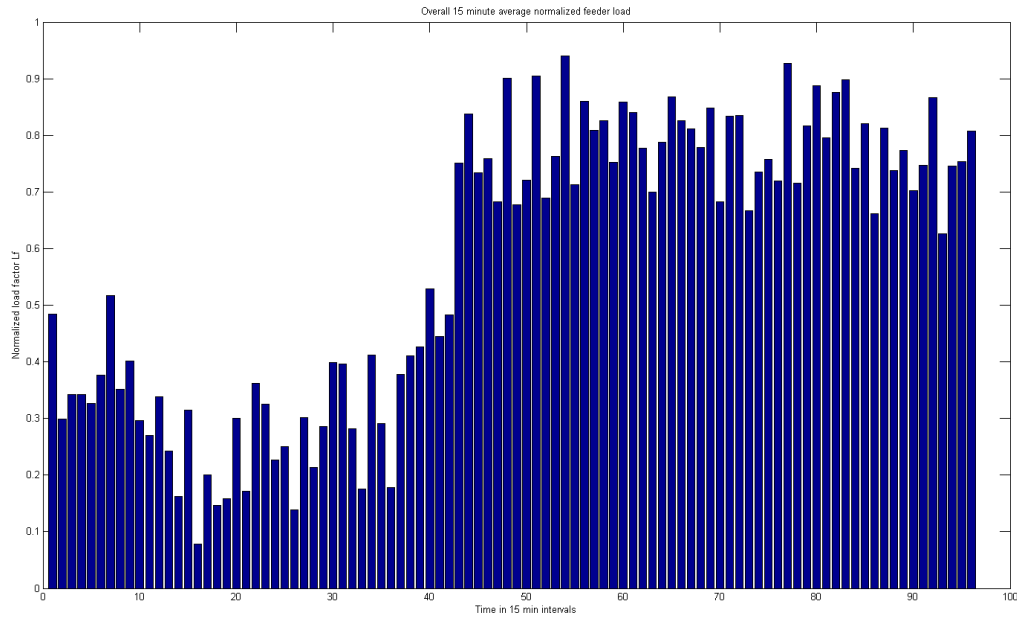


**Figure 6.17 Normalized fifteen minutes load histogram with direct wind connection and medium wind**

From the results obtained above, we see that the losses encountered in a distribution feeder decrease with the increase of locally generated power. The power flow results for the same data for low wind generation have been given in figures 6.18 through 6.21. The results obtained in the case of low wind generation prove that increase of locally generated power, especially renewables, reduces feeder losses.

<b>Amount of Wind Generation</b>	<b>Average Feeder losses (kW)</b>
High wind	12.4448
Medium wind	17.1213
Low wind	20.9120
No wind	22.9694

**Table 6.1 Comparison of feeder losses for different wind generation levels**

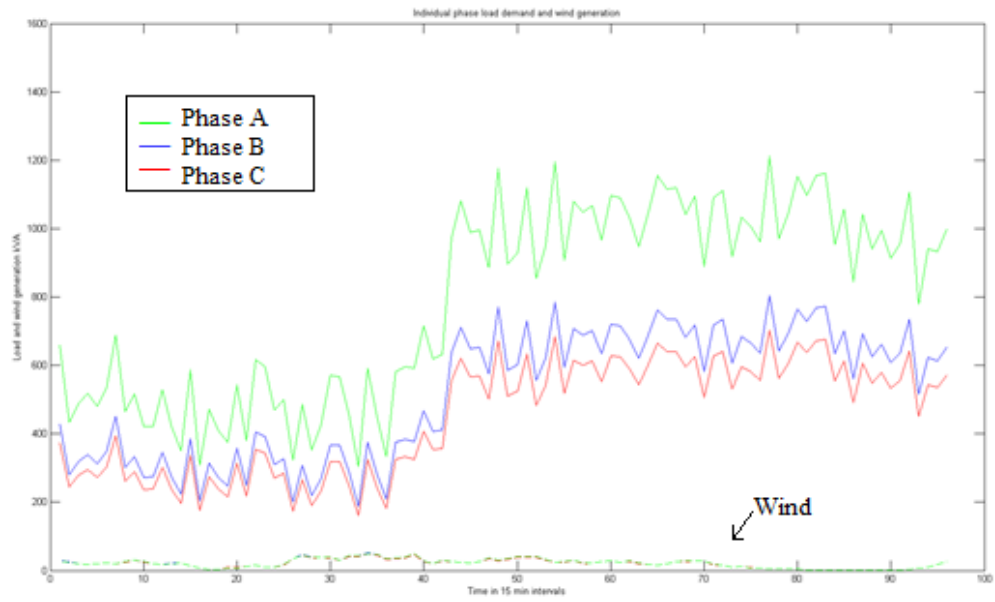


**Figure 6.18 Individual phase demands with direct wind generation connection and low wind for fifteen minute data**

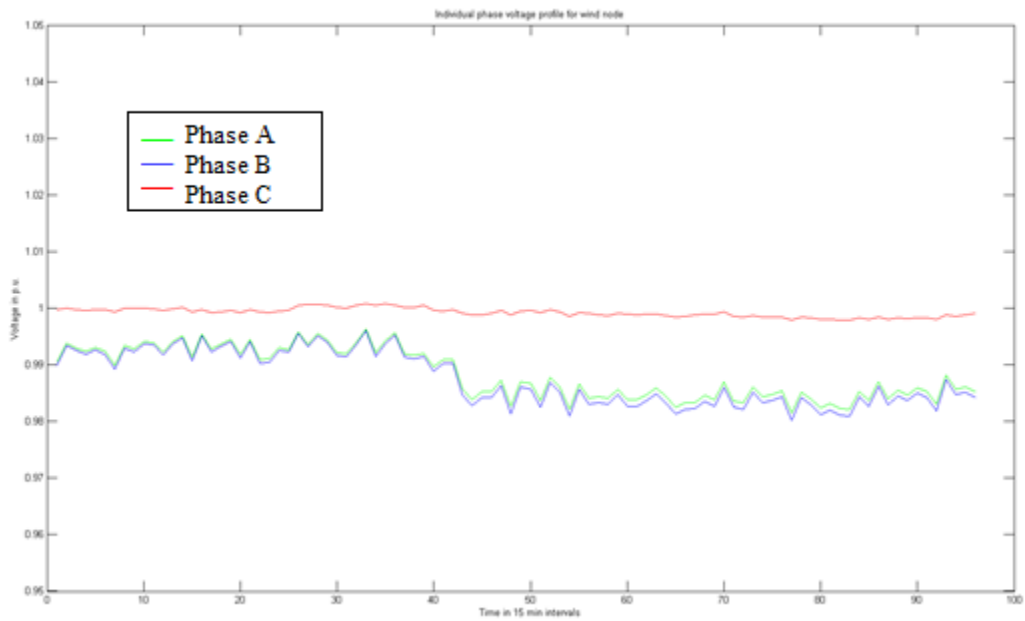


**Figure 6.19 Individual phase voltages for node 32 with direct wind connection and low wind for fifteen minute data**

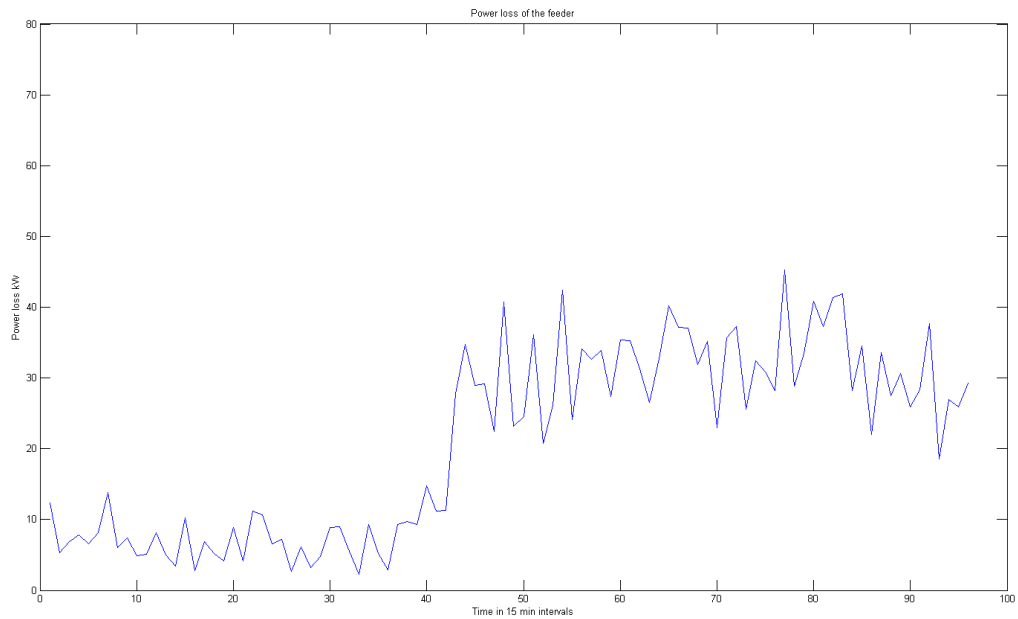


**Figure 6.20 Power losses for the feeder with direct wind connection and low wind for fifteen minute data**

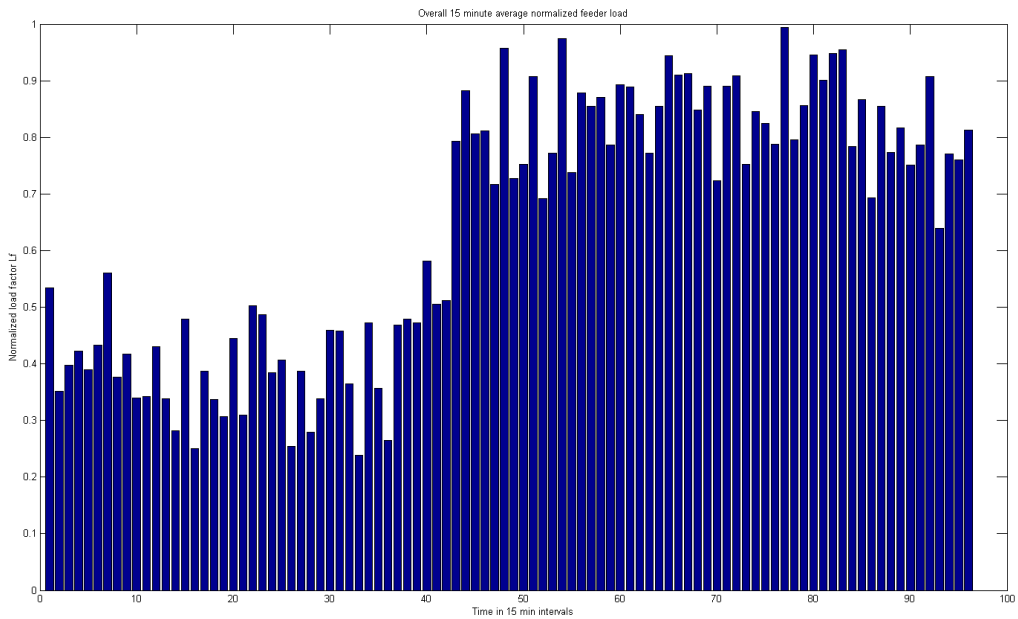


**Figure 6.21 Normalized fifteen minutes load histogram with direct wind connection and low wind**



The power flow results for one second basis forecasted load information and wind generation data have been given below in figures 6.22 through 6.26. It is seen that as in all the above cases, the peak load reduction is a direct function of wind generation availability, and the actual one second load of the feeder in spite of wind generation can be much higher than the average fifteen minute forecasted load. The peak reduction is also not very effective for one second wind generation as seen in the normalized demand plot. All the problems being observed in this section have been addressed in the next section.

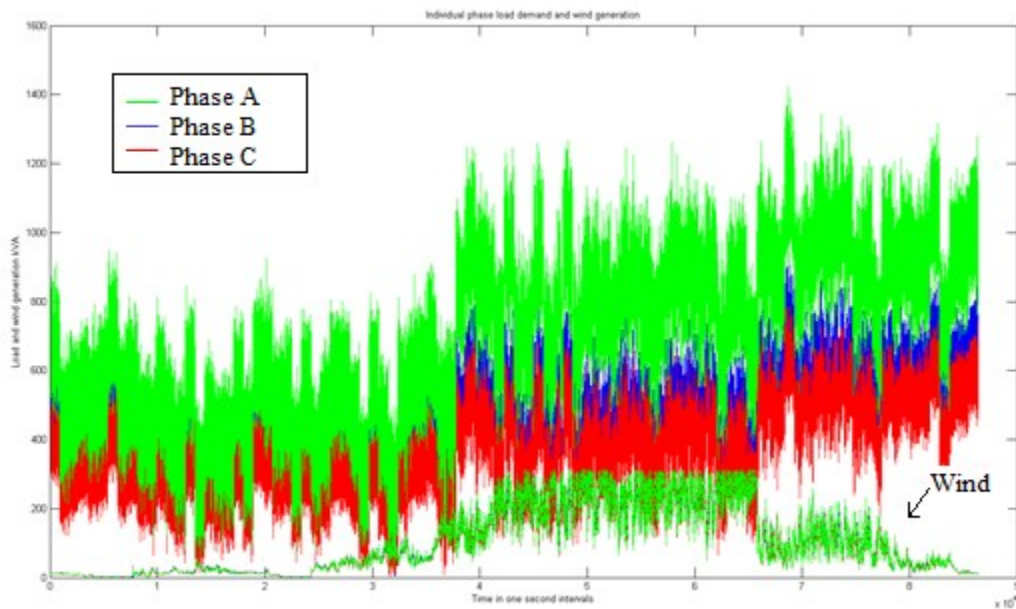


**Figure 6.22 Individual phase load demand for one second basis data with direct wind generation connection**

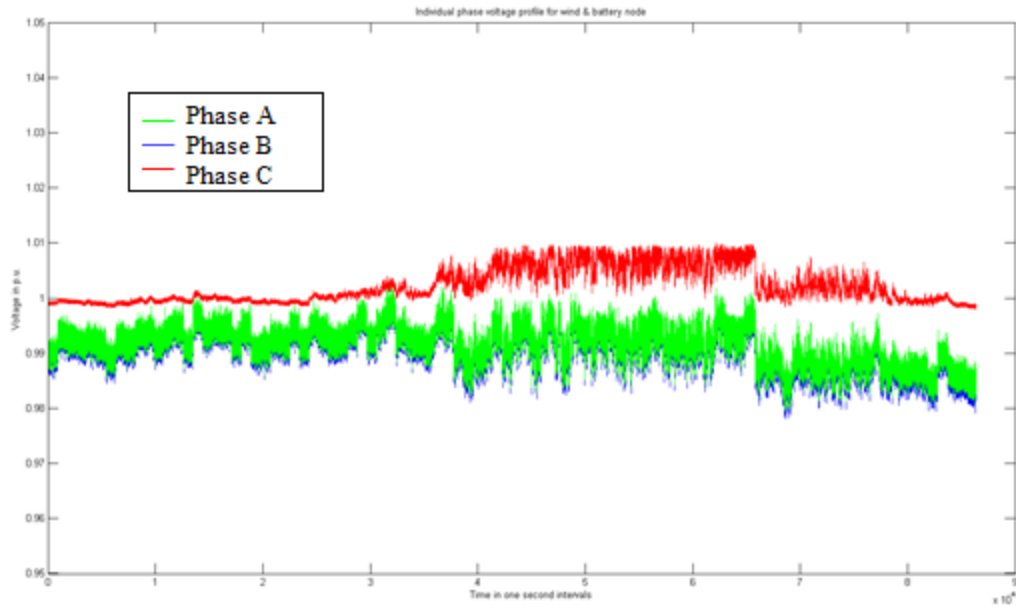


**Figure 6.23 Individual phase load voltages for one second basis data with direct wind generation connection**

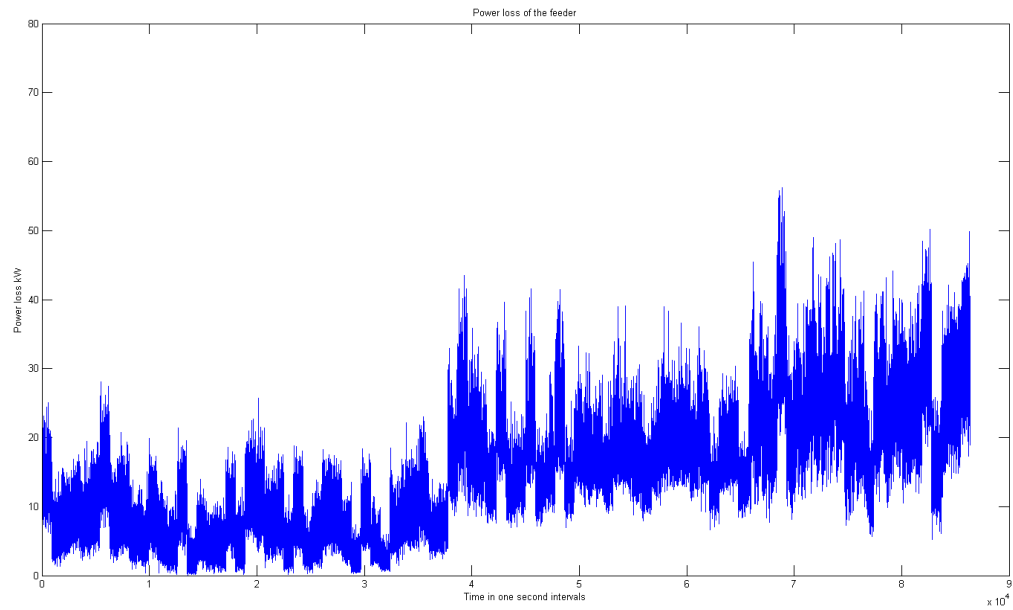


**Figure 6.24 Feeder power losses for one second basis data with direct wind generation connection**

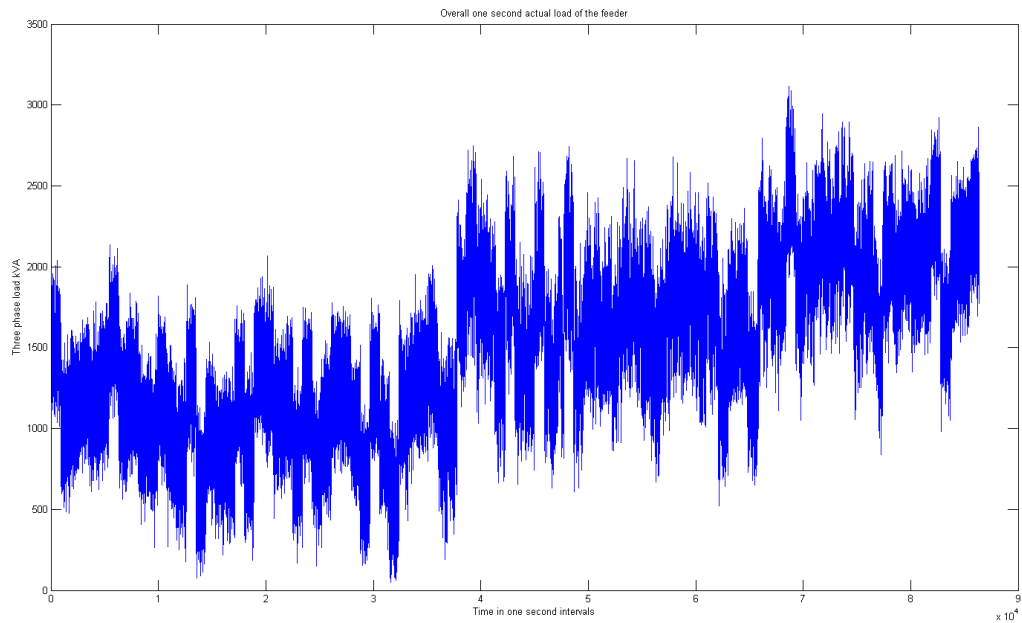


**Figure 6.25 Overall demand of the feeder for one second basis data with direct wind generation connection**

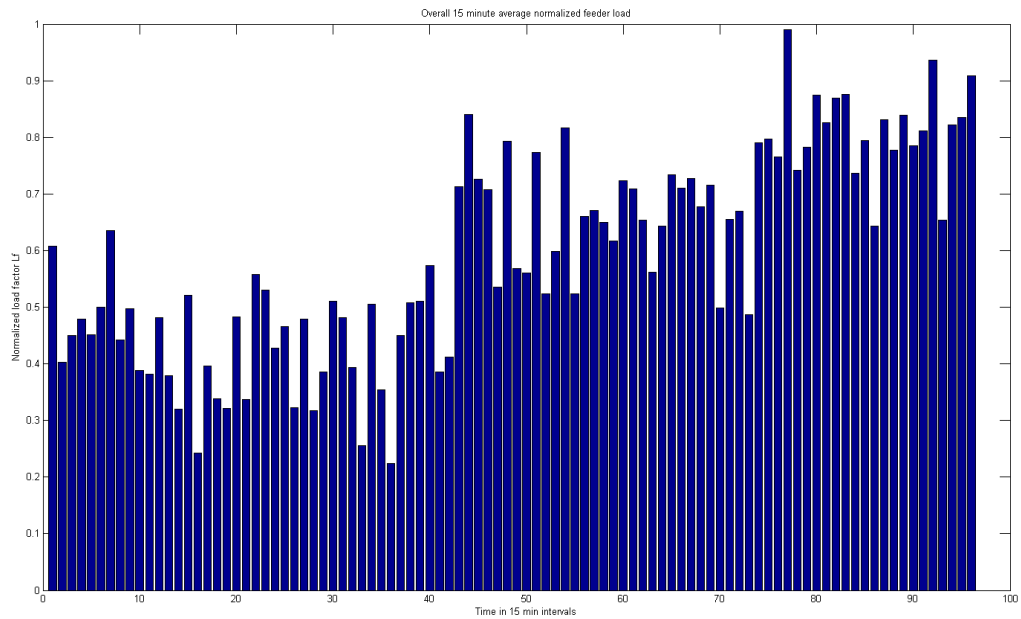


**Figure 6.26 Fifteen minute average normalized demand of the feeder for one second basis data with direct wind generation connection**

## 6.2 Results obtained for wind generation and battery storage integration for forecasted load information

In this section, results that were obtained for battery integration along with wind generation into the test feeder have been discussed. The results have been obtained for both fifteen minute data as well as one second data. In the results that follow, the plots obtained for individual phase loads, feeder losses and voltage profile of the critical feeder are not shown due to similarity and redundancy of results when battery storage is integrated into the system. The initial results shown are for wind and battery integration in case of fifteen minute data for low wind, medium wind and high wind conditions. The two methods of charging and discharging the battery that were described earlier, namely wind charging, sustained average load charging, free running discharge and conservative discharge methods and their results have been presented below for the fifteen minute data. The results shown only pertain to battery power of charging and discharging, energy level of the battery, overall one second actual load demand after storage integration, and the 15-minute normalized demand of the feeder. In all the energy plots, the black line indicates the minimum capacity beyond which the battery cannot be discharged any further. The results for high wind generation for fifteen minute data are given in figures 6.27 to 6.29.

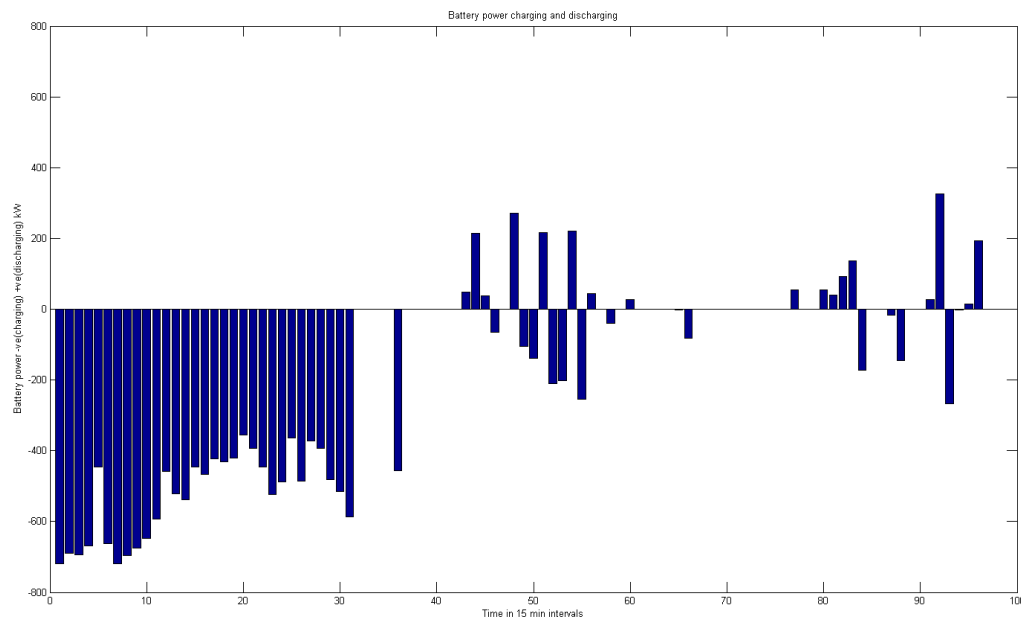


**Figure 6.27 Battery charging and discharging for fifteen minute data with high wind generation in free-running discharge and wind charging**

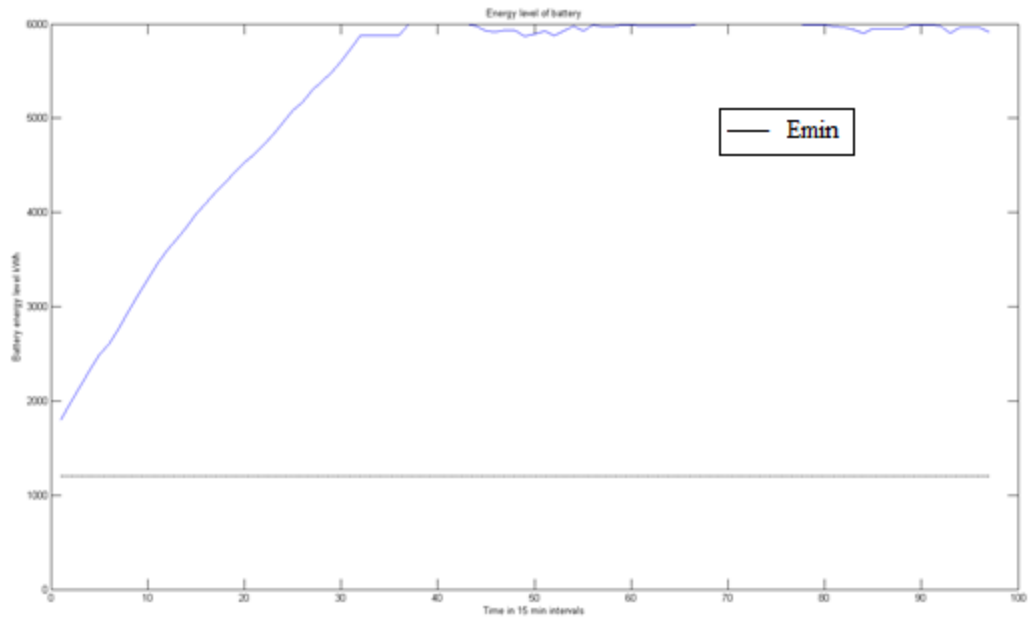


**Figure 6.28 Battery state of charge for fifteen minute data with high wind generation in free-running discharge and wind charging**

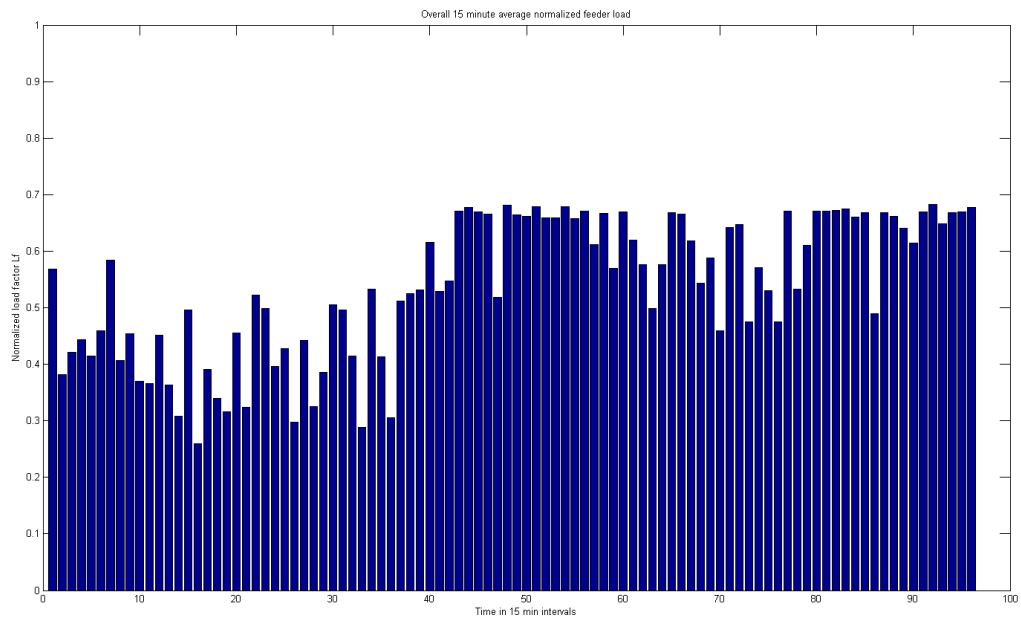


**Figure 6.29 Normalized overall feeder load demand for fifteen minute data with high wind generation in free-running discharge and wind charging**

The peak reduction achieved in case of even the fifteen minute low resolution data for battery discharging is high in cases of high wind generation. But the battery capacity cannot be effectively utilized as wind generation is available abundantly but cannot be stored effectively due to the non-availability of high resolution information. The results for free running discharge and sustained average load charging are given in figures 6.30 to 6.32.

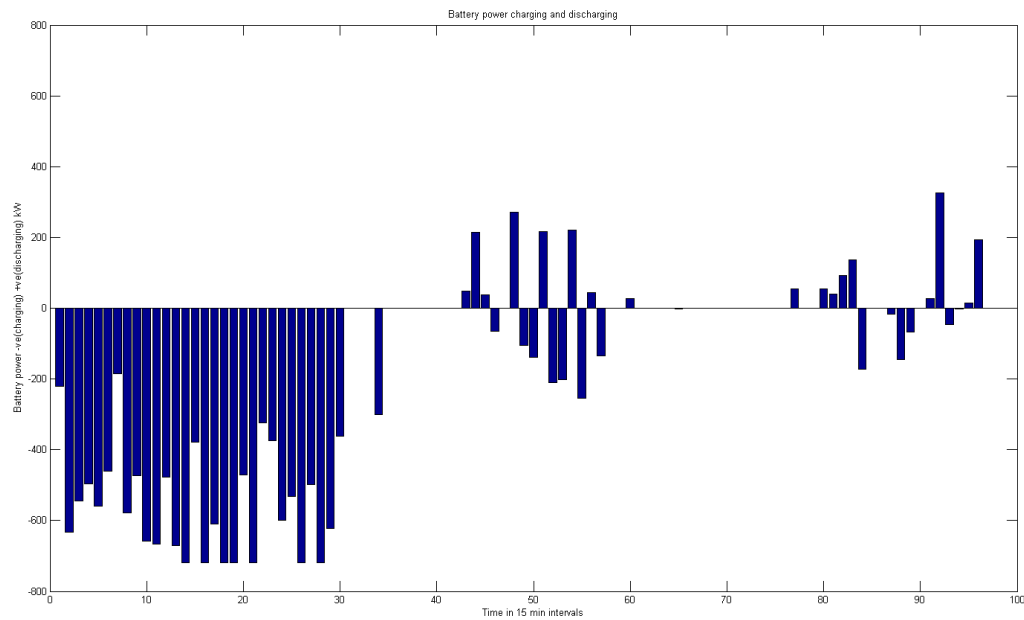


**Figure 6.30 Battery charging and discharging for fifteen minute data with high wind generation in free-running discharge and sustained average load charging**

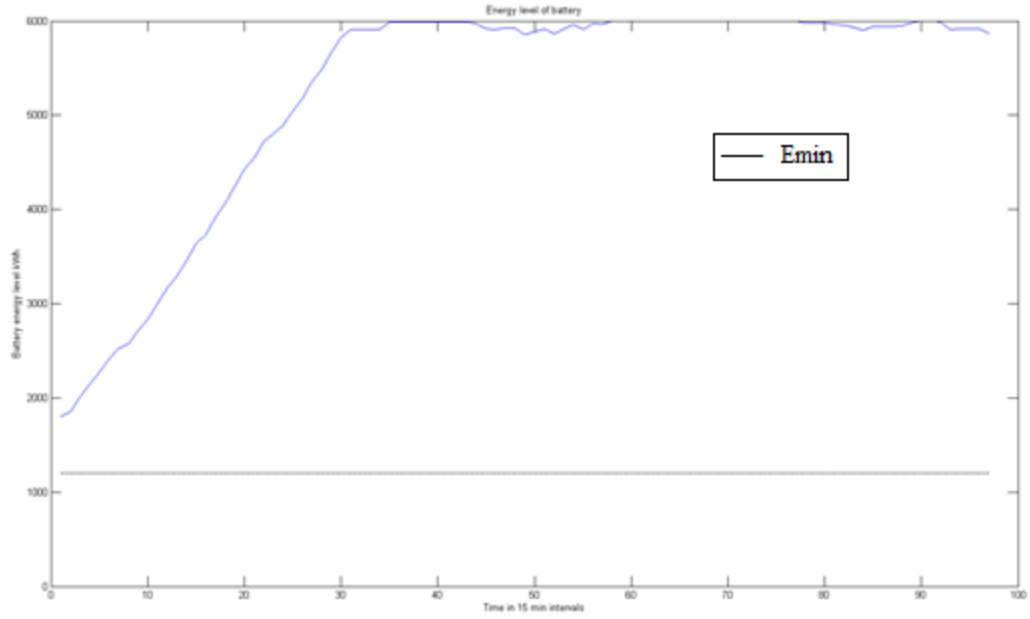


**Figure 6.31 Battery state of charge for fifteen minute data with high wind generation in free-running discharge and sustained average load charging**

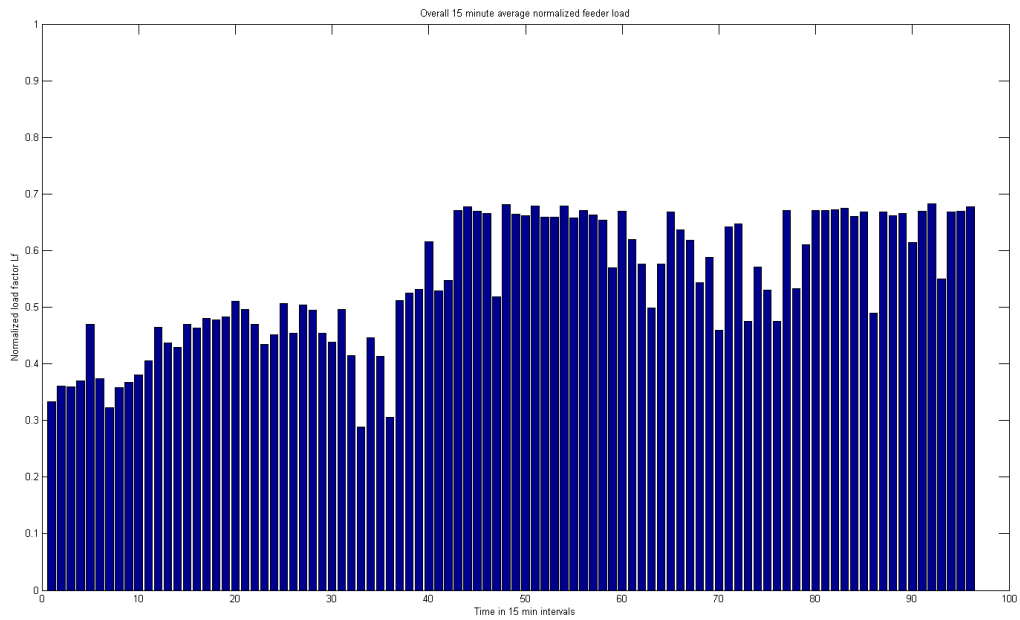


**Figure 6.32 Normalized overall fifteen minute demand histogram with high wind generation in free-running discharge and sustained average load charging**

The results obtained above are similar to the case without sustained average load charging. There is also no scope for the efficient utilization of wind generation due to lack of data resolution. The results obtained for conservative discharging mode with wind charging have been given in figures 6.33 to 6.35.

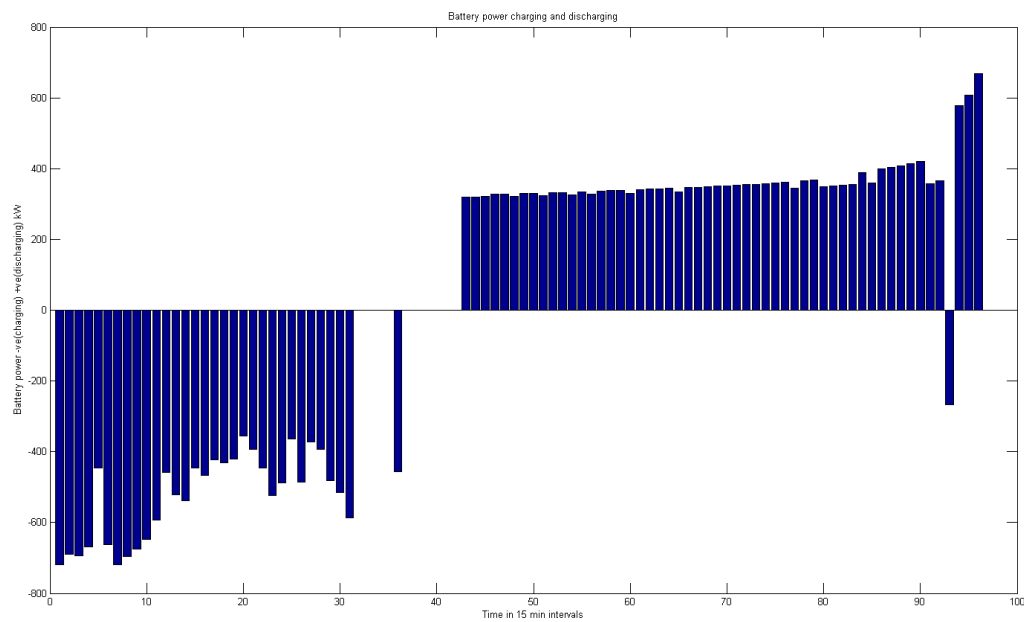


**Figure 6.33 Battery charging and discharging for fifteen minute data with high wind generation in conservative discharge and wind charging**



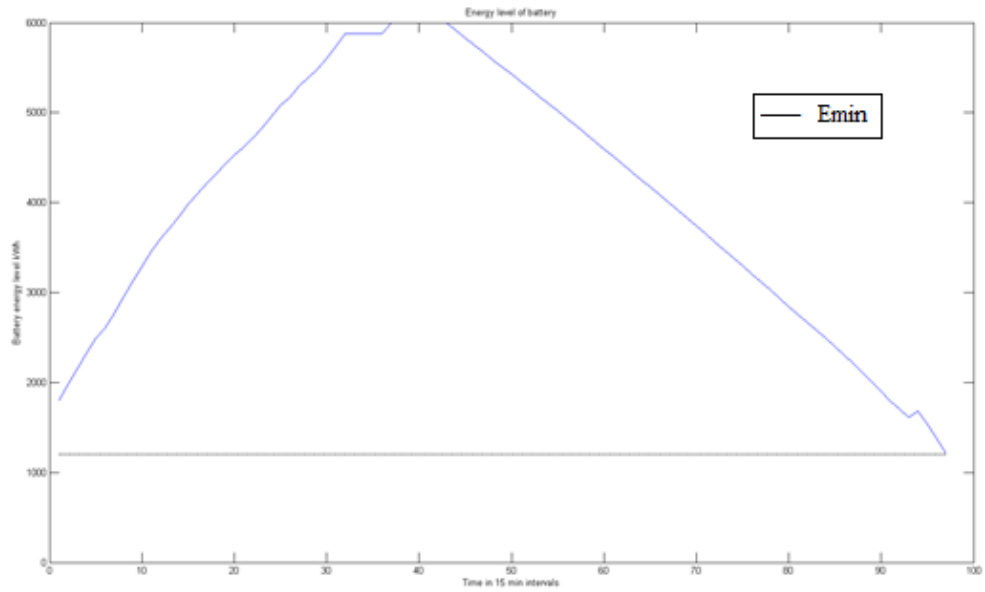


**Figure 6.34 Battery state of charge for fifteen minute data with high wind generation in conservative discharge and wind charging**

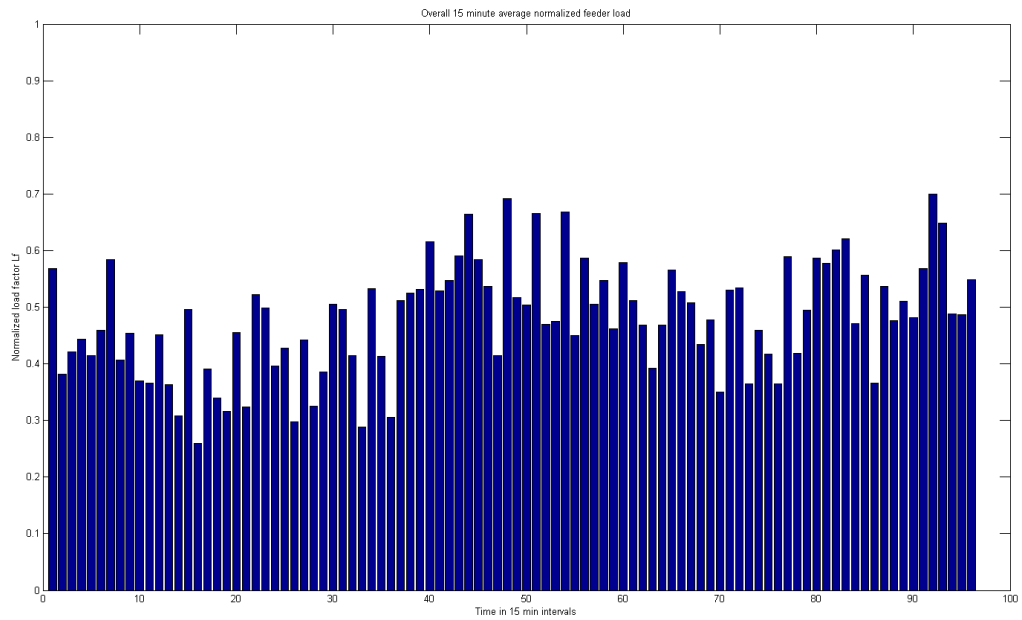


**Figure 6.35 Normalized demand histogram for fifteen minute data with high wind generation in conservative discharge and wind charging**

The peak reduction achieved in the case of conservative discharging with high wind generation and free running discharge is appreciable, but the battery is charged up to the highest level possible and also discharged to minimum in a single day. So, this method of discharge is only suitable for days during which wind generation is low in order to conserve battery capacity such that it is available for all the load intervals. The results obtained in case of high wind generation with sustained average load charging and conservative discharging are given in figures 6.36 to 6.38.

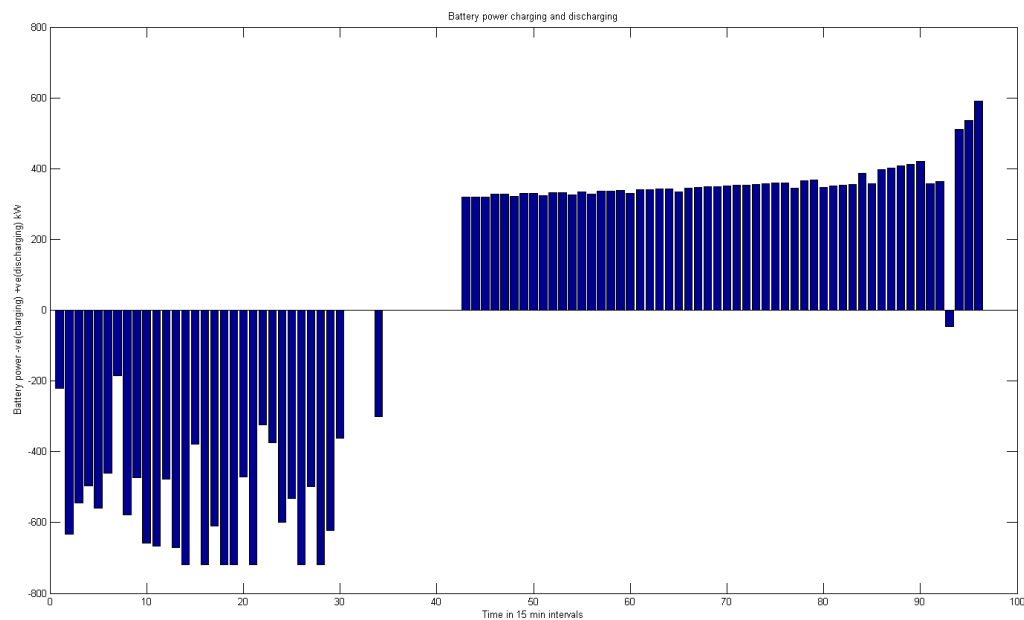


**Figure 6.36 Battery charging and discharging with high wind generation in conservative discharge and sustained average load charging**

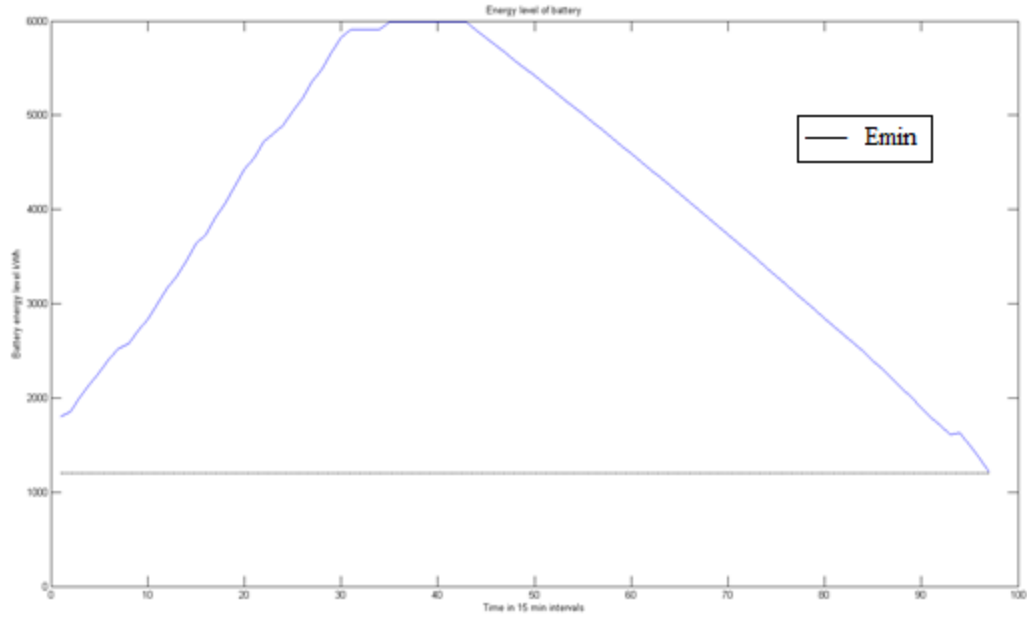


**Figure 6.37 Battery state of charge with high wind generation in conservative discharge and sustained average load charging**

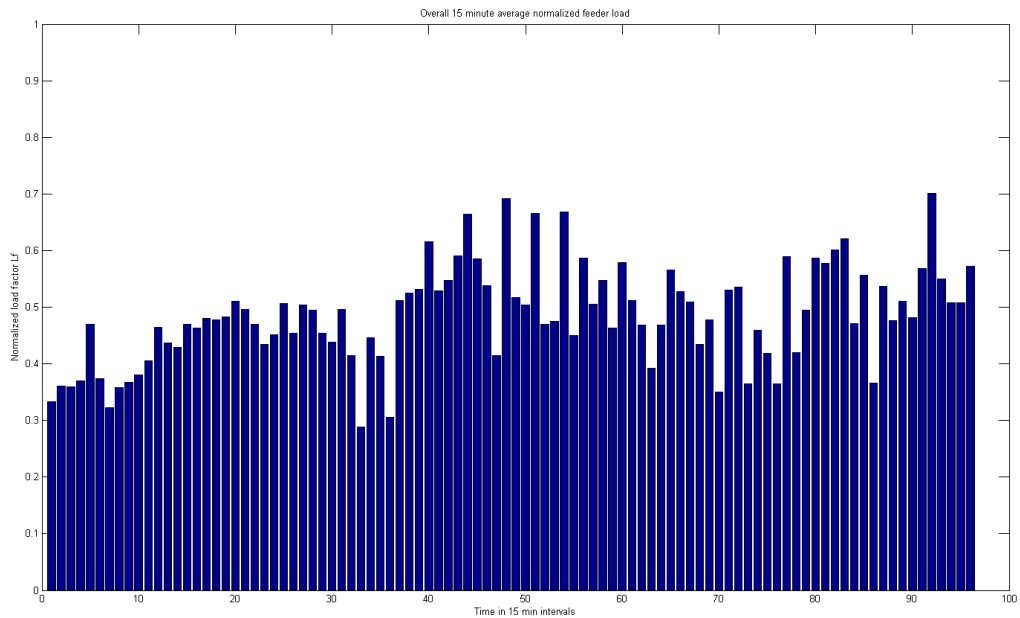


**Figure 6.38 Normalized demand histogram with high wind generation in conservative discharge and sustained average load charging**

The same results for all the four combinations of charging and discharging methods for the battery have been shown below for medium wind generation and low wind generation in figures 6.39 to 6.44.

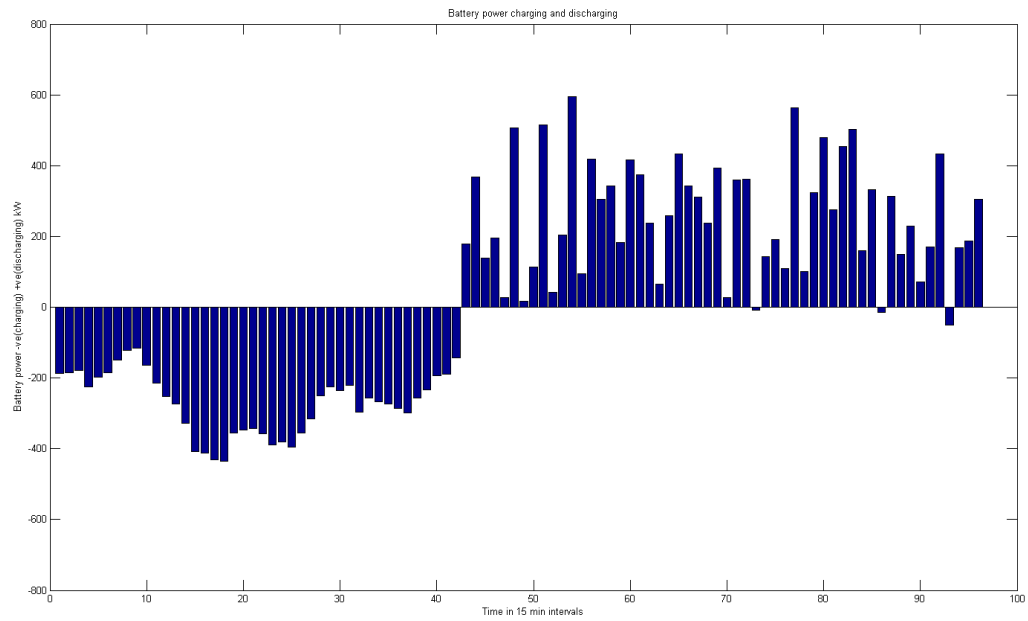


**Figure 6.39 Battery charging and discharging for fifteen minute data with medium wind generation in free-running discharge and wind charging**

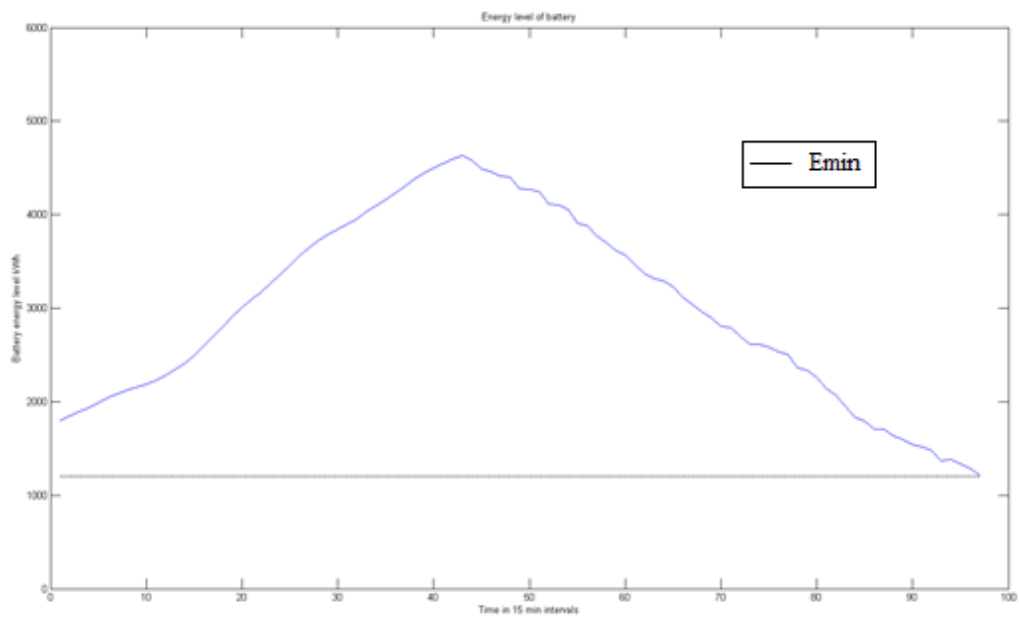


**Figure 6.40 Battery State of charge for fifteen minute data with medium wind generation in free-running discharge and wind charging**

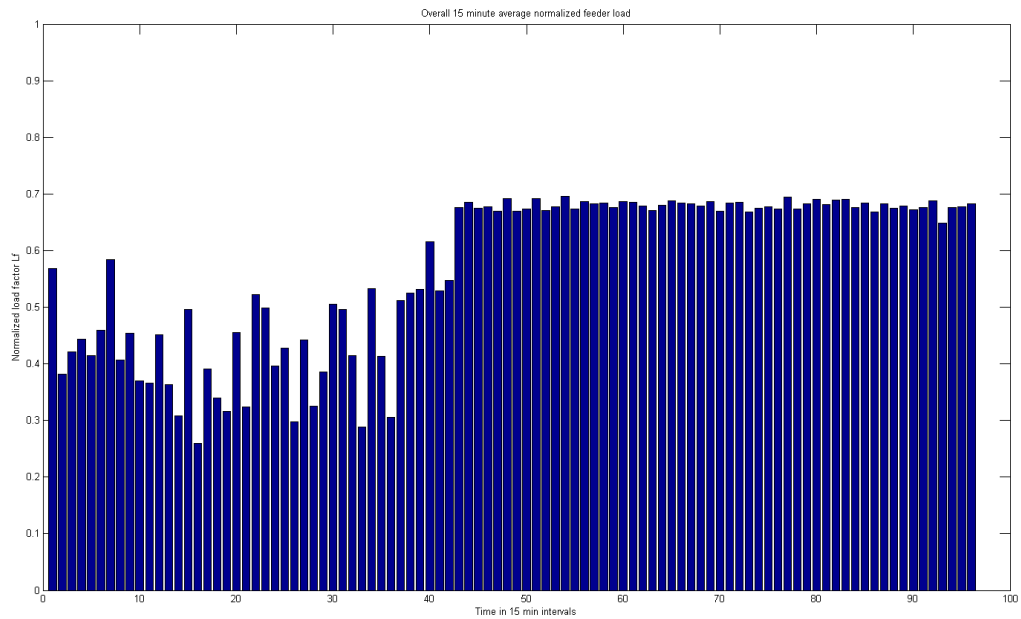


**Figure 6.41 Normalized overall feeder load demand for fifteen minute data with medium wind generation in free-running discharge and wind charging**

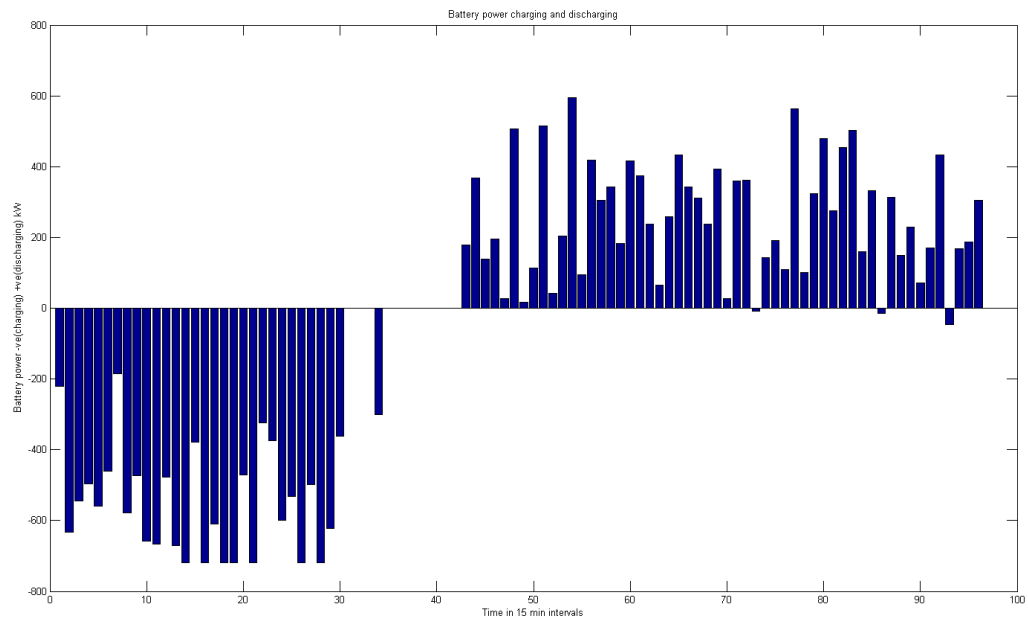


**Figure 6.42 Battery charging and discharging for fifteen minute data with medium wind generation in free-running discharge and sustained average load charging**

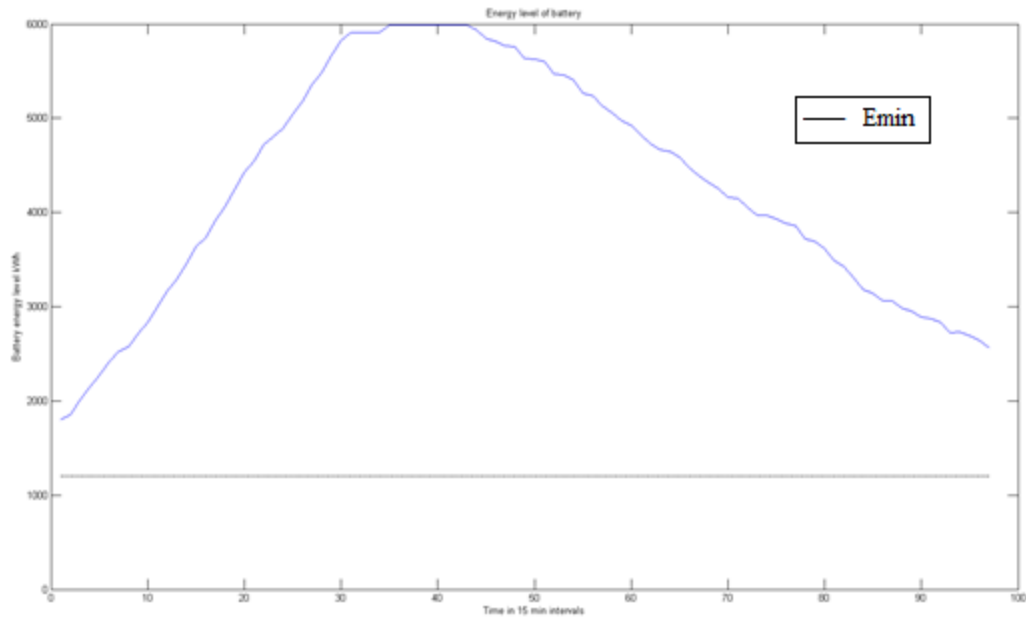


**Figure 6.43 Battery state of charge for fifteen minute data with medium wind generation in free-running discharge and sustained average load charging**

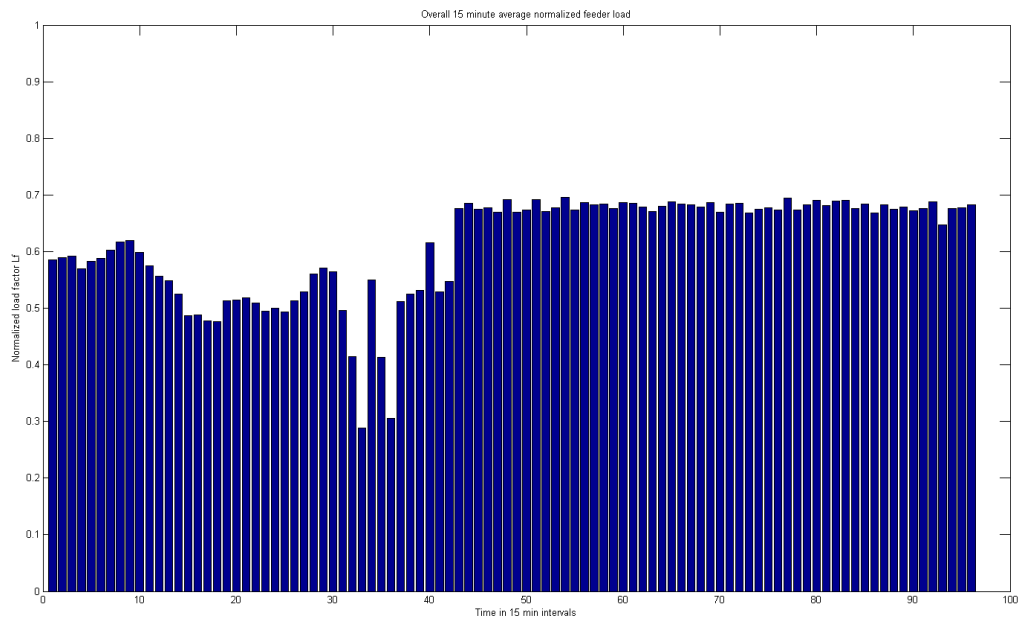


**Figure 6.44 Normalized overall fifteen minute demand histogram with medium wind generation in free-running discharge and sustained average load charging**

The difference that is clearly observed in this case is that on a given day during which an average amount of wind generation is available, if sustained average load charging is used, the average load tends to be higher than other cases. But the peak reduction is better than in other combinations of charging and discharging. The results for conservative discharging with wind charging as well as sustained average load charging have been given in figures 6.45 through 6.50.

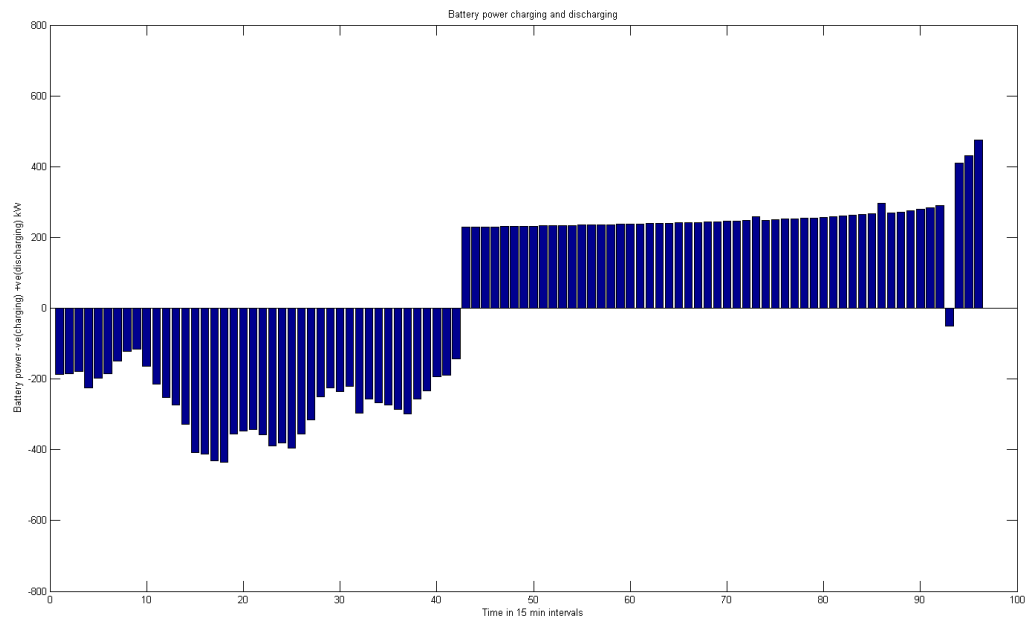


**Figure 6.45 Battery charging and discharging for fifteen minute data with medium wind generation in conservative discharge and wind charging**

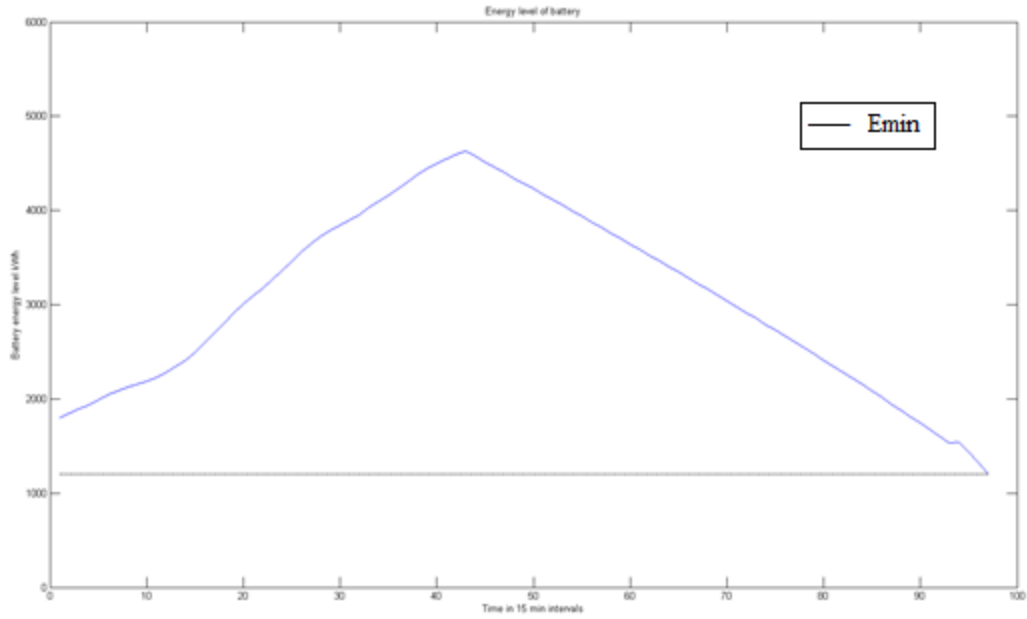


**Figure 6.46 Battery state of charge for fifteen minute data with medium wind generation in conservative discharge and wind charging**

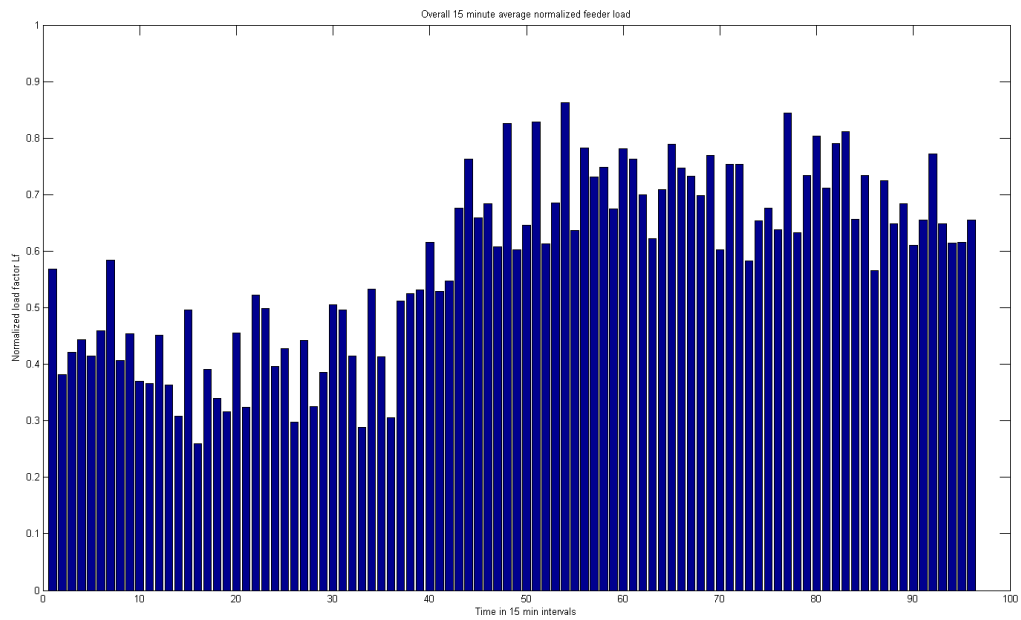


**Figure 6.47 Normalized overall fifteen minute demand histogram with medium wind generation in conservative discharge and wind charging**



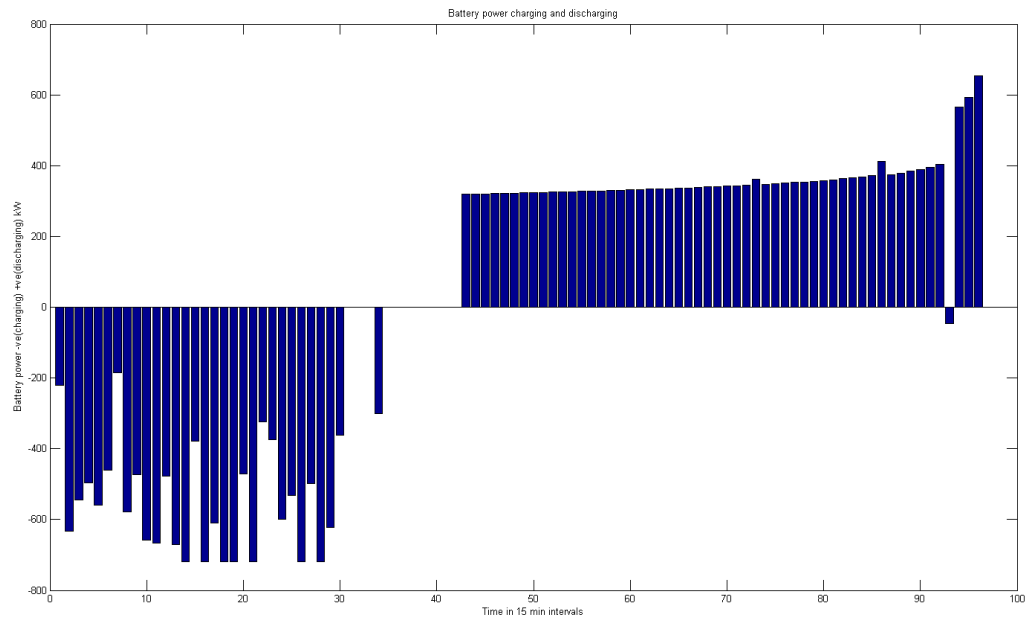


**Figure 6.48 Battery charging and discharging for fifteen minute data with medium wind generation in conservative discharge and sustained average load charging**

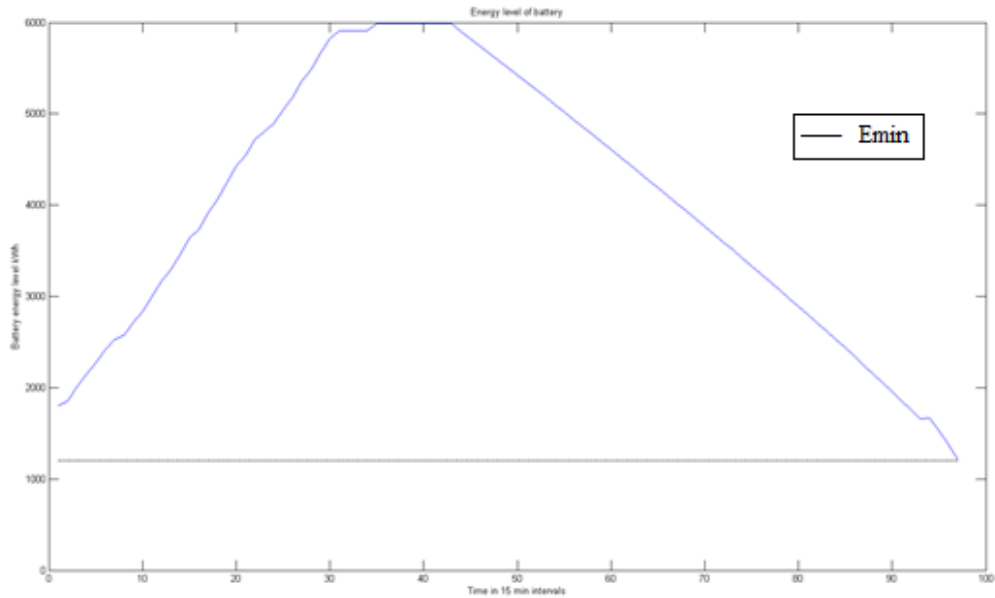


**Figure 6.49 Battery state of charge for fifteen minute data with medium wind generation in conservative discharge and sustained average load charging**

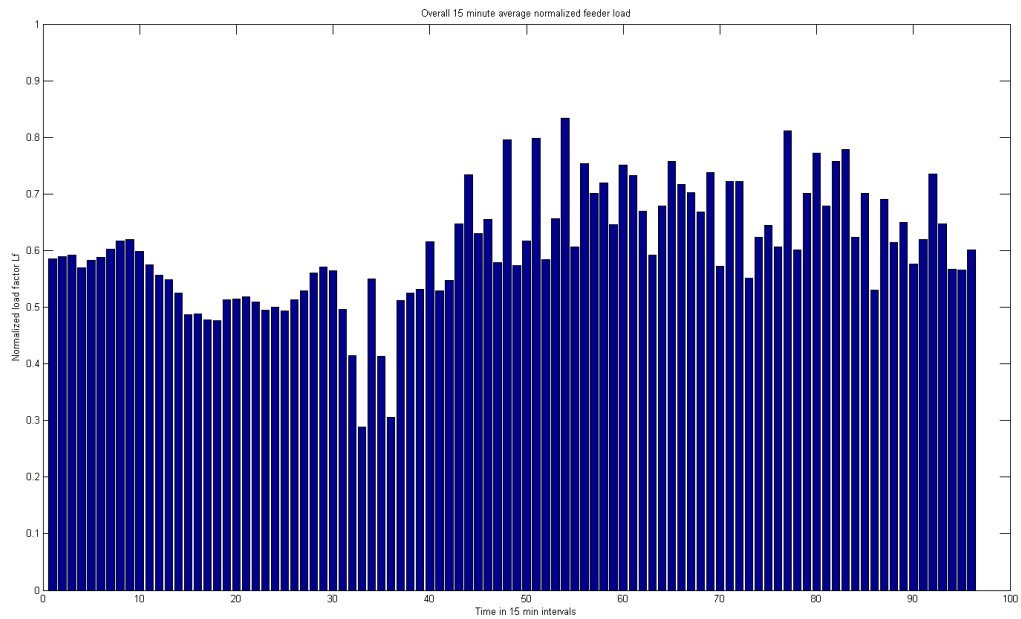


**Figure 6.50 Normalized overall fifteen minute demand histogram with medium wind generation in conservative discharge and sustained average load charging**

The results given below in figures 6.51 through 6.56 are for low wind generation with all the four combinations of charging and discharging methods for fifteen minute data.

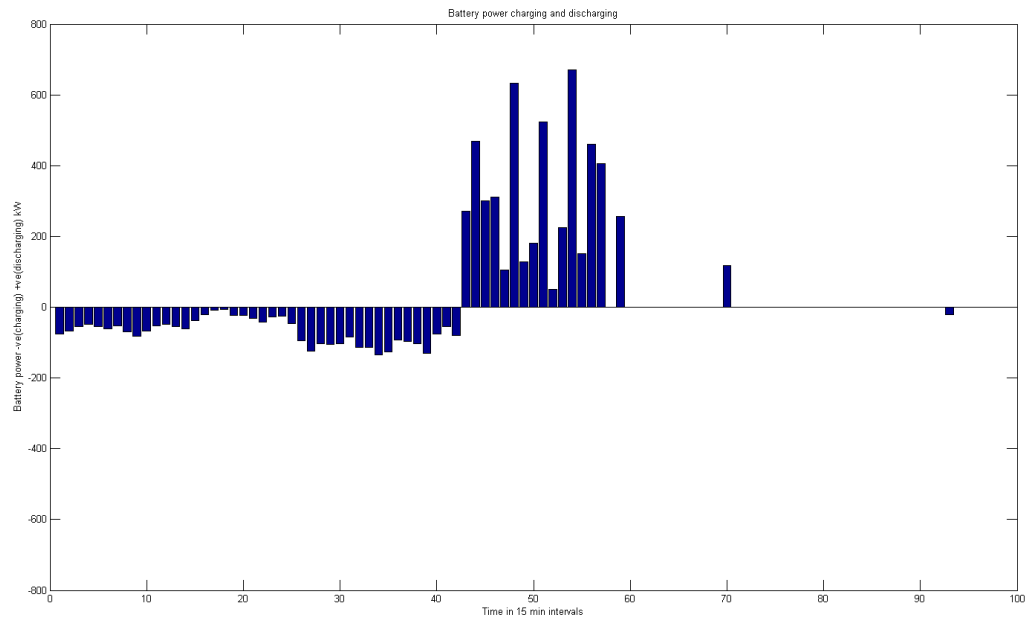


**Figure 6.51 Battery charging and discharging for fifteen minute data with low wind generation in free-running discharge and wind charging**

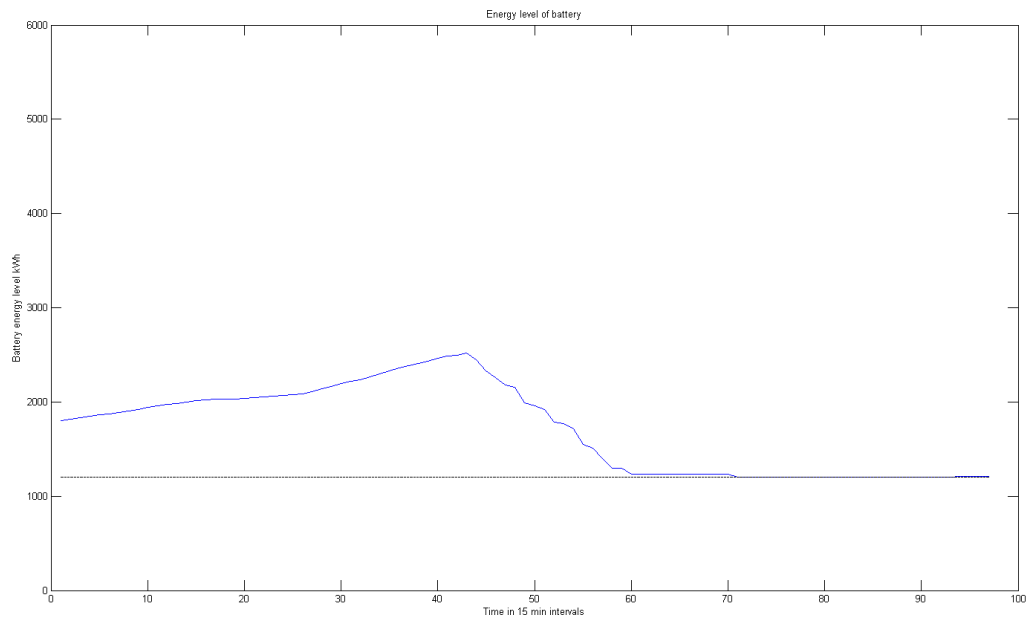


**Figure 6.52 Battery state of charge for fifteen minute data with low wind generation in free-running discharge and wind charging**

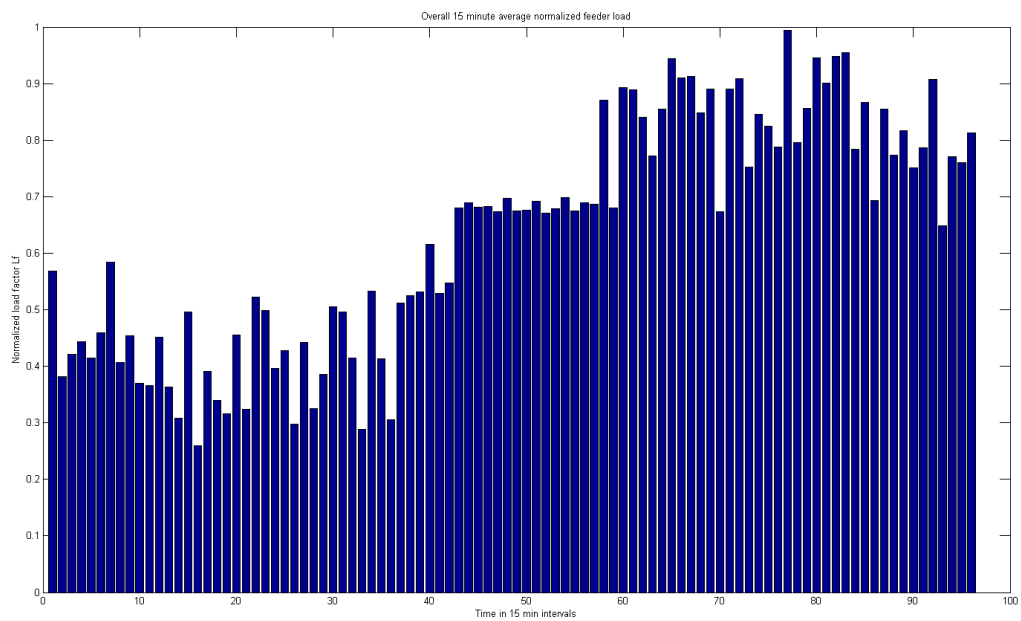


**Figure 6.53 Normalized overall feeder load demand for fifteen minute data with low wind generation in free-running discharge and wind charging**

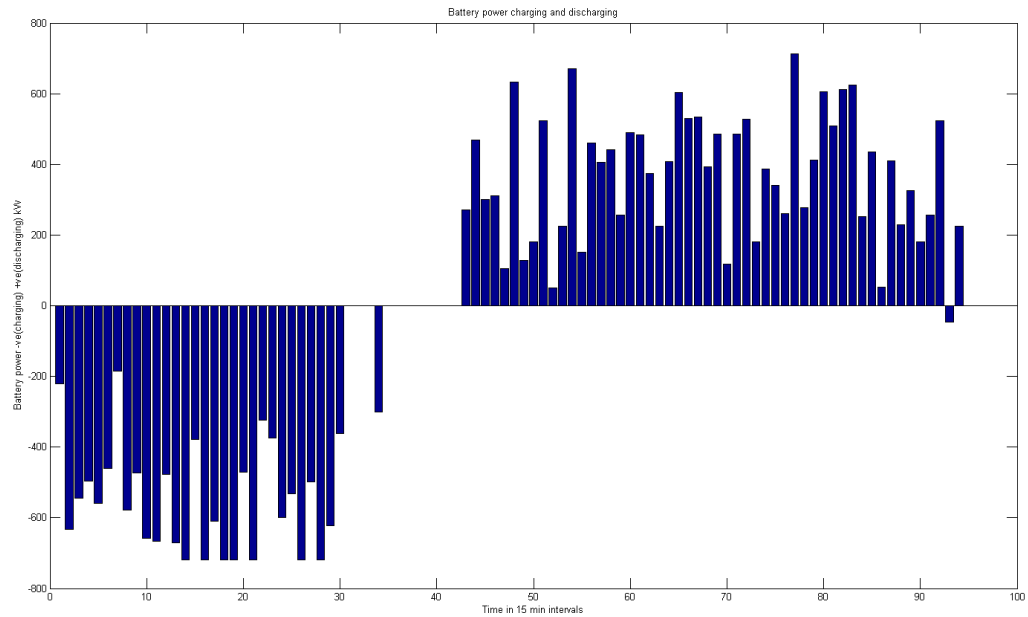


**Figure 6.54 Battery charging and discharging for fifteen minute data with low wind generation in free-running discharge and sustained average load charging**

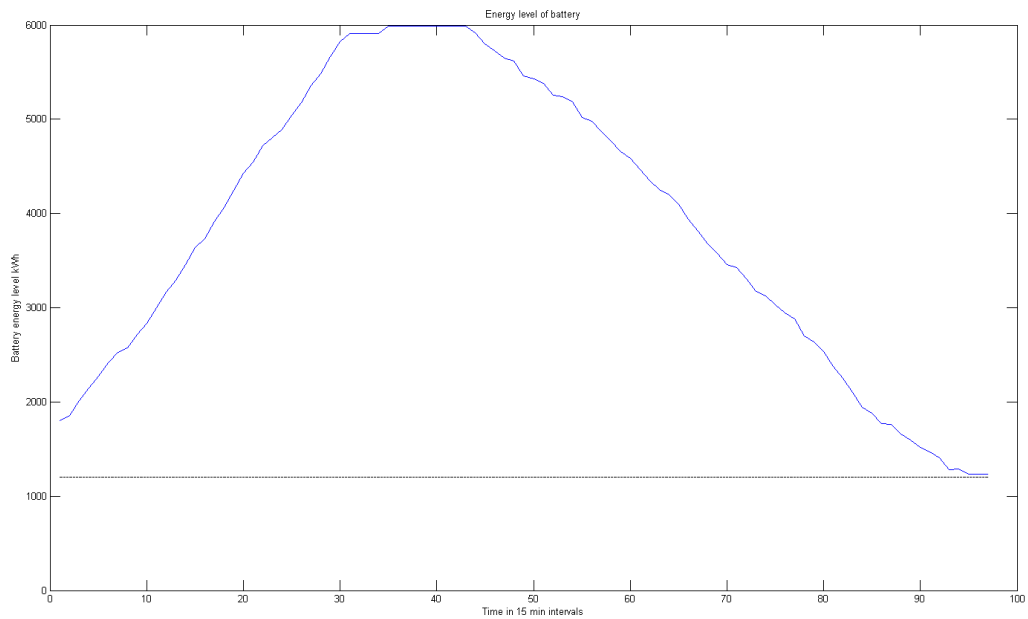


**Figure 6.55 Battery state of charge for fifteen minute data with low wind generation in free-running discharge and sustained average load charging**

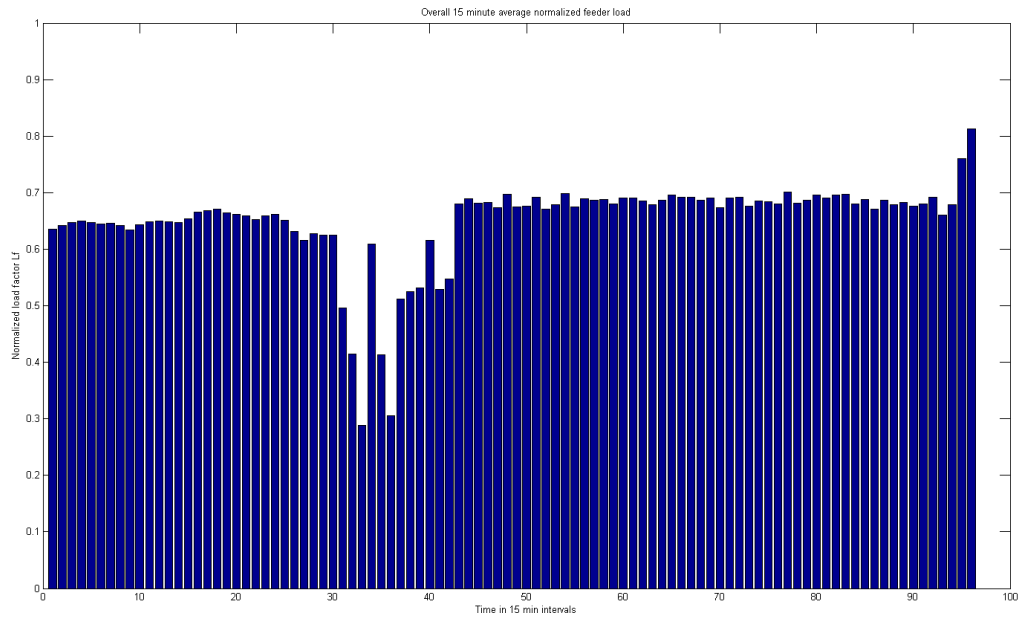


**Figure 6.56 Normalized overall fifteen minute demand histogram with low wind generation in free-running discharge and sustained average load charging**

As it can be seen from the results described above, free-running mode of discharging does not perform well under low wind conditions. This is one of the reasons that the sustained average load approach was developed in this research as a future alternative to solving the low wind generation problem. But it is also seen that, there are more losses associated with the distribution feeder when sustained average load approach is used to charge up the battery. The results given from figures 6.57 through 6.62 are for low wind generation using conservative discharging with both the kinds of charging methods.

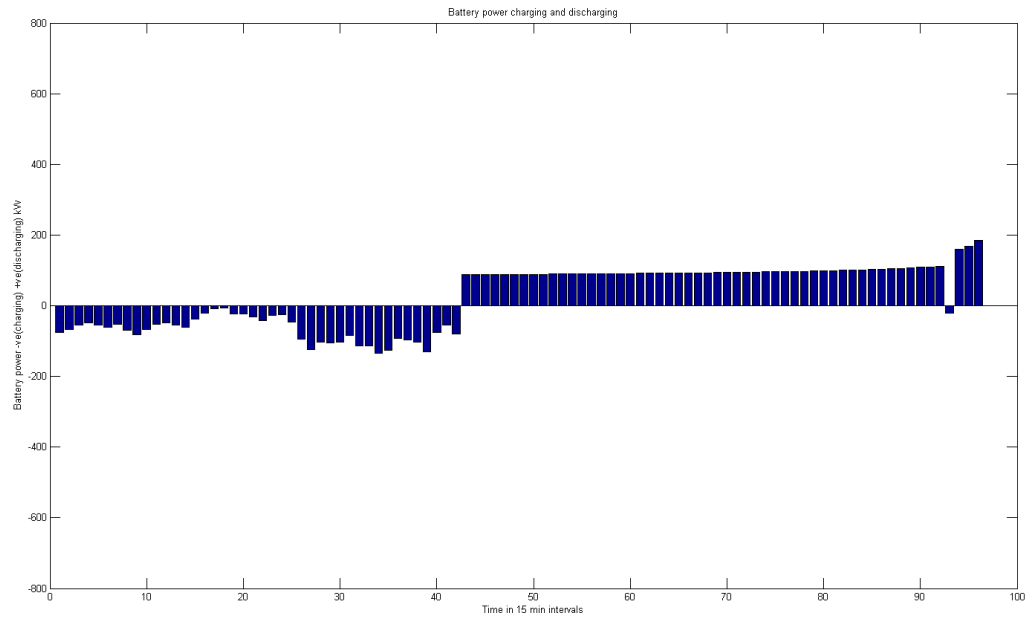


**Figure 6.57 Battery charging and discharging for fifteen minute data with low wind generation in conservative discharge and wind charging**

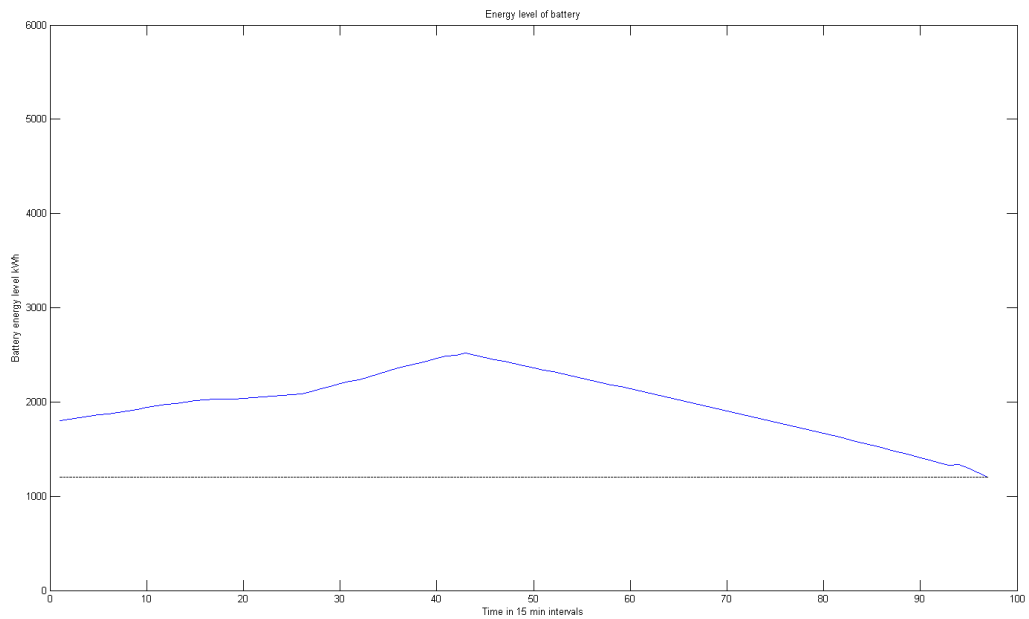


**Figure 6.58 Battery state of charge for fifteen minute data with low wind generation in conservative discharge and wind charging**

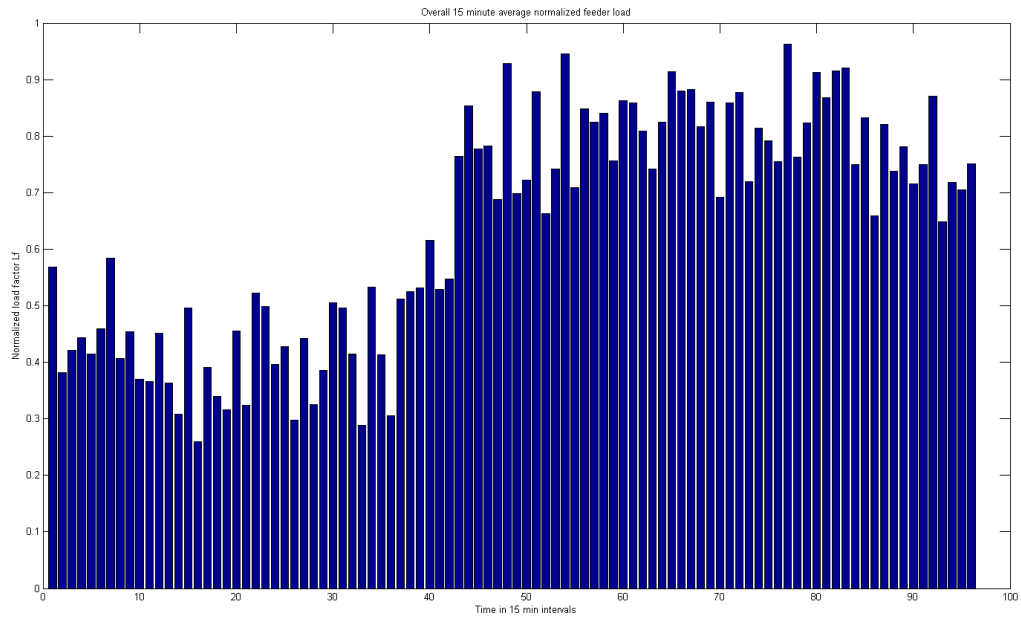


**Figure 6.59 Normalized overall fifteen minute demand histogram with low wind generation in conservative discharge and wind charging**

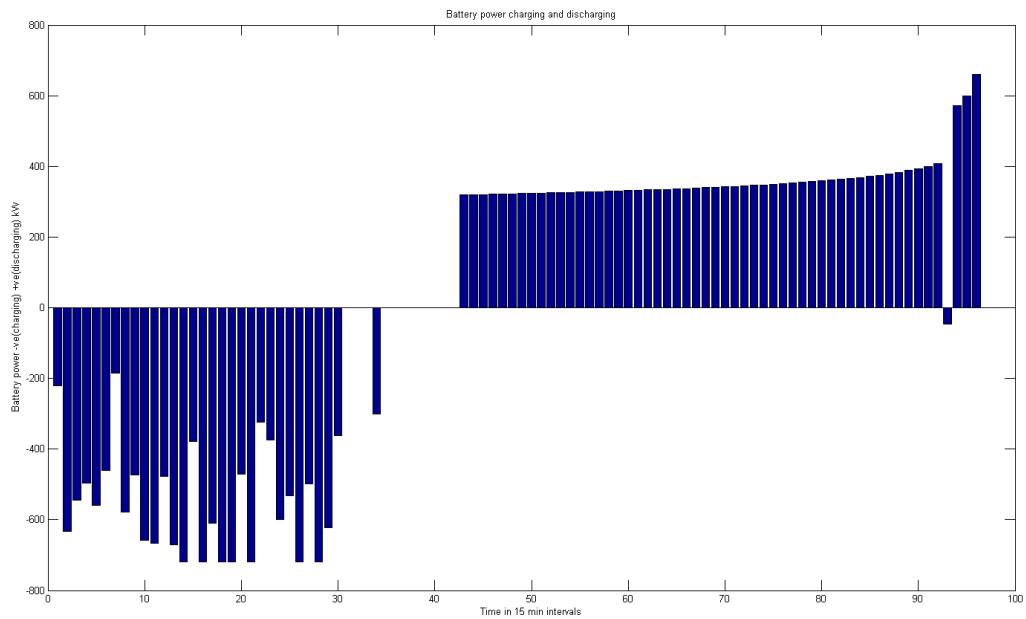


**Figure 6.60 Battery charging and discharging for fifteen minute data with medium wind generation in conservative discharge and sustained average load charging**

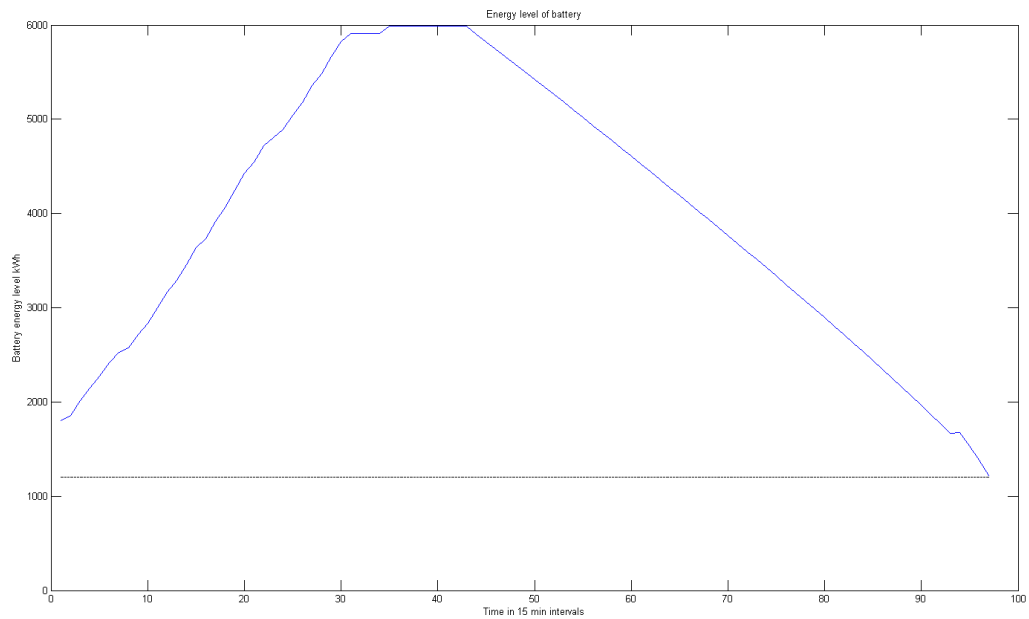


**Figure 6.61 Battery state of charge for fifteen minute data with medium wind generation in conservative discharge and sustained average load charging**

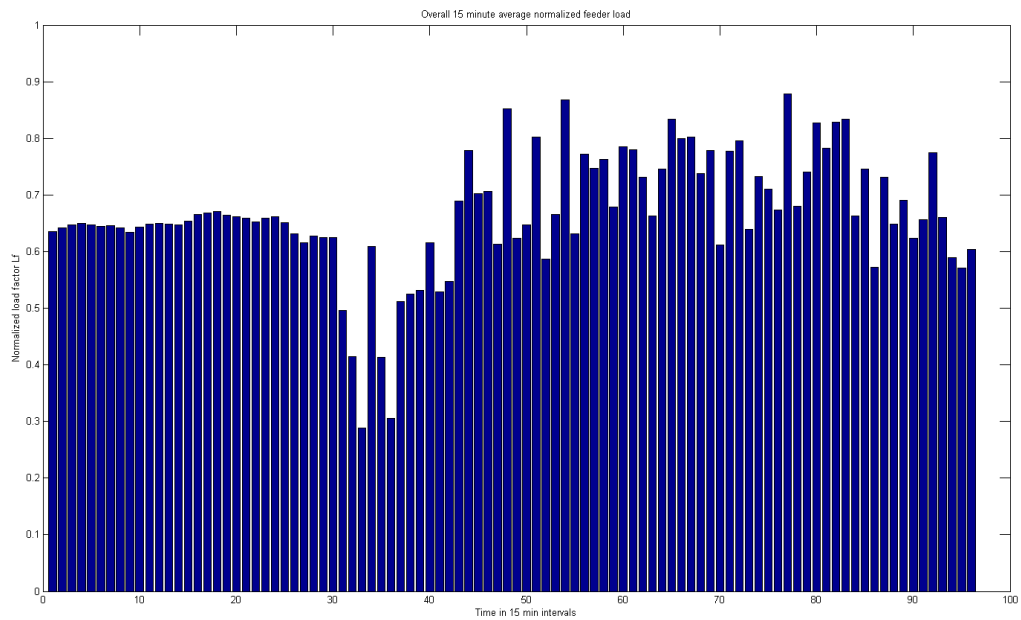


**Figure 6.62 Normalized overall fifteen minute demand histogram with medium wind generation in conservative discharge and sustained average load charging**



Many observations are made overall when fifteen minute data are used. The battery capacity is used completely most of the time even to the point of not effectively being able to store wind energy when its importance is not high. This is mainly due to the absence of dynamic load information which results in a fifteen minute averaged value of either charging or discharging the battery. The free running mode works best when medium to high level of wind generation is available. The conservative discharging mode of operation is best suited to days on which wind generation is very limited as it becomes possible to conserve battery capacity. Similarly, wind charging mode of operation is ideal for most days as wind generation is available, but if there is little or no wind generation, there might be no storage of wind energy in the battery to ensure peak reduction. This problem is overcome using sustained average load charging. This method is especially suitable for areas where wind generation is low, but under current technology trends, the advanced controller required for the operation in this method may not be available as yet. So, this is not a real time mode of operation.

The differences in performance that can be achieved when one second forecasted load is used are tremendous. The peak reduction, the reduction in average load, and the reduction in the battery capacity used are improved greatly when one second load forecast is used. The four combinations of charging and discharging methods described before have been tested here as well, for one case of wind generation data. Again, results obtained for individual phase demand, losses and voltage profile are not displayed due to redundancy and similarity in results, making them indistinguishable. However, battery charging and discharging, battery state of charge, overall one second demand of the feeder, and fifteen minute average normalized demand have been displayed. Also, the results for all cases have been tabulated for comparison at the end of this section.

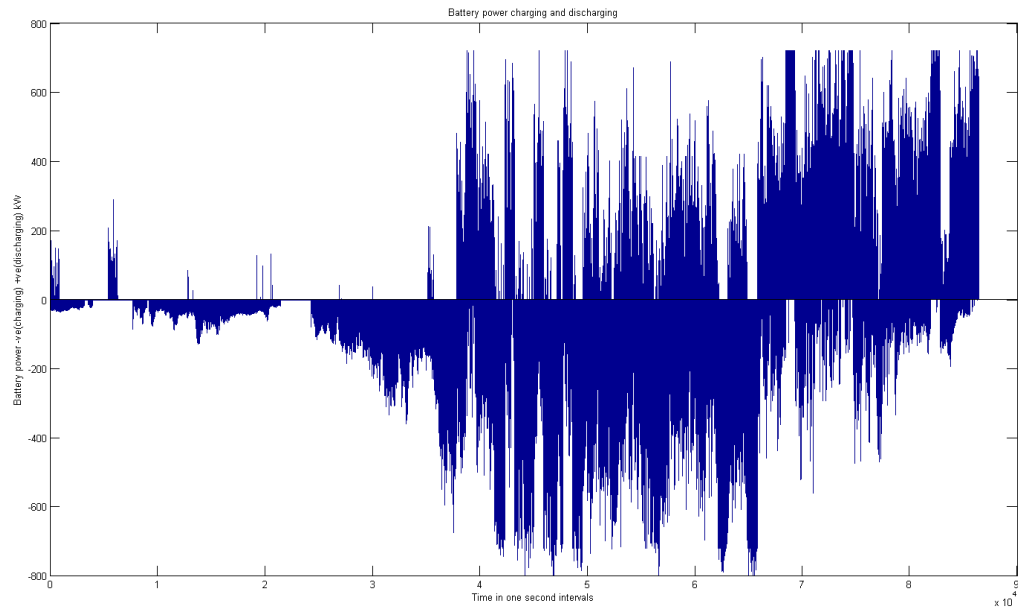


**Figure 6.63 Battery charging and discharging for one second forecasted load data in free-running discharging and wind charging modes**

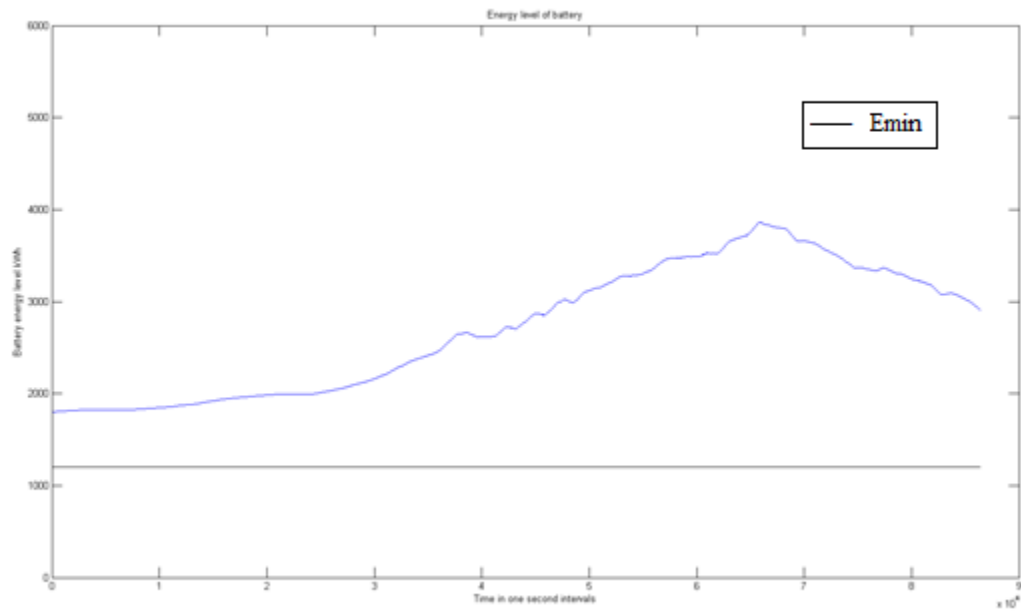


**Figure 6.64 Battery state of charge for one second forecasted load data in free-running discharging and wind charging modes**

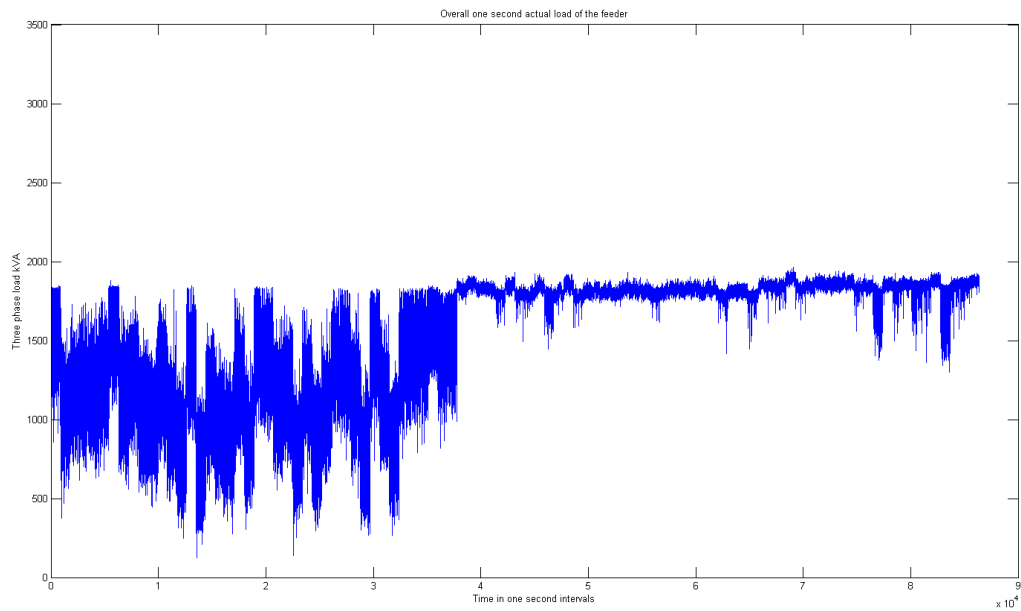


**Figure 6.65 Overall one second actual load demand after peak reduction for one second forecasted load data in free-running discharging and wind charging modes**

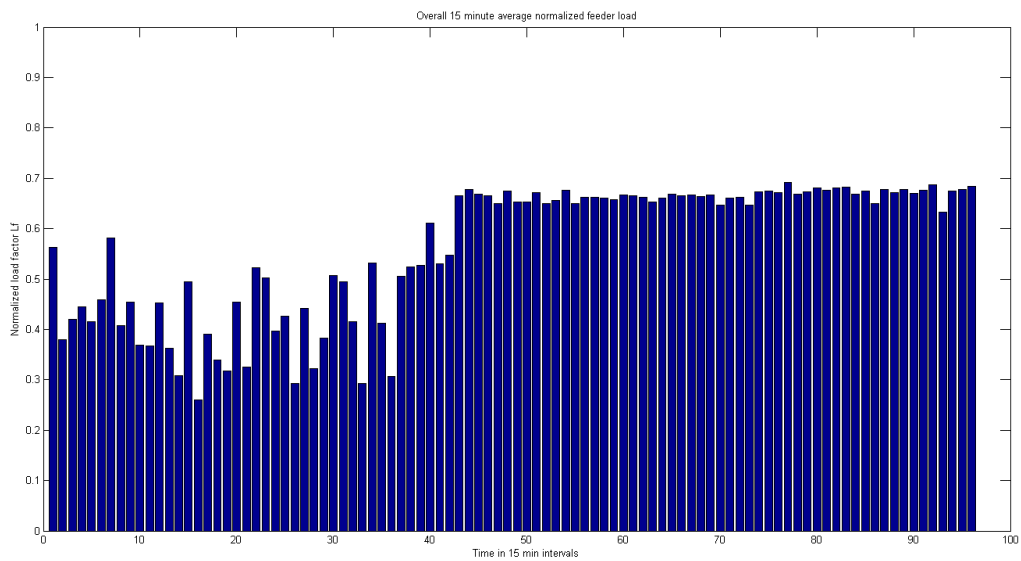


**Figure 6.66 Fifteen minute average normalized load demand after peak reduction for one second forecasted load data in free-running discharging and wind charging modes**

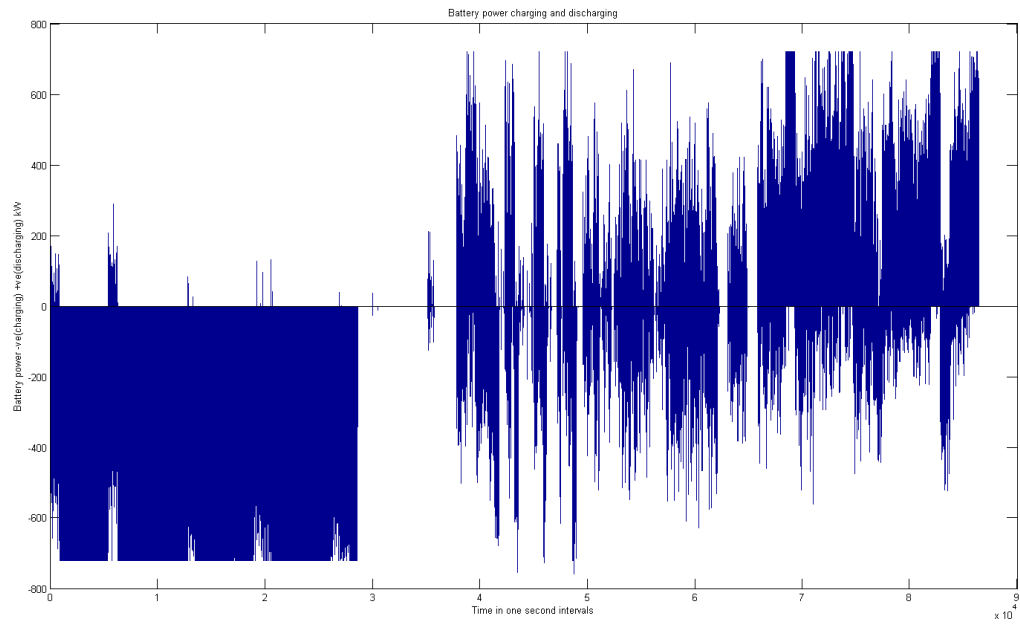


**Figure 6.67 Battery charging and discharging for one second forecasted load data in free-running discharging and sustained average load charging modes**

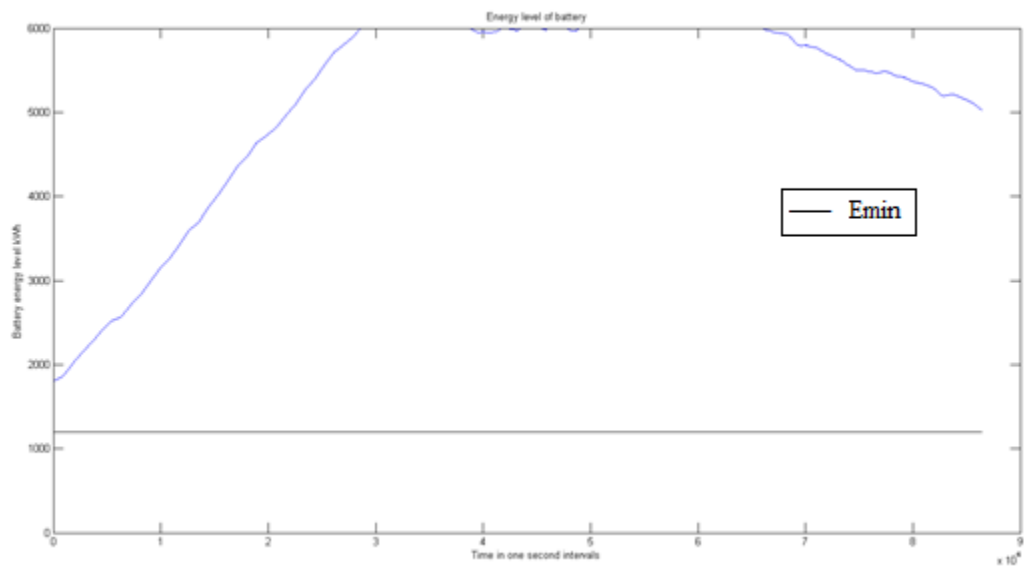


**Figure 6.68 Battery state of charge for one second forecasted load data in free-running discharging and sustained average load charging modes**

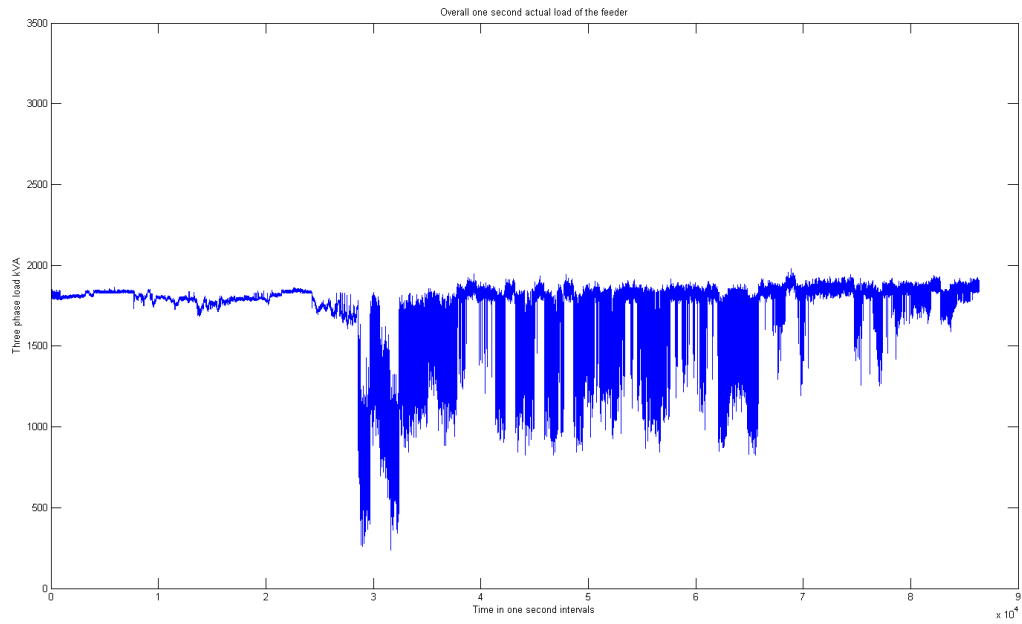


**Figure 6.69 Overall one second actual load demand after peak reduction for one second forecasted load data in free-running discharging and sustained average load charging modes**

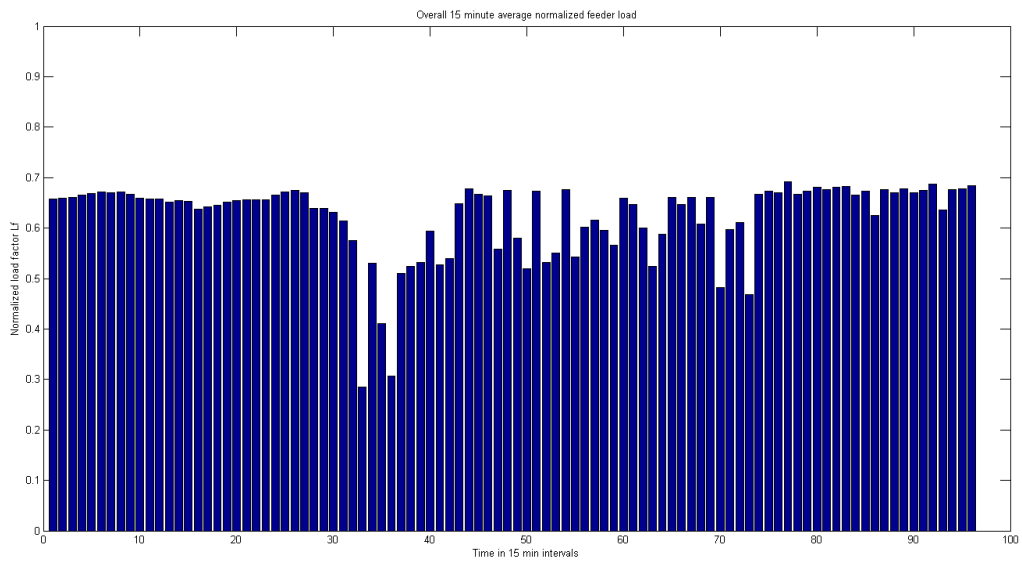


**Figure 6.70 Fifteen minute average normalized load demand after peak reduction for one second forecasted load data in free-running discharging and sustained average load charging modes**

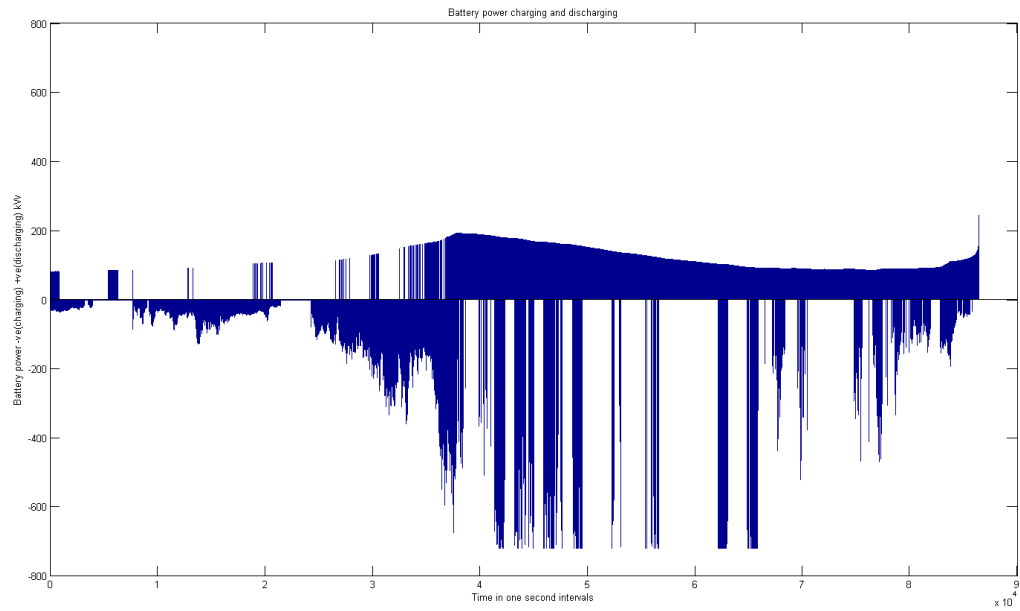


**Figure 6.71 Battery charging and discharging for one second forecasted load data in conservative discharging and wind charging modes**

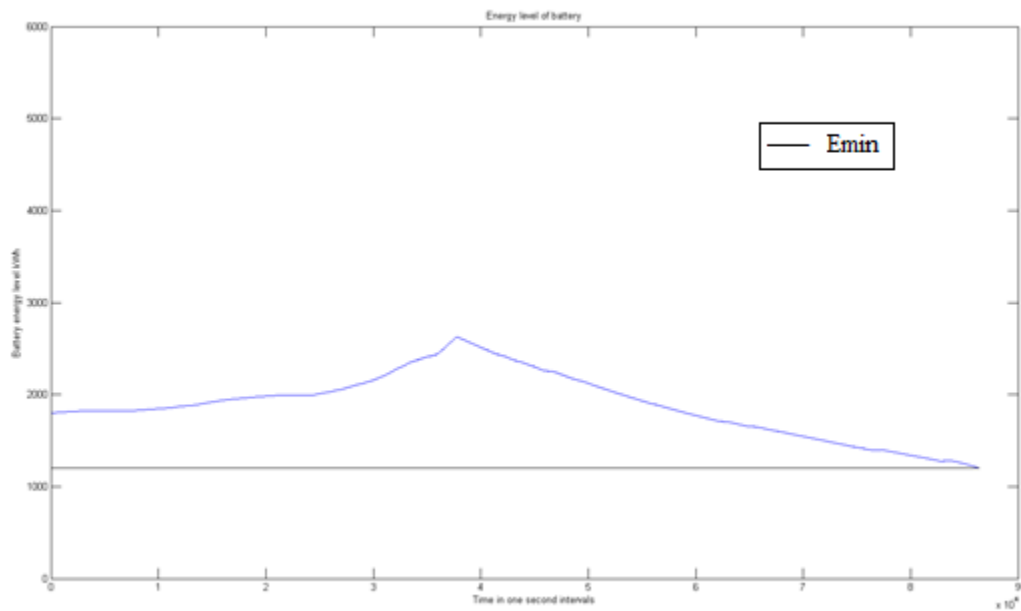


**Figure 6.72 Battery state of charge for one second forecasted load data in conservative discharging and wind charging modes**

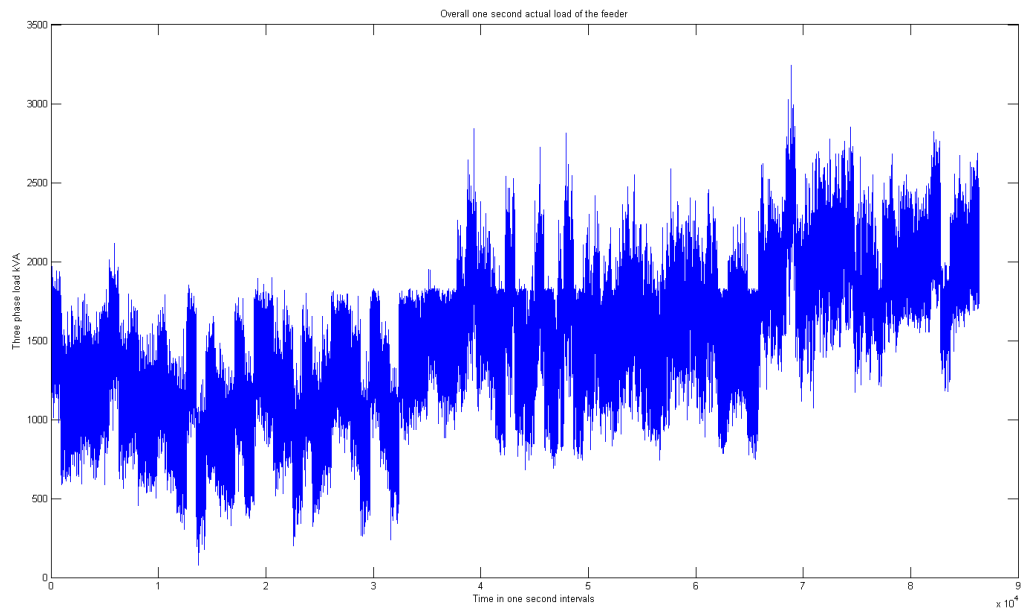


**Figure 6.73 Overall one second actual load demand after peak reduction for one second forecasted load data in conservative discharging and wind charging modes**

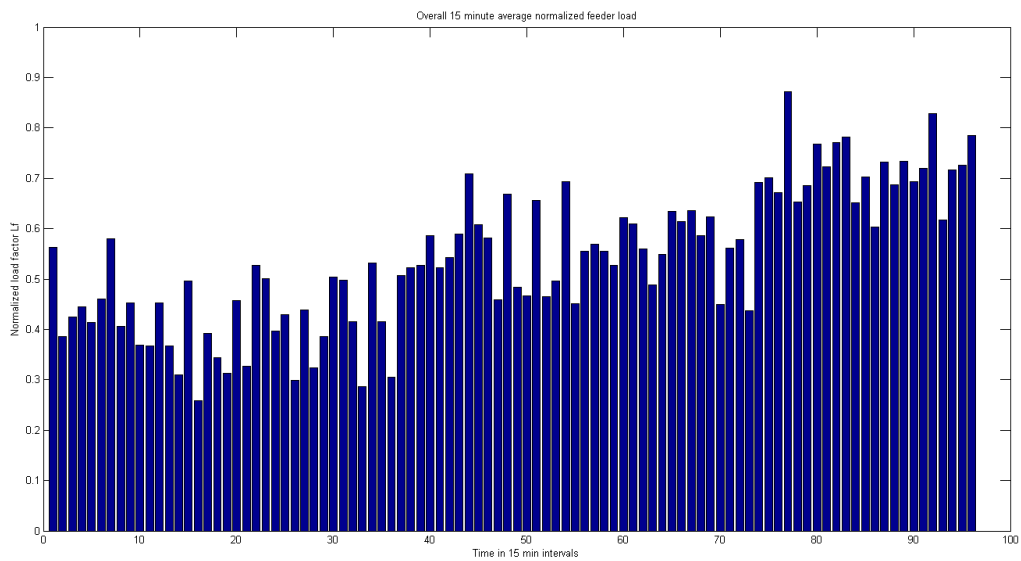


**Figure 6.74 Fifteen minute average normalized load demand after peak reduction for one second forecasted load data in conservative discharging and wind charging modes**

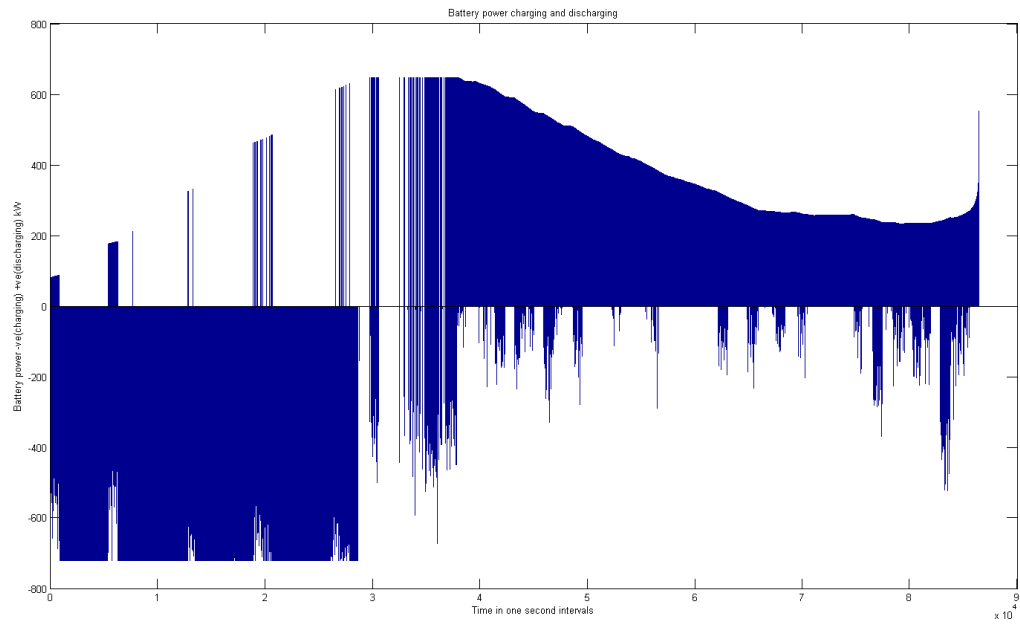


**Figure 6.75 Battery charging and discharging for one second forecasted load data in conservative discharging and sustained average load charging modes**

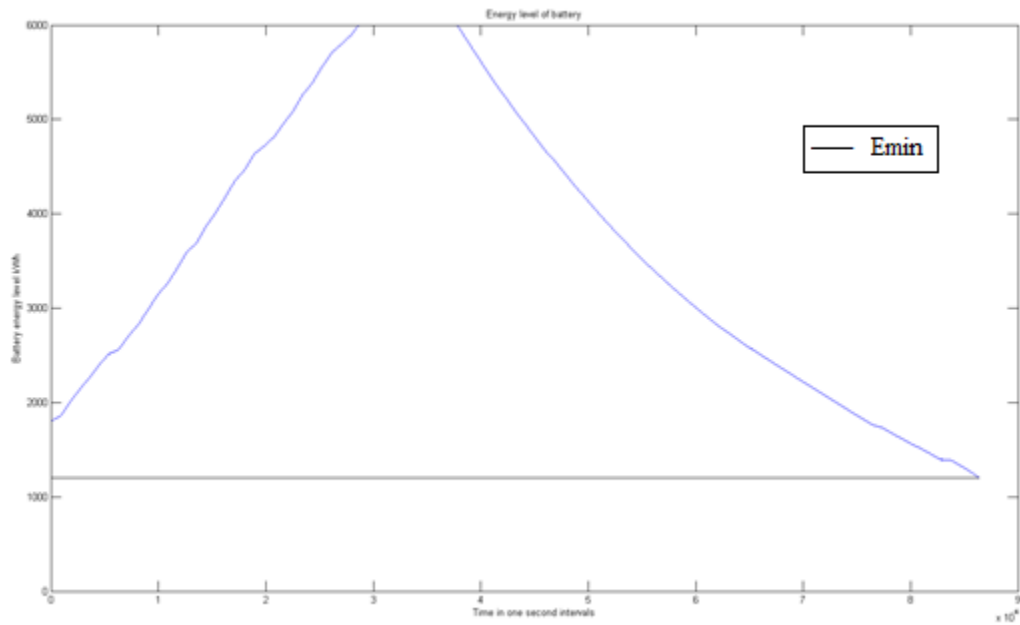


**Figure 6.76 Battery state of charge for one second forecasted load data in conservative discharging and sustained average load charging modes**



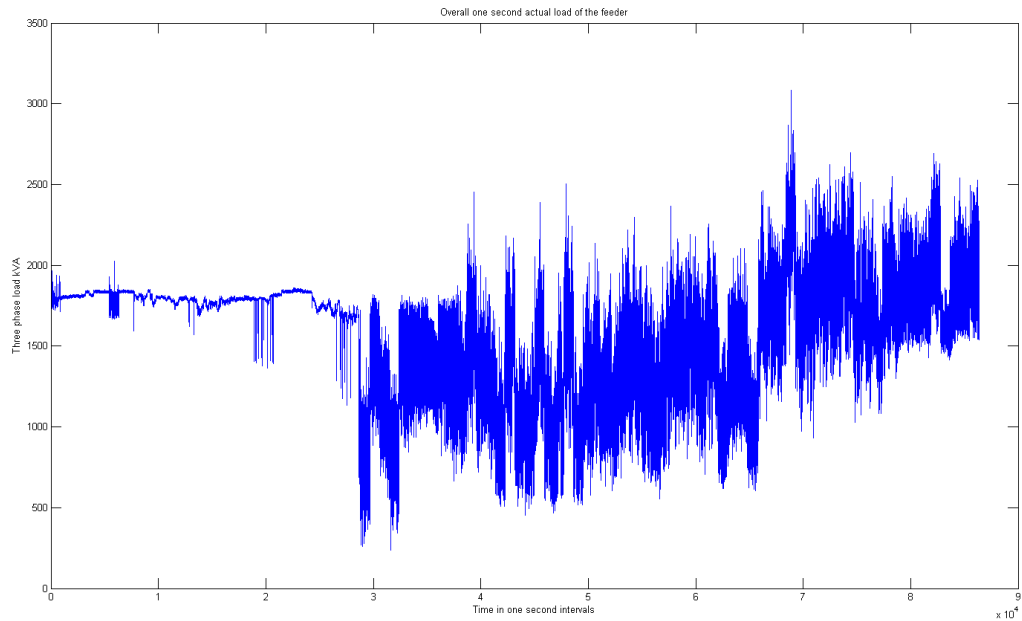


**Figure 6.77 Overall one second actual load demand after peak reduction for one second forecasted load data in conservative discharging and sustained average load charging modes**

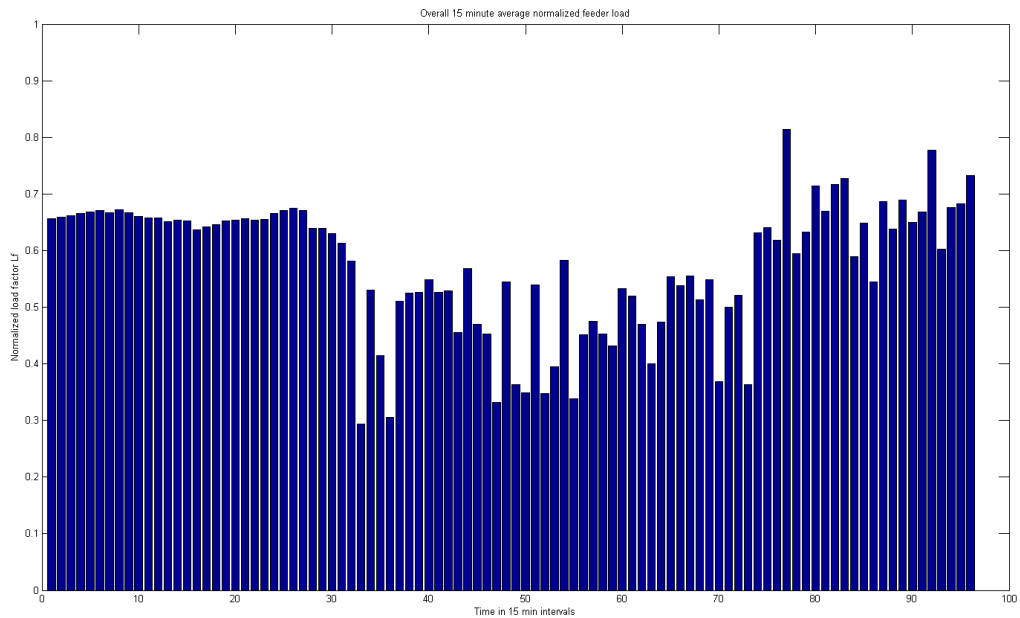


**Figure 6.78 Fifteen minute average normalized load demand after peak reduction for one second forecasted load data in conservative discharging and sustained average load charging modes**

The following observations were made for the average and maximum demand factors of the feeder and also for the battery capacity utilization. The table containing the comparison of the four methods with the base case of load flow without any wind generation has been given below.

Mode	Charging Method	Discharging Method	Average load factor	Peak load factor	Battery utilization factor
Base	--	--	0.6668	1.0000	--
Mode 1	Wind	Free – running	0.5631	0.6914	0.6431
Mode 2	SAL	Free – running	0.6237	0.6918	1.0000
Mode 3	Wind	Conservative	0.5422	0.8713	0.4376
Mode 4	SAL	Conservative	0.5767	0.8144	1.0000

(SAL – Sustained Average Load)

**Table 6.2 Summary of results obtained for one second load forecasted operation of wind generation with battery storage**

In the above table, the calculations of average and peak load factors and battery utilization factor were done as given below

$$\text{Average load factor} = \text{Mean}(\text{Normalized demand of all time instances during the period of operation}) \quad (6.1)$$

$$\text{Peak Load factor} = \text{Max}(\text{Normalized demand of all time instances during the period of operation}) \quad (6.2)$$

$$\text{Battery Utilization factor} = (\text{Max}(E_{ess}) - \text{Min}(E_{ess})) / E_{max} \quad (6.3)$$

In equation 6.3,  $E_{ess}$  is the operational energy level of the battery during all the instances of operation, and  $E_{max}$  is the full capacity of the battery. From the results displayed in the table above, we observe that all the methods cause a reduction in the average load as well as the peak load of the feeder. At any given instant of time during the operation of dispatch of battery storage in order to perform peak reduction operations with wind generation, it can be extended from the above results that during discharging, if the battery capacity is substantially available for usage,

it is better to use free-running mode of operation. However, if the battery capacity falls below a certain set minimum value necessary for dispatch operations, the performance of the conservative discharging mode seems to be better at reducing peak load by at least a slight margin over the remaining periods of time of the day. The charging methods used prove that battery capacity needs to be used to the highest extent possible within set maximum and minimum levels in order to effectively aid in the peak reduction process. In this regard, the sustained average load approach of battery charging makes sure that absence of wind generation does not render the battery unusable. But, the battery is charged up to maximum levels very quickly and usage of the battery becomes very limited and inefficient especially when wind generation is available. Also, the method is not suited for real time operations at this point of time due to non-availability or commercial unviability of the technology required to make the process a reality. Wind charging is a very viable option as the strategy used makes sure that wind generation is stored when close to base load conditions prevail irrespective of the amount available. Also, only a fraction of the overall battery capacity is always used, providing scope for battery size reduction leading to cost benefits. The lessons learned from the results presented in this section are that in order to have an effectively working real time strategy for dispatch operations of distributed wind generation using battery storage and PMUs in a distribution system, the charging of the battery needs to be done using only wind generation, free-running mode of operation has to be used in the discharging of the battery if capacity is available, and if the battery capacity falls below a certain set minimum value based on wind generation characteristics, conservative discharging of the battery should be carried out for all the remaining time intervals of the day.

### **6.3 Real time operation of storage dispatch with wind generation based on historical PMU measurements**

This section explains the most important results that have been obtained in this research work. The real time operations of battery storage with distributed wind generation using historical data obtained from PMU measurements of previous time instances has been investigated. In the study done here, PMU samples have been taken at the rate of one sample per second. For the purpose of research, PMU measurements have been recorded using the backward forward sweep power flow for every time instant. The sampling interval required to assess the

battery dispatch for the next time instant has been set at five minutes or 300 seconds of previous PMU data. The maximum load including wind generation and battery dispatch is calculated from each of these previous 300 time instances, and the difference between this maximum value, average load and wind generation of the immediately preceding time instant has been calculated to be the battery dispatch for the present time instance. For example, for a given time instance  $k$ , the battery discharge is calculated as follows.

$$S_{batt,k} = \text{Max}[(S_{pmu} + S_{wind} + S_{batt}) | k-1:k-301] - S_{avg} - S_{wind,k-1} \quad (6.4)$$

For all the cases, for a given power rating and energy rating of the battery, the following assumptions have been followed:

- The minimum permissible energy level of the battery has been set at 20% of the maximum value, and the switching level for this case of wind generation profile has been set at 30% of maximum value after analysis based on forecasted load. Higher switching energy levels may be assumed if wind generation profiles are weaker.
- The maximum power charging and discharging rate of the battery have been set as the power rating of the battery. For the case of 30% wind generation penetration into the feeder described in this research, the battery specifications have been discussed in chapter 4 section 4.1.4.

The only input information that the real time method described here would use are the average load of the feeder, and the switching energy level of battery capacity after which conservative dispatch operations can begin. Both of these values are feeder specific. The average load of the feeder is the recorded average value of load of an immediately preceding day for the given distribution feeder. The switching value of battery capacity can be decided based on the wind generation levels. The switching value of battery capacity and wind generation levels are inversely related, i.e., if wind generation levels are high, the switching capacity can be set at a smaller value and vice-versa.

The results shown below are for full capacity of battery storage. The maximum charge and discharge rates of the battery are equal to the full power rating of the battery equal to installed wind generation capacity. The initial analysis is done completely in free running mode without any conservative discharge in order to demonstrate the ineffective nature of the battery once it hits its minimum level. The total battery capacity and specifications have been tabulated below. The PMU based operation is also time specific as there is a fixed sampling rate associated

with the measurements. So, an effort has also been made to recover the execution time required to operate for all the one second intervals in a given day.

<b>Power Rating (P)</b>	800 kW
<b>Maximum Energy Level (E<sub>max</sub>)</b>	6000 kWh
<b>Minimum Energy Level (E<sub>min</sub>) 20%</b>	1200 kWh
<b>Initial Energy Level (E<sub>0</sub>) 30%</b>	1800 kWh
<b>Execution time (t)</b>	58 minutes

**Table 6.3 Battery Specifications for real time test system in free-running mode only at full capacity**

The results obtained for free-running mode of operation of real time storage dispatch based on historical PMU information have been displayed in figures 6.79 through 6.82.

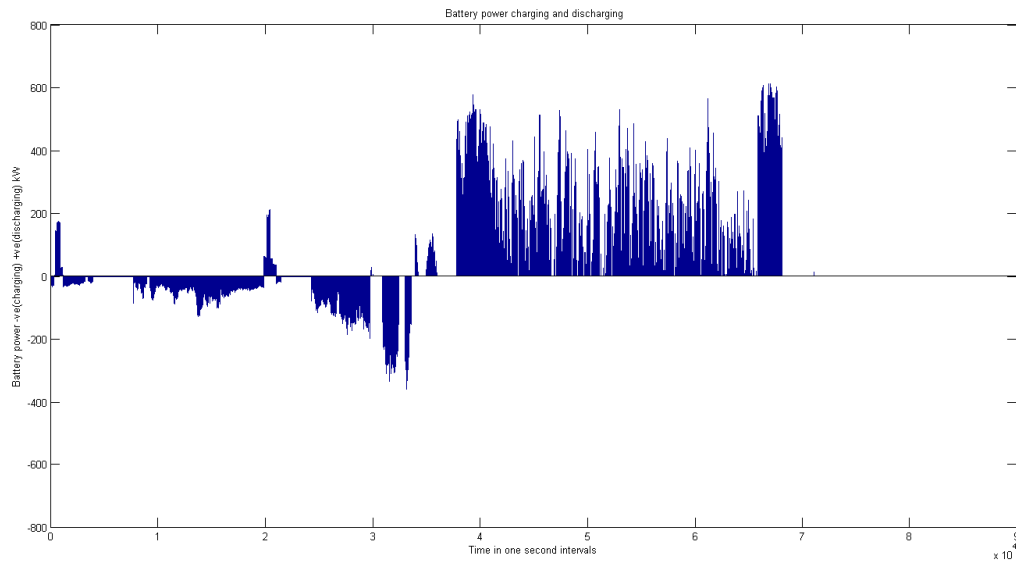


**Figure 6.79 Battery power charging and discharging under real time operation at full capacity in free-running mode only**

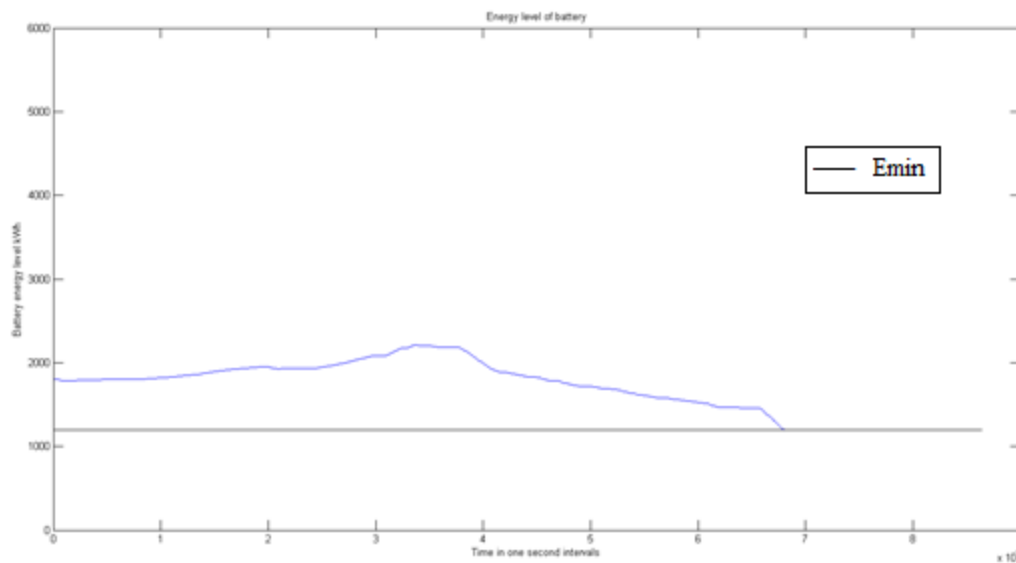


**Figure 6.80 Battery state of charge under real time operation at full capacity in free-running mode only**

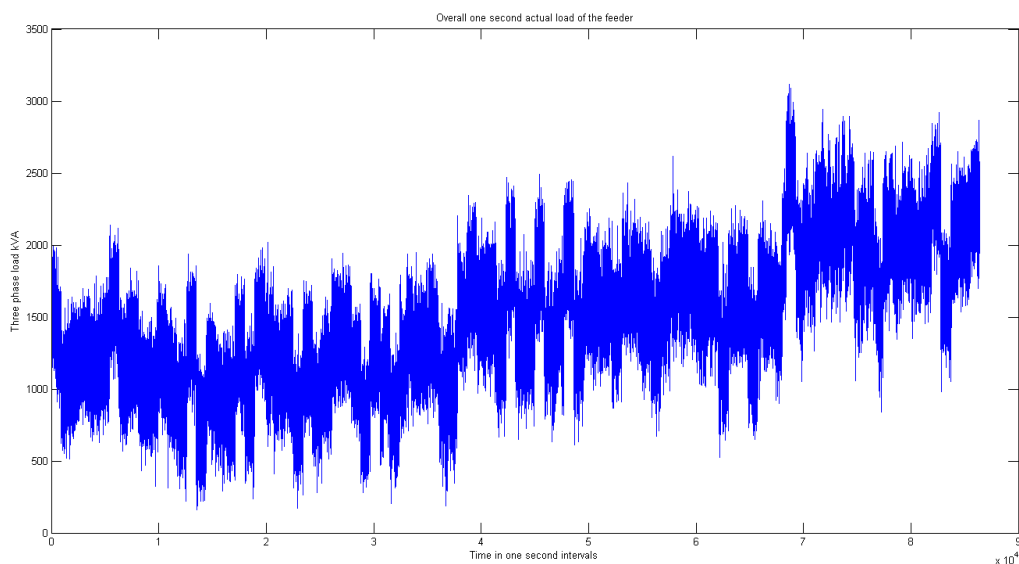


**Figure 6.81 Overall actual one second demand under real time operation at full battery capacity in free-running mode only**

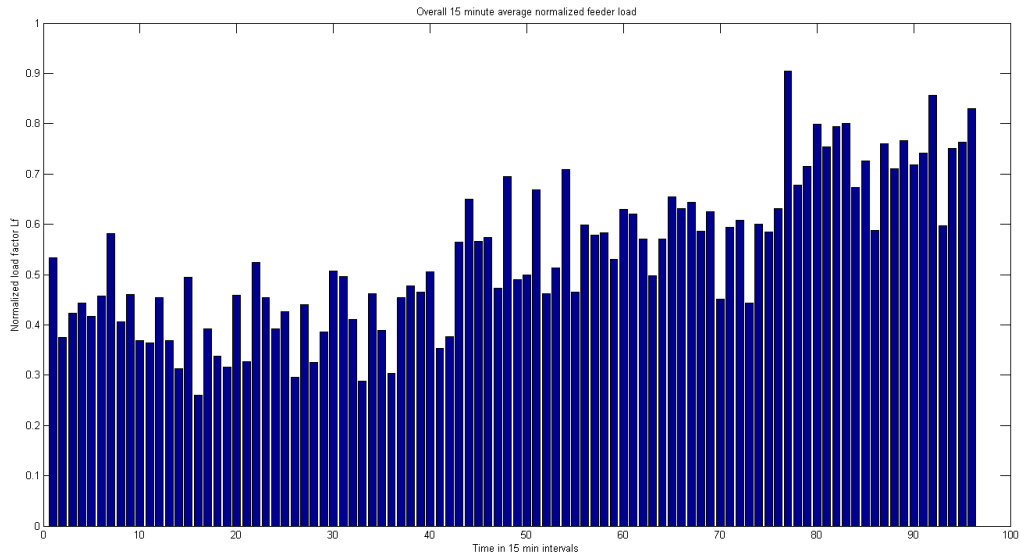


**Figure 6.82 Fifteen minute average normalized demand under real time operation at full battery capacity in free-running mode only**

The next step in the analysis involves the introduction of conservative discharge into the dispatch process once the battery energy level drops below a set minimum switching value. The table containing the specifications of the test battery is given below. The results are obtained in figures 6.83 through 6.86.

<b>Power Rating (P)</b>	800 kW
<b>Maximum Energy Level (E<sub>max</sub>)</b>	6000 kWh
<b>Minimum Energy Level (E<sub>min</sub>) 20%</b>	1200 kWh
<b>Initial Energy Level (E<sub>0</sub>) 30%</b>	1800 kWh
<b>Switching Energy level (E<sub>s</sub>) 30%</b>	1800 kWh
<b>Execution time (t)</b>	58 minutes

**Table 6.4 Battery Specifications for real time test system in free-running mode and conservative discharge at full installed capacity**

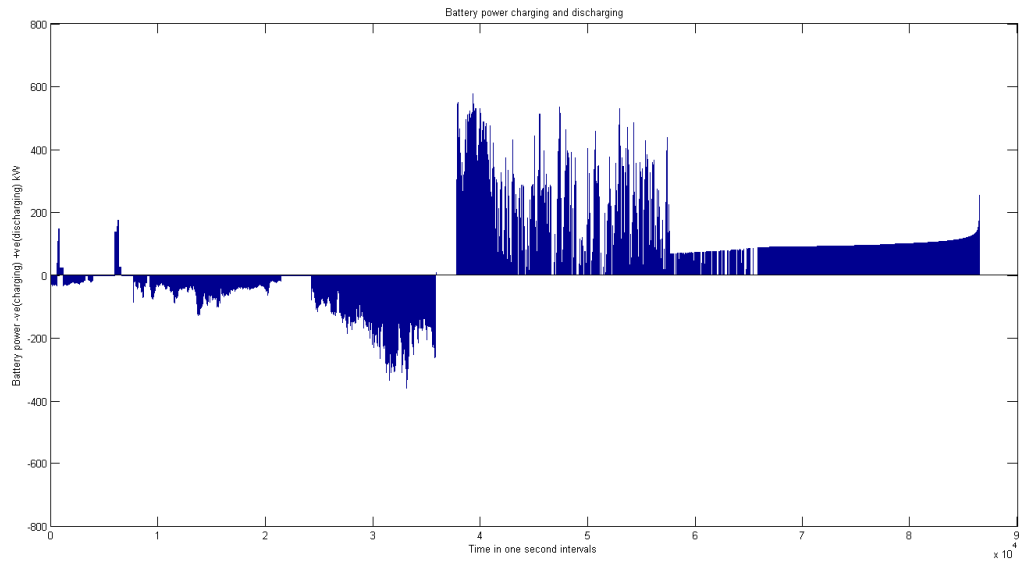


**Figure 6.83 Battery power charging and discharging under real time operation at full capacity in free-running mode and conservative discharging**

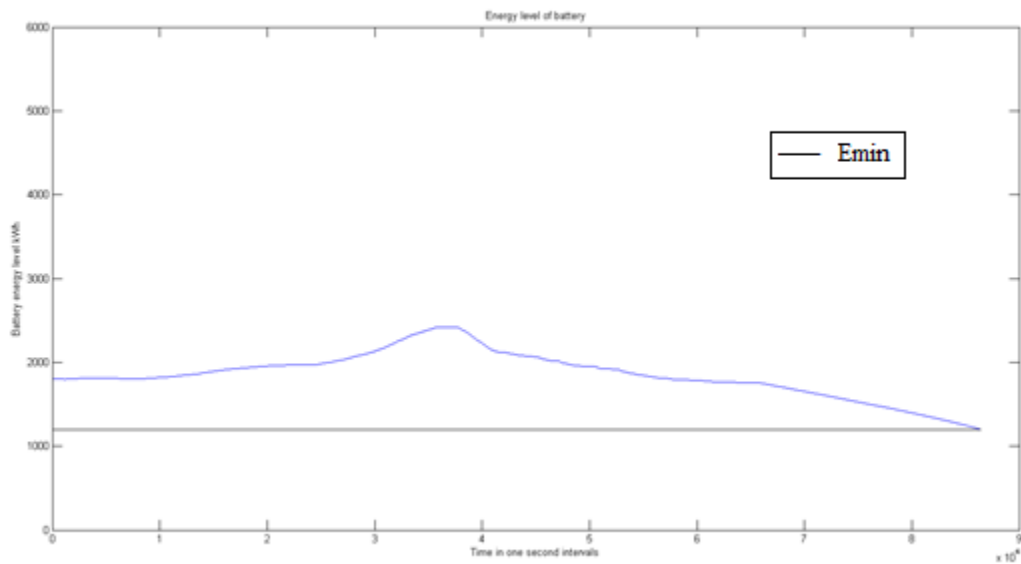


**Figure 6.84 Battery state of charge under real time operation at full capacity in free-running mode and conservative discharge**



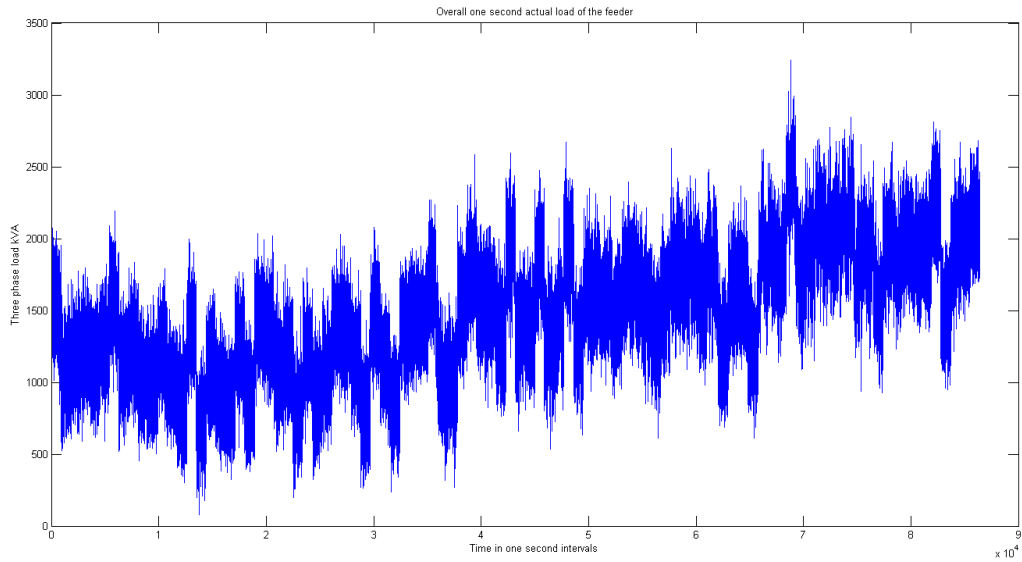


**Figure 6.85 Overall actual one second demand under real time operation at full battery capacity in free-running mode and conservative discharge**

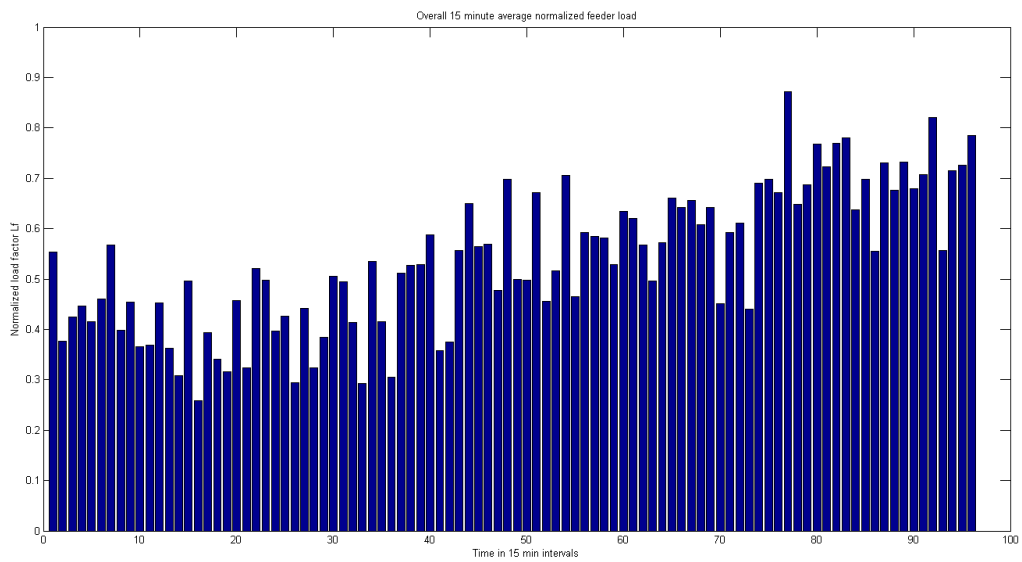


**Figure 6.86 Fifteen minute average normalized demand under real time operation at full battery capacity in free-running mode and conservative discharge**

From the results obtained above, it is observable that with the implementation of conservative discharge when the battery energy capacity falls below a set minimum switching value, the utilization of battery over the entire time interval of the day becomes possible. There are also better peak reduction characteristics with respect to the average fifteen minute normalized load. More clarity in this regard will be thrown when the results of all the real time analyses are tabulated at the end of this section.

The next analysis involves the reduction of the battery power and energy capacities to half of the actual values. The battery capacity is very minimally utilized in the previous two cases, and this provides the scope for the reduction of battery capacity in the next stage. The battery specifications for this analysis have been given below. The results are obtained in figures 6.87 through 6.90.

<b>Power Rating (P)</b>	400 kW
<b>Maximum Energy Level (E<sub>max</sub>)</b>	3000 kWh
<b>Minimum Energy Level (E<sub>min</sub>) 20%</b>	600 kWh
<b>Initial Energy Level (E<sub>0</sub>) 30%</b>	900 kWh
<b>Switching Energy level (E<sub>s</sub>) 30%</b>	900 kWh
<b>Execution time (t)</b>	58 minutes

**Table 6.5 Battery Specifications for real time test system in free-running mode and conservative discharge at half capacity**

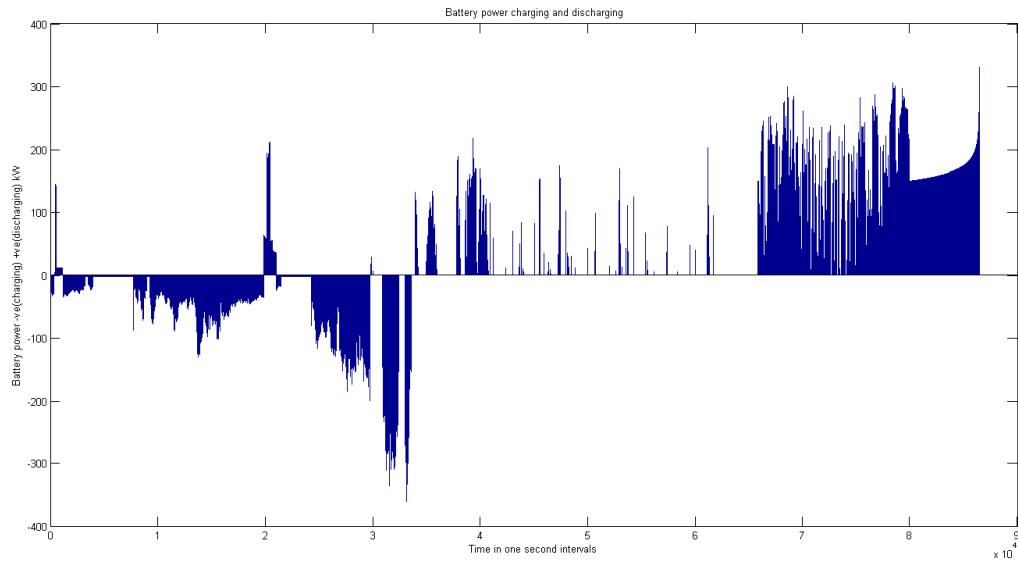


**Figure 6.87 Battery power charging and discharging under real time operation at half capacity in free-running mode and conservative discharging**

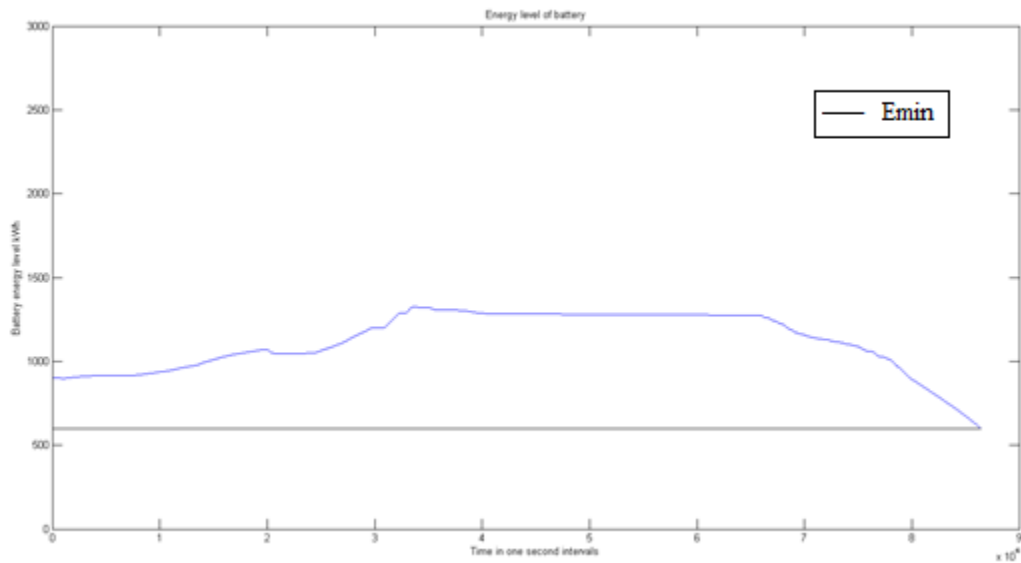


**Figure 6.88 Battery state of charge under real time operation at half capacity in free-running mode and conservative discharge**

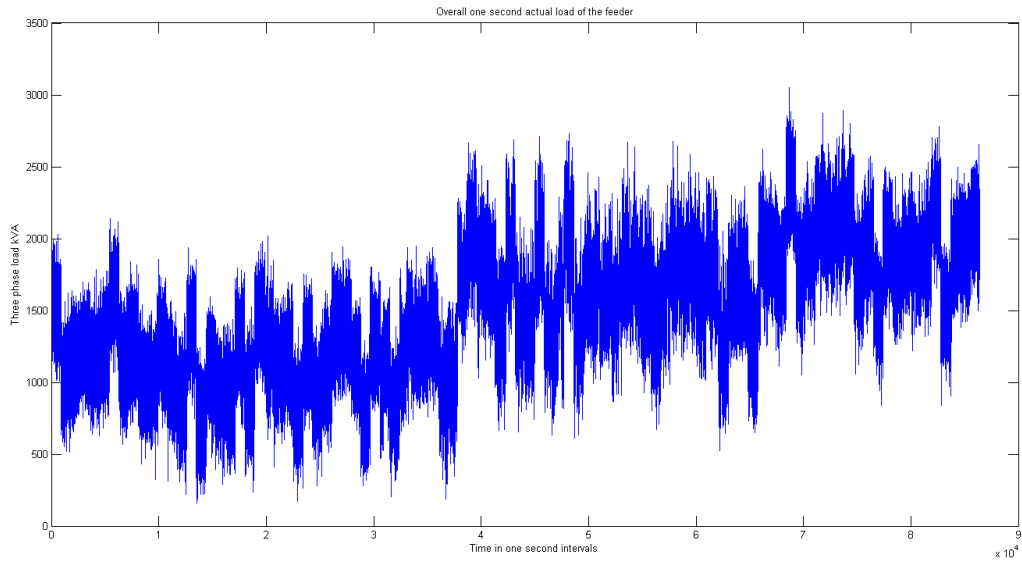


**Figure 6.89 Overall actual one second demand under real time operation at half battery capacity in free-running mode and conservative discharge**

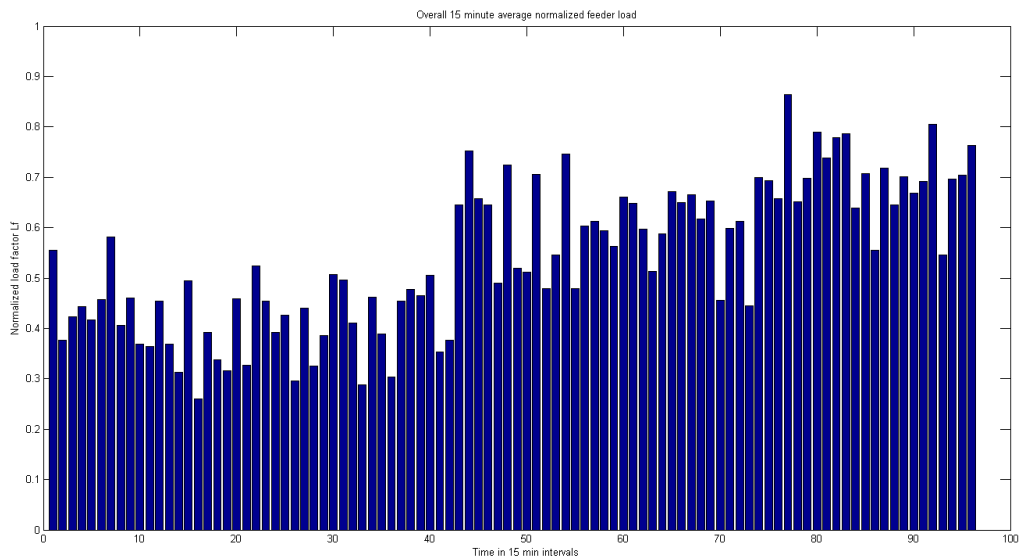


**Figure 6.90 Fifteen minute average normalized demand under real time operation at half battery capacity in free-running mode and conservative discharge**

It is seen from the results obtained for half battery capacity real time operation that there is a higher peak reduction ratio because of higher capacity utilization of the battery. Also, the average load of the feeder falls slightly more because of the same reason. The result shows that there is scope for further reduction in size of the battery. However, as this research work involves the usage of one particular type of battery, namely, the NAS battery, the effects of battery specific properties can be considered. The specialty of NAS batteries is to be able to pulse discharge at up to four times their rated power capacity for short periods of time. As the scope of real time operation investigated in this research work involves the change of battery discharge level at every second, pulsed operation can be considered in this case. Battery installed capacity is retained as in the previous case at half the original initial value, while the power level is bumped up to twice its value in the previous analysis. The battery specifications used are given below along with the execution time. The results have been obtained in figures 6.91 through 6.94.

<b>Power Rating (2P)</b>	800 kW
<b>Maximum Energy Level (E<sub>max</sub>)</b>	3000 kWh
<b>Minimum Energy Level (E<sub>min</sub>) 20%</b>	600 kWh
<b>Initial Energy Level (E<sub>0</sub>) 30%</b>	900 kWh
<b>Switching Energy level (E<sub>s</sub>) 30%</b>	900 kWh
<b>Execution time (t)</b>	58 minutes

**Table 6.6 Battery Specifications for real time test system in free-running mode and conservative discharge at half capacity for double pulse operation**

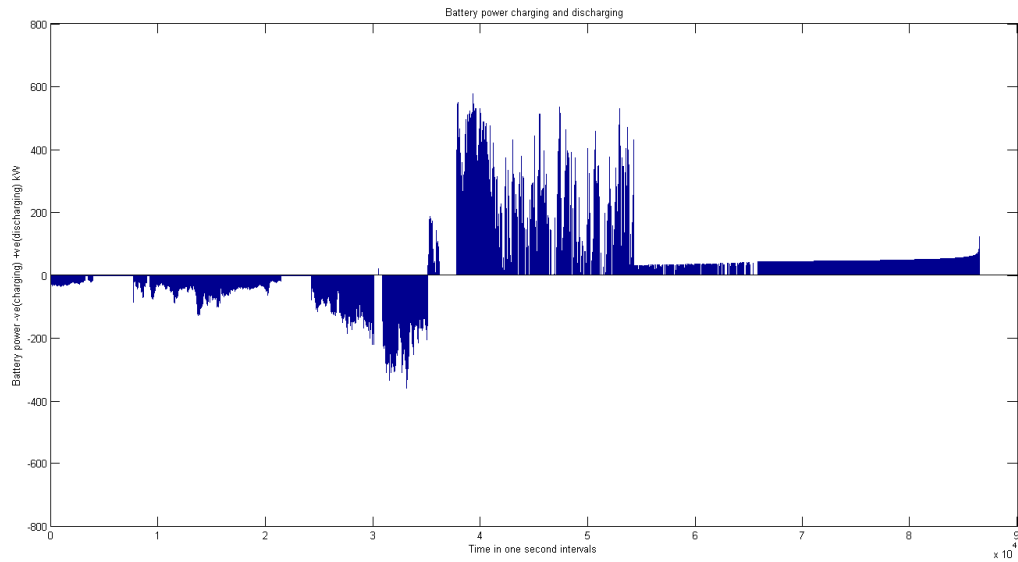


**Figure 6.91 Battery power charging and discharging under real time operation at half capacity and double pulse operation in free-running mode and conservative discharging**

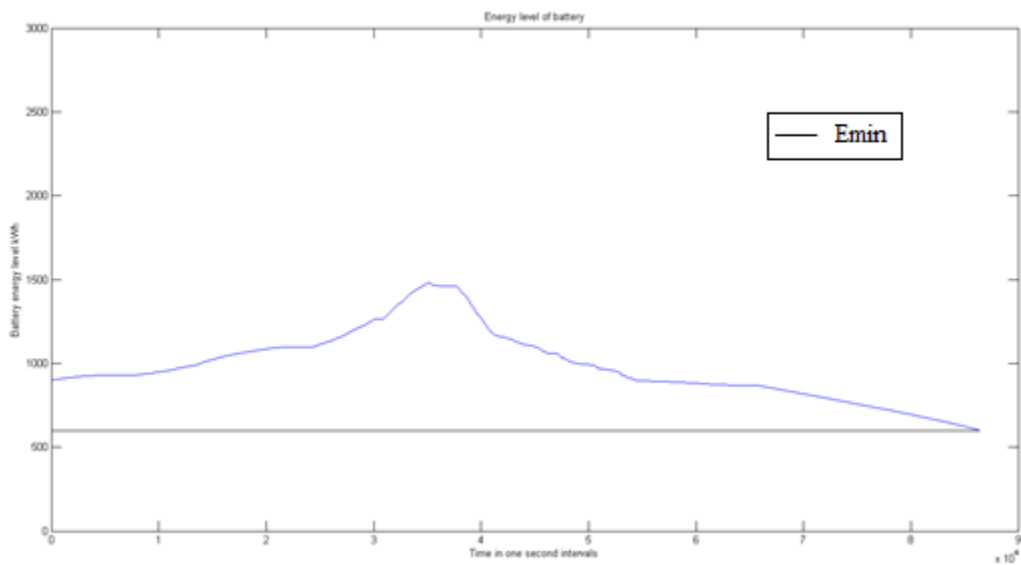


**Figure 6.92 Battery state of charge under real time operation at half capacity and double pulse operation in free-running mode and conservative discharge**

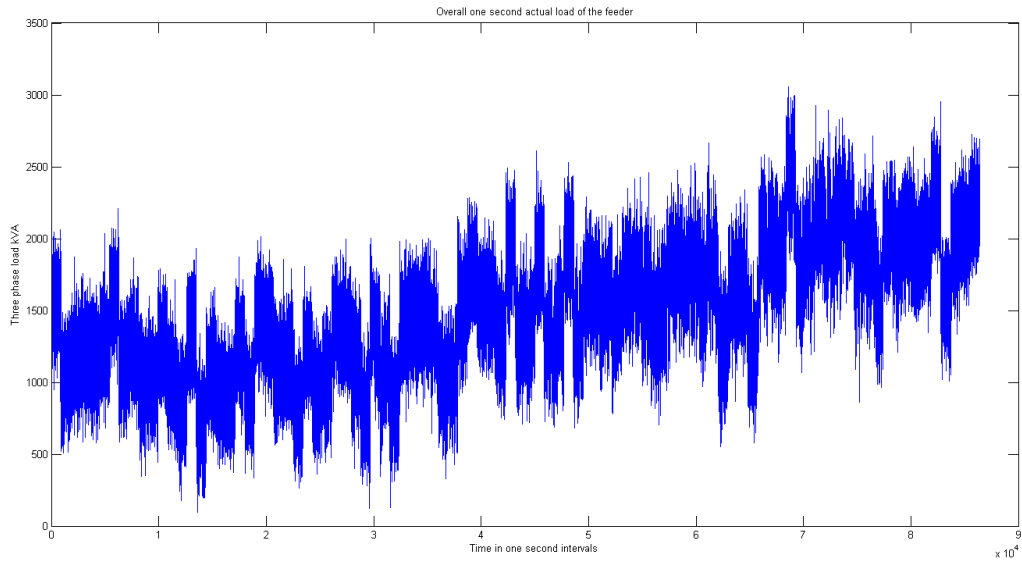


**Figure 6.93 Overall actual one second demand under real time operation at half battery capacity and double pulse operation in free-running mode and conservative discharge**

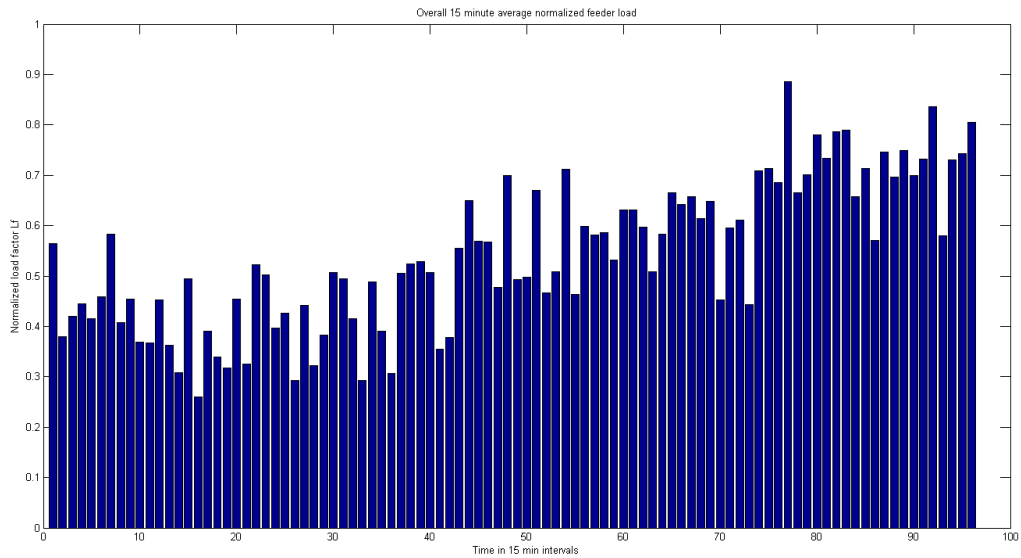


**Figure 6.94 Fifteen minute average normalized demand under real time operation at half battery capacity and double pulse operation in free-running mode and conservative discharge**

The results obtained above show that the improvements in peak reduction or mean load reduction of the feeder are not very appreciable. There is a slight improvement in the capacity usage of the battery although the battery is mostly unused. So, it may be inferred that the double pulse operation of the battery is unwarranted as there are no significant improvements, and also, prolonged operation of the battery in the double pulse mode could reduce the life span of operation.

The next step in the analysis involves using the battery in the same configuration as before without the double pulse operation. The only difference in this case is that the initial battery capacity is assumed to be at 60%. The analysis is done in this way in order to investigate if any changes occur in capacity utilization with higher initial battery energy level. The specifications in this case are given below. The results are obtained in figures 6.95 through 6.98.

<b>Power Rating (P)</b>	400 kW
<b>Maximum Energy Level (E<sub>max</sub>)</b>	3000 kWh
<b>Minimum Energy Level (E<sub>min</sub>) 20%</b>	600 kWh
<b>Initial Energy Level (E<sub>0</sub>) 60%</b>	1800 kWh
<b>Switching Energy level (E<sub>s</sub>) 30%</b>	900 kWh
<b>Execution time (t)</b>	58 minutes

**Table 6.7 Battery Specifications for real time test system in free-running mode and conservative discharge at half capacity for higher initial energy**



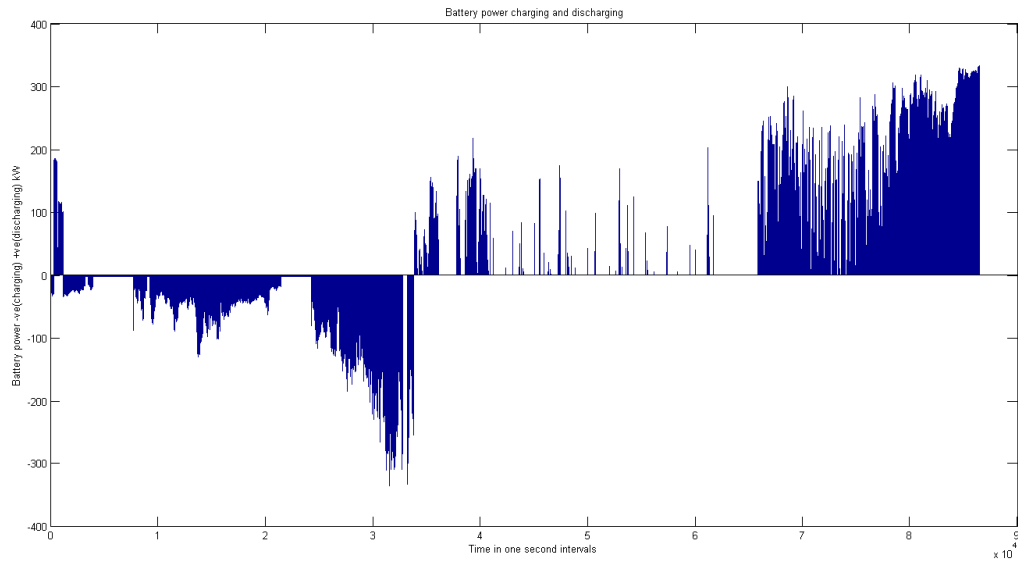


**Figure 6.95 Battery power charging and discharging under real time operation at half capacity and higher initial energy in free-running mode and conservative discharging**

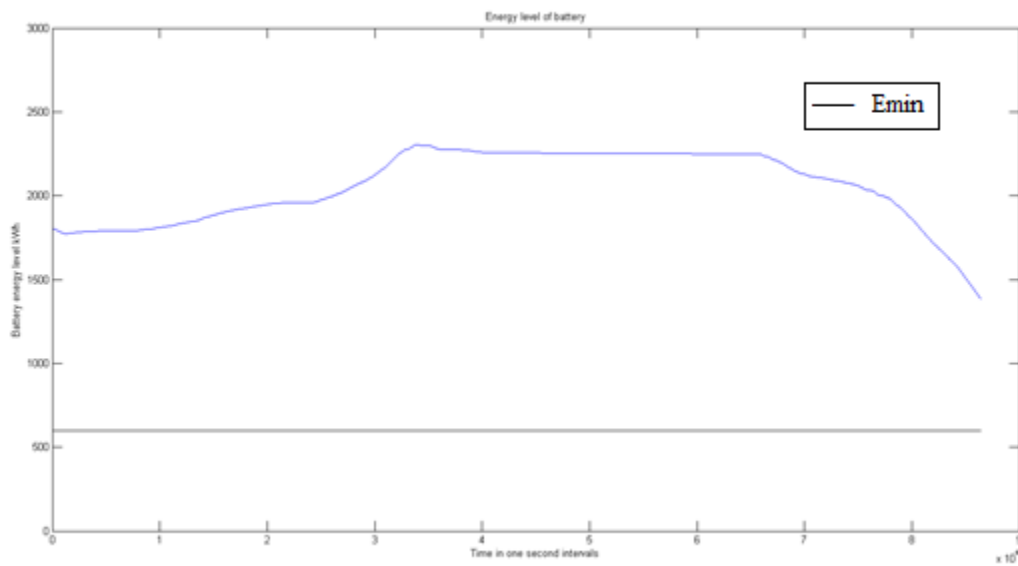


**Figure 6.96 Battery state of charge under real time operation at half capacity and higher initial energy in free-running mode and conservative discharge**

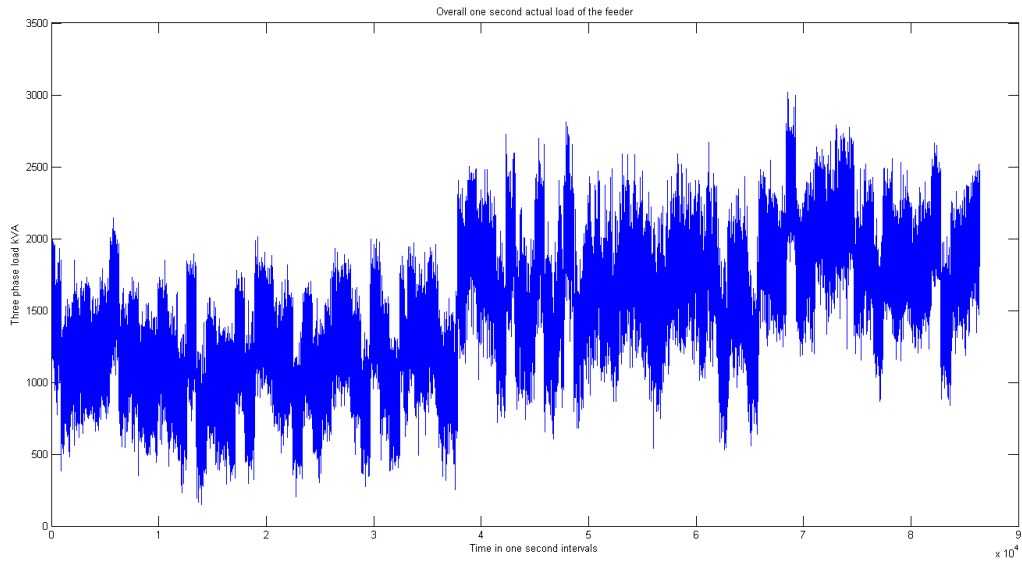


**Figure 6.97 Overall actual one second demand under real time operation at half battery capacity and higher initial energy in free-running mode and conservative discharge**

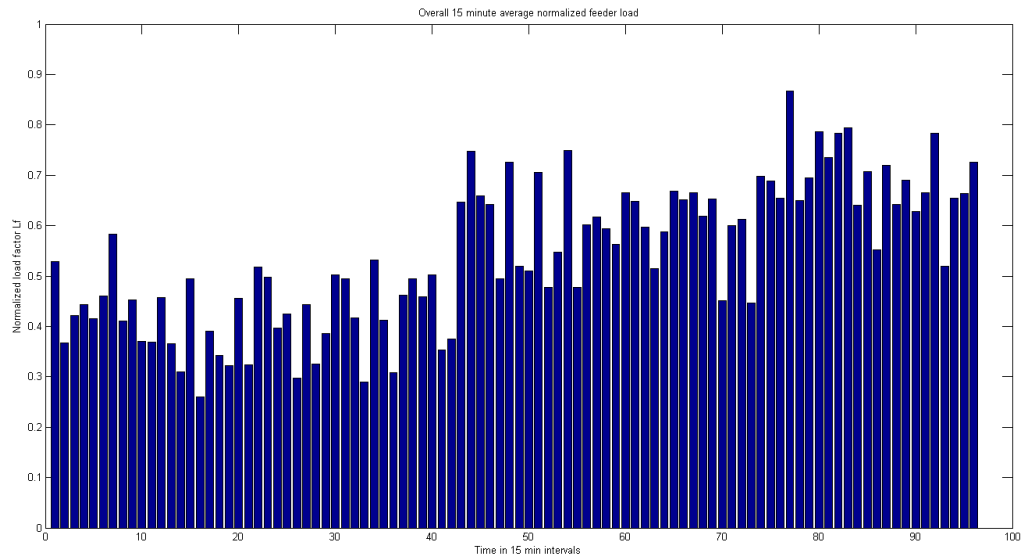


**Figure 6.98 Fifteen minute average normalized demand under real time operation at half battery capacity and higher initial energy in free-running mode and conservative discharge**

It is observed that in the above case where battery capacity starts at a higher initial energy level, there are no significant improvements in peak reduction and mean load reduction, and also the capacity utilization of the battery reduces as surplus amount of energy is available in the battery. This proves again that the capacity of the battery can be reduced further, which forms the basis for the next and final step in the battery size reduction process investigated along with dispatch operations in this research.

The battery is now reduced to one-fourth or 25% of its original capacity and the real time operation in free-running mode and conservative discharge is done under the following battery specifications. The results are obtained in figures 6.99 through 6.102.

<b>Power Rating (P)</b>	200 kW
<b>Maximum Energy Level (E<sub>max</sub>)</b>	1500 kWh
<b>Minimum Energy Level (E<sub>min</sub>) 20%</b>	300 kWh
<b>Initial Energy Level (E<sub>0</sub>) 30%</b>	450 kWh
<b>Switching Energy level (E<sub>s</sub>) 30%</b>	450 kWh
<b>Execution time (t)</b>	58 minutes

**Table 6.8 Battery Specifications for real time test system in free-running mode and conservative discharge at quarter capacity**

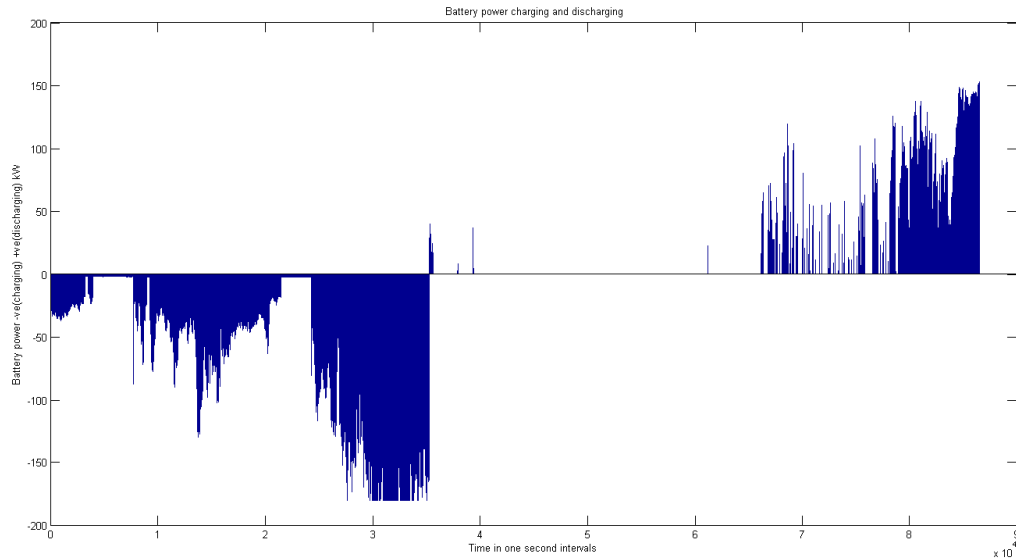


**Figure 6.99 Battery power charging and discharging under real time operation at quarter capacity in free-running mode and conservative discharging**

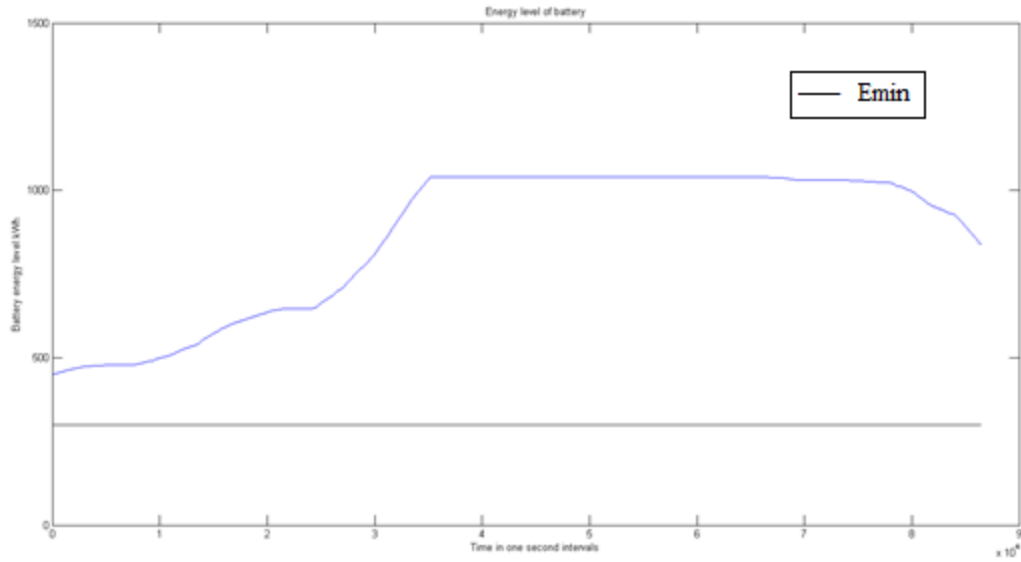


**Figure 6.100 Battery state of charge under real time operation at quarter capacity in free-running mode and conservative discharge**

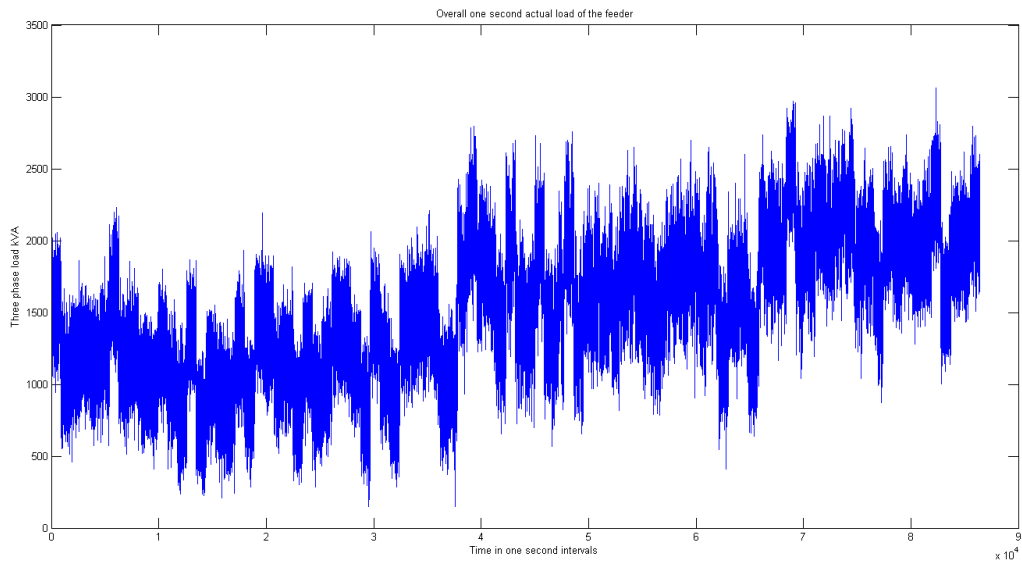


**Figure 6.101 Overall actual one second demand under real time operation at quarter battery capacity in free-running mode and conservative discharge**

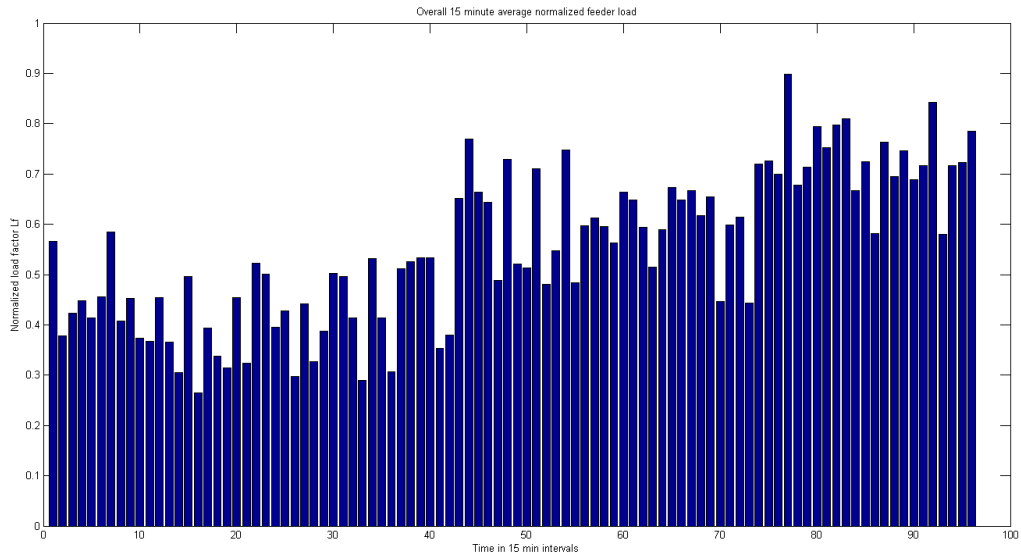


**Figure 6.102 Fifteen minute average normalized demand under real time operation at quarter battery capacity in free-running mode and conservative discharge**

The final results obtained for 25% of original assumed battery capacity show appreciable peak reduction and average load reduction and also high capacity utilization for the battery when compared to all of the previous results. So, it can be inferred that this could be the best case of battery sizing as the wind generation average for this case is between the medium and high levels and constantly high wind generation could actually end up utilizing the full capacity of the battery on such days.

A final tabulation of the results obtained for all the real time storage dispatch cases discussed so far has been presented below.

Mode	Specifications	Average load factor	Peak load factor	Battery utilization factor	Time of execution (minutes)
Base case	--	0.6668	1.0000	--	--
Free-running only	Full capacity + 30% initial	0.5393	0.9050	0.3681	58
Free-running and conservative discharge below switching energy level	Full capacity + 30% initial	0.5397	0.8716	0.4036	58
	Half capacity + 30% initial	0.5433	0.8641	0.4418	58
	Half capacity + 30% initial + double pulse operation	0.5434	0.8866	0.4940	58
	Half capacity + 60% initial	0.5421	0.8679	0.4681	58
	Quarter capacity + 30% initial	0.5539	0.8981	0.6939	58

**Table 6.9 Summary of results obtained for real time operation of wind generation with storage dispatch using historical PMU information**

In the analysis that has been done in this research work, PMU information of the previous 300 time instances or seconds is used to calculate the battery dispatch for the current time instant. So, it can be inferred that during every one second interval, one calculation for dispatch of the battery happens. For a total processing time of 58 minutes for all the 86400 time instances of dispatch calculation, the processing time per instance is calculated by dividing the total time by the total number of time instances. The processing time per time instant is calculated to be 40.27 milliseconds, which is slightly higher than the maximum PMU sampling time of 33.33 milliseconds. So, for this particular test feeder, it is possible to work with a high resolution of up to 15 samples per second of PMU data. This proves the dynamic real time characteristics of the

calculations analyzed in this research. Actual on field applications could be much faster with system components such as distribution SCADA computers which could put the full potential of the dynamic nature of PMU measurements to use.

## **Chapter 7 - Conclusions and Future Work**

### **7.1 Conclusions**

The integration of distributed storage into the distribution system in order to support wind generation provides some exciting advantages. The following contributions have been made in this research work.

- The possibility of storing wind generation and using it when it is most required is a valuable asset in the proper and efficient operation of a distribution system and has been accomplished with some degree of success in this research work.
- The unbalanced operation of power flow in a distribution system for dynamic load intervals in order to regulate storage and wind generation has been undocumented so far in literature and has been investigated in this research.
- The advantages of using dynamic load information available from advanced measurement devices in order to effectively achieve wind generation storage and dispatch operations have been established. The usage of Phasor Measurement Units (PMU) in order to perform the same function, especially in a distribution system has been handled newly in this research work.
- Some of the battery charging and discharging strategies developed in order to effectively support wind generation and achieve peak reduction in feeder load such as sustained average load approach and conservative discharging are unique to this research.
- The real time operation of battery storage dispatch using historical PMU information has also been newly developed in this research work. All of the methods developed here are purely based on math functions and involve no optimization, making them well suited to on field real time applications.
- When battery storage is to be used with wind generation in order to perform load support operations, battery size and cost can be a concern to be addressed. The step by step attempts made in the reduction of battery size for real time applications of load support, and the results obtained in the process greatly addressed this issue, and the stage is now set for other researchers trying to improve the methods and resources developed in this research even further.



## **7.2 Future Work**

The usage of PMUs in distribution systems is still a relatively unexplored area of study, and there might be a lot more scope for future research work in this area. As the PMU technology becomes cheaper, its usage in distribution systems can be expected to increase, as the benefits of this technology far outweigh the costs involved. Talking specifically in terms of the research done so far, the techniques and strategies used in this research can be applied through simulation to larger test feeders as well as for on field operation through test beds and actual experimental feeders. The techniques developed in this research have been applied primarily to centralized location of wind generation and storage technologies due to the size of the test feeder. But present trends in distributed generation are growing towards placement of distributed resources at multiple locations. So, there might be avenues for further studies in multiple sighting as well as measurement locations for PMUs, wind farms and storage. There is also scope for further optimization of storage installations with increasing penetration of renewables such as wind and solar energy. The entire power system has been moving towards smart grid technologies, and all the elements of the power system addressed in this research will need further investigation and validation with time.

## References

- [1] William H. Kersting, *Distribution System Modeling and Analysis*, CRC Press, New York, 2002.
- [2] Khushalani, S., Schulz, N., “Unbalanced Distribution Power Flow with Distributed Generation”, *Transmission and Distribution Conference and Exhibition*, pp. 301-306, 21-24 May 2006.
- [3] Kersting, W.H., “Radial Distribution Test Feeders”, *IEEE Power Engineering Society Winter Meeting, 2001.*, pp. 908-912 vol. 2, 2001.
- [4] Du, P., Huang, Z., Diao, R., Lee, B., Anderson, K.K., “PMU Placement for Enhancing Dynamic Observability of a Power Grid”, *Innovative Technologies for an Efficient and Reliable Electricity Supply (CITRES), 2010 IEEE Conference on*, pp.15-21, 27-29 Sept. 2010.
- [5] Zhang, J., Welch, G., Bishop, G., Huang, Z., “Optimal PMU Placement Evaluation for Power System Dynamic state Estimation”, *Innovative Smart Grid Technologies Conference Europe (ISGT Europe), 2010 IEEE PES*, pp. 1-7, 11-13 Oct. 2010.
- [6] Phadke, A.G., Thorp, J.S., “History and Applications of Phasor Measurements”, *Power Systems Conference and Exposition, 2006. PSCE '06. 2006 IEEE PES*, pp. 331-335, Oct. 29-Nov. 1 2006.
- [7] Chun-Line Su, “Effects of Distribution System Operations on Voltage Profiles in Distribution Grids connected Wind Power Generation”, *Power System Technology, 2006. PowerCon 2006. International Conference on*, pp. 1-7, 22-26 Oct. 2006.
- [8] Mota, W.S., Barros, L.S., “Dynamic Simulations of Wind Generators connected to Distribution Systems”, *Electricity Distribution, 2005. CIRED 2005. 18th International Conference and Exhibition on*, pp. 1-4, 6-9 June 2005.
- [9] Atwa, Y.M., El-Saadany, E.F., “Probabilistic Approach for Optimal Allocation of Wind-based Distributed Generation in Distribution Systems”, *Renewable Power Generation, IET*, pp. 79-88, January 2011.
- [10] Mills-Price, M. et al, “Interconnection Control of Distributed Generation with Time-Synchronized Phasors”, *Power Systems Conference and Exposition (PSCE), 2011 IEEE/PES*, pp. 1-8, 20-23 March 2011.

- [11] Roy, N.K., Hossain, M.J., Pota, H.R., “Effects of Load Modeling in Power Distribution System with Distributed Wind Generation”, *Universities Power Engineering Conference (AUPEC), 2011 21st Australasian*, pp. 1-6, 25-28 Sept. 2011.
- [12] Ding, F., Booth, C.D., “Applications of PMUs in Power Distribution Networks with Distributed Generation”, *Universities' Power Engineering Conference (UPEC), Proceedings of 2011 46th International*, pp. 1-5, 5-8 Sept. 2011.
- [13] Aly, Mohamed M., Abdel-Akher M., “Voltage Stability Assessment for Radial Distribution power system with Wind Power penetration”, *Renewable Power Generation (RPG 2011), IET Conference on*, pp. 1-6, 6-8 Sept. 2011.
- [14] Chung, L.W., Siam, M.F.M., Ismail A.B., Hussien Z.F., “Modeling and Simulation of Sodium Sulfur Batteries for Battery Energy Storage System and Custom Power Devices”, *Power and Energy Conference, 2004. PECon 2004. Proceedings. National*, pp. 205-210, 29-30 Nov 2004.
- [15] Iba, K., Ideta, R., Suzuki, K., “Analysis and Operational Records of NAS Battery”, *Universities Power Engineering Conference, 2006. UPEC '06. Proceedings of the 41st International*, pp. 491-495, 6-8 Sept. 2006.
- [16] Abbey, C., Strunz, K., Chahwan, J., Joos, G., “Impact and Control of Energy Storage Systems in Wind Power Generation”, *Power Conversion Conference - Nagoya, 2007. PCC '07*, pp. 1201-1206, 2-5 April 2007.
- [17] Khushalani, S., Solanki, J.M., Schulz, N.N., “Development of Three Phase Unbalanced Power Flow using PV and PQ models for Distributed Generation and Study of the Impact of DG Models”, *Power Systems, IEEE Transactions on*, pp. 1019-1025, Aug. 2007.
- [18] Abbey, C., Joos, G., “Coordination of Distributed Storage with Wind energy in a Rural Distribution System”, *Industry Applications Conference, 2007. 42nd IAS Annual Meeting. Conference Record of the 2007 IEEE*, pp. 1087-1092, 23-27 Sept. 2007.
- [19] Spahic, E., Balzer, G., Shakib A.D., “The Impact of the “Wind Farm – Battery” Unit on the Power System Stability and Control”, *Power Tech, 2007 IEEE Lausanne*, pp. 485-490, 1-5 July 2007.
- [20] Spahic, E., Balzer, G., Hellmich, B., Munch, W., “Wind Energy Storages – Possibilities”, *Power Tech, 2007 IEEE Lausanne*, pp. 615-620, 1-5 July 2007.

- [21] Shakib, A.D., Balzer, G., “Energy Storage Design and Optimization for Power System with Wind Feeding”, *Probabilistic Methods Applied to Power Systems (PMAPS), 2010 IEEE 11th International Conference on*, pp. 54-59, 14-17 June 2010.
- [22] Hida, Y., et al, “Load Following Operation of NAS Battery by setting Statistic Margins to avoid Risks”, *Power and Energy Society General Meeting, 2010 IEEE*, pp. 1-5, 25-29 July 2010.
- [23] Jintao Cui, et al, “Distributed Energy Storage System in Wind Power Generation”, *Electric Utility Deregulation and Restructuring and Power Technologies (DRPT), 2011 4th International Conference on*, pp. 1535-1540, 6-9 July 2011.
- [24] Such, M.C., Hill, C., “Battery Energy Storage and Wind Energy Integrated into the Smart grid”, *Innovative Smart Grid Technologies (ISGT), 2012 IEEE PES*, pp. 1-4, 16-20 Jan. 2012.
- [25] Ming-Shun Lu., et al, “Combining the Wind Power Generation System with Energy Storage Equipment”, *Industry Applications, IEEE Transactions on*, pp. 2109-2115, Nov.-Dec. 2009.
- [26] Pahwa, A., “ECE 887 – Textbook for Distribution System Engineering – Kansas State University”, 2009.
- [27] “Resourceful Kansas – Wind and Solar Information System”,  
<http://resourceks.ece.ksu.edu/>
- [28] Brooks, D.L., Pourbeik, P., “NERC’s integration of Variable Generation Task Force: Status Report – Planning work group update”, *Power and Energy Society General Meeting, 2010 IEEE*, pp. 1-4, 25-29 July 2010.
- [29] “1547.2-2008 – IEEE Application Guide for IEEE Std 1547, IEEE Standard for Interconnecting Distributed Resources with Electric Power Systems”, pp. 1-207, 15 April 2009.
- [30] “Advanced Metering Infrastructure (AMI)”,  
<http://www.ferc.gov/eventcalendar/Files/20070423091846-EPRI%20-%20Advanced%20Metering.pdf>, Feb. 2007.
- [31] Ulinuha, A., Masoum, M.A.S., Islam, S.M., “Unbalance power flow calculation for a radial distribution system using forward-backward propagation algorithm”, *Power Engineering Conference, 2007. AUPEC 2007. Australasian Universities*, pp. 1-6, 9-12 Dec. 2007.

- [32] “IEEE Distribution Test Feeders”,  
<http://ewh.ieee.org/soc/pes/dsacom/testfeeders/index.html>

## Appendix A – Test Feeder Information

### A.1 Test feeder Line, Load and Transformer details

Configuration	Phasing	Cable	Spacing ID
721	A B C	1,000,000 AA, CN	515
722	A B C	500,000 AA, CN	515
723	A B C	2/0 AA, CN	515
724	A B C	#2 AA, CN	515

**Table A.1 Underground Cable Configuration**

Node	Load	Ph-1	Ph-1	Ph-2	Ph-2	Ph-3	Ph-3
	Model	kW	kVAR	kW	kVAR	kW	kVAR
701	D-PQ	140	70	140	70	350	175
712	D-PQ	0	0	0	0	85	40
713	D-PQ	0	0	0	0	85	40
714	D-I	17	8	21	10	0	0
718	D-Z	85	40	0	0	0	0
720	D-PQ	0	0	0	0	85	40
722	D-I	0	0	140	70	21	10
724	D-Z	0	0	42	21	0	0
725	D-PQ	0	0	42	21	0	0
727	D-PQ	0	0	0	0	42	21
728	D-PQ	42	21	42	21	42	21
729	D-I	42	21	0	0	0	0
730	D-Z	0	0	0	0	85	40
731	D-Z	0	0	85	40	0	0
732	D-PQ	0	0	0	0	42	21
733	D-I	85	40	0	0	0	0
734	D-PQ	0	0	0	0	42	21
735	D-PQ	0	0	0	0	85	40
736	D-Z	0	0	42	21	0	0
737	D-I	140	70	0	0	0	0
738	D-PQ	126	62	0	0	0	0
740	D-PQ	0	0	0	0	85	40
741	D-I	0	0	0	0	42	21
742	D-Z	8	4	85	40	0	0
744	D-PQ	42	21	0	0	0	0
Total		727	357	639	314	1091	530

**Table A.2 Spot Loads**

	kVA	kV-high	kV-low	R - %	X - %
<b>Substation:</b>	2,500	230 D	4.8 D	2	8
<b>XFM -1</b>	500	4.8 D	.480 D	0.09	1.81

**Table A.3 Transformer data**

Node A	Node B	Length(ft.)	Configuration
701	702	960	722
702	705	400	724
702	713	360	723
702	703	1320	722
703	727	240	724
703	730	600	723
704	714	80	724
704	720	800	723
705	742	320	724
705	712	240	724
706	725	280	724
707	724	760	724
707	722	120	724
708	733	320	723
708	732	320	724
709	731	600	723
709	708	320	723
710	735	200	724
710	736	1280	724
711	741	400	723
711	740	200	724
713	704	520	723
714	718	520	724
720	707	920	724
720	706	600	723
727	744	280	723
730	709	200	723
733	734	560	723
734	737	640	723
734	710	520	724
737	738	400	723
738	711	400	723
744	728	200	724
744	729	280	724
775	709	0	XFM-1
799	701	1850	721

**Table A.4 Line Segment data**

## A.2 Phase Impedance Matrices for various configurations

Configuration 721:

Z (R +jX) in ohms per mile		
[ 0.2926+j0.1973	0.0673-j0.0368	0.0337-j0.0417
0.0673-j0.0368	0.2646+j0.1900	0.0673-j0.0368
0.0337-j0.0417	0.0673-j0.0368	0.2926+j0.1973 ]

Configuration 722:

Z (R +jX) in ohms per mile		
[ 0.4751+j0.2973	0.1629-j0.0326	0.1234-j0.0607
0.1629-j0.0326	0.4488+j0.2678	0.1629-j0.0326
0.1234-j0.0607	0.1629-j0.0326	0.4751+j0.2973 ]

Configuration 723:

Z (R +jX) in ohms per mile		
[ 1.2936+j0.6713	0.4871+j0.2111	0.4585+j0.1521
0.4871+j0.2111	1.3022+j0.6326	0.4871+j0.2111
0.4585+j0.1521	0.4871+j0.2111	1.2936+j0.6713 ]

Configuration 724:

Z (R +jX) in ohms per mile		
[ 2.0952+j0.7758	0.5204+j0.2738	0.4926+j0.2123
0.5204+j0.2738	2.1068+j0.7398	0.5204+j0.2738
0.4926+j0.2123	0.5204+j0.2738	2.0952+j0.7758 ]



## Appendix B – Input Files and Software Code

### B.1 Code for Input file used in Fifteen-minute Analysis

```
%Data Files creation for 3-ph load flow BFS method with wind and storage
%combined in the system - Manoj Vijayarengan
clear all
clc

Sb = 2500000;
Vb = 4800;
Zb = (Vb^2)/Sb;

%Load
%
% Node Renum Model kW kVAr kW kVAr kW kVAr
Node = [701 2 1 140 70 140 70 350 175
712 5 1 0 0 0 0 85 40
713 7 1 0 0 0 0 85 40
714 9 3 17 8 21 10 0 0
718 10 2 85 40 0 0 0 0
720 11 1 0 0 0 0 85 40
722 13 3 0 0 140 70 21 10
724 14 2 0 0 42 21 0 0
725 16 1 0 0 42 21 0 0
727 18 1 0 0 0 0 42 21
728 20 1 42 21 42 21 42 21
729 21 3 42 21 0 0 0 0
730 22 2 0 0 0 0 85 40
731 24 2 0 0 85 40 0 0
732 36 1 0 0 0 0 42 21
733 26 3 85 40 0 0 0 0
734 27 1 0 0 0 0 42 21
735 30 1 0 0 0 0 85 40
736 29 2 0 0 42 21 0 0
737 31 3 140 70 0 0 0 0
738 32 1 126 62 0 0 0 0
740 34 1 0 0 0 0 85 40
741 35 3 0 0 0 0 42 21
742 6 2 8 4 85 40 0 0
744 19 1 42 21 0 0 0 0 ];

S_peak = [0;0;0];
for i = 1:size(Node,1);
    S_peak = S_peak + 1000*[Node(i,4)+1j*Node(i,5) Node(i,6)+1j*Node(i,7)
Node(i,8)+1j*Node(i,9)].';
end
```

```
%Branch
%
% NodeA RenumA NodeB RenumB Length(ft.) Config.
Branch = [ 701 2 702 3 960 722
702 3 705 4 400 724
702 3 713 7 360 723
702 3 703 17 1320 722
703 17 727 18 240 724
703 17 730 22 600 723
704 8 714 9 80 724
704 8 720 11 800 723
```

705	4	742	6	320	724
705	4	712	5	240	724
706	15	725	16	280	724
707	12	724	14	760	724
707	12	722	13	120	724
708	25	733	26	320	723
708	25	732	36	320	724
709	23	731	24	600	723
709	23	708	25	320	723
710	28	735	30	200	724
710	28	736	29	1280	724
711	33	741	35	400	723
711	33	740	34	200	724
713	7	704	8	520	723
714	9	718	10	520	724
720	11	707	12	920	724
720	11	706	15	600	723
727	18	744	19	280	723
730	22	709	23	200	723
733	26	734	27	560	723
734	27	737	31	640	723
734	27	710	28	520	724
737	31	738	32	400	723
738	32	711	33	400	723
744	19	728	20	200	724
744	19	729	21	280	724
709	23	775	37	0	1
799	1	701	2	1850	721 ];

```

% Impedance matrices
z721 = [ 0.2926+1j*0.1973  0.0673-1j*0.0368  0.0337-1j*0.0417
         0.0673-1j*0.0368  0.2646+1j*0.1900  0.0673-1j*0.0368
         0.0337-1j*0.0417  0.0673-1j*0.0368  0.2926+1j*0.1973 ];
z721 = {z721};

z722 = [ 0.4751+1j*0.2973  0.1629-1j*0.0326  0.1234-1j*0.0607
         0.1629-1j*0.0326  0.4488+1j*0.2678  0.1629-1j*0.0326
         0.1234-1j*0.0607  0.1629-1j*0.0326  0.4751+1j*0.2973 ];
z722 = {z722};

z723 = [ 1.2936+1j*0.6713  0.4871+1j*0.2111  0.4585+1j*0.1521
         0.4871+1j*0.2111  1.3022+1j*0.6326  0.4871+1j*0.2111
         0.4585+1j*0.1521  0.4871+1j*0.2111  1.2936+1j*0.6713 ];
z723 = {z723};

z724 = [ 2.0952+1j*0.7758  0.5204+1j*0.2738  0.4926+1j*0.2123
         0.5204+1j*0.2738  2.1068+1j*0.7398  0.5204+1j*0.2738
         0.4926+1j*0.2123  0.5204+1j*0.2738  2.0952+1j*0.7758 ];
z724 = {z724};

Z = [z721;z722;z723;z724];

ftmi = 1.8939e-4;

```

```

% Transformer matrices

```

```

% For D-D transformer (in branch 709-775),
% at = (nt/3)*[2 -1 -1;-1 2 -1;-1 -1 2]
% bt = W*AV*Zabc*G1
% where W = (1/3)*[2 1 0;0 2 1;1 0 2]
%     AV = [nt 0 0;0 nt 0;0 0 nt]
%     Zabc = diagonal(Zab,Zbc,Zca)
%     G1 = (1/(Zab+Zbc+Zca))*[Zca -Zbc 0;Zca Zab+Zca 0;-Zab-Zbc -Zbc 0]
% dt = (1/nt)*eye(3)
% At = (1/(3*nt))*[2 -1 -1;-1 2 -1;-1 2 -1]
% Bt = W*Zabc*G1
nt = 10;
Zab = 0.0009+1j*0.0181;
Zbc = Zab;
Zca = Zab;
W = (1/3)*[2 1 0;0 2 1;1 0 2];
AV = [nt 0 0;0 nt 0;0 0 nt];
Zabc = [Zab 0 0;0 Zbc 0;0 0 Zca];
G1 = (1/(Zab+Zbc+Zca))*[Zca -Zbc 0;Zca Zab+Zca 0;-Zab-Zbc -Zbc 0];
at = (nt/3)*[2 -1 -1;-1 2 -1;-1 -1 2];
bt = W*AV*Zabc*G1;
dt = (1/nt)*eye(3);
At = (1/(3*nt))*[2 -1 -1;-1 2 -1;-1 -1 2];
Bt = W*Zabc*G1;

```

```

%Normalized Load fractions for 15-min divisions from profile 1
AggDem_Norm_1 = [ 0.5667
                  0.3805
                  0.4207
                  0.4425
                  0.4138
                  0.4586
                  0.5828
                  0.4057
                  0.4529
                  0.3690
                  0.3655
                  0.4506
                  0.3632
                  0.3080
                  0.4954
                  0.2598
                  0.3908
                  0.3391
                  0.3161
                  0.4540
                  0.3230
                  0.5207
                  0.4977
                  0.3954
                  0.4264
                  0.2966
                  0.4414
                  0.3241
                  0.3851
                  0.5034
                  0.4943
                  0.4138
                  0.2885]

```

0.5310  
0.4126  
0.3057  
0.5103  
0.5241  
0.5299  
0.6138  
0.5276  
0.5460  
0.8218  
0.9080  
0.8299  
0.8402  
0.7586  
0.9897  
0.7667  
0.7989  
0.9529  
0.7379  
0.8080  
1.0000  
0.7667  
0.9126  
0.8770  
0.8943  
0.8149  
0.9230  
0.9149  
0.8690  
0.7943  
0.8736  
0.9598  
0.9310  
0.9414  
0.8782  
0.9207  
0.7552  
0.9069  
0.9241  
0.7609  
0.8552  
0.8310  
0.7931  
0.9954  
0.7989  
0.8598  
0.9471  
0.8977  
0.9448  
0.9506  
0.7816  
0.8644  
0.6920  
0.8529  
0.7713  
0.8149  
0.7494  
0.7839

```

0.9080
0.6460
0.7793
0.7805
0.8414 ];

```

```

%           %Medium wind generation for a single day - 8 100kW
%           %Northwind Turbines
MedGen = [ 69.6000  68.1067  69.4133  31.3200  30.6480  31.2360
68.8533  67.3600  68.7200  30.9840  30.3120  30.9240
66.4267  64.9333  66.3200  29.8920  29.2200  29.8440
83.8133  82.2133  83.9200  37.7160  36.9960  37.7640
73.4133  72.1067  73.5200  33.0360  32.4480  33.0840
68.6667  67.4667  68.7733  30.9000  30.3600  30.9480
55.5200  54.4800  55.7333  24.9840  24.5160  25.0800
45.7067  44.5600  45.6533  20.5680  20.0520  20.5440
43.2533  42.1600  43.1200  19.4640  18.9720  19.4040
61.4933  60.2400  61.4667  27.6720  27.1080  27.6600
80.1067  78.7200  80.2400  36.0480  35.4240  36.1080
94.1867  92.4267  94.2133  42.3840  41.5920  42.3960
101.7600 100.0533 101.8133  45.7920  45.0240  45.8160
122.1867 120.5867 122.4533  54.9840  54.2640  55.1040
151.9200 149.7067 152.0533  68.3640  67.3680  68.4240
153.1467 150.8267 153.0667  68.9160  67.8720  68.8800
160.2133 157.9733 160.0000  72.0960  71.0880  72.0000
161.8667 159.5733 161.6000  72.8400  71.8080  72.7200
132.1333 129.9733 131.8133  59.4600  58.4880  59.3160
129.5733 127.5733 129.0933  58.3080  57.4080  58.0920
127.2800 125.6000 127.0133  57.2760  56.5200  57.1560
132.7200 131.0400 132.4000  59.7240  58.9680  59.5800
144.6933 143.0133 144.5600  65.1120  64.3560  65.0520
141.3867 139.5467 141.2533  63.6240  62.7960  63.5640
146.9867 145.2000 146.9067  66.1440  65.3400  66.1080
132.0533 130.4267 131.8667  59.4240  58.6920  59.3400
117.2267 115.7867 117.1467  52.7520  52.1040  52.7160
93.1733  91.7867  93.0933  41.9280  41.3040  41.8920
83.7067  82.5333  83.7067  37.6680  37.1400  37.6680
87.3333  86.1600  87.3867  39.3000  38.7720  39.3240
82.2133  80.8800  82.0267  36.9960  36.3960  36.9120
110.8000 109.1467 110.4533  49.8600  49.1160  49.7040
95.5467  93.5467  95.1200  42.9960  42.0960  42.8040
99.8667  97.9200  99.4933  44.9400  44.0640  44.7720
101.8667 100.0267 101.4667  45.8400  45.0120  45.6600
106.9867 105.0400 106.6933  48.1440  47.2680  48.0120
111.4933 109.4400 111.2800  50.1720  49.2480  50.0760
95.6533  93.8133  95.4400  43.0440  42.2160  42.9480
86.8000  85.1467  86.6667  39.0600  38.3160  39.0000
72.4000  70.9600  72.2667  32.5800  31.9320  32.5200
70.1333  68.8000  70.1600  31.5600  30.9600  31.5720
53.5467  52.4800  53.6800  24.0960  23.6160  24.1560
60.9867  59.6800  61.0400  27.4440  26.8560  27.4680
61.3067  60.1067  61.4667  27.5880  27.0480  27.6600
82.6933  80.9333  82.3733  37.2120  36.4200  37.0680
70.2667  68.8267  70.0533  31.6200  30.9720  31.5240
65.3067  64.1867  65.1733  29.3880  28.8840  29.3280
76.7733  75.4933  76.8533  34.5480  33.9720  34.5840
76.1333  74.4000  76.2667  34.2600  33.4800  34.3200
67.0133  65.2800  66.9333  30.1560  29.3760  30.1200

```

43.7067	42.6133	43.3867	19.6680	19.1760	19.5240
42.7467	41.9733	42.5333	19.2360	18.8880	19.1400
40.4533	39.7867	40.3200	18.2040	17.9040	18.1440
53.4133	52.2133	52.9600	24.0360	23.4960	23.8320
47.1733	46.0800	46.8267	21.2280	20.7360	21.0720
46.8000	45.8133	46.2933	21.0600	20.6160	20.8320
59.8933	58.8267	59.6000	26.9520	26.4720	26.8200
59.4667	58.3467	59.2267	26.7600	26.2560	26.6520
54.1867	52.9333	53.5733	24.3840	23.8200	24.1080
56.1600	54.9600	55.8133	25.2720	24.7320	25.1160
64.7467	63.3067	64.4533	29.1360	28.4880	29.0040
78.5067	76.8533	78.0000	35.3280	34.5840	35.1000
80.4533	79.3600	80.4000	36.2040	35.7120	36.1800
73.5733	72.3733	73.6800	33.1080	32.5680	33.1560
79.7600	78.2933	79.7067	35.8920	35.2320	35.8680
90.0533	88.6933	89.8933	40.5240	39.9120	40.4520
110.5333	108.5867	110.2933	49.7400	48.8640	49.6320
85.6267	84.0533	85.3867	38.5320	37.8240	38.4240
62.8000	61.4133	62.5867	28.2600	27.6360	28.1640
62.5867	61.0933	62.2667	28.1640	27.4920	28.0200
63.9467	62.4267	63.4933	28.7760	28.0920	28.5720
77.3867	75.7067	76.9867	34.8240	34.0680	34.6440
80.5600	78.9067	80.0533	36.2520	35.5080	36.0240
102.3200	100.4533	101.9200	46.0440	45.2040	45.8640
63.9733	62.4800	63.4133	28.7880	28.1160	28.5360
63.3333	62.1600	63.1467	28.5000	27.9720	28.4160
60.4267	59.2800	60.4000	27.1920	26.6760	27.1800
71.3600	70.1600	71.3867	32.1120	31.5720	32.1240
38.1067	37.3600	38.0267	17.1480	16.8120	17.1120
52.0800	51.2800	52.0533	23.4360	23.0760	23.4240
87.5733	86.3733	87.7867	39.4080	38.8680	39.5040
60.0000	59.1200	60.1600	27.0000	26.6040	27.0720
47.0400	46.1067	46.8533	21.1680	20.7480	21.0840
35.2533	34.3200	34.7467	15.8640	15.4440	15.6360
38.9067	37.9733	38.4800	17.5080	17.0880	17.3160
26.8000	26.0267	26.4267	12.0600	11.7120	11.8920
36.8000	35.7600	36.5067	16.5600	16.0920	16.4280
30.7733	29.7867	30.4800	13.8480	13.4040	13.7160
36.8800	35.9733	36.6133	16.5960	16.1880	16.4760
41.7333	40.7733	41.6800	18.7800	18.3480	18.7560
32.8533	32.1333	32.8000	14.7840	14.4600	14.7600
37.7067	36.7733	37.4400	16.9680	16.5480	16.8480
18.8267	18.0800	18.4533	8.4720	8.1360	8.3040
30.0267	29.0667	29.7067	13.5120	13.0800	13.3680
24.5867	23.5733	24.0800	11.0640	10.6080	10.8360
30.7733	29.6533	30.2133	13.8480	13.3440	13.5960 ];

```
%
%      High wind generation for a single day - 8 100kW
%Northwind Turbines
HighGen = [ 281.5501 275.5605 279.9189 126.6976 124.0022 125.9635
257.9286 252.7216 256.1336 116.0679 113.7247 115.2601
258.8540 254.7260 257.4784 116.4843 114.6267 115.8653
249.5892 245.2773 248.4009 112.3151 110.3748 111.7804
166.1852 163.1836 166.3977 74.7834 73.4326 74.8790
246.7829 242.1951 245.9837 111.0523 108.9878 110.6927
289.5928 285.1840 288.8539 130.3168 128.3328 129.9843
259.3332 255.5449 258.7695 116.6999 114.9952 116.4463
251.2633 247.5916 250.6554 113.0685 111.4162 112.7949
```

241.1937	237.3907	240.4628	108.5372	106.8258	108.2083
220.4890	216.7499	220.5590	99.2200	97.5374	99.2515
170.5276	167.2932	170.4710	76.7374	75.2819	76.7119
194.6946	190.9874	193.6259	87.6126	85.9443	87.1317
201.4305	197.2865	200.4182	90.6437	88.7789	90.1882
166.5257	163.6487	166.1027	74.9365	73.6419	74.7462
173.8276	171.2013	173.1800	78.2224	77.0406	77.9310
157.8256	155.1120	157.0649	71.0215	69.8004	70.6792
160.5729	157.9383	159.8133	72.2578	71.0722	71.9160
156.6348	154.0328	155.9338	70.4856	69.3148	70.1702
132.6656	130.3142	131.9406	59.6995	58.6414	59.3733
146.6556	143.6675	145.5267	65.9950	64.6504	65.4870
166.8968	163.6652	165.5689	75.1036	73.6493	74.5060
195.1793	191.8074	194.5388	87.8307	86.3133	87.5425
182.2967	179.2603	181.3677	82.0335	80.6672	81.6155
135.7996	133.3230	135.1459	61.1098	59.9954	60.8157
181.2490	177.8670	180.0255	81.5620	80.0401	81.0115
139.0507	136.1839	137.9074	62.5728	61.2828	62.0583
147.1830	144.2861	146.3829	66.2323	64.9288	65.8723
180.0165	176.5430	178.3378	81.0074	79.4444	80.2520
192.7610	189.0588	191.4471	86.7424	85.0765	86.1512
219.4664	215.4934	217.7267	98.7599	96.9720	97.9770
205.5480	201.7413	203.5906	92.4966	90.7836	91.6158
188.9781	186.0578	187.8556	85.0401	83.7260	84.5350
185.5239	182.8132	184.8639	83.4858	82.2659	83.1887
214.6119	211.3663	213.8163	96.5753	95.1148	96.2173
169.9298	166.8443	169.4745	76.4684	75.0799	76.2635
151.4000	148.5034	150.7789	68.1300	66.8265	67.8505
158.1906	155.3850	157.6438	71.1858	69.9232	70.9397
154.8747	152.3742	154.9013	69.6936	68.5684	69.7056
145.7215	143.2940	145.5506	65.5747	64.4823	65.4978
119.7136	117.7068	119.7499	53.8711	52.9681	53.8875
107.8217	106.1186	108.0676	48.5198	47.7534	48.6304
109.1439	107.3334	109.4081	49.1148	48.3000	49.2337
119.0752	116.7744	119.0558	53.5839	52.5485	53.5751
120.4739	117.9034	120.2289	54.2133	53.0565	54.1030
167.4364	164.3039	166.7815	75.3464	73.9368	75.0517
201.9840	199.1634	201.9390	90.8928	89.6235	90.8725
164.5809	162.0136	164.4520	74.0614	72.9061	74.0034
121.5801	119.6726	121.5301	54.7110	53.8527	54.6885
160.3128	157.8708	160.2114	72.1408	71.0418	72.0951
154.5830	152.1322	154.5418	69.5623	68.4595	69.5438
136.8201	134.5896	136.7365	61.5690	60.5653	61.5314
192.0582	188.4824	191.3688	86.4262	84.8171	86.1160
192.5512	188.6248	191.3867	86.6480	84.8812	86.1240
177.6566	174.1032	177.0777	79.9455	78.3464	79.6850
186.3555	182.8996	185.9392	83.8600	82.3048	83.6726
223.9334	219.7368	222.7411	100.7700	98.8815	100.2335
202.5944	198.5224	201.8154	91.1675	89.3351	90.8169
207.0331	203.2247	206.2358	93.1649	91.4511	92.8061
201.2881	197.6263	200.5627	90.5796	88.9318	90.2532
248.7264	244.3014	248.0414	111.9269	109.9356	111.6186
247.3148	242.4722	245.9475	111.2917	109.1125	110.6764
248.9380	244.0643	247.3982	112.0221	109.8289	111.3292
250.8993	245.9372	249.3291	112.9047	110.6717	112.1981
242.5997	238.1248	241.7165	109.1698	107.1561	108.7724
248.3843	243.9465	247.2201	111.7730	109.7759	111.2490
273.0356	267.9197	271.5799	122.8660	120.5639	122.2110

282.2504	277.0619	280.8363	127.0127	124.6779	126.3763
280.8353	275.4991	279.5669	126.3759	123.9746	125.8051
249.7466	245.0150	248.9040	112.3860	110.2567	112.0068
222.9976	219.4022	222.7584	100.3489	98.7310	100.2413
233.4804	229.5232	233.4604	105.0662	103.2855	105.0572
240.6930	236.2265	240.3427	108.3119	106.3019	108.1542
239.6281	235.0626	239.1987	107.8327	105.7782	107.6394
253.7524	249.1953	253.1141	114.1886	112.1379	113.9014
267.4458	262.6631	266.6065	120.3506	118.1984	119.9729
250.3672	245.8844	249.7498	112.6652	110.6480	112.3874
223.5473	219.6609	223.3517	100.5963	98.8474	100.5083
209.9352	206.4430	209.7836	94.4708	92.8994	94.4026
210.1597	206.7353	209.8198	94.5719	93.0309	94.4189
175.5417	172.6081	174.9504	78.9937	77.6737	78.7277
194.6614	191.3548	194.0840	87.5976	86.1096	87.3378
182.8304	179.4926	182.4156	82.2737	80.7717	82.0870
158.5451	155.5843	158.4632	71.3453	70.0129	71.3085
162.9233	160.0625	162.9225	73.3155	72.0281	73.3151
170.2485	167.0910	169.9036	76.6118	75.1910	76.4566
159.4286	156.3825	159.0667	71.7428	70.3721	71.5800
139.9951	137.1489	139.8089	62.9978	61.7170	62.9140
146.8990	144.0561	146.6753	66.1046	64.8253	66.0039
114.5270	112.1761	114.4074	51.5372	50.4793	51.4833
86.0956	83.9931	86.1375	38.7430	37.7969	38.7619
77.5236	75.4881	77.3301	34.8856	33.9697	34.7985
99.6748	97.2950	99.3048	44.8536	43.7827	44.6871
93.7251	91.4118	93.2710	42.1763	41.1353	41.9720
88.5965	86.6787	88.0478	39.8684	39.0054	39.6215
71.7157	70.0427	71.3719	32.2721	31.5192	32.1174

];

```
%
%                               %Low wind generation for a single day - 8 100kW
%                               %Northwind Turbines
LowGen = [ 28.8333  27.6133  28.5033  12.9750  12.4260  12.8265
25.3200  24.1000  25.1033  11.3940  10.8450  11.2965
20.8133  19.6267  20.5167   9.3660   8.8320   9.2325
18.1467  17.3067  17.9833   8.1660   7.7880   8.0925
20.3633  19.6500  20.3867   9.1635   8.8425   9.1740
22.7167  21.8700  22.5933  10.2225   9.8415  10.1670
20.1600  19.2833  20.0900   9.0720   8.6775   9.0405
25.6467  24.6367  25.7167  11.5410  11.0865  11.5725
31.1167  29.8367  30.9600  14.0025  13.4265  13.9320
25.2833  24.1633  25.2800  11.3775  10.8735  11.3760
19.9667  19.1700  20.0600   8.9850   8.6265   9.0270
17.9733  16.9500  17.8533   8.0880   7.6275   8.0340
21.0533  19.8467  20.9733   9.4740   8.9310   9.4380
22.7133  21.5533  22.3533  10.2210   9.6990  10.0590
14.2600  13.6800  14.2167   6.4170   6.1560   6.3975
 7.8333   8.1200   7.8233   3.5250   3.6540   3.5205
 3.2933   3.6833   3.0633   1.4820   1.6575   1.3785
 2.5667   2.8100   2.2767   1.1550   1.2645   1.0245
 8.3900   8.4900   8.3567   3.7755   3.8205   3.7605
 8.1833   8.5633   8.3233   3.6825   3.8535   3.7455
11.9600  11.7833  12.1900   5.3820   5.3025   5.4855
15.6400  15.0767  15.6500   7.0380   6.7845   7.0425
 9.8967   9.6967   9.8567   4.4535   4.3635   4.4355
 9.5700   9.3300   9.6367   4.3065   4.1985   4.3365
17.4833  16.8033  17.0933   7.8675   7.5615   7.6920
```



35.5367	34.3500	35.1733	15.9915	15.4575	15.8280
46.2867	44.8000	45.9500	20.8290	20.1600	20.6775
38.4333	37.1333	38.3300	17.2950	16.7100	17.2485
39.6133	38.2333	39.4100	17.8260	17.2050	17.7345
38.3133	36.9467	38.2100	17.2410	16.6260	17.1945
31.4667	30.2600	31.3933	14.1600	13.6170	14.1270
42.4000	40.9867	42.1467	19.0800	18.4440	18.9660
42.2300	41.0067	42.0600	19.0035	18.4530	18.9270
50.4767	49.0533	50.1667	22.7145	22.0740	22.5750
47.1867	46.0767	47.0733	21.2340	20.7345	21.1830
34.2733	33.2900	34.1600	15.4230	14.9805	15.3720
35.7900	34.8733	35.9100	16.1055	15.6930	16.1595
38.2500	36.9933	38.2633	17.2125	16.6470	17.2185
48.4467	47.0167	48.6500	21.8010	21.1575	21.8925
28.0533	27.0500	28.3367	12.6240	12.1725	12.7515
20.0133	19.3900	20.3933	9.0060	8.7255	9.1770
29.5467	28.5567	29.7733	13.2960	12.8505	13.3980
26.7867	25.9400	26.9633	12.0540	11.6730	12.1335
24.3600	23.3933	24.4433	10.9620	10.5270	10.9995
22.4233	21.2067	22.2700	10.0905	9.5430	10.0215
26.9567	26.0133	26.8900	12.1305	11.7060	12.1005
36.5900	35.3233	36.5700	16.4655	15.8955	16.4565
30.4100	29.3233	30.4567	13.6845	13.1955	13.7055
34.5200	33.2500	34.8100	15.5340	14.9625	15.6645
41.2800	39.9367	41.5500	18.5760	17.9715	18.6975
40.6333	39.7967	41.2233	18.2850	17.9085	18.5505
39.7267	38.7900	40.2500	17.8770	17.4555	18.1125
32.3500	31.3000	32.6700	14.5575	14.0850	14.7015
24.8833	24.0467	25.0167	11.1975	10.8210	11.2575
26.0467	25.0467	25.9567	11.7210	11.2710	11.6805
31.2333	30.4600	31.1767	14.0550	13.7070	14.0295
21.6933	20.9500	21.7567	9.7620	9.4275	9.7905
22.6800	21.8300	22.6033	10.2060	9.8235	10.1715
26.0967	25.4233	26.1867	11.7435	11.4405	11.7840
28.1433	27.3967	28.3933	12.6645	12.3285	12.7770
24.5467	23.8067	24.7300	11.0460	10.7130	11.1285
27.2200	26.3733	27.4700	12.2490	11.8680	12.3615
21.0100	20.3833	21.2867	9.4545	9.1725	9.5790
18.5700	17.9033	18.9067	8.3565	8.0565	8.5080
16.3667	15.8300	16.4267	7.3650	7.1235	7.3920
20.6400	20.0300	20.7067	9.2880	9.0135	9.3180
27.2433	26.4700	27.1733	12.2595	11.9115	12.2280
27.8900	27.0500	28.0933	12.5505	12.1725	12.6420
28.1833	27.3467	28.4633	12.6825	12.3060	12.8085
28.9367	28.3200	29.2567	13.0215	12.7440	13.1655
17.0367	16.5533	17.2300	7.6665	7.4490	7.7535
15.5900	15.3533	15.8767	7.0155	6.9090	7.1445
9.8733	9.9533	9.8933	4.4430	4.4790	4.4520
10.7467	10.6600	10.7467	4.8360	4.7970	4.8360
8.3633	8.5033	8.2533	3.7635	3.8265	3.7140
7.0700	7.2100	6.8333	3.1815	3.2445	3.0750
4.7967	5.1167	4.5167	2.1585	2.3025	2.0325
5.7233	6.0633	5.2700	2.5755	2.7285	2.3715
5.6633	6.1333	5.4300	2.5485	2.7600	2.4435
4.9700	5.4467	4.7433	2.2365	2.4510	2.1345
0.9867	1.0933	0.5833	0.4440	0.4920	0.2625
0.9800	1.1000	0.5633	0.4410	0.4950	0.2535
0.9800	1.0967	0.5633	0.4410	0.4935	0.2535

0.9800	1.1033	0.5633	0.4410	0.4965	0.2535
0.9900	1.1100	0.5733	0.4455	0.4995	0.2580
0.9900	1.1100	0.5867	0.4455	0.4995	0.2640
0.9900	1.1167	0.5733	0.4455	0.5025	0.2580
0.9900	1.1167	0.5733	0.4455	0.5025	0.2580
0.9933	1.1167	0.5933	0.4470	0.5025	0.2670
0.9933	1.1100	0.5933	0.4470	0.4995	0.2670
0.9900	1.1100	0.5767	0.4455	0.4995	0.2595
3.8767	3.9967	3.4967	1.7445	1.7985	1.5735
7.5000	7.9433	7.4333	3.3750	3.5745	3.3450
9.1400	9.1833	9.0400	4.1130	4.1325	4.0680
18.8133	18.2167	18.8200	8.4660	8.1975	8.4690
27.0667	26.0567	26.9267	12.1800	11.7255	12.1170 ];

```

%           %Load file creation for 24 hours on 15-minute basis with wind
%           %included
L = Node(1:size(Node,1),1:3);
C_Low = [];
C_Med = [];
C_High = [];
MeanDem = mean(AggDem_Norm_1);
S_avg = MeanDem.*S_peak;
for i = 1:length(AggDem_Norm_1)
    Load = [L(1:13,1:3) Node(1:13,4:9).*AggDem_Norm_1(i); L(14:25,1:3)
Node(14:25,4:9).*AggDem_Norm_1(i)];
    Load = [Load; 1000 32 1 LowGen(i,1) LowGen(i,4) LowGen(i,2)
LowGen(i,5) LowGen(i,3) LowGen(i,6)];
    Load = {Load};
    C_Low = [C_Low;Load];
    Load = cell2mat(Load);
    Load = [L(1:13,1:3) Node(1:13,4:9).*AggDem_Norm_1(i); L(14:25,1:3)
Node(14:25,4:9).*AggDem_Norm_1(i)];
    Load = [Load; 1000 32 1 MedGen(i,1) MedGen(i,4) MedGen(i,2)
MedGen(i,5) MedGen(i,3) MedGen(i,6)];
    Load = {Load};
    C_Med = [C_Med;Load];
    Load = cell2mat(Load);
    Load = [L(1:13,1:3) Node(1:13,4:9).*AggDem_Norm_1(i); L(14:25,1:3)
Node(14:25,4:9).*AggDem_Norm_1(i)];
    Load = [Load; 1000 32 1 HighGen(i,1) HighGen(i,4) HighGen(i,2)
HighGen(i,5) HighGen(i,3) HighGen(i,6)];
    Load = {Load};
    C_High = [C_High;Load];
    Load = cell2mat(Load);
end

%Proximity matrix creation
N = max(max(Branch(:,2)), max(Branch(:,4)));
Prox = zeros(N,N);
for i = 1:N-1
    if Branch(i,6) == 1
        Prox(Branch(i,2),Branch(i,4)) = 0.5;
    else
        Prox(Branch(i,2),Branch(i,4)) = 1;
    end
    Prox(i,i) = 1;
end

```

```

Prox(N,N) = 1;

Zline = {N};
for i = 1:size(Branch,1)
    if Branch(i,6) ~= 1
        Zline{Branch(i,2),Branch(i,4)} =
Branch(i,5)*ftmi*cell2mat(Z(Branch(i,6)-720))./Zb;
    end
end

```

## B.2 Code for Input file used in One-second Analysis

%Data Files creation for 3-ph load flow BFS method with wind and storage  
%combined in the system - Manoj Vijayarengan

```
clear all
```

```
clc
```

```
tic
```

```
Sb = 2500000;
```

```
Vb = 4800;
```

```
Zb = (Vb^2)/Sb;
```

```

                                %Load
%   Node  Renum  Model  kW  kVAr  kW  kVAr  kW  kVAr
Node = [701      2      1    140  70    140  70    350 175
        712      5      1      0   0      0   0      85  40
        713      7      1      0   0      0   0      85  40
        714      9      3     17   8     21  10      0   0
        718     10      2     85  40      0   0      0   0
        720     11      1      0   0      0   0      85  40
        722     13      3      0   0     140  70     21  10
        724     14      2      0   0     42  21      0   0
        725     16      1      0   0     42  21      0   0
        727     18      1      0   0      0   0     42  21
        728     20      1     42  21     42  21     42  21
        729     21      3     42  21      0   0      0   0
        730     22      2      0   0      0   0     85  40
        731     24      2      0   0     85  40      0   0
        732     36      1      0   0      0   0     42  21
        733     26      3     85  40      0   0      0   0
        734     27      1      0   0      0   0     42  21
        735     30      1      0   0      0   0     85  40
        736     29      2      0   0     42  21      0   0
        737     31      3     140  70      0   0      0   0
        738     32      1    126  62      0   0      0   0
        740     34      1      0   0      0   0     85  40
        741     35      3      0   0      0   0     42  21
        742      6      2      8   4     85  40      0   0
        744     19      1     42  21      0   0      0   0 ];

```

```
S_peak = [0;0;0];
```

```
for i = 1:size(Node,1);
```

```
    S_peak = S_peak + 1000.*[Node(i,4)+1j*Node(i,5)
```

```
Node(i,6)+1j*Node(i,7) Node(i,8)+1j*Node(i,9)].';
```

```
end
```

```
%Branch
```

%	NodeA	RenumA	NodeB	RenumB	Length(ft.)	Config.
Branch = [	701	2	702	3	960	722
	702	3	705	4	400	724
	702	3	713	7	360	723
	702	3	703	17	1320	722
	703	17	727	18	240	724
	703	17	730	22	600	723
	704	8	714	9	80	724
	704	8	720	11	800	723
	705	4	742	6	320	724
	705	4	712	5	240	724
	706	15	725	16	280	724
	707	12	724	14	760	724
	707	12	722	13	120	724
	708	25	733	26	320	723
	708	25	732	36	320	724
	709	23	731	24	600	723
	709	23	708	25	320	723
	710	28	735	30	200	724
	710	28	736	29	1280	724
	711	33	741	35	400	723
	711	33	740	34	200	724
	713	7	704	8	520	723
	714	9	718	10	520	724
	720	11	707	12	920	724
	720	11	706	15	600	723
	727	18	744	19	280	723
	730	22	709	23	200	723
	733	26	734	27	560	723
	734	27	737	31	640	723
	734	27	710	28	520	724
	737	31	738	32	400	723
	738	32	711	33	400	723
	744	19	728	20	200	724
	744	19	729	21	280	724
	709	23	775	37	0	1
	799	1	701	2	1850	721 ];

```

% Impedance matrices
z721 = [ 0.2926+1j*0.1973    0.0673-1j*0.0368    0.0337-1j*0.0417
         0.0673-1j*0.0368    0.2646+1j*0.1900    0.0673-1j*0.0368
         0.0337-1j*0.0417    0.0673-1j*0.0368    0.2926+1j*0.1973 ];
z721 = {z721};

z722 = [ 0.4751+1j*0.2973    0.1629-1j*0.0326    0.1234-1j*0.0607
         0.1629-1j*0.0326    0.4488+1j*0.2678    0.1629-1j*0.0326
         0.1234-1j*0.0607    0.1629-1j*0.0326    0.4751+1j*0.2973 ];
z722 = {z722};

z723 = [ 1.2936+1j*0.6713    0.4871+1j*0.2111    0.4585+1j*0.1521
         0.4871+1j*0.2111    1.3022+1j*0.6326    0.4871+1j*0.2111
         0.4585+1j*0.1521    0.4871+1j*0.2111    1.2936+1j*0.6713 ];
z723 = {z723};

z724 = [ 2.0952+1j*0.7758    0.5204+1j*0.2738    0.4926+1j*0.2123
         0.5204+1j*0.2738    2.1068+1j*0.7398    0.5204+1j*0.2738

```

```

        0.4926+1j*0.2123    0.5204+1j*0.2738    2.0952+1j*0.7758 ];
z724 = {z724};

Z = [z721;z722;z723;z724];

ftmi = 1.8939e-4;

% Transformer matrices
% For D-D transformer (in branch 709-775),
% at = (nt/3)*[2 -1 -1;-1 2 -1;-1 -1 2]
% bt = W*AV*Zabc*G1
% where W = (1/3)*[2 1 0;0 2 1;1 0 2]
%      AV = [nt 0 0;0 nt 0;0 0 nt]
%      Zabc = diagonal(Zab,Zbc,Zca)
%      G1 = (1/(Zab+Zbc+Zca))*[Zca -Zbc 0;Zca Zab+Zca 0;-Zab-Zbc -Zbc 0]
% dt = (1/nt)*eye(3)
% At = (1/(3*nt))*[2 -1 -1;-1 2 -1;-1 2 -1]
% Bt = W*Zabc*G1
nt = 10;
Zab = 0.0009+1j*0.0181;
Zbc = Zab;
Zca = Zab;
W = (1/3)*[2 1 0;0 2 1;1 0 2];
AV = [nt 0 0;0 nt 0;0 0 nt];
Zabc = [Zab 0 0;0 Zbc 0;0 0 Zca];
G1 = (1/(Zab+Zbc+Zca))*[Zca -Zbc 0;Zca Zab+Zca 0;-Zab-Zbc -Zbc 0];
at = (nt/3)*[2 -1 -1;-1 2 -1;-1 -1 2];
bt = W*AV*Zabc*G1;
dt = (1/nt)*eye(3);
At = (1/(3*nt))*[2 -1 -1;-1 2 -1;-1 -1 2];
Bt = W*Zabc*G1;

%Normalized Load fractions for 15-min divisions from profile 1
AggDem_Norm_1 = [ 0.5667
                  0.3805
                  0.4207
                  0.4425
                  0.4138
                  0.4586
                  0.5828
                  0.4057
                  0.4529
                  0.3690
                  0.3655
                  0.4506
                  0.3632
                  0.3080
                  0.4954
                  0.2598
                  0.3908
                  0.3391
                  0.3161
                  0.4540
                  0.3230
                  0.5207

```

0.4977  
0.3954  
0.4264  
0.2966  
0.4414  
0.3241  
0.3851  
0.5034  
0.4943  
0.4138  
0.2885  
0.5310  
0.4126  
0.3057  
0.5103  
0.5241  
0.5299  
0.6138  
0.5276  
0.5460  
0.8218  
0.9080  
0.8299  
0.8402  
0.7586  
0.9897  
0.7667  
0.7989  
0.9529  
0.7379  
0.8080  
1.0000  
0.7667  
0.9126  
0.8770  
0.8943  
0.8149  
0.9230  
0.9149  
0.8690  
0.7943  
0.8736  
0.9598  
0.9310  
0.9414  
0.8782  
0.9207  
0.7552  
0.9069  
0.9241  
0.7609  
0.8552  
0.8310  
0.7931  
0.9954  
0.7989  
0.8598  
0.9471

```

0.8977
0.9448
0.9506
0.7816
0.8644
0.6920
0.8529
0.7713
0.8149
0.7494
0.7839
0.9080
0.6460
0.7793
0.7805
0.8414 ];

pmudem = [];
for i = 1:length(AggDem_Norm_1)
    pmudem = [pmudem; AggDem_Norm_1(i) + 0.065.*randn(900,1)];
end

WindGen = [10.25572044  9.80057883  10.33032044  4.615074197  4.410260473
4.6486442
10.28637074  9.783267048  10.1704822  4.628866834  4.402470172  4.576716992
10.46965067  9.722066756  10.32026748  4.7113428  4.37493004  4.644120368
% 86400 lines of data
10.61390701  9.938559808  10.51708218  4.776258154  4.472351914  4.732686981
10.33531363  9.640236161  10.28735141  4.650891136  4.338106272  4.629308135 ];

%           %Load file creation for 24 hours on 1-second basis with wind
%           %included
L = Node(1:size(Node,1),1:3);
C = [];
MeanDem = mean(AggDem_Norm_1);
S_avg = MeanDem.*S_peak;
for i = 1:length(pmudem)
    Load = [L(1:13,1:3) Node(1:13,4:9).*pmudem(i); L(14:25,1:3)
Node(14:25,4:9).*pmudem(i)];
    Load = [Load; 1000 32 1 WindGen(i,1) WindGen(i,4) WindGen(i,2)
WindGen(i,5) WindGen(i,3) WindGen(i,6)];
    Load = {Load};
    C = [C;Load];
    Load = cell2mat(Load);
end

%Proximity matrix creation
N = max(max(Branch(:,2)), max(Branch(:,4)));
Prox = zeros(N,N);
for i = 1:N-1
    if Branch(i,6) == 1
        Prox(Branch(i,2),Branch(i,4)) = 0.5;
    else
        Prox(Branch(i,2),Branch(i,4)) = 1;
    end
end

```

```

    Prox(i,i) = 1;
end
Prox(N,N) = 1;
Zline = {N};
    for i = 1:size(Branch,1)
        if Branch(i,6) ~= 1
            Zline{Branch(i,2),Branch(i,4)} =
Branch(i,5)*ftmi*cell2mat(Z(Branch(i,6)-720))./Zb;
        end
    end
end

```

### B.3 Code for Analysis used for fifteen-minute forecasted load data

```

% 3-ph load flow BFS method %% with wind and storage combined in the system
% - Manoj Vijayarengan
tic
VRes_Low = [];
VRes_Med = [];
VRes_High = [];
IRes_Low = [];
IRes_Med = [];
IRes_High = [];
Iplot = zeros(96,3);
Vplot = zeros(96,3);
P = 800;
Emax = 6000;
Emin = 1200;
E0 = 1800;
E_ess = [E0; zeros(96,1)];
P_ess = zeros(96,1);
State = zeros(96,1);
count = zeros(96,1);
ILoss = zeros(96,1);
% S_batt = [0;0;0];
for m = 1:96
    % Node = cell2mat(C_Low(m));
    % Node = cell2mat(C_Med(m));
    Node = cell2mat(C_High(m));
    V = ones(3,N);
    I = zeros(3,N);
    Inode = zeros(3,N);
    znode = zeros(3,N);
    S = zeros(4,N);

    V_nom = [1; exp(-1j*120*pi/180); exp(1j*120*pi/180)];
    Wind = size(Node,1);
    for i = 1:Wind-1
        S(1:3,Node(i,2)) = 1000*[Node(i,4)+1j*Node(i,5)
Node(i,6)+1j*Node(i,7) Node(i,8)+1j*Node(i,9)].';
        S(4,Node(i,2)) = Node(i,3);
    end

    % % Battery integration
    % % Charging
    % % Always charging in Free-running mode
    % if E_ess(m)>Emin && E_ess(m)<=Emax && AggDem_Norm_1(m) <= MeanDem
    %     State(m) = -1;

```



```

%           %Sustained Average load approach in next 2 lines
% %           P_mains = max([0;0;0] S_avg -
1000.*[Node(Wind,4)+1j*Node(Wind,5) Node(Wind,6)+1j*Node(Wind,7)
Node(Wind,8)+1j*Node(Wind,9)].' - sum(S(1:3,:),2)], [], 2);
% %           P_ess(m) = 0.9*(max(-1*P, (-1.*real(Node(Wind,4)+1j*Node(Wind,5)
+ Node(Wind,6)+1j*Node(Wind,7) + Node(Wind,8)+1j*Node(Wind,9)) -
(1/1000).*real(sum(P_mains,1)))));
%           P_ess(m) = 0.9*(max(-1*P, (-1.*real(Node(Wind,4)+1j*Node(Wind,5) +
Node(Wind,6)+1j*Node(Wind,7) + Node(Wind,8)+1j*Node(Wind,9))))); %This line
only for no mains compensation
%           Elevel = E_ess(m) - P_ess(m)*0.25;
%           if Elevel <= Emax && Elevel > Emin
% %           S(1:3,Node(Wind,2)) = S(1:3,Node(Wind,2)) + P_mains; % This
line only for mains compensation
%           for l = m+1:length(E_ess)
%               E_ess(l) = Elevel;
%           end
%           else
%               P_ess(m) = 0;
%               for l = m+1:length(E_ess)
%                   E_ess(l) = E_ess(m);
%               end
%           end
%           % % Discharging
%           % % % Optimal Discharging
% %           elseif E_ess(m)>Emin && E_ess(m)<=Emax && AggDem_Norm_1(m) > MeanDem
% %           State(m) = 1;
% %           S(1:3,Node(Wind,2)) = S(1:3,Node(Wind,2)) -
1000*[Node(Wind,4)+1j*Node(Wind,5) Node(Wind,6)+1j*Node(Wind,7)
Node(Wind,8)+1j*Node(Wind,9)].';
% %           count(m) = 0;
% %           Snod = zeros(3,1);
% %           S_crit = zeros(3,1);
% %           for ins = m:96
% % %           Rem = cell2mat(C_Low(ins));
% % %           Rem = cell2mat(C_Med(ins));
% % %           Rem = cell2mat(C_High(ins));
% %           Wind = size(Rem,1);
% %           for i = 1:Wind-1
% %               Snod = Snod + 1000.*[Rem(i,4)+1j*Rem(i,5)
Rem(i,6)+1j*Rem(i,7) Rem(i,8)+1j*Rem(i,9)].';
% %           end
% %           Snod = Snod - 1000.*[Rem(Wind,4)+1j*Rem(Wind,5)
Rem(Wind,6)+1j*Rem(Wind,7) Rem(Wind,8)+1j*Rem(Wind,9)].';
% %           if abs(sum(Snod,1)) >= abs(sum(S_avg,1))
% %               count(m) = count(m) + 1;
% %               S_crit = S_crit + Snod;
% %           end
% %           end
% %           S_req = real(S_crit)./count(m);
% %           P_req = 1000.*(E_ess(m) - Emin)/(count(m)*0.25);
% % %           Netload(S_batt,S);
% % %           S_batt = fmincon(@Netload,[-50;-50;-50],[[],[],[],[],[-50;-50;-
50],min(S_req./1000,(P_req/(sum(S_req,1))).*S_req./1000));
% %           S_batt = 0.9*min([(P./(sum(S_req,1))).*S_req S_req./1000
(P_req/(sum(S_req,1))).*S_req./1000],[[], 2]);
% %           S(1:3,Node(Wind,2)) = S(1:3,Node(Wind,2)) - 1000.*S_batt;
% %           P_ess(m) = sum(S_batt,1);

```

```

% %
% %      Elevel = E_ess(m) - P_ess(m).*0.25;
% %      if Elevel <= Emax && Elevel > Emin
% %          for l = m+1:length(E_ess)
% %              E_ess(l) = Elevel;
% %          end
% %      else
% %          P_ess(m) = 0;
% %          for l = m+1:length(E_ess)
% %              E_ess(l) = E_ess(m);
% %          end
% %      end
% %
% % % Free-running mode
% % elseif E_ess(m)>Emin && E_ess(m)<=Emax && AggDem_Norm_1(m) > MeanDem
% %     State(m) = 1;
% %     S(1:3,Node(Wind,2)) = S(1:3,Node(Wind,2)) -
1000*[Node(Wind,4)+1j*Node(Wind,5) Node(Wind,6)+1j*Node(Wind,7)
Node(Wind,8)+1j*Node(Wind,9)].';
% %     P_ess(m) = 0.9*min(P, (real(sum(sum(S(1:3,:),2) -
S_avg,1)))./1000);
% %     Elevel = E_ess(m) - P_ess(m)*0.25;
% %     if Elevel <= Emax && Elevel > Emin
% %         S(1:3,Node(Wind,2)) = S(1:3,Node(Wind,2)) -
0.9*(sum(S(1:3,:),2) - S_avg);
% %         for l = m+1:length(E_ess)
% %             E_ess(l) = Elevel;
% %         end
% %     else
% %         P_ess(m) = 0;
% %         for l = m+1:length(E_ess)
% %             E_ess(l) = E_ess(m);
% %         end
% %     end
% % else
% %     State(m) = 0;
% %     S(1:3,Node(Wind,2)) = S(1:3,Node(Wind,2)) -
1000*[Node(Wind,4)+1j*Node(Wind,5) Node(Wind,6)+1j*Node(Wind,7)
Node(Wind,8)+1j*Node(Wind,9)].';
% % end
% upto here
S(4,Node(Wind,2)) = Node(Wind,3);
S(1:3,:) = S(1:3,:)./Sb;
Iline = {N};

% Forward sweep
for i = 1:N
    if sum(Prox(i,:)) == 1 || sum(Prox(i,:)) == 0.5
        V(:,i) = V_nom;
    end
end
for i = 1:N-1
    if S(4,N-i+1) == 1
        I(:,N-i+1) = conj(S(1:3,N-i+1)./V(:,N-i+1));
    elseif S(4,N-i+1) == 2
        znode(:,N-i+1) = (abs(V_nom).^2)./conj(S(1:3,N-i+1));
        I(:,N-i+1) = V(:,N-i+1)./znode(:,N-i+1);
    elseif S(4,N-i+1) == 3

```

```

        Inode(:,N-i+1) = conj(S(1:3,N-i+1))./V_nom;
        I(:,N-i+1) = Inode(:,N-i+1);
    end
    Iline{N-i+1,N-i+1} = I(:,N-i+1);
    if sum(Prox(N-i+1,:)) == 1 || sum(Prox(N-i+1,:)) == 0.5
        for k = 1:N-i+1
            if (Prox(k,N-i+1) == 1 || Prox(k,N-i+1) == 0.5) && k ~= N-i+1
                Iline{k,N-i+1} = I(:,N-i+1);
                if Prox(k,N-i+1) == 0.5
                    V(:,k) = at*V(:,N-i+1)*0.1 + bt*I(:,N-i+1)*0.1;
                else
                    V(:,k) = V(:,N-i+1) + cell2mat(Zline(k,N-
i+1))*cell2mat(Iline(k,N-i+1));
                end
            end
        end
    elseif sum(Prox(N-i+1,:)) > 1
        Temp = zeros(3,1);
        for j = N-i+1:N
            if Prox(N-i+1,j) == 1 || Prox(k,N-i+1) == 0.5
                Temp = Temp + cell2mat(Iline(N-i+1,j));
                if N-i+1~=j
                    if Prox(N-i+1,j) == 0.5
                        V(:,N-i+1) = (at*V(:,j) + bt*I(:,j))*0.1;
                    else
                        V(:,N-i+1) = V(:,j) + cell2mat(Zline(N-
i+1,j))*cell2mat(Iline(N-i+1,j));
                    end
                end
            end
        end
    end
    for j = 1:N-i+1
        if Prox(j,N-i+1) == 1 && j ~= N-i+1
            Iline{j,N-i+1} = Temp;
        end
    end
end
V(:,1) = V(:,2) + cell2mat(Zline(1,2))*cell2mat(Iline(1,2));

% Loop for tolerance check of source node
for n = 1:5
    delV = abs(V(:,1) - V_nom);
    if delV(1)>1e-5 || delV(2)>1e-5 || delV(3)>1e-5
        %Backward Sweep
        V(:,1) = V_nom;
        for i = 1:N
            for j = i:N
                if (Prox(i,j) == 1 || Prox(i,j) == 0.5) && i ~= j
                    if Prox(i,j) == 0.5
                        V(:,j) = (At*V(:,i) - Bt*I(:,i))*10;
                    else
                        V(:,j) = V(:,i) -
cell2mat(Zline(i,j))*cell2mat(Iline(i,j));
                    end
                end
            end
        end
    end
end
end

```

```

%Forward Sweep
for i = 1:N-1
    if S(4,N-i+1) == 1
        I(:,N-i+1) = conj(S(1:3,N-i+1)./V(:,N-i+1));
    elseif S(4,N-i+1) == 2
        I(:,N-i+1) = V(:,N-i+1)./znnode(:,N-i+1);
    elseif S(4,N-i+1) == 3
        I(:,N-i+1) = conj(S(1:3,N-i+1)./V(:,N-i+1));
        I(:,N-i+1) = abs(Inode(:,N-i+1)).*exp(1j.*angle(I(:,N-
i+1))));
    end
    Iline{N-i+1,N-i+1} = I(:,N-i+1);
    if sum(Prox(N-i+1,:)) == 1 || sum(Prox(N-i+1,:)) == 0.5
        for k = 1:N-i+1
            if (Prox(k,N-i+1) == 1 || Prox(k,N-i+1) == 0.5) && k
~= N-i+1
                Iline{k,N-i+1} = I(:,N-i+1);
                if Prox(k,N-i+1) == 0.5
                    V(:,k) = at*V(:,N-i+1)*0.1 + bt*I(:,N-
i+1)*0.1;
                else
                    V(:,k) = V(:,N-i+1) + cell2mat(Zline(k,N-
i+1))*cell2mat(Iline(k,N-i+1));
                end
            end
        end
    end
    elseif sum(Prox(N-i+1,:)) > 1
        Temp = zeros(3,1);
        for j = N-i+1:N
            if Prox(N-i+1,j) == 1 || Prox(k,N-i+1) == 0.5
                Temp = Temp + cell2mat(Iline(N-i+1,j));
                if N-i+1~=j
                    if Prox(N-i+1,j) == 0.5
                        V(:,N-i+1) = (at*V(:,j) + bt*I(:,j))*0.1;
                    else
                        V(:,N-i+1) = V(:,j) + cell2mat(Zline(N-
i+1,j))*cell2mat(Iline(N-i+1,j));
                    end
                end
            end
        end
    end
    for j = 1:N-i+1
        if Prox(j,N-i+1) == 1 && j ~= N-i+1
            Iline{j,N-i+1} = Temp;
        end
    end
end
end
V(:,1) = V(:,2) + cell2mat(Zline(1,2))*cell2mat(Iline(1,2));
end

%Backward Sweep
V(:,1) = V_nom;
for i = 1:N
    for j = i:N
        if (Prox(i,j) == 1 || Prox(i,j) == 0.5) && i ~= j
            if Prox(i,j) == 0.5

```

```

        V(:,j) = (At*V(:,i) - Bt*I(:,i))*10;
    else
        V(:,j) = V(:,i) -
cell2mat(Zline(i,j))*cell2mat(Iline(i,j));
    end
end
end
end

VRes = [(1:N)' (abs(V))' (angle(V)*180/pi)'];
VRes = {VRes};
% VRes_Low = [VRes_Low; VRes];
Vplot(m,:) = abs(V(:,32))';
% VRes_Med = [VRes_Med; VRes];
VRes_High = [VRes_High; VRes];
IRes = zeros(N-1,8);
Loss = zeros(3,1);
for k = 1:N-1
    IRes(k,:) = [Branch(k,2) Branch(k,4)
(abs(cell2mat(Iline(Branch(k,2),Branch(k,4))))*Sb/Vb)'
(angle(cell2mat(Iline(Branch(k,2),Branch(k,4))))*180/pi)'];
    if k ~= N-2
        Loss = Loss +
real(cell2mat(Zline(Branch(k,2),Branch(k,4))))*((abs(cell2mat(Iline(Branch(k,
2),Branch(k,4))))).^2).*Sb;
    end
end
Iloss(m) = sum(Loss,1);
Iplot(m,:) = Vb*IRes(size(IRes,1),3:5);
IRes = {IRes};
% IRes_Low = [IRes_Low; IRes];
% IRes_Med = [IRes_Med; IRes];
IRes_High = [IRes_High; IRes];
end
toc
plot(1:96,Iplot(:,1)./1000)
hold on
plot(1:96,HighGen(:,1),'b--')
hold on
plot(1:96,Iplot(:,2)./1000,'r')
hold on
plot(1:96,HighGen(:,2),'r--')
hold on
plot(1:96,Iplot(:,3)./1000,'g')
hold on
plot(1:96,HighGen(:,3),'g--')
title('Individual phase load demand and wind generation')
xlabel('Time in 15 min intervals')
ylabel('Load and wind generation kVA')
axis([0 100 0 1600])
figure(2)
plot(1:96,Vplot(:,1))
hold on
plot(1:96,Vplot(:,2),'r')
hold on
plot(1:96,Vplot(:,3),'g')
title('Individual phase voltage profile for wind node & battery node')
xlabel('Time in 15 min intervals')

```

```

ylabel('Voltage in p.u.')
axis([0 100 0.95 1.05])
figure(3)
bar(1:length(P_ess),P_ess)
title('Battery power charging and discharging')
xlabel('Time in 15 min intervals')
ylabel('Battery power -ve(charging) +ve(discharging) kW')
axis([0 100 -P P])
figure(4)
plot(1:length(E_ess),E_ess)
hold on
plot(1:0.1:length(E_ess),1200,'k')
title('Energy level of battery')
xlabel('Time in 15 min intervals')
ylabel('Battery energy level kWh')
axis([0 100 0 6000])
figure(5)
plot(1:length(ILoss),ILoss./1000)
title('Power loss of the feeder')
xlabel('Time in 15 min intervals')
ylabel('Power loss kW')
axis([0 100 0 80])
figure(6)
bar(1:96,sum(Iplot(:,1:3),2)./(1000*abs(sum(S_peak./1000,1))))
title('Overall 15 minute average normalized feeder load')
xlabel('Time in 15 min intervals')
ylabel('Normalized load factor Lf')
axis([0 100 0 1])

```

## B.4 Code for Analysis used for one-second forecasted load data

```

% 3-ph load flow BFS method %% with wind and storage combined in the system
% - Manoj Vijayarengan
tic
VRes_1s = [];
IRes_1s = [];
Iplot = zeros(86400,3);
Vplot = zeros(86400,3);
P = 800;
Emax = 6000;
Emin = 1200;
E0 = 1800;
E_ess = [E0; zeros(86400,1)];
P_ess = zeros(86400,1);
State = zeros(86400,1);
count = zeros(86400,1);
ILoss = zeros(86400,1);
% S_batt = [0;0;0];
for m = 1:86400
    Node = cell2mat(C(m));
    V = ones(3,N);
    I = zeros(3,N);

```

```

Inode = zeros(3,N);
znnode = zeros(3,N);
S = zeros(4,N);

V_nom = [1; exp(-1j*120*pi/180); exp(1j*120*pi/180)];
Wind = size(Node,1);
for i = 1:Wind-1
    S(1:3,Node(i,2)) = 1000*[Node(i,4)+1j*Node(i,5)
Node(i,6)+1j*Node(i,7) Node(i,8)+1j*Node(i,9)].';
    S(4,Node(i,2)) = Node(i,3);
end
% % Battery integration
% % Charging
% % Always charging in Free-running mode
if E_ess(m)>Emin && E_ess(m)<=Emax && pmudem(m) <= MeanDem
    State(m) = -1;
    %Sustained Average load approach in next 2 lines
    P_mains = max([0;0;0] S_avg - 1000.*[Node(Wind,4)+1j*Node(Wind,5)
Node(Wind,6)+1j*Node(Wind,7) Node(Wind,8)+1j*Node(Wind,9)].' -
sum(S(1:3,:),2)], [], 2);
    P_ess(m) = 0.9*(max(-1*P, (-1.*real(Node(Wind,4)+1j*Node(Wind,5) +
Node(Wind,6)+1j*Node(Wind,7) + Node(Wind,8)+1j*Node(Wind,9)) -
(1/1000).*real(sum(P_mains,1)))));
% P_ess(m) = 0.9*(max(-1*P, (-1.*real(Node(Wind,4)+1j*Node(Wind,5) +
Node(Wind,6)+1j*Node(Wind,7) + Node(Wind,8)+1j*Node(Wind,9)))));% This line
only for no mains compensation
    Elevel = E_ess(m) - P_ess(m)*(1/3600);
    if Elevel <= Emax && Elevel > Emin
        S(1:3,Node(Wind,2)) = S(1:3,Node(Wind,2)) + P_mains; % This line
only for mains compensation
        for l = m+1:length(E_ess)
            E_ess(l) = Elevel;
        end
    else
        P_ess(m) = 0;
        for l = m+1:length(E_ess)
            E_ess(l) = E_ess(m);
        end
    end
% % Discharging
% % Optimal Discharging
elseif E_ess(m)>Emin && E_ess(m)<=Emax && pmudem(m) > MeanDem
    State(m) = 1;
    S(1:3,Node(Wind,2)) = S(1:3,Node(Wind,2)) -
1000*[Node(Wind,4)+1j*Node(Wind,5) Node(Wind,6)+1j*Node(Wind,7)
Node(Wind,8)+1j*Node(Wind,9)].';
    count(m) = 0;
    S_crit = zeros(3,1);
    Snod = zeros(3,1);
    for ins = m:86400
        Rem = cell2mat(C(ins));
% Wind = size(Rem,1);
% for i = 1:Wind-1
% Snod = Snod + 1000.*[Rem(i,4)+1j*Rem(i,5)
Rem(i,6)+1j*Rem(i,7) Rem(i,8)+1j*Rem(i,9)].';
% end
        Snod = pmudem(ins).*S_peak;

```

```

        Snod = Snod - 1000.*[Rem(Wind,4)+1j*Rem(Wind,5)
Rem(Wind,6)+1j*Rem(Wind,7) Rem(Wind,8)+1j*Rem(Wind,9)].';
        if abs(sum(Snod,1)) >= abs(sum(S_avg,1))
            count(m) = count(m) + 1;
            S_crit = S_crit + Snod;
        end
    end
    S_req = real(S_crit)./count(m);
    P_req = 1000.*(E_ess(m) - Emin)/(count(m)*(1/3600));
    % Netload(S_batt,S);
    % S_batt = fmincon(@Netload,[-50;-50;-50],[[],[],[],[],[-50;-50;-
50],min(S_req./1000,(P_req/(sum(S_req,1)).*S_req./1000));
    S_batt = 0.9*min([(P./(sum(S_req,1)).*S_req S_req./1000
(P_req./sum(S_req,1)).*S_req./1000],[], 2);
    S(1:3,Node(Wind,2)) = S(1:3,Node(Wind,2)) - 1000.*S_batt;
    P_ess(m) = sum(S_batt,1);
    Elevel = E_ess(m) - P_ess(m).*(1/3600);
    if Elevel <= Emax && Elevel > Emin
        for l = m+1:length(E_ess)
            E_ess(l) = Elevel;
        end
    else
        P_ess(m) = 0;
        for l = m+1:length(E_ess)
            E_ess(l) = E_ess(m);
        end
    end
end
% % Free-running mode
% elseif E_ess(m)>Emin && E_ess(m)<=Emax && pmudem(m) > MeanDem
%     State(m) = 1;
%     S(1:3,Node(Wind,2)) = S(1:3,Node(Wind,2)) -
1000*[Node(Wind,4)+1j*Node(Wind,5) Node(Wind,6)+1j*Node(Wind,7)
Node(Wind,8)+1j*Node(Wind,9)].';
%     P_ess(m) = 0.9*min(P, (real(sum(sum(S(1:3,:),2) -
S_avg,1)))./1000);
%     Elevel = E_ess(m) - P_ess(m).*(1/3600);
%     if Elevel <= Emax && Elevel > Emin
%         S(1:3,Node(Wind,2)) = S(1:3,Node(Wind,2)) -
0.9*(sum(S(1:3,:),2) - S_avg);
%         for l = m+1:length(E_ess)
%             E_ess(l) = Elevel;
%         end
%     else
%         P_ess(m) = 0;
%         for l = m+1:length(E_ess)
%             E_ess(l) = E_ess(m);
%         end
%     end
end
else
    State(m) = 0;
    S(1:3,Node(Wind,2)) = S(1:3,Node(Wind,2)) -
1000*[Node(Wind,4)+1j*Node(Wind,5) Node(Wind,6)+1j*Node(Wind,7)
Node(Wind,8)+1j*Node(Wind,9)].';
end
%upto here
S(4,Node(Wind,2)) = Node(Wind,3);
S(1:3,:) = S(1:3,:)./Sb;
Iline = {N};

```



```

% Forward sweep
for i = 1:N
    if sum(Prox(i,:)) == 1 || sum(Prox(i,:)) == 0.5
        V(:,i) = V_nom;
    end
end
for i = 1:N-1
    if S(4,N-i+1) == 1
        I(:,N-i+1) = conj(S(1:3,N-i+1)./V(:,N-i+1));
    elseif S(4,N-i+1) == 2
        znode(:,N-i+1) = (abs(V_nom).^2)./conj(S(1:3,N-i+1));
        I(:,N-i+1) = V(:,N-i+1)./znode(:,N-i+1);
    elseif S(4,N-i+1) == 3
        Inode(:,N-i+1) = conj(S(1:3,N-i+1))./V_nom;
        I(:,N-i+1) = Inode(:,N-i+1);
    end
    Iline{N-i+1,N-i+1} = I(:,N-i+1);
    if sum(Prox(N-i+1,:)) == 1 || sum(Prox(N-i+1,:)) == 0.5
        for k = 1:N-i+1
            if (Prox(k,N-i+1) == 1 || Prox(k,N-i+1) == 0.5) && k ~= N-i+1
                Iline{k,N-i+1} = I(:,N-i+1);
                if Prox(k,N-i+1) == 0.5
                    V(:,k) = at*V(:,N-i+1)*0.1 + bt*I(:,N-i+1)*0.1;
                else
                    V(:,k) = V(:,N-i+1) + cell2mat(Zline(k,N-
i+1))*cell2mat(Iline(k,N-i+1));
                end
            end
        end
    elseif sum(Prox(N-i+1,:)) > 1
        Temp = zeros(3,1);
        for j = N-i+1:N
            if Prox(N-i+1,j) == 1 || Prox(k,N-i+1) == 0.5
                Temp = Temp + cell2mat(Iline(N-i+1,j));
                if N-i+1~=j
                    if Prox(N-i+1,j) == 0.5
                        V(:,N-i+1) = (at*V(:,j) + bt*I(:,j))*0.1;
                    else
                        V(:,N-i+1) = V(:,j) + cell2mat(Zline(N-
i+1,j))*cell2mat(Iline(N-i+1,j));
                    end
                end
            end
        end
    end
    for j = 1:N-i+1
        if Prox(j,N-i+1) == 1 && j ~= N-i+1
            Iline{j,N-i+1} = Temp;
        end
    end
end
end
V(:,1) = V(:,2) + cell2mat(Zline(1,2))*cell2mat(Iline(1,2));

% Loop for tolerance check of source node
for n = 1:5

```

```

delV = abs(V(:,1) - V_nom);
if delV(1)>1e-5 || delV(2)>1e-5 || delV(3)>1e-5
    %Backward Sweep
    V(:,1) = V_nom;
    for i = 1:N
        for j = i:N
            if (Prox(i,j) == 1 || Prox(i,j) == 0.5) && i ~= j
                if Prox(i,j) == 0.5
                    V(:,j) = (At*V(:,i) - Bt*I(:,i))*10;
                else
                    V(:,j) = V(:,i) -
cell2mat(Zline(i,j))*cell2mat(Iline(i,j));
                end
            end
        end
    end
    %Forward Sweep
    for i = 1:N-1
        if S(4,N-i+1) == 1
            I(:,N-i+1) = conj(S(1:3,N-i+1)./V(:,N-i+1));
        elseif S(4,N-i+1) == 2
            I(:,N-i+1) = V(:,N-i+1)./znnode(:,N-i+1);
        elseif S(4,N-i+1) == 3
            I(:,N-i+1) = conj(S(1:3,N-i+1)./V(:,N-i+1));
            I(:,N-i+1) = abs(Inode(:,N-i+1)).*exp(1j.*angle(I(:,N-
i+1))));
        end
        Iline{N-i+1,N-i+1} = I(:,N-i+1);
        if sum(Prox(N-i+1,:)) == 1 || sum(Prox(N-i+1,:)) == 0.5
            for k = 1:N-i+1
                if (Prox(k,N-i+1) == 1 || Prox(k,N-i+1) == 0.5) && k
~= N-i+1
                    Iline{k,N-i+1} = I(:,N-i+1);
                    if Prox(k,N-i+1) == 0.5
                        V(:,k) = at*V(:,N-i+1)*0.1 + bt*I(:,N-
i+1)*0.1;
                    else
                        V(:,k) = V(:,N-i+1) + cell2mat(Zline(k,N-
i+1))*cell2mat(Iline(k,N-i+1));
                    end
                end
            end
        elseif sum(Prox(N-i+1,:)) > 1
            Temp = zeros(3,1);
            for j = N-i+1:N
                if Prox(N-i+1,j) == 1 || Prox(k,N-i+1) == 0.5
                    Temp = Temp + cell2mat(Iline(N-i+1,j));
                    if N-i+1~=j
                        if Prox(N-i+1,j) == 0.5
                            V(:,N-i+1) = (at*V(:,j) + bt*I(:,j))*0.1;
                        else
                            V(:,N-i+1) = V(:,j) + cell2mat(Zline(N-
i+1,j))*cell2mat(Iline(N-i+1,j));
                        end
                    end
                end
            end
        end
        for j = 1:N-i+1

```

```

        if Prox(j,N-i+1) == 1 && j ~= N-i+1
            Iline{j,N-i+1} = Temp;
        end
    end
end
end
V(:,1) = V(:,2) + cell2mat(Zline(1,2))*cell2mat(Iline(1,2));
end
end

%Backward Sweep
V(:,1) = V_nom;
for i = 1:N
    for j = i:N
        if (Prox(i,j) == 1 || Prox(i,j) == 0.5) && i ~= j
            if Prox(i,j) == 0.5
                V(:,j) = (At*V(:,i) - Bt*I(:,i))*10;
            else
                V(:,j) = V(:,i) -
cell2mat(Zline(i,j))*cell2mat(Iline(i,j));
            end
        end
    end
end

VRes = [(1:N)' (abs(V))' (angle(V)*180/pi)'];
VRes = {VRes};
Vplot(m,:) = abs(V(:,32))';
VRes_1s = [VRes_1s; VRes];
IRes = zeros(N-1,8);
Loss = zeros(3,1);
for k = 1:N-1
    IRes(k,:) = [Branch(k,2) Branch(k,4)
(abs(cell2mat(Iline(Branch(k,2),Branch(k,4))))*Sb/Vb)'
(angle(cell2mat(Iline(Branch(k,2),Branch(k,4))))*180/pi)'];
    if k ~= N-2
        Loss = Loss +
real(cell2mat(Zline(Branch(k,2),Branch(k,4))))*((abs(cell2mat(Iline(Branch(k,
2),Branch(k,4))))).^2).*Sb;
    end
end
ILoss(m) = sum(Loss,1);
Iplot(m,:) = Vb*IRes(size(IRes,1),3:5);
IRes = {IRes};
IRes_1s = [IRes_1s; IRes];
end
toc
plot(1:86400,Iplot(:,1)./1000)
hold on
plot(1:86400,WindGen(:,1),'b--')
hold on
plot(1:86400,Iplot(:,2)./1000,'r')
hold on
plot(1:86400,WindGen(:,2),'r--')
hold on
plot(1:86400,Iplot(:,3)./1000,'g')
hold on

```

```

plot(1:86400, WindGen(:, 3), 'g--')
title('Individual phase load demand and wind generation')
xlabel('Time in one second intervals')
ylabel('Load and wind generation kVA')
axis([0 90000 0 1600])
figure(2)
plot(1:86400, Vplot(:, 1))
hold on
plot(1:86400, Vplot(:, 2), 'r')
hold on
plot(1:86400, Vplot(:, 3), 'g')
title('Individual phase voltage profile for wind & battery node')
xlabel('Time in one second intervals')
ylabel('Voltage in p.u.')
axis([0 90000 0.95 1.05])
figure(3)
bar(1:length(P_ess), P_ess)
title('Battery power charging and discharging')
xlabel('Time in one second intervals')
ylabel('Battery power -ve(charging) +ve(discharging) kW')
axis([0 90000 -P P])
figure(4)
plot(1:length(E_ess), E_ess)
hold on
plot(1:length(E_ess), 1200, 'k')
title('Energy level of battery')
xlabel('Time in one second intervals')
ylabel('Battery energy level kWh')
axis([0 90000 0 6000])
figure(5)
plot(1:length(ILoss), ILoss./1000)
title('Power loss of the feeder')
xlabel('Time in one second intervals')
ylabel('Power loss kW')
axis([0 90000 0 80])
F = sum(Iplot(:, 1:3), 2)./1000;
figure(6)
plot(1:86400, F)
title('Overall one second actual load of the feeder')
xlabel('Time in one second intervals')
ylabel('Three phase load kVA')
axis([0 90000 0 3500])
F_15 = [];
out = 0;
for i = 1:96
    out = out + 1;
    F_15 = [F_15; mean(F(out:i*900))./abs(sum(S_peak, 1))./1000)];
    out = out + 900;
end
figure(7)
bar(1:96, F_15)
title('Overall 15 minute average normalized feeder load')
xlabel('Time in 15 min intervals')
ylabel('Normalized load factor Lf')
axis([0 100 0 1])
Avg_Dem = mean(F_15)
Peak_Dem = max(F_15)
Batt_util = max(E_ess)./Emax

```

## B.5 Code for Analysis used for one-second load data based on historical PMU measurements

```

% 3-ph load flow BFS method %% with wind and storage combined in the system
% - Manoj Vijayarengan
tic
VRes_1s = [];
IRes_1s = [];
Iplot = zeros(86400,3);
Vplot = zeros(86400,3);
P = 200;
Emax = 1500;
Emin = 300;
E0 = 450;
E_ess = [E0; zeros(86400,1)];
P_ess = zeros(86400,1);
State = zeros(86400,1);
count = zeros(86400,1);
ILoss = zeros(86400,1);
Vpmu2 = [];
x = 60;
for m = 1:86400
    Node = cell2mat(C(m));
    V = ones(3,N);
    I = zeros(3,N);
    Inode = zeros(3,N);
    znode = zeros(3,N);
    S = zeros(4,N);

    V_nom = [1; exp(-1j*120*pi/180); exp(1j*120*pi/180)];
    Wind = size(Node,1);
    for i = 1:Wind-1
        S(1:3,Node(i,2)) = 1000*[Node(i,4)+1j*Node(i,5)
Node(i,6)+1j*Node(i,7) Node(i,8)+1j*Node(i,9)].';
        S(4,Node(i,2)) = Node(i,3);
    end
    % Battery integration
    if m <= x && E_ess(m) <= Emax % Preliminary
        State(m) = -1;
        P_ess(m) = 0.9*(max(-1*P, (-1.*real(Node(Wind,4)+1j*Node(Wind,5) +
Node(Wind,6)+1j*Node(Wind,7) + Node(Wind,8)+1j*Node(Wind,9)))));
        Elevel = E_ess(m) - P_ess(m)*(1/3600);
        if Elevel <= Emax && Elevel > Emin
            for l = m+1:length(E_ess)
                E_ess(l) = Elevel;
            end
        else
            P_ess(m) = 0;
            for l = m+1:length(E_ess)
                E_ess(l) = E_ess(m);
            end
        end
    end
end

```

```

elseif m > x && E_ess(m) >= Emin && E_ess(m) <= Emax
    S_det = [];
    for ins = m-x:m-1
        Inod = (cell2mat(Zline(1,2)))\'(V_nom - (Vpmu2(ins,:)).');
        Snod = V_nom.*conj(Inod).*Sb;
        if P_ess(ins) >= 0;
            S_det = [S_det (Snod +
1000.*P_ess(ins).*real(Snod)./sum(real(Snod),1)) +
1000.*[WindGen(ins,1)+1j*WindGen(ins,4) WindGen(ins,2)+1j*WindGen(ins,5)
WindGen(ins,3)+1j*WindGen(ins,6)].'];
        end
    end
    S_crit = max(S_det, [],2);
    if abs(sum(S_crit,1)) >= abs(sum(S_avg,1)) % Discharging
        State(m) = 1;
        S(1:3,Node(Wind,2)) = S(1:3,Node(Wind,2)) -
1000*[Node(Wind,4)+1j*Node(Wind,5) Node(Wind,6)+1j*Node(Wind,7)
Node(Wind,8)+1j*Node(Wind,9)].';
        S_batt = 0.9.*min([(1000*P.*real(S_crit -
S_avg))./(sum(real(S_crit - S_avg))) real(S_crit - S_avg)], [],2) -
1000.*[WindGen(m-1,1) WindGen(m-1,2) WindGen(m-1,3)].');
        if E_ess(m) <= 0.3*Emax
            S_batt = min([S_batt (0.9*1000.*(E_ess(m) - Emin)/((86400-
m)*(1/3600))).*S_batt./sum(S_batt,1)], [],2);
        end
        if sum(S_batt,1)>0
            P_ess(m) = sum(S_batt,1)./1000;
            Elevel = E_ess(m) - P_ess(m).*(1/3600);
            if Elevel <= Emax && Elevel > Emin
                S(1:3,Node(Wind,2)) = S(1:3,Node(Wind,2)) - S_batt;
                for l = m+1:length(E_ess)
                    E_ess(l) = Elevel;
                end
            else
                P_ess(m) = 0;
                State(m) = 0;
                for l = m+1:length(E_ess)
                    E_ess(l) = E_ess(m);
                end
            end
        end
    end
elseif abs(sum(S_crit,1)) < abs(sum(S_avg,1)) % Charging
    State(m) = -1;
    P_ess(m) = 0.9*(max(-1*P, (-1.*real(Node(Wind,4)+1j*Node(Wind,5)
+ Node(Wind,6)+1j*Node(Wind,7) + Node(Wind,8)+1j*Node(Wind,9)))));
    Elevel = E_ess(m) - P_ess(m).*(1/3600);
    if Elevel <= Emax && Elevel > Emin
        for l = m+1:length(E_ess)
            E_ess(l) = Elevel;
        end
    else
        P_ess(m) = 0;
        for l = m+1:length(E_ess)
            E_ess(l) = E_ess(m);
        end
    end
end
end
else % Default

```

```

        State(m) = 0;
        S(1:3,Node(Wind,2)) = S(1:3,Node(Wind,2)) -
1000*[Node(Wind,4)+1j*Node(Wind,5) Node(Wind,6)+1j*Node(Wind,7)
Node(Wind,8)+1j*Node(Wind,9)].';
    end
    %upto here

    S(4,Node(Wind,2)) = Node(Wind,3);
    S(1:3,:) = S(1:3,:)./Sb;
    Iline = {N};

    % Forward sweep
    for i = 1:N
        if sum(Prox(i,:)) == 1 || sum(Prox(i,:)) == 0.5
            V(:,i) = V_nom;
        end
    end
    for i = 1:N-1
        if S(4,N-i+1) == 1
            I(:,N-i+1) = conj(S(1:3,N-i+1)./V(:,N-i+1));
        elseif S(4,N-i+1) == 2
            znode(:,N-i+1) = (abs(V_nom).^2)./conj(S(1:3,N-i+1));
            I(:,N-i+1) = V(:,N-i+1)./znode(:,N-i+1);
        elseif S(4,N-i+1) == 3
            Inode(:,N-i+1) = conj(S(1:3,N-i+1))./V_nom;
            I(:,N-i+1) = Inode(:,N-i+1);
        end
        Iline{N-i+1,N-i+1} = I(:,N-i+1);
        if sum(Prox(N-i+1,:)) == 1 || sum(Prox(N-i+1,:)) == 0.5
            for k = 1:N-i+1
                if (Prox(k,N-i+1) == 1 || Prox(k,N-i+1) == 0.5) && k ~= N-i+1
                    Iline{k,N-i+1} = I(:,N-i+1);
                    if Prox(k,N-i+1) == 0.5
                        V(:,k) = at*V(:,N-i+1)*0.1 + bt*I(:,N-i+1)*0.1;
                    else
                        V(:,k) = V(:,N-i+1) + cell2mat(Zline(k,N-
i+1))*cell2mat(Iline(k,N-i+1));
                    end
                end
            end
        elseif sum(Prox(N-i+1,:)) > 1
            Temp = zeros(3,1);
            for j = N-i+1:N
                if Prox(N-i+1,j) == 1 || Prox(k,N-i+1) == 0.5
                    Temp = Temp + cell2mat(Iline(N-i+1,j));
                    if N-i+1~=j
                        if Prox(N-i+1,j) == 0.5
                            V(:,N-i+1) = (at*V(:,j) + bt*I(:,j))*0.1;
                        else
                            V(:,N-i+1) = V(:,j) + cell2mat(Zline(N-
i+1,j))*cell2mat(Iline(N-i+1,j));
                        end
                    end
                end
            end
        end
        for j = 1:N-i+1

```

```

        if Prox(j,N-i+1) == 1 && j ~= N-i+1
            Iline{j,N-i+1} = Temp;
        end
    end
end
end
V(:,1) = V(:,2) + cell2mat(Zline(1,2))*cell2mat(Iline(1,2));

% Loop for tolerance check of source node
for n = 1:5
    delV = abs(V(:,1) - V_nom);
    if delV(1)>1e-5 || delV(2)>1e-5 || delV(3)>1e-5
        %Backward Sweep
        V(:,1) = V_nom;
        for i = 1:N
            for j = i:N
                if (Prox(i,j) == 1 || Prox(i,j) == 0.5) && i ~= j
                    if Prox(i,j) == 0.5
                        V(:,j) = (At*V(:,i) - Bt*I(:,i))*10;
                    else
                        V(:,j) = V(:,i) -
cell2mat(Zline(i,j))*cell2mat(Iline(i,j));
                    end
                end
            end
        end
    end
    %Forward Sweep
    for i = 1:N-1
        if S(4,N-i+1) == 1
            I(:,N-i+1) = conj(S(1:3,N-i+1)./V(:,N-i+1));
        elseif S(4,N-i+1) == 2
            I(:,N-i+1) = V(:,N-i+1)./znode(:,N-i+1);
        elseif S(4,N-i+1) == 3
            I(:,N-i+1) = conj(S(1:3,N-i+1)./V(:,N-i+1));
            I(:,N-i+1) = abs(Inode(:,N-i+1)).*exp(1j.*angle(I(:,N-
i+1))));
        end
        Iline{N-i+1,N-i+1} = I(:,N-i+1);
        if sum(Prox(N-i+1,:)) == 1 || sum(Prox(N-i+1,:)) == 0.5
            for k = 1:N-i+1
                if (Prox(k,N-i+1) == 1 || Prox(k,N-i+1) == 0.5) && k
~= N-i+1
                    Iline{k,N-i+1} = I(:,N-i+1);
                    if Prox(k,N-i+1) == 0.5
                        V(:,k) = at*V(:,N-i+1)*0.1 + bt*I(:,N-
i+1)*0.1;
                    else
                        V(:,k) = V(:,N-i+1) + cell2mat(Zline(k,N-
i+1))*cell2mat(Iline(k,N-i+1));
                    end
                end
            end
        end
    elseif sum(Prox(N-i+1,:)) > 1
        Temp = zeros(3,1);
        for j = N-i+1:N
            if Prox(N-i+1,j) == 1 || Prox(k,N-i+1) == 0.5
                Temp = Temp + cell2mat(Iline(N-i+1,j));
                if N-i+1~=j

```



```

        if Prox(N-i+1,j) == 0.5
            V(:,N-i+1) = (at*V(:,j) + bt*I(:,j))*0.1;
        else
            V(:,N-i+1) = V(:,j) + cell2mat(Zline(N-
i+1,j))*cell2mat(Iline(N-i+1,j));
        end
    end
end
    end
    for j = 1:N-i+1
        if Prox(j,N-i+1) == 1 && j ~= N-i+1
            Iline{j,N-i+1} = Temp;
        end
    end
end
    end
    V(:,1) = V(:,2) + cell2mat(Zline(1,2))*cell2mat(Iline(1,2));
end
end

%Backward Sweep
V(:,1) = V_nom;
for i = 1:N
    for j = i:N
        if (Prox(i,j) == 1 || Prox(i,j) == 0.5) && i ~= j
            if Prox(i,j) == 0.5
                V(:,j) = (At*V(:,i) - Bt*I(:,i))*10;
            else
                V(:,j) = V(:,i) -
cell2mat(Zline(i,j))*cell2mat(Iline(i,j));
            end
        end
    end
end
end

Vpmu2 = [Vpmu2; V(:,2).'];
VRes = [(1:N)' (abs(V))' (angle(V)*180/pi)'];
VRes = {VRes};
Vplot(m,:) = abs(V(:,32)).';
VRes_1s = [VRes_1s; VRes];
IRes = zeros(N-1,8);
Loss = zeros(3,1);
for k = 1:N-1
    IRes(k,:) = [Branch(k,2) Branch(k,4)
(abs(cell2mat(Iline(Branch(k,2),Branch(k,4))))*Sb/Vb)'
(angle(cell2mat(Iline(Branch(k,2),Branch(k,4))))*180/pi)'];
    if k ~= N-2
        Loss = Loss +
real(cell2mat(Zline(Branch(k,2),Branch(k,4))))*((abs(cell2mat(Iline(Branch(k,
2),Branch(k,4))))).^2).*Sb;
    end
end
    ILoss(m) = sum(Loss,1);
    Iplot(m,:) = Vb*IRes(size(IRes,1),3:5);
    IRes = {IRes};
    IRes_1s = [IRes_1s; IRes];
end
end

```

```

toc
plot(1:86400,Iplot(:,1)./1000)
hold on
plot(1:86400,WindGen(:,1),'b--')
hold on
plot(1:86400,Iplot(:,2)./1000,'r')
hold on
plot(1:86400,WindGen(:,2),'r--')
hold on
plot(1:86400,Iplot(:,3)./1000,'g')
hold on
plot(1:86400,WindGen(:,3),'g--')
title('Individual phase load demand and wind generation')
xlabel('Time in one second intervals')
ylabel('Load and wind generation kVA')
axis([0 90000 0 1600])
figure(2)
plot(1:86400,Vplot(:,1))
hold on
plot(1:86400,Vplot(:,2),'r')
hold on
plot(1:86400,Vplot(:,3),'g')
title('Individual phase voltage profile for wind & battery node')
xlabel('Time in one second intervals')
ylabel('Voltage in p.u.')
axis([0 90000 0.95 1.05])
figure(3)
bar(1:length(P_ess),P_ess)
title('Battery power charging and discharging')
xlabel('Time in one second intervals')
ylabel('Battery power -ve(charging) +ve(discharging) kW')
axis([0 90000 -P P])
figure(4)
plot(1:length(E_ess),E_ess)
hold on
plot(1:length(E_ess),Emin,'k')
title('Energy level of battery')
xlabel('Time in one second intervals')
ylabel('Battery energy level kWh')
axis([0 90000 0 Emax])
figure(5)
plot(1:length(ILoss),ILoss./1000)
title('Power loss of the feeder')
xlabel('Time in one second intervals')
ylabel('Power loss kW')
axis([0 90000 0 80])
F = sum(Iplot(:,1:3),2)./1000;
figure(6)
plot(1:86400,F)
title('Overall one second actual load of the feeder')
xlabel('Time in one second intervals')
ylabel('Three phase load kVA')
axis([0 90000 0 3500])
F_15 = [];
out = 0;
for i = 1:96
    out = out + 1;
    F_15 = [F_15;mean(F(out:i*900))./abs(sum(S_peak,1)./1000)];

```

```

        out = out + 900;
    end
    figure(7)
    bar(1:96,F_15)
    title('Overall 15 minute average normalized feeder load')
    xlabel('Time in 15 min intervals')
    ylabel('Normalized load factor Lf')
    axis([0 100 0 1])
    Avg_Dem = mean(F_15)
    Peak_Dem = max(F_15)
    Batt_util = max(E_ess)./Emax

```